Development of a Serum-Free Chemically Defined Medium for Adherent and Suspension Culture

by

Megan Logan

A thesis
presented to the University of Waterloo
in fulfillment of the
thesis requirement for the degree of
Doctor of Philosophy
in
Chemical Engineering

Waterloo, Ontario, Canada, 2021

Examining Committee Membership

The following served on the Examining Committee for this thesis. The decision of the Examining Committee is by majority vote.

External Examiner:	Mario Jolicoeur Professor, Dept. of Chemical Engineering, Polytechnique Montreal
Supervisor:	Marc G. Aucoin Professor, Dept. of Chemical Engineering, University of Waterloo
Internal Member:	Evelyn Yim Associate Professor, Dept. of Chemical Engineering, University of Waterloo
Internal-External Member:	Maud Gorbet Associate Professor, Dept. of Systems Design Engineering, University of Waterloo
Internal-External Member:	Roderick Slavcev Associate Professor, School of Pharmacy, University of Waterloo

Author's Declaration

This thesis consists of material all of which I authored or co-authored: see Statement of Contributions included in the thesis. This is a true copy of the thesis, including any required final revisions, as accepted by my examiners.

I understand that my thesis may be made electronically available to the public.

Statement of Contributions

Megan Logan was the sole author of Chapters 1 and 3, which were written under the supervision of Dr. Marc Aucoin and were not written for publication.

This thesis consists in part of two manuscripts that were written for publication. Exceptions to sole authorship are as follows:

Research presented in Chapter 2:

This research was conducted at the University of Waterloo by Megan Logan under the supervision of Dr. Marc Aucoin. Megan Logan completed the data collection and data analysis. Megan Logan drafted the manuscript, with the exception of the *Osmolarity* section which was written by Scott Boegel, and Dr. Ali Jahanian-Najafabadi contributed to the *Vitamins* section.

Research presented in Chapter 3:

This research was conducted at the University of Waterloo by Megan Logan under the supervision of Dr. Marc Aucoin. Megan Logan completed the data collection, data analysis, and drafted the manuscript.

Research presented in Chapter 4

This research was conducted at the University of Waterloo by Megan Logan and Karsten Rinas under the supervision of Dr. Marc Aucoin and Dr. Brendan McConkey. Megan Logan performed the cell culture and the design of the experiments. Karsten Rinas performed the data analysis of the RNA-seq data that was collected by Centre for Applied Genomics, Sick Kids Hospital, Toronto, Canada. Megan Logan and Karsten Rinas reviewed the data, drafted the manuscript and each author provided intellectual input on manuscript drafts.

Research presented in Chapter 5

This research was conducted at the University of Waterloo by Megan Logan and Karsten Rinas under the supervision of Dr. Marc Aucoin and Dr. Brendan McConkey. Megan Logan performed the cell culture and the design of the experiments. Karsten Rinas performed the data analysis of the RNA-seq data that was collected by Centre for Applied Genomics, Sick Kids Hospital, Toronto, Canada. Megan Logan reviewed the data and drafted the manuscript.

As lead author, or co-author of these four chapters, I was responsible for contributing and conceptualizing study design, data collection and analysis, and drafting and submitting manuscripts. My co-authors provided help with the data analysis, data representation and provided feedback on draft manuscripts.

Abstract

The development of suspension cell lines is a sought after holy grail for bioprocess development. Suspension cell lines allow for easier scale up and better volumetric productivity for most biotherapeutics, including vaccine manufacturing. Various cell lines have readily adapted to suspension growth through the modification of the cell culture medium, but Vero cells have resisted the trend of becoming a suspension cell line. For Vero cells and other cell lines that remain anchorage-dependent, researchers have found methods such as roller bottles and microcarriers to scale up production of biotherapeutics. Although these technologies have enabled the use of anchorage-dependent cell lines for biomanufacturing, the industry prefers suspension cultures and will design new cell lines, or design their processes around existing suspension cell lines to avoid the extra complexity of using anchorage-dependent cell lines.

Medium development has been the main method to adapt cells from adherent culture to suspension. This was first done by reducing the amount of serum that is supplemented in cell culture media. Serum is animal derived and contains many essential nutrients, growth factors, and adhesion proteins that traditional basal mediums do not contain. While serum has been essential for the establishment of many cell lines, it has safety concerns when producing biotherapeutics. Since serums are animal-derived, they can contain viruses, prions, or be contaminated with chemicals that the animal has ingested. Not only do these safety concerns create problems for the biomanufacturing industry, but also the lot-to-lot variability of serums can lead to poor product consistency. To overcome these challenges, the industry has developed animal component-free medium supplements that can contain plant hydrolysates or peptones. These are undefined bioactive fractions of hydrolyzed plant proteins, and while they do not have the same safety concerns as animal derived

materials, they also suffer for lot-to-lot variability since the raw materials can depend on soil conditions, weather patterns, and pesticide use. Nevertheless, industry has overcome these challenges by developing chemically defined media. Every component's concentration in this medium is known and therefore this reduces the lot-to-lot variability. Additionally, many of the compounds that are commonly used in chemically defined medium can be manufactured using animal origin-free materials.

As cell culture media have eliminated serum, cells have become more anchorage-independent and have been slowly adapted to suspension growth. Although this has not been historically true for Vero cells, which have been grown in tight cell aggregates in serum-free medium. More recently, however, Vero cells have been successfully grown as single cell suspensions using two different undisclosed medium formulations that contain undefined plant hydrolysates or peptones. While this was a major achievement, the medium formulations are unknown, and they contain undefined proteins which can possibly suffer lot-to-lot variability. This thesis seeks to develop a chemically defined medium to support suspension Vero cells and to identify the transcriptomic differences between adherent and suspension Vero cells.

This work began by creating a data set of the previously reported medium formulations for Vero, CHO, HEK293, and various other commercial cell lines for adherent and suspension cell culture. Classic basal mediums that require serum supplementation were first compared to serum-free medium formulations to identify compounds that were added to media to replace serum. These compounds included glucose, amino acids, vitamins, trace metals, lipids and fatty acids, along with growth factors and proteins. A second comparison was done within the serum-free medium formulations to compare adherent versus suspension mediums. Suspension media were found to be more enriched that the adherent media and contained higher concentrations of amino acids and fatty acids. This review resulted

in theoretical chemically defined, serum-free medium formulations that could support the growth of adherent and suspension commercial cell lines.

From this data set, a design space was laid out for the creation of a chemically defined medium formulation that supports Vero cell suspension culture. Through this work, recombinant epidermal growth factor was found to be essential for Vero cell proliferation along with the addition of trace metals, lipids, amino acids, and vitamins. Even without any serum, Vero cells continued to adhere to non-tissue culture treated flasks, while it was found that other cell lines (CHO-K1, HEK293T and MDCK) could grow as single cell suspension in the same novel medium. In an effort to coerce the Vero cells to grow in suspension the concentration of calcium and magnesium was reduced 10x. While this did cause the Vero cells to detach and form a single cell suspension, the growth rate dramatically decreased. Nevertheless, this work demonstrated that a chemically defined medium can be developed for Vero cell suspension, although compounds need to be added to ensure that Vero cells continue to grow.

To further investigate the cause of the low growth rate of the suspension Vero cells, RNA-seq was performed to compare the suspension Vero cells to Vero cells grown adherently in the chemically defined medium, and Vero cells grown in DMEM/F12+10% FBS. This data set demonstrated that the suspension Vero cells had down-regulated cell cycle genes, and had begun to express kidney-associated genes. Since Vero cells were originally isolated from a female Green African monkey's kidney, it is hypothesized that the suspension Vero cells were reverting back to kidney cells. Key genes that were found to be differentially expressed by the suspension Vero cells included *tgfb1*, *c-myc*, and genes that are associated with the epithelial-mesenchymal transition.

Finally, different methods for improving the medium formulation were compared in the final chapter. Comparing a literature search, NMR metabolite analysis and RNA-seq

transcriptomics found that the transcriptomic data provided the most insight on the compounds that were beneficial for cell growth. The literature did not have enough specific information about Vero cell metabolism and the compounds that were identified using this method did not result in significant improvements in the medium formulation. NMR was more specific for Vero cells, but because it can only track relatively high concentrations (micromolar) of metabolites, changes in vitamins and growth factors could not be tracked. The metabolite analysis did show a disfunctional tricarboxylic acid cycle, and some compounds that were identified using the analysis did significantly improve the cell's growth rate. Overall, the compounds that were identified using the transcriptomic data had the largest effect on the growth rate. Through RNA-seq analysis, we identified retinyl acetate, progesterone, β-estradiol and prostaglandin E_2 as growth enhancing compounds. Using the compounds identified through RNA-seq, NMR and a literature review, the doubling time of Vero cells was reduced from 38 hours to 32.1 hours, which is better than the animal component-free commercially available media currently on the market today.

Acknowledgements

I am eternally grateful to Marc Aucoin as my PhD supervisor. His style of supervision has taught me much about myself and has been crucial in my development as a person and as a researcher. He offered me the freedom to develop my own project, along with planning my own experiments, data analysis and collaborations with other groups.

I am also indebted to my committee members - Professors Mario Jolicoeur, Maud Gorbet, Evelyn Yim and Roderick Slavcev - for attending my defense, and for providing thoughtful feedback on my work and questions that helped guide my research.

I would also like to thank the support staff at the University of Waterloo, whom have made my PhD journey more enjoyable and I could always count on for some good chats, especially Bert Habicher, Rose Guderian, Judy Caron, Ralph Dickout, Ingrid Sherrer, Rick Hecktus, and Pauline Ferfolja.

Finally I would like to thank my labmates. Specifically Stan, Jann, Sandi, and Mark. I can't thank all of you enough for your mentoring with experiment designs, lab techniques, data analysis, and I think you have all had the largest influence on who I am as a researcher today. I am so happy to know that we have become life long friends.

Dedication

This is dedicated to my parents, my sister and Mark. The year 2020 has been a tumultuous one, but I am glad we still have each other.

Table of Contents

Examining Committee Membership ii

Author's Declaration iii

Statement of Contributions iv

Abstract vi

Acknowledgements x

Dedication xi

List of Tables xvii

List of Figures xxv

List of Abbreviations xxxviii

1 Introduction **1**

1.1 Area for Improvement 2

1.2 Brief History of Vero Cells in Suspension 3

1.3 Hypothesis Statement 5

1.4 Research Objectives 5

1.5 Thesis Outline 6

2 Literature Review **7**

2.1 Media Formulations 8

2.1.1 Basic Needs of the Cell 13

2.1.2 Fatty Acids, Steroids and Phospholipids 14

2.1.3 Amino Acids 19

2.1.4 Metals 33

2.1.5 Vitamins 46

2.1.6 Purines and Pyridines 57

2.1.7 Osmolarity 58

2.2 Summary 60

3 The Development of a Chemically Defined Media for Mammalian Cells in Suspension **61**

3.1 Introduction 61

3.2 Materials and methods 65

3.2.1 Cell culture . . . 65
3.2.2 Media development . . . 66
3.2.3 Data Analysis . . . 67
3.3 Results . . . 69
3.3.1 Medium component screening using Plackett-Burman design of experiments . . . 69
3.3.2 CDM2 medium formulation supports suspension growth of CHO, MDCK, and HEK293T cells and robust adherent growth of Vero cells 87
3.4 Discussion . . . 90
3.5 Conclusion . . . 96

4 Transcriptomics to Identify Differences in Gene Expression Between Adherent and Suspension Vero Cells 97

4.1 Introduction . . . 97
4.2 Materials and Methods . . . 100
4.2.1 RNA-seq Analysis . . . 100
4.2.2 Gene set enrichment analysis . . . 101
4.2.3 Housekeeping gene expression for quality control . . . 102
4.2.4 RNA-seq heatmaps . . . 102
4.2.5 Visualization . . . 103
4.3 Results . . . 104

4.3.1 RNA-seq analysis of Vero cell adaptation to CDM as adherent and suspension culture . . . 104
4.3.2 Changes in Regulation of Proliferation and Apoptosis . . . 107
4.3.3 Up-regulation of Kidney Related Genes . . . 112
4.3.4 Membrane Transporters . . . 116
4.3.5 Up-regulation of Cell Adhesion Genes . . . 120
4.3.6 Up-regulation of Fatty Acid β-Oxidation . . . 120
4.4 Discussion . . . 126
4.5 Conclusions . . . 133

5 Improvement of Chemically Defined Media Using Transcriptomics 135

5.1 Introduction . . . 135
5.2 Materials and Methods . . . 139
5.2.1 Cell Culture and Media Development . . . 139
5.2.2 RNA-seq Analysis . . . 140
5.2.3 NMR Analysis . . . 141
5.2.4 Visualization . . . 142
5.3 Results . . . 143
5.3.1 NMR Metabolite Analysis . . . 143
5.3.2 Using Transcriptomic Data to Identify Up-Regulated Metabolic Pathways . . . 151

5.3.3 Design of Experiments to Test Media Components 156
5.4 Discussion 163
5.5 Conclusions 169

6 Original Contributions and Recommendations 170

6.1 Original Contributions 170
6.1.1 Serum-Free Media Formulations Database 170
6.1.2 Chemically Defined Media Formulation for Suspension Vero Cells . 171
6.1.3 RNA-seq Analysis Comparing Suspension to Adherent Vero Cells . 172
6.1.4 Using RNA-seq Data to Improve Media Formulations 173
6.2 Recommendations and future prospects 174

References 176

Appendices 249

A Media Database Summary 250

B Medium Formulation Tables 254

C RNA-seq Cell Cycle 265

D RNA-seq Differentially Expressed Genes and Pathways 279

E Formulation for CDM4 293

List of Tables

2.1 **Vero Cell Propagation Strategies and Maximum Cell Densities** . . 11

2.1 **Vero Cell Propagation Strategies and Maximum Cell Densities** . . 12

2.2 Percent Composition of Fatty Acids in various lots of FBS determined by gas chromatography measurement. The chain length is written as (a:bn-c), where a is the number of carbon atoms in the chain, b is the number of double bonds and c is the location of the first double bond from the methyl end of the fatty acid. * indicates essential fatty acids that cannot be synthesized in animal cells 16

2.3 Iron Chelators 41

2.4 List of trace metals that are commonly included in chemically defined media. This table also lists their known use in cell functions and associated proteins in mammalian cells. 44

2.4 List of trace metals that are commonly included in chemically defined media. This table also lists their known use in cell functions and associated proteins in mammalian cells. 45

2.5 List of vitamins, their use and associated proteins for mammalian cells. (*indicates lipid soluble vitamin, ** indicates not a true vitamin, but included here because of their importance for growth) 55

2.5 List of vitamins, their use and associated proteins for mammalian cells. (*indicates lipid soluble vitamin, ** indicates not a true vitamin, but included here because of their importance for growth) 56

3.1 An example layout of a 23 factor (A-W) Plackett Burman experiment with 24 runs. 68

3.2 List of significant ($p<0.1$) main effects of the first Plackett-Burman experiment. 73

3.3 List of significant ($p<0.052$) main effects of the third Plackett-Burman experiment. 81

3.4 List of significant ($p<0.05$) main effects of the last Plackett-Burman experiment. 86

4.1 List of differentially expressed genes between adherent and suspension Vero cells grown in CDM2-A and CDM2-S. All information was acquired from UniProt. 123

5.1 The doubling times and conversion ratio of glucose to lactate of Vero cells grown in DMEM/F12 + 10% FBS, CDM2, NutriVero Flex 10, or OptiPRO™ SFM. The doubling time was calculated from the exponential growth phase of the adherent cell culture. $Y_{Lactate/Glucose}$ is the ratio of the lactate concentration that had accumulated since day 0, to the day the media was refreshed (media was refreshed on day 4 for cells grown in NutriVero Flex 10 and CDM2, and on day 7 for cells grown in OptiPRO™ SFM). 146

5.2 The conversion ratios of asparagine, GlutaMax™, or pyruvate to biomass of Vero cells grown in CDM2, NutriVero Flex 10, or OptiPRO™ SFM. $Y_{10^8\ cells/Carbon\ Source}$ is the ratio of the change in the cell concentration divided by the change in the concentration of the compound over the first 4 days of culture. 149

5.3 The formulation differences between CDM2, CDM3 and CDM4. 162

5.4 The doubling times of Vero cells grown in DMEM/F12 + 10% FBS, CDM2, CDM3, CDM4, NutriVero Flex 10, or OptiPRO™ SFM. The doubling time was calculated from the exponential growth phase of the adherent cell culture. 163

A.1 Median concentrations in millimolar for serum-free media formulations that support adherent, suspension, or both types of culture methods. 250

A.1 Median concentrations in millimolar for serum-free media formulations that support adherent, suspension, or both types of culture methods. 251

A.1 Median concentrations in millimolar for serum-free media formulations that support adherent, suspension, or both types of culture methods. 252

A.1 Median concentrations in millimolar for serum-free media formulations that support adherent, suspension, or both types of culture methods. 253

B.1 Formulation for Millipore Sigma's Chemically Defined Lipid Mixture 1. . . 254

B.2 The medium recipe for Formulation 8 from Plackett-Burman Experiment 2 255

B.2 The medium recipe for Formulation 8 from Plackett-Burman Experiment 2 256

B.2 The medium recipe for Formulation 8 from Plackett-Burman Experiment 2 257

B.3 The medium recipe for basal medium from Plackett-Burman Experiment 3 258

B.3 The medium recipe for basal medium from Plackett-Burman Experiment 3 259

B.3 The medium recipe for basal medium from Plackett-Burman Experiment 3 260

B.3 The medium recipe for basal medium from Plackett-Burman Experiment 3 261

B.4 The medium recipe for Formulations 11, 17, 23 from Plackett-Burman Experiment 4 261

B.4 The medium recipe for Formulations 11, 17, 23 from Plackett-Burman Experiment 4 262

B.4 The medium recipe for Formulations 11, 17, 23 from Plackett-Burman Experiment 4 263

B.4 The medium recipe for Formulations 11, 17, 23 from Plackett-Burman Experiment 4 264

C.1 Name and description of genes in the cell cycle that were up or downregulated in suspension (Sus_CDM2) cells compared to cells grown adherently in CDM2 (Adh_CDM2). The descriptions were acquired from Genecards or UniProt. 267

C.1 Name and description of genes in the cell cycle that were up or downregulated in suspension (Sus_CDM2) cells compared to cells grown adherently in CDM2 (Adh_CDM2). The descriptions were acquired from Genecards or UniProt. 268

C.1 Name and description of genes in the cell cycle that were up or downregulated in suspension (Sus_CDM2) cells compared to cells grown adherently in CDM2 (Adh_CDM2). The descriptions were acquired from Genecards or UniProt. 269

C.1 Name and description of genes in the cell cycle that were up or downregulated in suspension (Sus_CDM2) cells compared to cells grown adherently in CDM2 (Adh_CDM2). The descriptions were acquired from Genecards or UniProt. 270

C.1 Name and description of genes in the cell cycle that were up or downregulated in suspension (Sus_CDM2) cells compared to cells grown adherently in CDM2 (Adh_CDM2). The descriptions were acquired from Genecards or UniProt. 271

C.1 Name and description of genes in the cell cycle that were up or downregulated in suspension (Sus_CDM2) cells compared to cells grown adherently in CDM2 (Adh_CDM2). The descriptions were acquired from Genecards or UniProt. 272

C.2 A list of the 25 genes that were identified as upregulated in the HPA kidney tissue gene dataset, along with their associated ligand and description of the protein function according to UniProt. 273

C.2 A list of the 25 genes that were identified as upregulated in the HPA kidney tissue gene dataset, along with their associated ligand and description of the protein function according to UniProt. 274

C.2 A list of the 25 genes that were identified as upregulated in the HPA kidney tissue gene dataset, along with their associated ligand and description of the protein function according to UniProt. 275

C.3 List of transporter genes that are downregulated in suspension Vero cells compared to adherent Vero cells that are grown in CDM2 or in DMEM/F12 + 10% FBS. Descriptions of the genes were taken from Human Protein Atlas and UniProt. 276

C.3 List of transporter genes that are downregulated in suspension Vero cells compared to adherent Vero cells that are grown in CDM2 or in DMEM/F12 + 10% FBS. Descriptions of the genes were taken from Human Protein Atlas and UniProt. 277

C.3 List of transporter genes that are downregulated in suspension Vero cells compared to adherent Vero cells that are grown in CDM2 or in DMEM/F12 + 10% FBS. Descriptions of the genes were taken from Human Protein Atlas and UniProt. 278

D.1 A list of the genes that are up or down-regulated in the KEGG pathways that were identified during the RNA-Seq analysis when comparing suspension to adherent Vero cells grown in CDM2. 279

D.1 A list of the genes that are up or down-regulated in the KEGG pathways that were identified during the RNA-Seq analysis when comparing suspension to adherent Vero cells grown in CDM2. 280

D.1 A list of the genes that are up or down-regulated in the KEGG pathways that were identified during the RNA-Seq analysis when comparing suspension to adherent Vero cells grown in CDM2. 281

D.1 A list of the genes that are up or down-regulated in the KEGG pathways that were identified during the RNA-Seq analysis when comparing suspension to adherent Vero cells grown in CDM2. 282

D.1 A list of the genes that are up or down-regulated in the KEGG pathways that were identified during the RNA-Seq analysis when comparing suspension to adherent Vero cells grown in CDM2. 283

D.1 A list of the genes that are up or down-regulated in the KEGG pathways that were identified during the RNA-Seq analysis when comparing suspension to adherent Vero cells grown in CDM2. 284

D.1 A list of the genes that are up or down-regulated in the KEGG pathways that were identified during the RNA-Seq analysis when comparing suspension to adherent Vero cells grown in CDM2. 285

D.1 A list of the genes that are up or down-regulated in the KEGG pathways that were identified during the RNA-Seq analysis when comparing suspension to adherent Vero cells grown in CDM2. 286

E.1 The medium recipe for CDM4. Use Sigma DMEM/F12 media (cat#D9785-10L) (w/o bicarbonate, phenol red, and glutamine, leucine, lysine, methionine) for suspension media for CHO-K1 or Vero cells, or Corning DMEM/F12 for suspension MDCK and HEK293T, or adherent Vero. 293

E.1 The medium recipe for CDM4. Use Sigma DMEM/F12 media (cat#D9785-10L) (w/o bicarbonate, phenol red, and glutamine, leucine, lysine, methionine) for suspension media for CHO-K1 or Vero cells, or Corning DMEM/F12 for suspension MDCK and HEK293T, or adherent Vero. 294

E.1 The medium recipe for CDM4. Use Sigma DMEM/F12 media (cat#D9785-10L) (w/o bicarbonate, phenol red, and glutamine, leucine, lysine, methionine) for suspension media for CHO-K1 or Vero cells, or Corning DMEM/F12 for suspension MDCK and HEK293T, or adherent Vero. 295

E.1 The medium recipe for CDM4. Use Sigma DMEM/F12 media (cat#D9785-10L) (w/o bicarbonate, phenol red, and glutamine, leucine, lysine, methionine) for suspension media for CHO-K1 or Vero cells, or Corning DMEM/F12 for suspension MDCK and HEK293T, or adherent Vero. 296

E.1 The medium recipe for CDM4. Use Sigma DMEM/F12 media (cat#D9785-10L) (w/o bicarbonate, phenol red, and glutamine, leucine, lysine, methionine) for suspension media for CHO-K1 or Vero cells, or Corning DMEM/F12 for suspension MDCK and HEK293T, or adherent Vero. 297

List of Figures

2.1 Comparison of media formulations on their fatty acid composition. This plot also includes other common additives that are found in lipid supplements such as Pluronic™ F68 (also known as poloxamer 188) and Tween® 80 (also known as polysorbate 80). 18

2.2 Amino Acid concentration for basal media and SFM formulations 20

2.3 Amino acid concentrations for SFM formulations. Media formulations were categorized based on the type of culture they supported (suspension, adherent or both) 21

2.4 Aspartate Synthesis in the cell 26

2.5 Metal concentrations in basal and serum-free mediums 34

2.6 Metal concentrations in serum-free mediums 35

2.7 Vitamin concentrations in basal and serum-free mediums 47

2.8 Vitamin concentrations in serum-free mediums. Teal coloured boxplots are media that support adherent growth, the pink colour represents media that support both adherent and suspension culture methods, and purple represents media that support suspension grwoth. 48

3.1 The results from the first Plackett-Burman media screening experiment. The concentrations for each component at the high (+1) and low (-1) levels are listed in the table and the viable cell density (VCD) is on the y-axis of each of the plots. Vero cells were adapted to the media over 14 days and then grown for another 14 days in the various media. The VCD is from day 28 of the experiment. 72

3.2 The viable cell counts for the second Plackett-Burman experiment. The viable suspension cells were tracked over 75 days. Vero cells were adapted to the media over 14 days and then grown for another 61 days in the various media. A 10x brightfield image of the cells grown in Formulation 8 is displayed in the top right corner to demonstrate the morphology of the cells on day 75. 75

3.3 The results from the second Plackett-Burman media screening experiment. The concentrations for each component at the high (+1) and low (-1) levels are listed in the table and the viable cell density (VCD) for suspension cells is on the y-axis of each of the plots. Vero cells were adapted to the media over 14 days and then grown for another 14 days in the various media. The VCD is from day 28 of the experiment. 76

3.4 10x brightfield images of Vero cells grown in Formulation 8, without OptiPRO™ SFM for 13 days in 3 different conditions after 83 days of culture (Tissue Culture Treated Tflask, Non-treated Tflask with static liquid, and Non-treated Tflask with shaking). 77

3.5 The results from the third Plackett-Burman media screening experiment. The concentrations for each component at the high (+1) and low (-1) levels are listed in the table and the growth rate for adherent cells is on the y-axis of each of the plots. Vero cells were adapted to the media over 14 days and then grown for another 61 days in the various media. The growth rate is from day 75 of the experiment. 80

3.6 A. Brightfield images of Vero cells as they adapt to low-calcium and magnesium media over the course of 120 days. Vero cells grown in DMEM/F12 + 10% FBS is used as a reference for normal morphology, compared to the cells growing in the chemically defined media (top right image). Vero cells were unable to adhere to non-treated Tflasks in the chemically defined media, and with the addition of shaking (40 rpm, bottom right image) single cells and small aggregates were observed. B. The doubling time of Vero cells increased dramatically as they were adapted to the low-calcium and magnesium media over the course of 118 days. The shortest doubling time at the end of the experiment was approximately 20 days (500 hours). C. The growth rate of Vero cells as they adapted to the new medium formulations for PB4 over 118 days. D. A zoomed in image of the growth rate of the medium formulations between days 65 and 120. 84

3.7 The results from the last Plackett-Burman media screening experiment. The concentrations for each component at the high (+1) and low (-1) levels are listed in the table and the growth rate ($hours^{-1}$) for adherent cells is on the y-axis of each of the plots. Vero cells were adapted to the media over 12 days and then grown for another 168 days in the various media. The growth rate data is from day 83 of the experiment. 85

3.8 The chemically defined media that was formulated from the series of Plackett-Burman experiments was modified to include 1 mM Ca^{2+} and 0.7 mM Mg^{2+} (called CDM2-A) to support a higher growth rate in Vero cells. CHO-K1, HEK293T and MDCK cells were slowly adapted to CDM2-A from serum-containing basal media in static Tflasks. All three cell types were able to grow in suspension when they were fully adapted to CDM2-A and were cultured in 125 mL shake flasks. Vero cells remained adherent for all media formulations. 89

4.1 **A.** The growth rate of Vero cells adapted to various medium formulations grown over 105 days with low calcium and magnesium concentrations to encourage single cell suspension. **B.** The viability of the cells from each medium formulation over time as the cells adapted to the new media. Each formulation is represented by a number (1-24) and as indicated by the number on the plot and with a different color. 105

4.2 Analysis of RNA-seq data variance. **A.** A two-dimensional plot of principal component analysis (PCA) for all 13 samples of the 500 most variable genes. Each symbol represents one sample. Group affiliation is shown in the legend on the right side. **B.** Pearson's correlation between all samples for 3122 detected housekeeping genes. Correlation coefficients r values are annotated and colour coded according to the legend on the right side of the figure. Vero cells grown adherently in basal medium (DMEM/F12) supplemented with 10% FBS are labeled 'Cont', 'Adh' is Vero cells grown adherently in CDM2 with the same calcium and magnesium concentrations as DMEM/F12 are and 'Sus' are Vero cells grown in suspension in CDM2. 106

4.3 Enrichment map for significant down-regulated GO-terms in biological processes for the comparison of Sus against Adh (threshold at FDR of 0.05). The size of the node is proportional to the number of identified genes annotated to the GO-term. The thickness of edges represents the level of overlap between the GO-terms. A: DNA templated transcription termination, B: Aerobic respiration, C: Response to increased oxygen levels, D: Protein peptidyl prolyl isomerization, E: Cofactor transport, F: positive regulation of inflammatory response,G: Cellular response to fluid shear stress, H: Regulation of ubiquitin protein ligase activity, I: Establishment of endothelial barrier, J: Hyperosmotic response, K: Regulation of protein oligomerization, L: Excitatory synapse assembly, M: Regulation of calcineurin mediated signaling, N: Modified amino acid transport, O: Cell migration involved in sprouting angiogenesis, P: Low density lipoprotein receptor particle metabolic process, Q: Endosome organization, R: Pyrimidine nucleotide triphosphate biosynthetic process, S: Water soluble vitamin metabolic process, T: Collagen catabolic process, U: Drug metabolic process. NES: Normalized enrichment score. . . 110

4.4 Expression regulation of cell cycle related genes in relation to the interphase cycle using BioRender. Genes that were identified as differentially expressed in the KEGG cell cycle pathway are mapped onto a cell cycle image with their respective proteins. Up-regulated genes between Sus and Adh are highlighted in green and down-regulated genes are in red. G1: Gap phase 1 of the cell cycle, G1/S: Gap 1 to synthesis transition phase, S: synthesis phase, G2: Gap phase 2, G2/M: Gap2 to mitosis transition phase, M: mitosis phase.**B.** Log fold-change for genes linked to anti- or pro-apoptosis according to Gene Ontology. The comparison of the expression levels between Vero cells grown adherently in CDM2 to the control group (DMEM/F12 + 10% FBS) for apoptosis related genes is shown in blue and the comparison of the suspension Vero cells compared to the control group is shown in red. 111

4.5 Kidney related type of suspension cells. HPA tissue related gene set enrichment analysis of Sus_CDM2 samples compared to Adh_CDM2 samples (FDR < 0.05). Tissue profiles were developed with the package TissueEnrich. Only tissue enriched genes were selected for the profiles, and only profiles with size of at least 5 specific genes were considered for the analysis. The proportion of the genes related to that profile and contributing to the enrichment scores are annotated at the side of the bars. The coloring of the bars depicts the FDR values according to the legend on the right side of the figure. 114

4.6 Kidney related type of suspension cells. Mean Difference plot of identified kidney enriched genes with log fold-change and log(CPM) values. Red labels are specifically to identify renal tubules, and the green labels represent the genes that are associated with the whole kidney according to Human Protein Atlas database, respectively. 115

4.7 Heatmaps of differentially expressed membrane transporters (FDR < 0.001). The x-axis shows the samples, and the y-axis represents the HGNC symbols. The colouring of the heatmap represents the standardized, normalized expression log(CPM) values according to the legend at the top left side of each heatmap. **A.** Heatmap of differentially regulated solute carrier. **B.** Heatmap of differentially regulated subunits of V-type proton ATP (ATP6V). **C.** Heatmap of differentially regulated ATP-binding cassette (ABC)-transporters. The name of each gene has colouring overlaid on the text to show if the transporter is associated with the transport of amino acids (red), bicarbonate ions (yellow), small ions (dark green), organic ions (pink) or other (grey). Control is Vero cells grown in DMEM/F12+10% FBS and Adherent is Vero cells grown in CDM2-A. 118

4.8 A scheme of the significantly up-regulated membrane transporters with the target molecules and the direction of transport in a nephron. The transporters whose location are unknown are mentioned in the center of the image. Red colored arrows or gene names indicate an log fold-change > 5. Image created using *BioRender.com*. 119

4.9 Heat map of tight junctions associated claudins (FDR < 0.001). The x-axis shows the samples and the y-axis represents the HGNC symbols. The colouring of the heatmap represents the standardized, normalized expression $\log_2$CPM values according to the legend at the top left side of each heatmap. Control is Vero cells grown in DMEM/F12+10% FBS and Adherent is Vero cells grown in CDM2-A. 121

4.10 Up-regulation of fatty acid beta oxidation related genes (GO:0006635). A heatmap of differentially regulated genes. The x-axis shows the samples and the y-axis represents the HGNC symbols. Colouring of the samples is the same as in Figure 4.11. The colouring of the heatmap represents the standardized, normalized expression $\log_2$CPM values according to the legend at the top left side of each heatmap. 124

4.11 Up-regulation of fatty acid beta oxidation related genes (GO:0006635). Diagram of fatty acid beta oxidation with the main reactions and enzymes in mitochondria. Green arrows label significant up-regulation of at least one gene in that reaction group with an FDR threshold of 0.001. Red arrows emphasize the fatty acid and derivatives flow through the process until Acetyl-CoA. 125

5.1 Vero cells were adapted from DMEM/F12 + 10% FBS into three different serum-free and animal origin-free media (CDM2, OptiPRO™ SFM, and NutriVero Flex 10). The cells were cultured over 10 days without being passaged, but the media was refreshed as indicated by the arrows. Each colour represents a different media formulation that Vero cells were cultured in and one replicate was taken per sample. 145

5.2 Media samples were collected from Vero cells being cultured in either CDM2, NutriVero Flex 10 or OptiPRO™ SFM for 10 days. The metabolites were analyzed using NMR, and specifically compounds that have large changes (glucose, lactate, citric acid and pyruvate) are shown here. 147

5.3 Media samples were collected from Vero cells being cultured in either CDM2, NutriVero Flex 10 or OptiPRO™ SFM for 10 days. The metabolites were analyzed, and amino acids that can be profiled by NMR are shown here. . 148

5.4 The expression of genes associated with fatty acid degradation in suspension compared to adherent Vero cells grown in CDM2-S media. Genes that are differentially expressed are highlighted in green (down-regulated) and red (up-regulated) to demonstrate the changes in suspension cells compared to adherent cells using the Pathview package. 153

5.5 The expression of genes associated with retinol metabolism in suspension compared to adherent Vero cells grown in CDM2-S media. Genes that are differentially expressed are highlighted in green (down-regulated) and red (up-regulated) to demonstrate the changes in suspension cells compared to adherent cells using the Pathview package. 154

5.6 The expression of genes associated with steroid hormone biosynthesis in suspension compared to adherent Vero cells grown in CDM2-S media. Genes that are differentially expressed are highlighted in green (down-regulated) and red (up-regulated) to demonstrate the changes in suspension cells compared to adherent cells using the Pathview package. 155

5.7 A map of the TCA cycle, the urea cycle and the malate-aspartate shuttle. The compounds that were identified by NMR as depleted in the extracellular space are outlined in red, and the compounds that accumulated are outlined in green. The TCA cycle has arrows marked in dark blue to show the pathway, the urea cycle is dark yellow and the malate-aspartate shuttle is in dark green. The names of the dehydrogenase enzymes are marked in teal. 156

5.8 The results from the first Plackett-Burman media screening experiment using components identified through RNA-seq, NMR and a literature search. The concentrations for each component at the high (+1) and low (-1) levels are listed in the table and the growth rate for adherent Vero cells was calculated while the cells were 100% in the new media formulation for 3 passages. Each formulation was numbered 1 through 8 and is represented by a different colour in the plot. 159

5.9 The results from the second Plackett-Burman media screening experiment using components identified through RNA-seq, NMR and a literature search. The concentrations for each component at the high (+1) and low (-1) levels are listed in the table and the growth rate for adherent Vero cells was calculated while the cells were 100% in the new media formulation for 2 passages. Each formulation was numbered 1 through 8 and is represented by a different colour in the plot. 160

5.10 The results from the last Plackett-Burman media screening experiment using components identified through RNA-seq, NMR and a literature search. The concentrations for each component at the high (+1) and low (-1) levels are listed in the table and the growth rate for adherent Vero cells was calculated while the cells were 100% in the new media formulation for 3 passages. Each formulation was numbered 1 through 8 and is represented by a different colour in the plot. 161

C.1 Expression regulation of cell cycle related genes. **A.** KEGG cell cycle showing differentially regulated genes for the comparison of Sus_CDM2 against Adh_CDM2 rendered with Pathview. The color code determines the direction of significantly differentially regulated genes (FDR < 0.001)according to the legend at the top of the figure. A white background of a text box means that the gene was not identified as expressed. **B.** LFC for the top 500 cell cycle related genes from Cyclebase 3.0 grouped to their peak expression phase. Non-periodic: no known expressional changes during the cell cycle, G1: Gap phase 1 of the cell cycle, G1/S: Gap 1 to synthesis transition phase, S: synthesis phase, G2: Gap phase 2, G2/M: Gap2 to mitosis transition phase, M: mitosis phase. **C.** LFC for genes linked to positive or negative regulation of apoptosis according to Gene Ontology. 266

D.1 The expression of genes associated with phospholipase D signalling pathway in suspension compared to adherent Vero cells grown in CDM2 media. Genes that are differentially expressed are highlighted in green (downregulated) and red (upregulated) to demonstrate the changes in suspension cells compared to adherent cells using the Pathview package. 287

D.2 The expression of genes associated with tryptophan metabolism pathway in suspension compared to adherent Vero cells grown in CDM2 media. Genes that are differentially expressed are highlighted in green (downregulated) and red (upregulated) to demonstrate the changes in suspension cells compared to adherent cells using the Pathview package. 288

D.3 The expression of genes associated with cell adhesion molecule signalling pathway in suspension compared to adherent Vero cells grown in CDM2 media. Genes that are differentially expressed are highlighted in green (downregulated) and red (upregulated) to demonstrate the changes in suspension cells compared to adherent cells using the Pathview package. 289

D.4 The expression of genes associated with cytokine-cytokine receptor interaction signalling pathway in suspension compared to adherent Vero cells grown in CDM2 media. Genes that are differentially expressed are highlighted in green (downregulated) and red (upregulated) to demonstrate the changes in suspension cells compared to adherent cells using the Pathview package. . . 290

D.5 Mean difference plot of identified pro-mesenchymal (blue) or anti-mesenchymal (red) genes with log fold-change between Sus and Adh (adherent Vero cells grown in CDM2) groups (y-axis), or Sus and Con (adherent Vero cells grown in DMEM/F12 + 10% FBS) (x-axis). Gene targets associated with EMT were identified in Byers *et al.* [60] 291

D.6 Mean difference plot of identified pro-mesenchymal (blue) or anti-mesenchymal (red) genes with log fold-change between Sus and Adh (adherent Vero cells grown in CDM2) groups (y-axis), or Sus and Con (adherent Vero cells grown in DMEM/F12 + 10% FBS) (x-axis). Gene targets associated with EMT were identified in Kalluri *et al.* [208] 292

List of Abbreviations

AdoCbl adenosylcobalamin 53

AHB α-hydroxybutyrate 25

AKB α-ketobutyrate 25

AMP adenosine monophosphate 23

ATA aurintricarboxylic acid 40

ATP adenosine triphosphate 25

BCAA branched chain amino acids 28

BHK Baby Hamster Kidney 3, 5

CDM2-A Chemically Defined Medium 2 Adherent 87

CDM2-S Chemically Defined Medium 2 Suspension 87

cGMP cyclic guanosine monophosphate 52

CoA coenzyme A 28, 51

DHA dehydroascorbic acid 49

DNA deoxyribonucleic acid 30

EDTA ethylenediaminetetraacetic acid 33

EGFR epidermal growth factor receptor 42

EMA European Medicines Agency 7

ER endoplasmic reticulum 37, 51

ETC electron transport chain 24

FAD flavin adenine dinucleotide 51, 56

FBS Fetal Bovine Serum 5

FDA Food and Drug Administration of the U.S.A 7

FMN flavin mononucleotide 51, 56

GTP Guanosine triphosphate 57

IMP inosine 5'-monophosphate 23

LC liquid chromatography 135

mAb monoclonal antibody 31

MAPK mitogen-activated protein kinase 42

MDCK Madin Darby Canine Kidney 4, 5

MeCbl methylcobalamin 53

MS mass spectrometry 135

mTORC1 mammalian target of rapamycin complex 1 24

NADH nicotinamide adenine dinucleotide (reduced form) 25

NADPH nicotinamide adenine dinucleotide phosphate (reduced form) 27

NMR nuclear magnetic resonanace 135

NO nitric oxide 22

ODC ornithine decarboxylase 22

PLP pyridoxal-5'-phosphatase 52, 55

PMCA plasma membrane Ca^{2+} ATPases 37

RNA ribonucleic acid 30

ROS reactive oxygen species 49

SAM S-adenosylmethionine 29, 32, 93

SCM serum-containing media 136

SERCA sarcoendoplasmic reticular Ca^{2+} ATPases 37

SOD superoxide dismutase 38

TCA tricarboxylic acid cycle 39

TEPA Tetraethylenepentamine 39

THF tetrahydrofolate 53

TPO thrombopoietin 59

TPP thiamine pyrophosphate 51, 56

Chapter 1

Introduction

Vero cells were first established in 1962 by Y. Yasumura and Y. Kawakita from the kidney of a female African green monkey [432, 355] and are considered a non-transformed continuous cell line. They have been used to manufacture human vaccines for over 30 years, making them one of the most widely accepted continuous cell lines by regulatory authorities in over 60 countries [30, 328]. Over the years, the cell line has been extensively characterized; shown to be free of adventitious agents and have low tumorgenicity at passage numbers below 191 [432]. More recently, through genome work on the Vero cell line, many full length viral genomes have been uncovered [355]. Nonetheless, these cells are used to make vaccines and vaccine candidates against polio (Imovax® Polio) [327, 475, 178], rabies (Imovax® Rabies)[327, 479], rotavirus [204, 502], Japanese encephalitis (Ixiaro®) [271, 121], dengue fever [250, 357], West Nile encephalitis [264], Chikungunya fever [166, 384, 478], Ross River fever [512], SARS [390], smallpox [30], and influenza (Perflucel®, Celvapan®) [115, 147, 310, 364]. Researchers found a large deletion on chromosome 12, explaining the inability of Vero cells to produce type 1 interferon, which may

be a reason why they are susceptible to infection by a plethora of different viruses [355]. Newer suspension cell lines such as Madin-Darby canine kidney (MDCK) cells [144] and PER.C6 have been used as alternatives to Vero cells, but face regulatory hurdles by not having the same long history as the Vero cells. One of the major drawbacks of using Vero cells for virus production is their anchorage dependence. Common methods of scaling up anchorage dependent cells is to grow them in roller bottles, cell stacks or on microcarriers. Microcarriers can be used in suspension making them more attractive as they can be scaled up using bioreactors, but they are often very costly and add extra obstacles to manufacturing. In 1992, Litwin demonstrated that Vero cells could be grown as aggregates in serum-free media [269]. More recently, two groups have achieved Vero cells in single cell suspension using animal component-free media [412, 433]. Growing Vero cells in single cell suspension greatly improves the ease of scaling up vaccine production, although Vero cells have a higher doubling time as single cell suspension (40-44 hours) compared to adherent cells (31-43 hours) [433, 414].

1.1 Area for Improvement

Given the wide array of viruses that can be replicated in Vero cells and the pressure on industry to reduce costs, and increase speed [115], the optimization of the Vero cells in terms of cell density and virus yields are the next major challenges associated with producing human vaccines. The major limitation associated with Vero cells is their anchorage dependence, requiring a burdensome propagation strategy and large working volumes compared to suspension cells such as Chinese hamster ovary cells (CHO) or MDCK. The development of a robust method for adapting Vero cells for growth in suspension and at high densities would greatly ease the scale up process for vaccine production and minimize

the risk of contamination when working with microcarriers [144].

1.2 Brief History of Vero Cells in Suspension

Methods to culture anchorage dependent cells at large scale include propagation on microcarriers, roller bottles or stacks of tissue culture plates. Microcarriers have the benefit of allowing for easy media exchanges during bioreactor cultivation because they can be filtered out of solution or can be allowed to settle to the bottom of the reactor, allowing the medium to be removed without removing the microcarriers or cells. The use of cell factories/stacks, or roller bottles are also a common method of propagating Vero cells for vaccine production, but these require large amounts of space and material, which are not easily scaled up. Even with the use of microcarriers in perfusion reactors or with medium recirculation, the Vero cell density is no greater than 5-6x10^6 cells/mL [475, 316] which is a relatively low density compared to what can be achieved theoretically from closely packed, tissue-like geometries (10^9 cells/mL) [359]. A review of various propagation strategies for Vero cells, along with their maximum cell density can be seen in Table 2.1. Given no limitations in nutrients or growth inhibiting products, the maximum cell density depends on the concentration of oxygen in the media. The theoretical maximum cell density, using todays conventional bioreactors, is approximately 10^8 cells/mL which has been reported for suspension CHO cells [473]. It is possible that a higher cell density can be achieved by increasing the available surface area on microcarriers, but this requires the use of a solid support matrix for the proliferation of Vero cells. A suspension Vero (sVero) cell line would allow for higher cell densities using less space and volume than conventional methods, and ease scale up during production.

Manufacturers have turned to alternatives to Vero cells such as suspension PER.C6, Baby

Hamster Kidney (BHK) or Madin Darby Canine Kidney (MDCK) cell lines, but these cells face regulatory hurdles by not having the same extended safe history as the Vero cells and may not produce the virus of interest as efficiently as Vero cells. Therefore, a renewed interest in developing suspension Vero cells has occurred in the past 10 years. Attempts to culture Vero cells in suspension were first made using small dextran microspheres (diameter = 32 μm) which cells could adhere to, but could not elongate on, to obtain cell aggregates in suspension [153]. Later, J. Litwin demonstrated that Vero cells could be grown as cell aggregates without microspheres in serum-free media reaching densities of 1-3x10^6 cell/mL [269]. Unfortunately, it proved difficult to control the aggregate size causing mass transport problems within the aggregate, which led to necrosis at the center of the aggregate. In 2007, Paillet *et al*, published findings of a Vero cell line that could grow in single cell suspension, reaching cell densities of up to 2.5x10^6 cells/mL using in-house serum free media (SMIF-6), in batch and perfusion reactors [363]. As the composition of the media was not described in the paper, and there was limited characterization of the sVero cell line, the cell line was not used further in the literature [364, 363, 90, 476]. Even though work with this particular cell line appeared to die out for a moment, researchers did not stop trying. In fact, in 2019 two papers from separate groups were published with Vero cells in suspension. One paper from the National Research Council in Canada [433], and another paper from Tunisia [412]. These groups used different media (both in-house media), but the same method of adapting cells to serum-free media, and then shaking them at 90-120 rpm in 125 mL shaker flask for a considerable amount of time (>8 passages)at 37°C in a 5% CO_2 incubator. Both groups were able to successfully amplify virus, and Shen *et al.*, also confirmed that the cells were non-tumorigenic [433]. Although the ability for two separate groups to produce single-cell suspension Vero cells is very exciting, the media formulations and methods are not fully disclosed, which limits other academic labs from

replicating their results, but provides opportunities for commercialization.

1.3 Hypothesis Statement

Vero cells, along with other cell lines such as MDCK and BHK, were once believed to be anchorage dependent, but with the advancement in media technology these cells lines have been successfully adapted to suspension growth. However, many media formulations that were developed contain undefined protein mixtures and none of the commercially available media formulations support the adaptation of Vero cells to suspension. The driving hypothesis of this work is that through the use of designed experiments, a defined, animal-component free media can be developed specifically to adapt Vero cells to suspension. This media formulation is not solely limited to Vero cells, but can be used to grow other industrially relevant cell lines in suspension.

1.4 Research Objectives

The primary objectives of this research can be described as follows:

1. Use design of experiments to create a defined, animal-component free media formulation for suspension Vero cells. This objective includes the screening of various different media components using seven Plackett-Burman styled design of experiments and slowly adapting cells to the new media formulations over 30-180 days.

2. Compare the growth kinetics of Vero cells in the newly developed medium and basal media supplemented with Fetal Bovine Serum (FBS) and commercial animal-component free media. This objective is accomplished by modifying the media to

support adherent growth of Vero cells and other mammalian cell lines (CHO-K1, HEK293T and MDCK) used in the production of biopharmaceuticals.

3. Analyze the differences between adherent and suspension Vero cells by using transcriptomic data acquired through RNA-seq. This objective includes evaluating over or under expressed genes in pathways of interest that are associated with the suspension phenotype.

4. Use the transcriptomic data to identify upregulated signaling and metabolic pathways in the cell to create a better designed Plackett-Burman experiment to encourage Vero cell growth.

1.5 Thesis Outline

This thesis is comprised of a literature review presented in Chapter 2 to inform the readers on what media formulations have been developed for serum-free adherent and suspension cultures and the general differences between the formulations. The review also briefly describes the biological relevance of each compound that is added to medium. From the information that was gathered through the literature search, sets of experiments are described in Chapter 3 which attempts to create a medium formulation for suspension growth of Vero cells. RNA-seq was conducted to identify key differences between adherent and suspension Vero cells in Chapter 4. The last chapter (Chapter 5) uses the transcriptomic data to make specific modifications to the cell culture media to increase the growth rate of adherent Vero cells. This final formulation is compared to various commercially available media for Vero cells.

Chapter 2

Literature Review

Suspension cell lines have gained widespread acceptance in vaccine manufacturing as a platform that can increase production efficiency and yield while maintaining the stringent safety standards of regulatory agencies such as the Food and Drug Administration of the U.S.A (FDA) and the European Medicines Agency (EMA). Many cell lines have been adapted to grow in suspension through manipulation of the cell culture medium. Commercial media have been used to successfully grow a variety of cell lines in suspension, but have so far failed to support long term growth of Vero cells in suspension, despite numerous attempts. To address this gap, this review will scrutinize the suspension and adherent media formulations that are currently available in an effort to identify commonalities between the formulations. We first compared basal media formulations formulated in preceding decades to serum-free media (SFM) formulations developed more recently to identify compounds that are used to replace serum. Then, SFM formulations were analyzed based on the type of growth they support; adherent, suspension, or both.

2.1 Media Formulations

The ability of researchers to grow and study cells in tissue culture dishes has been supported by the development of many specialized media. When cell culture media were first being developed in the 1960s, they contained undefined supplements such as serum and extracts from biological sources that were comprised of essential nutrients for propagation of many different cell lines. As research progressed, scientists tried to replace these undefined supplements with defined concentrations of trace metals, vitamins, proteins and lipids to avoid batch-to-batch variability and possible contaminants (viruses, prions, toxins), and to improve our understanding of cell metabolism. Recent advancements in media development have been protected as trade secrets or under patents and our understanding of cell culture media has stagnated since the development of first basal media. Specifically, serum-free and animal component-free media have gained increased attention as biopharmaceutical companies and regulatory agencies, such as the FDA and the EMA, applied more stringent safety measures on production of biopharmaceuticals. The potential presence of adventitious agents in serum and animal derived supplements has fueled research into SFM and replacement supplements such as yeast extracts and plant hydrolysates. SFM refers to media formulations that do not contain animal serums, while animal component-free media do not contain any material derived from an animal source. Further media development has led to chemically defined media, which do not contain any supplements of unknown composition such as serum, extracts or hydrolysates. Plant extracts and hydrolysates are still considered undefined and provide the nutrients needed by the cells for robust growth and protein production, but like serum, suffer from batch-to-batch variability. The Gold Standard for a medium formulation would be a protein and animal-component free chemically-defined media so there would be limited batch-to-batch

variability, a reduced risk of adventitious agents in the final media formulation, and less complicated downstream processing. Chemically defined and completely protein-free media have been developed for CHO cells (PowerCHO Advance by Westburg or CD CHO by Gibco) and hybridoma cells (PFHM II by ThermoFisher). PowerCHO contains peptides (<10 kDa) and small amounts of a recombinant hormone, while CD CHO does not contain any proteins or peptides. All of these formulations are proprietary and therefore researchers have little understanding of the environment their cells are being cultured in. This creates a problem for researchers that are trying to improve protein production, since the media is essentially a black box of unknown variables that affect cell growth and productivity. A review conducted by Rodrigues *et al.*, tested 7 different commercial SFM on monoclonal antibody production in CHO cells showed that there were large variations in cell viability, max cell density, and protein production [403]. However, because the media formulations are unknown, little could be said about what led to the differences in cell viability, cell density and productivity of the cells.

For Vero cells, most of the work for suspension culture was achieved using microcarriers and serum-containing media, although more recently Vero cells were grown as single cell suspension using in-house media. Table 2.1 summarises the media formulations, suspension growth conditions and maximum cell densities that were achieved for Vero cells. Leibovitz-15 (L-15) is the most common media, which was first created in 1977 and was originally designed for diagnostic virology [253]. This medium replaced glucose with D(+) galactose, sodium pyruvate and DL α-alanine to reduce the pH drop that is normally seen with glucose as the sole carbon source. It also replaces bicarbonate with L-arginine (free base) to prevent the increase of pH at atmospheric conditions. Lastly, L-15 has higher amounts of each essential amino acid (histidine, valine, leucine, isoleucine, tryptophan, phenylalanine, threonine, methionine) to prevent their exhaustion during virus production. Although L-

15 is a useful media for virus production, it needs to be supplemented to make up for the lack of trace metals, fatty acids, vitamins, purines, and polyamines that would normally be supplemented through serum addition.

Another basal media that is commonly used used is Minimum Essential Medium (MEM), which was developed by Eagle in 1959. It contains 28 essential metabolites and is supplemented with 5-10% animal serum [114, 113]. This media is thought to contain the minimum amount of nutrients needed to culture a variety of cell types (Walker carcinosarcoma cells, rabbit fibroblasts, rabbit embryonic limb-bud cells, primary monkey kidney cells, L cells, 388 cells, mouse embryonic cells, and HeLa cells). This medium formulation was later improved upon by Dulbecco and Freeman to create a more enriched medium called Dulbecco's Modified Eagle Medium (DMEM) [109]. Dulbecco increased the concentration of many amino acids (L-cystine, L-glutamine, L-isoleucine, L-leucine, L-lysine, L-methionine, L-phenylalanine, L-threonine, L-tryptophan, L-tyrosine, and L-valine), all of the vitamins, and added glycine, L-serine and ferric nitrate to the formulation. DMEM is often mixed with Ham's F-12 Nutrient Mixture (F12). F12 contains many of the nutrients that DMEM lacks, and contains lower concentrations of the amino acids [168]. In addition to the amino acids that are already present in DMEM, F12 also contains L-alanine, L-asparagine, L-aspartic acid, L-cysteine, L-glutamic acid, L-proline, additional vitamins (D-biotin, and Vitamin B_{12}), metals (cupric sulfate, ferric sulfate, and zinc sulfate), and other compounds (hypoxanthine, linoleic acid, lipoic acid, putrescine, sodium pyruvate and thymidine). DMEM and F12 are often combined in a 50:50 mixture to create a nutrient rich medium for cells to grow in with the addition of serum, since this basal media does not contain any growth factors. This basal medium is recommended as a good starting point when developing a novel medium [486].

Table 2.1: **Vero Cell Propagation Strategies and Maximum Cell Densities**

	Media	Suspension Method	Cell Density	Ref
Batch	IHM03	Single Cell Suspension	2.2x10^6 cells/mL	[433]
	IPT-AFM with 20% Ca^{2+} and Mg^{2+}	Single Cell Suspension	2.9x10^6 cells/mL	[412]
	DMEM+5% FBS	100-360 μm aggregates	2x10^6 cells/mL	[153, 378]
	HyQ SFM4Mega Vir	Cytodex 1 (6 g/L)	4.5x10^5 cells/mL	[69]
	OptiPro SFM	Cytodex 1 (6 g/L)	1.2x10^6 cells/mL	[69]
	VP-SFM	Cytodex 1 (6 g/L)	1.2x10^6 cells/mL	[69]
	Provero-1 SFM	Cytodex 1 (6 g/L)	1.2x10^6 cells/mL	[69]
	EX-CELL Vero SFM	Cytodex 1 (6 g/L)	2.6x10^6 cells/mL	[69, 233]
	SFM	Cell aggregates	1-3x10^6 cells/mL	[269]
	VP-SFM+ 4mM Glutamax	Cytodex 1 (3 g/L)	1.77x10^6 cells/mL	[297]
	M-VSFM	Cytodex 1 (2 g/L)	1.0x10^6 cells/mL	[57]
	SMIF-6	Single cell suspension	2.5x10^6 cells/mL	[363]
	VP-SFM + 1% FCS	Cytodex 3 (2.7 g/L)	3.3x10^6 cells/mL	[131]
	L15+5% FCS	Cytodex 3 (2.7 g/L)	1x10^6 cells/mL	[131]
	L15+0.9g/L D-galactose+0.3g/L L-glutamine+5%FBS	Cytodex 1 (2 g/L)	1.76x10^6 cells/mL	[314]
	L15+5% FCS+2mM L-Gln	Cytodex 1 (10 g/L)	1.4x10^6 cell/mL	[316]
	L15+5% FCS+2mM L-Gln	Cytodex 1 (10 g/L)	2.7x10^6 cell/mL	[315]
	M199+10% FBS	Cytodex (5 g/L)	1.9x10^6 cells/mL	[514]
	VP-SFM with 10mM glucose and 2 mM glutamine feeding	Cytodex 1 (3 g/L)	1.0x10^6 cells/mL	[475]
	MEM+10% FCS+0.2 mM serine +0.2 mM methionine	Cytodex 1 (3 g/L)	2.2x10^6 cells/mL	[479]
Fed-Batch	L15+5% FCS+2mM L-Gln 1/3 vol/day	Cytodex (10 g/L)	4.0x10^6 cells/mL	[316]
	L15+5% FCS+2mM L-Gln 1/2 vol/day	Cytodex 1 (2 g/L)	2.5x10^5 cells/mL	[315]
	VP-SFM with 20mM glucose and 2 mM glutamine feeding 1/3 vol/day	Cytodex 1 (3 g/L)	1.8^6 cells/mL	[475]
Perfusion	IHM03 1 vol/day	Single Cell Suspension	6.8x10^6 cells/mL	[433]
	Modified L15 (galactose replaced with 10mM fructose)	Cytodex 1	3x10^7 cells/mL	[339]

Continued on next page

Table 2.1: **Vero Cell Propagation Strategies and Maximum Cell Densities**

	Media	Suspension Method	Cell Density	Ref
	4mM L-glutamine and 5% FBS) Fed with 50% diluted L15 with PBS at 8 vol/day			
	VP-SFM, recirculation of media 5 vol/day up to 10 vol/day	Cytodex 1 (3 g/L)	$5x10^6$ cells/mL	[475]
	SMIF-6	Single cell suspension	$1.9x10^7$ cells/mL	[363]
Perfusion	L15+5% FCS+2mM L-Gln 1.5 vol/day	Cytodex 1 (10 g/L)	$6x10^6$ cells/mL	[316]
	L15+5% FCS+2mM L-Gln 1 vol/day	Cytodex 1 (2 g/L)	$2.5x10^6$ cells/mL	[315]
	VP-SFM 3 vol/day	Cytodex 1 (2 g/L)	$2.6x10^6$ cells/mL	[414]
	MDSS2 0.91 vol/day	Superbead (6.25 g/L)	$3x10^6$ cells/mL	[321]
	EGB2 no dilution data given	Biosilon (30 g/L)	$3x10^6$ cells/mL	[539]
	MEM+10% FCS+0.2 mM serine +0.2 mM methionine 0.5 vol/day	Cytodex 1 (3 g/L)	$4.73x10^6$ cells/mL	[479]
	L15+10% FBS	Cytopore (0.5 g/L)	$2.1x10^6$ cells/mL	[528]
	L15+10% FBS	Cytodex 1 (2 g/L)	$2.2x10^6$ cells/mL	[528]
	L15+10% FBS	Cultispher G (1.7 g/L)	$1.8x10^6$ cells/mL	[528]

The goal of this review is to collect media formulations for mammalian cell lines over the past 60 years to show trends and improvements that have been made from basal, serum-containing media to serum-free and suspension media. Over 35 media formulations were catalogued from literature and patents from over the past 60 years [56, 79, 80, 109, 112, 113, 120, 128, 158, 157, 162, 168, 189, 198, 230, 253, 295, 294, 309, 330, 332, 334, 366, 367, 368, 387, 386, 396, 427, 1, 3, 435, 499, 506]. The components in media formulations have been categorized into 4 major sections of this chapter: lipids and fatty acids, amino acids, trace metals, and vitamins, with smaller sections on purines and pyrimidines, osmolarity and reducing agents. Within each section, we compare the basal media formulations to serum-free formulations to show changes in component concentrations that can be used to replace serum. We then look further into SFM and discern whether the component concentrations

support adherent or suspension growth. This review should give the reader a framework of a basic media formulation that can support serum-free growth of most mammalian cell lines, which researchers can then optimize for robust cell growth or productivity for their specific cell line.

2.1.1 Basic Needs of the Cell

It is instrumental to understand how the nutrients support cell growth and how the cell uses these nutrients. A cell culture medium surrounds the cells with the correct environment that helps stimulate proliferation and protein production. As a starting point for any medium development, the basic culture conditions for mammalian cells need to be met such as correct pH, buffers to help maintain the pH, temperature, and an adequate carbon source. Mammalian cell culture is typically done at 37°C in a humidified incubator. Incubators can be equipped with a CO_2 injector, which helps maintain pH around 7.4 when coupled with a bicarbonate buffered medium. Depending on the concentration of bicarbonate in the medium, CO_2 levels are maintained from 5-10%. Bicarbonate and CO_2 work in conjunction to maintain the proper pH using the equilibrium reaction listed below:

$$CO_2 + H_2O \rightleftharpoons H_2CO_3 \rightleftharpoons HCO_3^- + H^+$$

When larger amounts of bicarbonate (HCO_3^-) are added to media, the above equation shifts to the left and increases the pH (becomes more basic). For media containing 1.2-2.2 g/L of sodium bicarbonate, CO_2 levels should be kept at 5% and for 3.7 g/L of sodium bicarbonate, incubators should be set to 10% CO_2 [24]. There is no difference between the average concentration of sodium bicarbonate in classical media and SFM (1.8 g/L sodium

bicarbonate). Other types of biological buffers that are commonly used are listed by N. Good, *et al.* (including HEPES,MES, and TES) [156]. In addition to the optimum pH and temperature, cells require a carbon source. The carbon source is usually supplied by glucose, but cells can also use galactose, which is the main carbon source in Leibovitz L-15 medium [253]. Classic media formulations on average contain approximately 17 mM of glucose, while SFM formulations have approximately 22-25 mM (see Appendix A for median values for various categories of media).

2.1.2 Fatty Acids, Steroids and Phospholipids

Fatty acids are long carbon chains (containing 4 to 28 carbon atoms) that have a carboxylic acid group at one end and a methyl group at the other end. The chains can contain carbon-carbon double bonds (unsaturated fatty acids) or no double bonds (saturated fatty acids) and their structure strongly influences how they will be used by the cell. Mammalian cells do not have the ability to synthesize fatty acids that have a double bond between the 3^{rd} and 4^{th} carbon atoms from the terminal methyl group (called n-3 fatty acids or n-6 type fatty acids). Therefore, these fatty acids have to be supplied in the media, usually in the form of linoleic or linolenic acid. Linoleic and linolenic acid are important building blocks for other fatty acids and are precursors for prostaglandins, prostacyclins, thromboxanes, phospholipids, glycolipids and vitamins [15, 58, 449]. In general, fatty acids are used by the cell for five main functions; building phospholipids or glycolipids, hydrophobic linkages to target proteins to membranes, to store energy as triglycerides, to make hormones, or to make cell signaling molecules [37]. For the production of phospholipids and glycolipids, cells combine two non-polar fatty acids with a polar head group (serine, ethanolamine, inositol, choline, sphingosine and glycerol). The inner side of the plasma membrane (the

part facing the cytosol) has a higher abundance of specific phospholipids such as phosphatidylethanolamine and phosphatidylserine, while the outer side is mainly made up of sphingomyelin, phosphatidylcholine and glycosphingolipids [521] There are hundreds of possible different kinds of phospholipids because of the variability in the carbon chain length and location of carbon double bonds in the fatty acids, as well as the different head groups. The composition of the membrane can vary depending on components available in the medium and environmental factors such as temperature [13, 450, 456]. For example, cells can alter the permeability and fluidity of their membrane by incorporating cholesterol into the lipid bilayer in response to changes in its environment [195]. Cholesterol is classified as a steroid, but it makes up a large portion of the plasma membrane (30-40% in some mammalian cells [298]) and is a precursor to make steroid hormones (testosterone, progesterone, estradiol, cortisol) and Vitamin D in the cell [323]. Most basal media are supplemented with FBS and do not contain linoleic acid or linolenic acid (with the exception of DMEM/F12 and William's E media). Typical ranges of fatty acid composition in FBS are listed in Table 2.2, along with total cholesterol, phospholipid, free fatty acid content and total lipids. The most abundant fatty acids include palmitic, stearic, oleic, linoleic and arachidonic acids. In the presence of free iron or copper, peroxyl radicals can be generated via Fenton chemistry, which initiates peroxidation of the fatty acids [141]. If fatty acids begin to oxidize, it can create a chain reaction that can lead to destabilization of the cell membrane and cell death [283]. In serum-containing media, proteins such as transferrin and albumin protect and transport fatty acids to the cells [345]. In protein-free media formulations anti-oxidants such as α-tocopherol (Vitamin E) [283], lipoic acid, urate [164], cyclodextrins, liposomes and micelles are used to stabilize unsaturated fatty acids long term in culture media [94, 126, 396, 503].

Table 2.2: Percent Composition of Fatty Acids in various lots of FBS determined by gas chromatography measurement. The chain length is written as (a:bn-c), where a is the number of carbon atoms in the chain, b is the number of double bonds and c is the location of the first double bond from the methyl end of the fatty acid. * indicates essential fatty acids that cannot be synthesized in animal cells

Chain Length	Common Name	% Composition [160, 456]
14:00	Myristic acid	0-0.8
16:00	Palmitic acid	20.1-23
18:00	Stearic acid	12.6-18.8
16:1n-7	Palmitoleic acid	0-1.3
18:1n-9	Oleic acid	15.3-28.1
18:1n-7	Vaccenic acid	0-2
18:2n-6	*Linoleic acid	6.2-7.6
18:3n-6	γ-Linolenic acid	0.3
20:3n-6	Dihomo-γ-linolenic acid	0-3.4
20:4n-6	Arachidonic acid	9.9-10.4
18:3n-3	*α-Linolenic acid	0
20:5n-3	Eicosapentaenoic acid	0-0.3
22:6n-3	Docosahexaenoic acid	4-4.1
	Total Cholesterol (mg/ 100mL) [45]	45
	Phospholipids (mg/100mL) [45]	35
	Free Fatty Acids (mEq/L) [45]	0.21
	Total Lipids (mg/100mL) [45]	310

Figure 2.1 shows the range of fatty acids concentrations used in SFM (SFM) based on the type of growth (adherent, suspension or both types). Both adherent and suspension media contain linoleic and linolenic acids, although suspension media contain higher concentrations of these fatty acids along with many other types of fatty acids. Butler *et al.*, reported that higher amounts of linoleic acid improved cell growth and viability with increasing agitation speeds for murine hybridoma cells [58]. There appears to be limited attention paid to optimizing the concentration of fatty acids in cell culture media, and this could prove to be an area that can be improved upon in future media formulations.

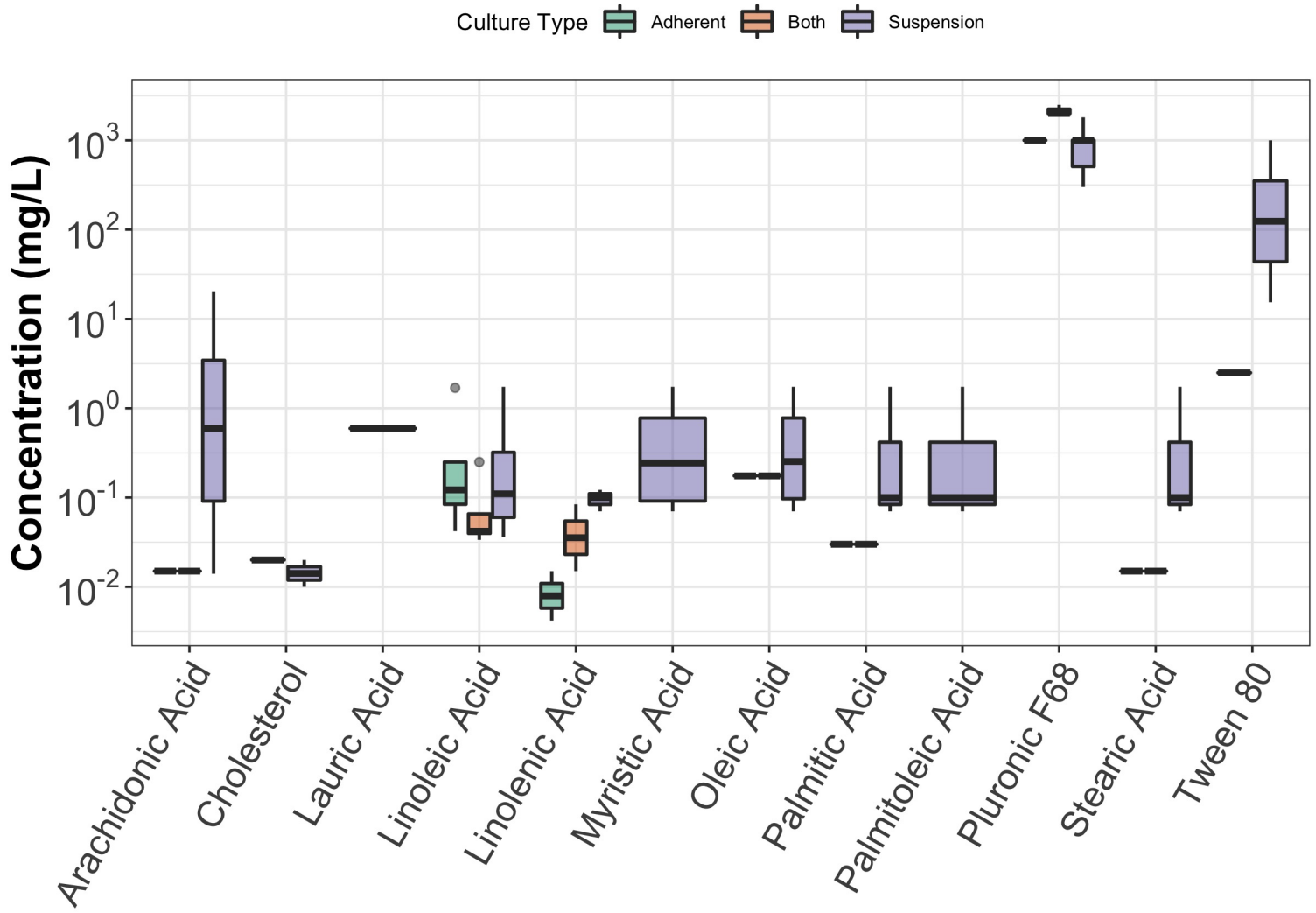

Figure 2.1: Comparison of media formulations on their fatty acid composition. This plot also includes other common additives that are found in lipid supplements such as Pluronic™ F68 (also known as poloxamer 188) and Tween® 80 (also known as polysorbate 80).

2.1.3 Amino Acids

Amino acids are the building blocks for proteins, and can also be used to make neurotransmitters, polyamines, and nucleotides [341]. They consist of 20 organic compounds that contain an amine and carboxyl functional group, along with a specific side chain group. The side chain group gives the amino acids specific characteristics, such as being polar or non-polar, aromatic or aliphatic, and acidic or basic at physiological pH. Cells have the ability to synthesize many amino acids, but they are supplied in excess concentrations in media to enhance cell growth. Some amino acids, however, cannot be made by the cell and are considered essential amino acids' (arginine, cystine, histidine, isoleucine, leucine, lysine, methionine, phenylalanine, threonine, tryptophan, tyrosine and valine) [114]. These amino acids must be provided in the medium [114]. Most basal media contain all 20 standard amino acids at various concentrations (Figure 2.2). Serum contains a mixture of amino acids or short peptides that can be broken down by the cells. In animal component-free media, yeast extract or plant hydrolysates can be used to supplement the amount of amino acids or short peptides that are normally supplemented using serum. In defined media, all the amino acids can be individually supplemented, or supplemented as dipeptides (e.g. L-alanyl-L-glutamine or glycyl-L-glutamine). SFM contain greatly elevated levels of most amino acids including arginine, glutamine, isoleucine, leucine, lysine, methionine, phenylalanine, proline, serine, threonine, tryptophan and valine (Figure 2.2). Figure 2.3 demonstrates that within SFM, suspension media have even greater amounts of most amino acids, compared to adherent media. Suspension media specifically have much greater amounts of asparagine, aspartic acid, glutamine, glutamic acid, histidine, isoleucine, leucine, lysine, proline, serine, and threonine. This section will focus on the amino acids that are supplemented in higher amounts for SFM.

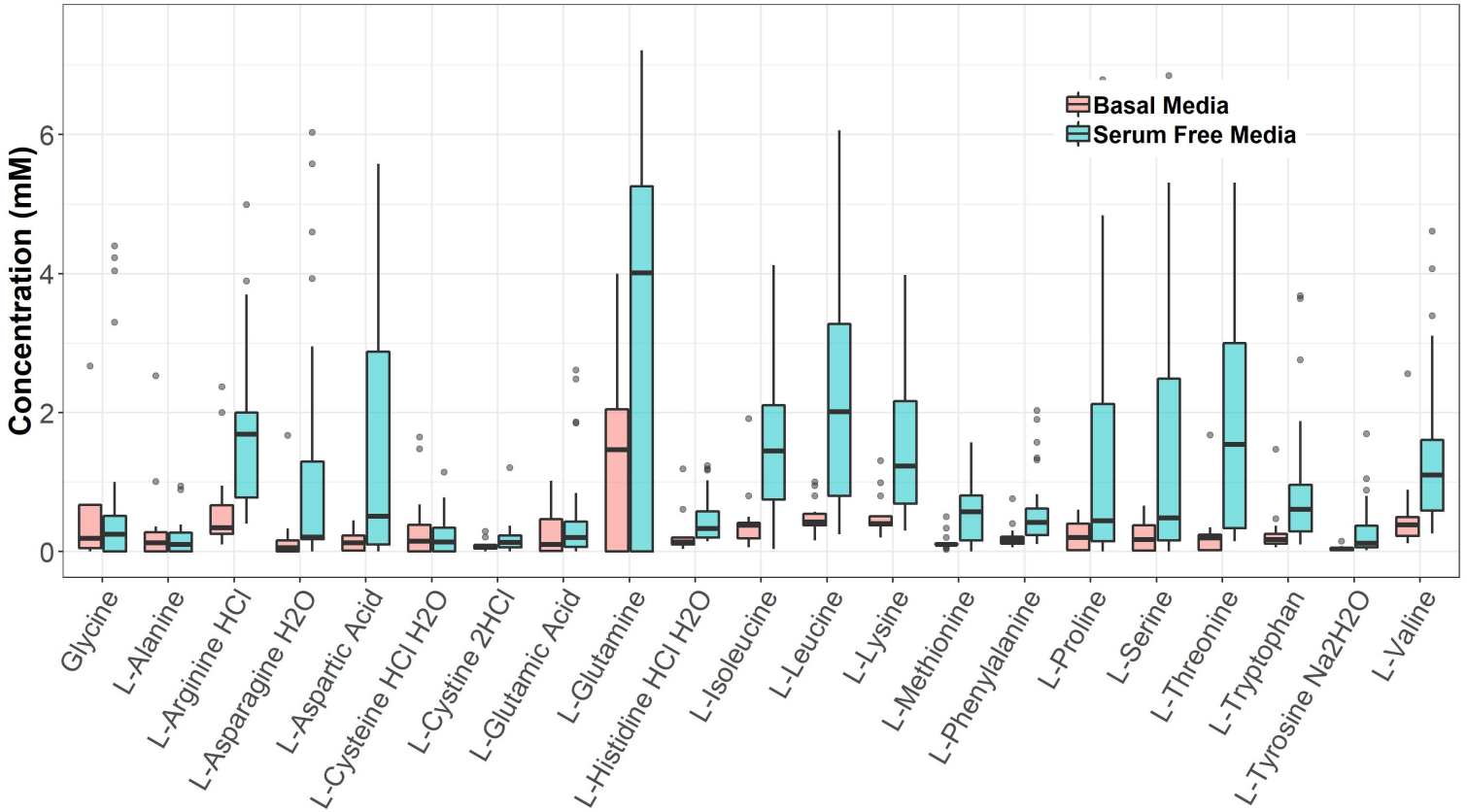

Figure 2.2: Amino Acid concentration for basal media and SFM formulations

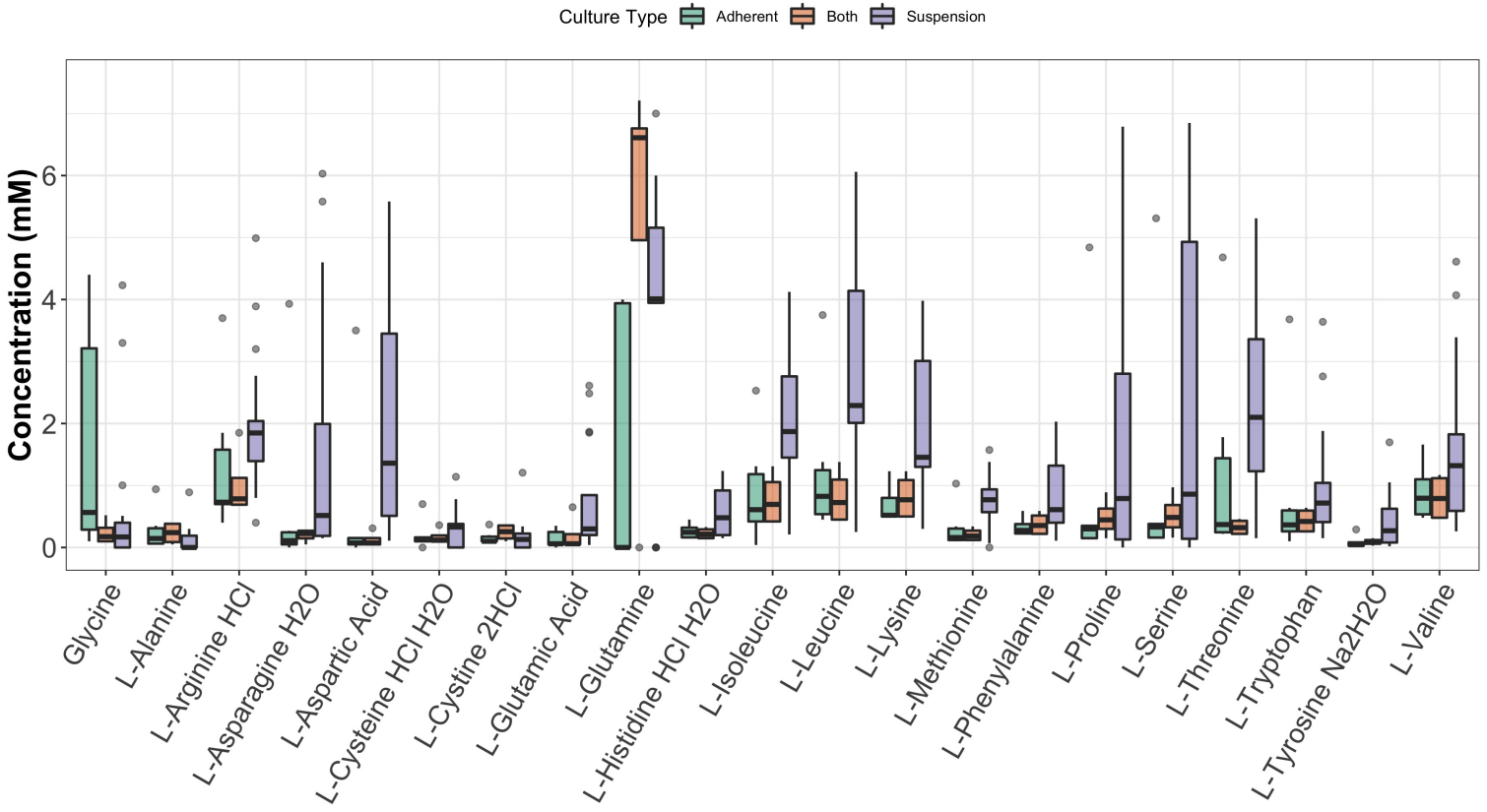

Figure 2.3: Amino acid concentrations for SFM formulations. Media formulations were categorized based on the type of culture they supported (suspension, adherent or both)

Arginine and Polyamines

Arginine is an extremely versatile amino acid that is utilized to produce nitric oxide (NO), polyamines, proline and glutamate [513]. Arginine metabolism is controlled by a multitude of enzymes, often interacting in a complex manner [333]. NO has been shown to modulate the proliferation of cells by inhibiting arginase and ornithine decarboxylase (ODC) in vascular smooth muscle cells [194]. The inhibition of these two enzymes interfere with the production of cellular polyamines. ODC is known to be highly regulated and is the first step in the polyamine biosynthesis pathway [373], and its degradation has been demonstrated to result in reduced polyamine levels and subsequent inhibition of cell proliferation [36]. The natural polyamines (putrescine, spermidine and spermine) are organic cations that are typically found in millimolar concentrations and are known to be involved in cell cycle progression [474]. Polyamine levels fluctuate during the cell cycle [353]. Researchers have found that when polyamines are replaced with inhibitors or ODC is inhibited, the cells are unable to continue their cell cycle [374] and cell proliferation resumes once polyamines are added back into the media or when the inhibitors are removed [474]. Polyamines are not only associated with cell cycle, but also iron uptake [135], and translation initiation and elongation of the cell [243, 287]. Spearman *et al.*, achieved similar viable cell densities in CHO cells when yeast extract was replaced with a combination of the polyamines putrescine, spermidine and spermine, and the related compounds, ornithine and citrulline [448]. Similarly, Burnette *et al.* found spermidine to be a critical component in the long term culturing of *Drosophila* insect cell lines in a chemically defined medium [53]. The exact role of polyamines within the cell is still not comprehensively understood [324], however it is clear that they are an important group of compounds in cell culture. SFM has increased concentrations of arginine compared to basal media (Figure 2.2). All media formulations included in this review contained arginine. The majority of the media formu-

lations also contained putrescine (60%), but only 8% contained spermine, 11% contained ornithine, 3% contained citrulline and none contained spermidine. Given the necessity of the polyamines in cell cycle progression, this class of compounds should be included in more media formulations. Due to the highly regulated nature of cellular polyamine levels, care should be taken to determine appropriate formulation concentrations.

Asparagine and Aspartate

Asparagine, aspartic acid and glutamic acid are all non-essential amino acids and have been used to replace glutamine in cell culture. Asparagine can be made from aspartate using the asparagine synthase enzyme, which takes an ammonium group from glutamine and transfers it to aspartate to create asparagine [463]. Glutamate and aspartate are negatively charged at physiological pH and can be degraded into Kreb's cycle intermediates oxaloacetate and α-ketoglutarate, respectively [491]. Glutamate can then be used to build other amino acids such as glutamine, aspartate, ornithine, proline, arginine, and is important for the formation of neurotransmitters [491]. Aspartate is used by cells for protein production, and as the backbone for pyrimidine synthesis, and is required for the conversion of inosine 5'-monophosphate (IMP) to adenosine monophosphate (AMP) for purine synthesis [244, 462, 491]. Due to cancer cells' dependence on glutamine, many researchers have looked at targeting it for therapeutic purposes [507]. Through this vein of research, it was discovered that asparagine played a large role in rescuing cells from death after glutamine starvation. Zhang *et al.* found that cancer cells could be rescued from glutamine starvation by the addition of asparagine, although they did not restore cell proliferation [536]. Asparagine is essential for CHO-GS cell lines that are not supplemented with glutamine and the addition of higher concentrations of asparagine in the medium improves cell viability, and productivity but not growth [108, 517]. Krall *et al.* attempted to elu-

cidate the mechanism of asparagine on cancer cell survival through asparagine synthase knockdown and altering asparagine media concentrations [236]. They were able to find that asparagine can act as an amino acid exchange factor, especially for serine, arginine and histidine. Cells would import asparagine into the intracellular space, only to export it as it imported other essential amino acids. Asparagine was also used to promote mammalian target of rapamycin complex 1 (mTORC1) activation, protein and nucleotide synthesis and cell proliferation under normal feeding conditions. The mTORC1 protein promotes growth in response to many different amino acids using a two-step mechanism that consists of a priming step followed by activation [111]. The activation of mTORC1 is a two-step process, where it is first sensitized by asparagine, glycine, glutamine, threonine, arginine, proline, serine, alanine or glutamic acid, and then leucine is used to activate the complex. The activation of this complex promotes growth in the cell. The recent findings clarify that asparagine plays a larger role than simply being a substrate for protein synthesis and that it can influence cell growth and amino acid transport into the cell. Figure 2.3 shows that the concentration of asparagine is greatly increased for suspension media formulations.

Recently, in cancer cells where respiration via the electron transport chain (ETC) is chemically inhibited, aspartate or pyruvate have been shown to restore cell proliferation [44, 462]. Under normal conditions, aspartate is made in the mitochondria and exported out using the malate-aspartate shuttle, but when there is a reduction of electron acceptors in the mitochondria, aspartate can no longer be made in the mitochondria, and cells attempt to make aspartate by consuming oxaloacetate in the cytoplasm (Figure 2.4). Birsoy *et al.*, found that in Jurkat cells with the *got1* gene knocked out and ETC inhibited, high amounts of aspartate (10 mM) could rescue the cells and allow them to proliferate (Figure 2.4) [44]. Further studies were done to elucidate how aspartate is made in cells where the ETC is dysfunctional and there is a lack of electron acceptors, such as low oxygen

levels, in the mitochondria. Sullivan *et al.* and Birsoy *et al.* both found that the loss of a functional ETC affected the NAD^+/ nicotinamide adenine dinucleotide (reduced form) (NADH) ratio, and cells will attempt to produce more NAD^+ in the cytosol by converting pyruvate into lactate, or α-ketobutyrate (AKB) to α-hydroxybutyrate (AHB) [44, 462]. NAD^+ could then be used as a substrate, along with malate, to produce oxaloacetate, which could then be converted to aspartate. In rapidly growing cancer cells, where there is a greater need for purine and pyrimidine synthesis, the ability to quickly produce large amounts of aspartate by replenishing NAD^+ pools may be one of the reasons for the inefficient conversion of pyruvate to lactate. These findings also give rise to the idea that the purpose of the ETC may not be for adenosine triphosphate (ATP) production, but rather to act as a source of electron acceptors during aspartate synthesis. Cells still require a functional ETC for uridine synthesis since the dihydroorotate dehydrogenase enzyme transfers electrons directly to the ETC when dihydroorotate is converted to orotate [159]. Given that aspartate is such an important substrate, increasing aspartate in the media formulation should increase cell growth, but aspartate is poorly transported into the cell using the SLC1A3 transporter [139, 463]. Garcia-Bermudez *et al.*, found that when cancer cells were overexpressing SLC1A3, they could overcome ETC inhibition or low oxygen conditions, which allowed them to import more aspartate. Researchers add very high concentrations (10-20 mM) of aspartate to get sufficient levels of aspartate in the cells [44, 462].

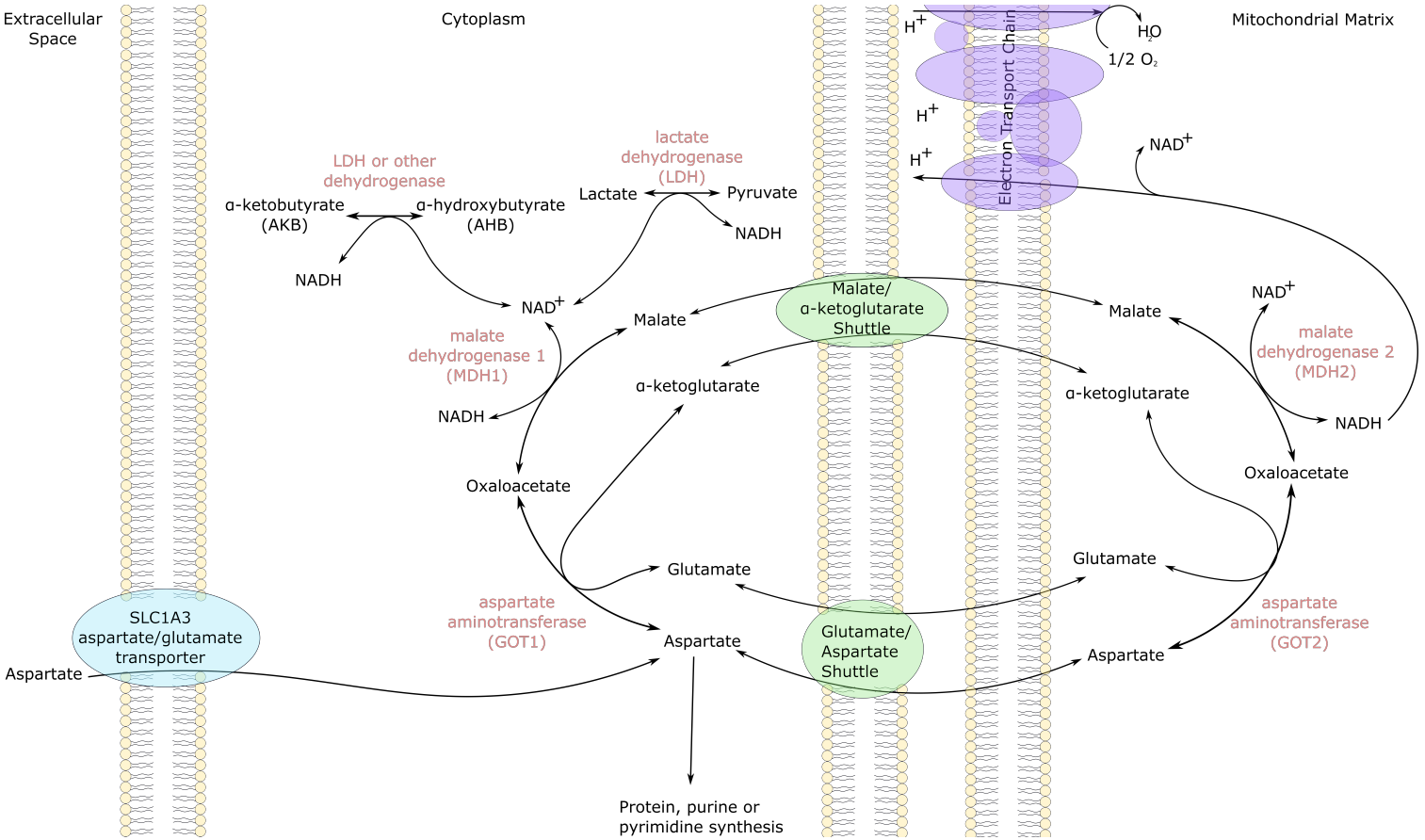

Figure 2.4: Aspartate Synthesis in the cell

Glutamine

L-glutamine is commonly added at much higher concentrations (10- to 100- fold) compared to other amino acids due to its ability to enhance cell growth [114] by being a source of nitrogen for purine and pyrimidine synthesis and acting as an alternative energy source to glucose. SFM has a much higher concentration of glutamine compared to basal media (Figure 2.2). Glutamine is commonly used to enhance cell growth in SFM and it is added at higher concentrations in media tailored for suspension cultures (Figure 2.3). In rapidly dividing cells, glutamine is inefficiently used and the cells produce alanine and ammonia [179, 490, 529]. Some media formulations developed for CHO cells contain 8-10 mM of glutamine, but this often increases the amount of ammonium that accumulates in the culture. Heiden *et al.* hypothesized that the inefficient catabolism of glutamine into lactate is to repopulate the pool of nicotinamide adenine dinucleotide phosphate (reduced form) (NADPH) and to redirect metabolites to nucleotide and fatty acid biosynthesis to support rapid cell proliferation [179]. Nevertheless, glutamine that is quickly converted into ammonia in rapidly dividing cell cultures inhibits cell growth at high concentrations. Researchers have looked for alternatives to glutamine in order to control the amount of ammonia produced in cell culture [11, 148]. Common methods to control ammonia levels in cell culture include fed-batch or perfusion bioreactor modes of operation that dilute the media to keep ammonia level below growth inhibiting concentrations (3-4 mM) [425]. Another method is to introduce more stable forms of glutamine to avoid the degradation of glutamine into ammonia and pyroglutamate [439, 511]. These substitutions include dipeptides such as alanyl-glutamine and glycyl-glutamine, or plant hydrolysates and peptones [486]. A final method to lower the amount of ammonia produced in cell culture is to completely substitute glutamine for another compound such as glutamate or pyruvate [148, 380]. A recent patent completely replaced glutamine with asparagine and aspartic acid (10 mM each) to

lower the amount of ammonium produced in CHO cells [143]. An additional approach is to explore increasing the concentration of purines and pyrimidines in the cell culture media to reduce the cell's dependence on glutamine, although Boza *et al.* showed that in Caco-2 cells, nucleotides could not replace glutamine [47]. When nucleotides and nucleosides were added to medium already containing glutamine, proliferation in Caco-2 cells increased, which demonstrates a positive correlation [522].

Branched Chain Amino Acids: Isoleucine, Leucine and Valine

Isoleucine, leucine and valine are supplemented in higher concentrations for SFM compared to basal media (Figure 2.2). All of these amino acids are non-polar and have large aliphatic hydrophobic side chains, which make them important for the hydrophobic regions in proteins. These branched amino acids are essential amino acids for mammalian cell culture and can be catabolized into many different products such as propionyl-coenzyme A (CoA), acetyl-CoA, or succinyl-CoA [175], which are important building blocks for proteins and fatty acids [106]. Leucine is catabolized into acetoacetate and acetyl-CoA, while isoleucine is catabolized into propionyl-CoA, and acetyl-CoA and valine yields succinyl-CoA [41]. Dorai *et al.*, found that in apoptosis-resistant CHO cells, all three branched chain amino acids (BCAA) were consumed more rapidly than the control cells [106]. The control CHO cells rapidly accumulated high amounts of ammonia (12 mM), while the apoptosis-resistant cells accumulated 8 mM of ammonia and plateaued after 8 days of culture, which indicates that the apoptosis-resistant cells were able to reuse the ammonia that was being produced. Work done by Johansen *et al.* who studied ammonium-induced inhibition in neurons and astrocytes, found that cells were able to use BCAA catabolism to support ammonium detoxification through the production of glutamate or glutamine [206]. Therefore, BCAA are not only important for fatty acid and protein synthesis, but

can also play a role in controlling the levels of ammonia in cell culture.

Lysine

Lysine is an essential alipahtic amino acid that is positively charged at physiological pH [18]. This charged structure allows lysine to make hydrogen bonds and salt bridges that are important for protein structure and function. It is important for helix formation in protein secondary structure and also crosslinking between proteins, such as between collagen fibers and fibrin molecules [490, 523]. Mammalian cells are able to catabolize lysine to acetyl-CoA or acetoacetate through two major pathways: the saccharopine pathway and the pipecolate pathway [458]. Lysine is able to be used to form L-pipecolic acid and carnitine [52, 188]. Carnitine's role is to transport fatty acids and products of peroxisomal β-oxidation into the mitochondria for further degradation, which fuels the Kreb's cycle and ATP synthesis [283, 488]. This amino acid is added at much higher concentrations in suspension media compared to adherent media (Figure 2.3).

Methionine and Cysteine

Both methionine and cysteine are sulfur containing amino acids that are commonly added to cell culture media. Other sulfur containing components that are added to cell culture media are β-mercaptoethanol, cystine, taurine, and N-acetylcysteine. Methionine is an essential, non-polar amino acid that contains a thiol ether group and it is often the donor of a methyl group for many reactions inside the cell [491]. Methionine can be converted to propionyl-CoA, which can be converted to succinyl-CoA using biotin and cobalamin to replenish the Kreb's cycle. The beginning steps during the degradation of methionine produce S-adenosylmethionine (SAM). SAM is responsible for being the methyl

donor for many different reactions such as during the synthesis of phosphatidylcholine to phosphatidylethanolamine, or deoxyribonucleic acid (DNA) or ribosomal ribonucleic acid (RNA) methylation. The methylation reactions result in a methyl group being donated to the substrate and the formation of homocysteine, which can be methylated again to form methionine. Homocysteine can also combine with serine to create cystathionine, which can then form cysteine and α-ketobutyrate. Not only can the cells produce cysteine from methionine, but it can also be transported directly into the cells through a neutral amino acid transporter from the extracellular space [29, 268]. Cysteine can be oxidized with itself to form cystine, which uses a different transporter that exchanges glutamate for cystine [28]. Once cystine enters the cell, it is quickly reduced to cysteine, which can be used to make glutathione. Glutathione is a tripeptide (γ-L-glutamyl-L-cysteinylglycine) and is very important for maintaining the redox balance inside the cell. It can non-enzymatically reduce cystine, plays a role in ascorbate recycling, and can chelate cuprous copper [132, 299]. Glutathione (reduced form) is commonly added to cell culture media at a concentration of 1 mg/L. Taurine is also a product of cysteine that is commonly added to cell culture media. It is formed from the degradation of cysteine and is one of the most abundant compounds in many different tissues, although it is not used to synthesize proteins [259]. It has been shown to be a cytoprotectant, prevent superoxide generation, be an osmotic pressure regulator, help maintain cation homeostasis in cell culture and improve the proliferation of neural stem cells at concentrations of 10 mM [119, 182, 207, 423]. Interestingly, cysteine and cystine concentrations are only slightly increased in SFM compared to basal media (Figure 2.2), although the concentration of methionine is increased, especially for suspension media (Figure 2.3). Taurine is not included in any basal media formulations that were reviewed and in only one serum-free medium formulation at a concentration of 0.03 mM.

Aromatic Rings: Phenylalanine, Tryptophan and Tyrosine

Amino acids that contain aromatic rings (phenylalanine, tryptophan and tyrosine) are important precursors for cell signaling molecules and hormones. Tryptophan can be used to make a variety of compounds including tryptamine, serotonin, melatonin, niacin, NAD^+ and $NADP^+$ [370]. Phenylalanine is an essential amino acid and can be degraded into tyrosine. Tyrosine is used to make various signaling molecules such as thyroxine, triiodothyronine, neurotransmitters such as dopamine, epinephrine, noepinephrine, phenylethylamine and tyramine, and can be catabolized into fumarate and acetoacetate. Tyrosine is not very soluble at neutral pH, and alternative sources of the amino acid can be added through dipeptides containing tyrosine, phosphotyrosine disodium salt, N-acetyl-tyrosine, glycyl-tyrosine or alanyl-tyrosine [212, 541].

To address the poor solubility of tyrosine Kang *et al.* tested various tyrosine dipeptides (Tyr-His and Tyr-Lys) in an attempt to improve specific productivity of various monoclonal antibody (mAb) producing cell lines in a fed-batch system [212]. They showed that when tyrosine and asparagine where fed in their monomeric form at the beginning of culture, these amino acids were depleted after 11 days and lactate accumulated in the culture [212]. When Tyr-Lys and Tyr-His were added to the bioreactors, cells began to metabolize lactate after 10 days, and tyrosine depletion was not detected. They also found that there was enhanced antibody productivity and viability, but they did not improve the maximum cell density. Similarily, Zimmer *et al.*, found that using 2.5 mM tyrosine and 30 mM phosphotyrosine disodium in the feed for a fed-batch CHO cultivation yielded better mAb titers, although it did not achieve higher peak cell densities [541].

Threonine

Threonine is an essential, polar, uncharged amino acid that can be degraded into pyruvate, acetyl-CoA, propionyl-CoA and succinyl-CoA [490]. In the SFM formulation review (Figure 2.2) it is supplemented higher than in basal media, which may be due to its ability to be catabolized into the aforementioned compounds. Shyh-Chang *et al.* looked at why pluripotent mouse embryonic stem cells used threonine at a higher rate than mouse embryonic fibroblasts using 13C labelling [438]. They were able to detect that threonine was the main source of glycine and acetyl-CoA in the cells, and that threonine metabolism is linked to SAM metabolism and histone methylation. For serum-free suspension media, the median for threonine is approximately 5x higher than for adherent cultures (2.1 mM vs 0.37 mM) (Figure 2.3). In fed-batch culture of CHO cells, threonine has been reported to act as a growth inhibitor if it is above 0.5-1 mM [65, 377]. Conversely, deZengotita *et al.* showed that threonine improved the growth rate of CHO cells under elevated osmolarity levels [101]. Various commercially available CHO media (CD-CHO, OptiCHO, FortiCHO, Acti CHO-P) contain 1.5-3.1 mM threonine [366]. Additionally, threonine is able to form hydrogen bonds and is an important amino acid in building proteins. Kisselev *et al.* found that threonine provides a greater capacity to cleave peptides compared to serine in the active sites of proteasomes [226]. This indicates that threonine is a key amino acid for the function of proteasomes and plays an important role in degradation of proteins in the cytosol and nucleus. It is also an important amino acid for cell signaling as it is the site of phosphorylation by serine/threonine-specific protein kinases [520]. The phosphorylation of threonine by different kinases is involved in many different pathways such as cell growth [25, 331], death [88, 151], and stress responses [118, 192, 210].

2.1.4 Metals

Trace metals play a vital role in cell growth and function. During the beginning of media development, trace metals were incorporated into the formulations through serum, extracts, leaching from processing materials, or contaminants of water or impure compounds [152]. Glassman *et al.* found that in 11 different commercial media, all of them contained trace amounts of lead, copper, tin and zinc and that these trace metals could have been acquired from contact with surfaces [152]. As processing techniques improve and ultrapure water is more widely available, researchers increasingly appreciate the importance of trace metals. Hamilton and Ham first published a protein-free media for CHO cells in 1977 [161]. At first glance, this media appears quite similar to previous mediums in terms of vitamins, amino acids, and lipids, but Hamilton and Ham added 23 different trace metals to the medium. This wide array of metal ions included many divalent cations in very small quantities. In 1988, Cleveland *et al.* patented a trace metal solution containing 18 different trace metals in addition to 8 metals that are already present in most serum-free mediums (calcium, copper, iron, potassium, magnesium, sodium, zinc and selenium) [84]. Kenerson patented another trace metal supplement in 2005 for PER.C6 cells, which incorporates the same trace metals as Cleveland, with the addition of titanium [218]. Metal ions play a crucial role in protein conformations, catalysts in cellular reactions, and as electron acceptors. The necessary concentration of these metal ions can vary from millimolar to nanomolar concentrations. In undefined media supplements, metal ions can be contained in protein complexes, which act as chelators reducing the toxicity of the ion and can transport the metal ion to a cellular receptor to be taken up by the cell. In serum-free or chemically defined media, chemical chelators (tropolone [126], ethylenediaminetetraacetic acid (EDTA), sodium citrate, cyclodextrins, or hydroxypyridine derivatives [79, 235]) or lower amounts of metal ions must be used to reduce the toxicity of the ions on the cells.

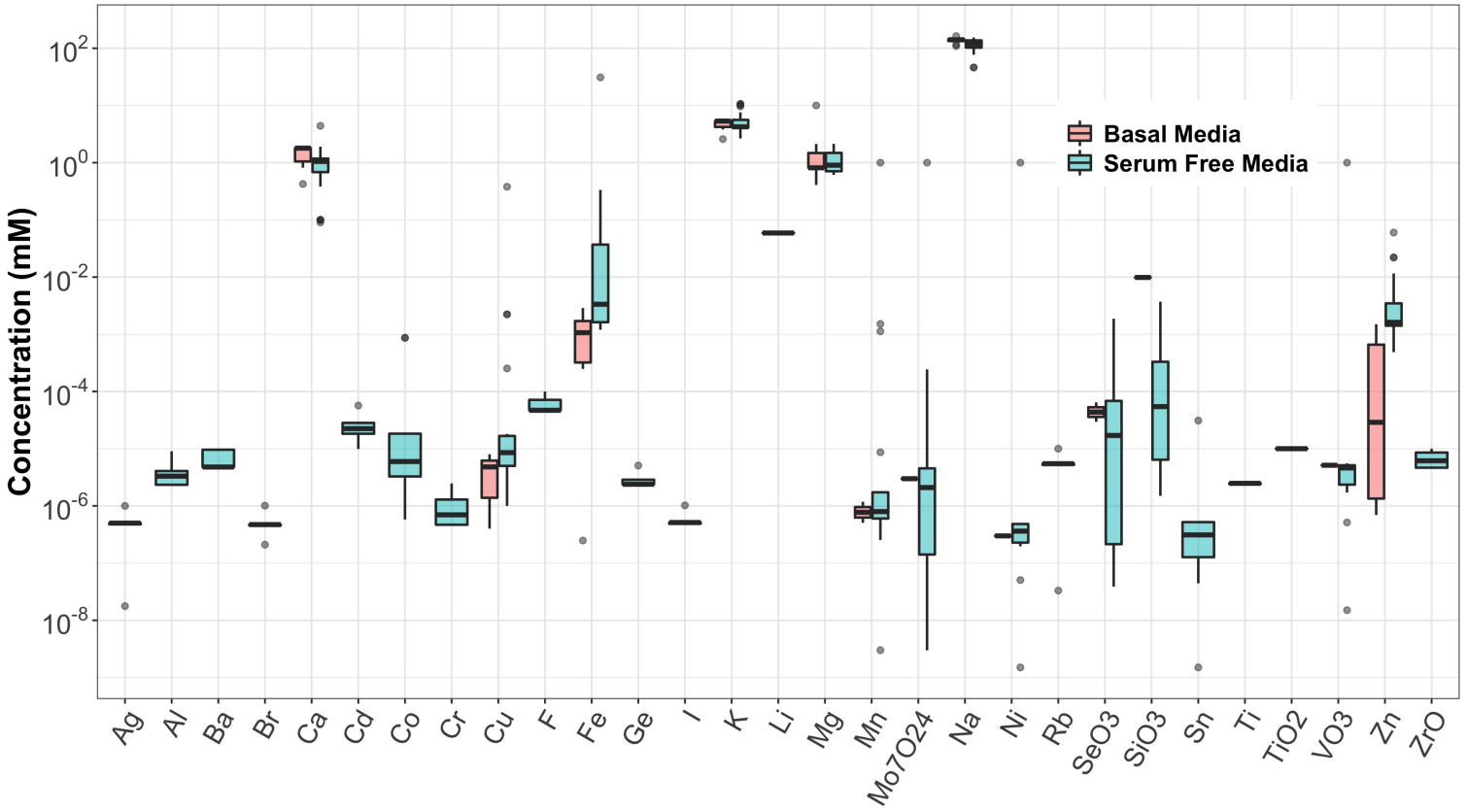

Figure 2.5: Metal concentrations in basal and serum-free mediums

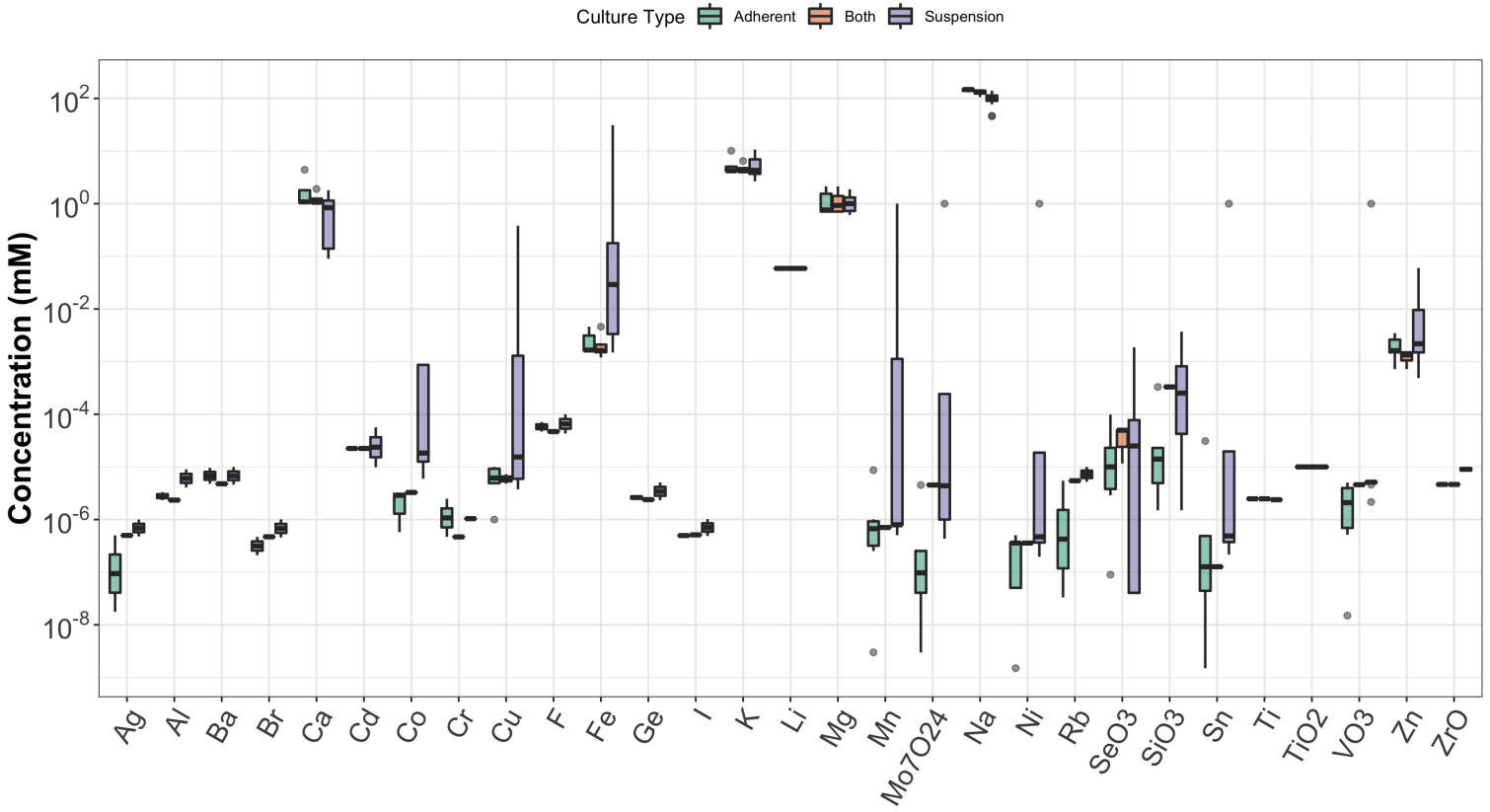

Figure 2.6: Metal concentrations in serum-free mediums

Sodium and Potassium

Sodium and potassium are two of the metal ions in the highest concentration in cell culture. At physiological conditions in mammalian systems, their extracellular concentrations are 145mM Na^+ and 4 mM K^+ (ratio of 36:1), and the intracellular concentration is typically 12 mM Na^+ and 139 mM K^+ (ratio of 1:12)[273]. The cell maintains this large concentration gradient to drive many biological processes such as transport of materials across the plasma membrane against their concentration gradient, cell volume, migration and growth [525]. Ion transporters for potassium and sodium have been well studied and consist of the active transmembrane Na/K transporter (NA,K-ATPase), and passive Na^+ and K^+ ion pumps [83]. Sodium and potassium are actively transported across the cell membrane using ATP to maintain the cell membrane potential, and then the ions can pass across the membrane, down their concentration gradient. This passive transport of sodium or potassium can be coupled to other transport systems in the cell to help transport a range of compounds such as sugars, amino acids, and other ions [83, 397]. The ratio of sodium to potassium has been linked to cell growth and can influence protein production in L and CHO cells [127, 254, 497]. Most classic mediums contain a Na:K molar ratio of 26-29 and serum-free mediums are slightly higher > 30 [254]. Wang *et al.* tested different ratios of Na:K in CHO cell media to optimize growth rate and protein production in perfusion reactors [497]. They were able to reduce the growth rate of CHO cells by lowering the ratio to 0.5 Na:K and protein production per cell was increased. Leist *et al.* created CHO cell media with Na:K molar ratios of 5.7-7.8 and a ratio of ions to amino acids of 2.1 to improve cell growth and polypeptide production [254].

Calcium and Magnesium

Calcium is an important divalent cation that is involved in many cellular processes such as cell adhesion [273], cell signaling [38], enzyme activity, apoptosis [354]. Healthy cells maintain a large concentration gradient between the cytosol (0.1 µM) and extracellular space (1-2 mM) [273]. Due to this large gradient, cells must continuously pump calcium out of the cytoplasm. This is accomplished through several different pumps on the surface of the plasma and the endoplasmic reticulum (ER) membranes. The sarcoendoplasmic reticular Ca^{2+} ATPases (SERCA) pump calcium into the ER, while plasma membrane Ca^{2+} ATPases (PMCA) pump calcium out of the cytosol [82]. Cells also use proton exchangers such as a sodium-calcium exchanger, and potassium and calcium pumps to move ions around the cell. Cell adhesion molecules such as cadherins, require a certain concentration (>55 µM) of calcium to maintain the correct rigid conformation and remain active [385]. Cadherins are a family of transmembrane proteins that binds to other cadherins on the cell surface. This leads to an adhesive signal, which creates a cascade of other signaling events by β-catenin [485]. Integrins are another family of adhesion molecules, but unlike cadherins, these proteins do not require calcium to function. Although the protein itself does not require calcium, integrin α-subunits associate with calreticulin, which does bind calcium [85, 257, 447]. Coppolino *et al.* found that calreticulin is essential for integrin-mediated calcium signaling and adhesion [86].

Magnesium is the second most abundant cation (after potassium) inside the cell and ranges from 17-20 mM in most mammalian cells [407, 406]. Most of the magnesium is bound to various cellular structures, and only about 0.8-1.2 mM is free Mg^{2+} [407]. It is essential for the most basic functions in the cell, for example ATP requires magnesium to be biologically active. It is an important cofactor for over 180 cellular proteins includ-

ing membrane proteins and enzymes, cytosolic signaling components, glycolytic enzymes, endoplasmic reticulum functions, mitochondrial enzymes and functions, and nuclear functions [237]. Interestingly, because of magnesium ion's similar coordination chemistry to calcium, magnesium ions can also bind to endogenous calcium-binding proteins [237]. For example, when the concentration of extracellular calcium is below 50 µM, E-cadherins can no longer maintain their functional conformation, but they can regain their rigid structure by using magnesium [519]. Since magnesium is such a vital metal for cellular functions, basal media and SFM have approximately the same concentration of magnesium (1 mM), and there is little difference in magnesium concentrations between suspension and adherent SFM (Figure 2.6).

Copper

Copper is an essential metal for cell culture. It exists mainly in two forms Cu^{+} and Cu^{2+} and it plays a critical role in cellular respiration and as a cofactor for many proteins in the cell [215]. Copper is transported into the cells in its Cu^{+} state by the CTR1 transporter in mammalian cells [214]. Once inside the cell, it is usually transported by chaperones, P-type ATPases, or glutathione [215, 352, 381]. There are almost no free copper ions (10^{-8} M, less than one free copper ion per cell) [267, 393]. The copper ions are incorporated into proteins that are used in the mitochondria for cellular respiration such as cytochrome c oxidase and NADH dehydrogenase, the free radical scavenger Cu/Zn superoxide dismutase (SOD), and in oxidases ceruloplasmin, multicopper ferroxidase and lysyl oxidase, which also help transport iron into the cell [125]. Many basal medium formulations do not include copper because FBS contains sufficient amounts. In serum, copper is chelated by ceruloplasmin, which has 6 copper binding sites [180]. Basal mediums that contain extra copper include Ham's F12K (8 nM), William's E (0.4 nM), MCDB 131 (4.8 nM) and modified forms of

Ham's F12 (such as DMEM/F12, 5.2 nM) (Figure 2.5). Without chelation, copper has the ability to form free radicals that damage other media components. Cysteine is a media component that will react with copper to form cystine and subsequently reduces the pool of available cysteine for cell growth [286]. Therefore, when adding copper in serum-free formulations, it is important to also provide a chelator or extra antioxidants to the media to protect other media components from free radical damage, and lipid peroxidation.

Serum-free medium formulations contain approximately the same concentration of copper as basal formulations (6.2-7.5 nM) (Figure 2.6). In serum-free protein-containing media, albumin can be used used to chelate copper, but in protein-free media synthetic copper chelators must be used. Glutathione (reduced form) can also be used to chelate copper and is included in many serum-free adherent media formulations at a concentration of 1 mg/L. Other synthetic copper chelators have been investigated for the effects of copper concentration on HL-60 cells and human hematopoietic progenitor cells [376, 388, 429]. Tetraethylenepentamine (TEPA) has been used to chelate copper and reduce the amount of copper in the cell and lower the oxidative stress on cells. Given how important copper is to many different proteins, and the transport of iron, this is an essential micronutrient that needs careful attention, because of its ability to form free radicals and damage other media components.

Iron

Iron is a vital cofactor in cellular respiration, the tricarboxylic acid cycle (TCA) cycle, lipid metabolism and DNA synthesis [62, 389]. Given that iron is used in so many aspects of the cell, one would think the cell requires large amounts of this metal. The main problem with trying to incorporate large quantities of iron is that it is toxic at higher concentrations if it is not properly chelated. Free iron in media can exist in the ferric (Fe^{3+}) or ferrous

(Fe^{2+}) state. Ferric ions can be converted into ferrous ions by strong reducing agents in cell culture media. Ferrous ions are a major source of oxidative stress on the cell. It can catalyze the conversion of hydrogen peroxide to hydroxide and a hydroxyl ion [234]. The hydroxyl free radical is extremely reactive and can damage many of the media components [6, 325]. One particular class of compounds that are prone to peroxidation are polyunsaturated fatty acids. Researchers have found that catalase, desferrioxamine, and mannitol inhibit lipid peroxide formation [6, 325]. Ferric (Fe^{3+}) ions are much more stable and is the normal oxidative state that is used by the cells [2]. One of the major challenges of maintaining free ferric ions in the media, is that they quickly form ferric hydroxides and precipitate out of solution. In serum containing media, iron is chelated by transferrin outside the cell, and it is stored by ferritin inside the cell. When designing serum-free, protein-free media, researchers have looked to other chelating compounds that are able to loosely bind iron and maintain it in its ferric state, while also being able to be taken up by the cell.

Researchers have looked at alternatives to transferrin to create protein free media. Nagira *et al.*, screened various iron salts and chelating agents to create a protein-free media for human-human hybridoma [338]. They found that 8.0 µM ferric citrate was the most favorable for cell viability and antibody production. Bertheussen also found that citric acid was a good iron chelator when creating a synthetic serum replacement for the cultivation of L929, HeLa, S3, and 1E6 hybridoma cells in RPMI media [39]. Bertheussen found that ferric citrate and trace metals would precipitate out of the medium, but this could be prevented by adding EDTA and citric acid. When the final synthetic serum replacement was complete, it contained various trace metals along with 3 µM iron ($FeCl_3 \cdot 6H_2O$), 4.3 µM EDTA, 40 µM citric acid, and 3 µM aurintricarboxylic acid (ATA) to replace transferrin for a protein-free medium formulation [39]. ATA is not only reported as a trivalent metal chelator [202], but also an apoptosis inhibitor [35] and it inhibits protein-nucleic acid

interactions [155]. Table 2.3 lists various chelators that have been used for iron addition in culture media.

Table 2.3: Iron Chelators

Proteins	**Chemical**
Transferrin	Citric acid
Ferritin	Iminodiacetic acid
Troponin	Gluconic acid
	Pyridoxal isonicotinyl hydrazine
	EDTA
	2-hydroxypyridine-N-oxide

Some basal mediums contain iron, but many do not have any iron in their formulation (Figure 2.5). Most of the iron for cell culture in basal mediums comes from supplements such as FBS. FBS provides iron chelators, such as transferrin, to the media, but since there is variability between different lots of serum, the amount of chelators isn't constant and can vary between experiments. Ham's F12 medium contains 2.99 µM of $FeSO_4$, which contains iron in the Fe^{2+} state, whereas DMEM contains 0.247 µM $Fe(NO_3)_3$, which contains iron in the Fe^{3+} state. Since many SFM formulations are based off DMEM/F12 basal media, the addition of the ferrous ions from F12 can be problematic without the proper chelator. M-199 medium may be a better choice for SFM development because it contains 1.78 µM $Fe(NO_3)_3$. For SFM formulations, the amount of iron that is used for adherent cultures is not much larger than the amount in M-199. The median for adherent SFM is approximately 1.62 µM without any clear preference for ferric citrate, $FeSO_4$ or $Fe(NO_3)_3$. For serum-free suspension culture, the amount of iron is much larger (18.6 µM). This may be due to the higher cell densities that can be achieved in suspension culture. Given the large importance

of iron in almost all cell functions, it is an essential nutrient that can either greatly enhance cell growth and viability or cause large amounts of stress on the cells if it is not chelated properly.

Zinc

Zinc (Zn^{2+}) is another transition metal that is extremely important to cellular function. Unlike copper and iron, zinc is more stable in cell culture conditions and does not form free radicals. The optimal internal levels of zinc inside a mammalian cell is approximately 0.1-0.5 mM [116, 461]. It also protects the cell from oxidative damage by stabilizing membranes, inducing metallothionein synthesis, and inhibiting nicotinamide adenine dinucleotide phosphate oxidase [89, 292].

Interestingly, nutritional studies performed on rats showed that circulating IGF-1 levels in their blood depended on adequate amounts of zinc in their diets [281]. The zinc-deficient diet led to a 28% decrease in serum IGF-1 compared to a zinc-adequate diet when rats were fed the same caloric value [411]. It is known that zinc can be used to replace insulin, and zinc ions affect the phosphorylation of the insulin receptor β subunit [347, 472, 532]. In protein-free media for hybridoma, myeloma and CHO-K1 cells, zinc was found to be a replacement for insulin [509, 510]. Zinc has been shown to affect different signaling pathways that involve various proteins besides the insulin receptor, such as the epidermal growth factor receptor (EGFR) [420, 514], mitogen-activated protein kinase (MAPK) [187, 532], and protein kinase C [74]. These protein families have influence on cell signaling cascades that can lead to cell survival (Src-c, Akt/PKB, Ras, ERK).

In basal media, zinc is not included in the formulation with the exception of Ham's F12, MCDB 131 and William's E media. Of the basal media that do contain zinc in their formulation, the mean concentration is 0.0005 mM (Figure 2.5). Zinc is normally supplied

through the addition of serum. In serum, zinc can be bound to albumin, histidine, cysteine, citrate, or phosphate [48]. In SFM formulations, the zinc that is normally provided by FBS must be replaced. For SFM that is meant for adherent cell culture, the mean zinc concentration used is 0.0016 mM; for suspension growth this value is increased to 0.0022 mM (Figure 2.6). Given the importance of zinc in signaling pathways, it is not surprising that SFM contains 3-4x the amount of zinc compared to serum supplemented media. The addition of this metal is vitally important for the development of an effective SFM.

Trace Metals

Other transition metals (Ag, Al, As, B, Ba, Br, Cd, Co, Cr, I, F, Ge, Li, Mn, Mo, Ni, Rb, Se, Si, Sn, Ti, V, W, Zr) are added to cell culture media in micromolar to nanomolar concentrations. Table 2.4 list all the metals that are commonly added to cell culture media along with their use and some of the proteins they are associated with in the cell. Many of the trace metals are added to cell culture media, because they are commonly found in mammalian tissues, even though their functions remain unknown. Studies have shown that these metals are essential for the health and proper development of whole organisms such as rats or humans [342]. For SFM formulations, many of these metals could have been unknowingly included in DI water, or could have been leached from glass vessels. With the improvement in water quality and using higher quality plastics for media bottles, these metals need to be added manually. Additionally, as industry moved towards protein-free media, metals that were bound to albumin or transferrin, also need to be added manually. Therefore, although their purpose is unknown, these metals are beneficial to cell growth and should be included in SFM formulations.

Table 2.4: List of trace metals that are commonly included in chemically defined media. This table also lists their known use in cell functions and associated proteins in mammalian cells.

Metal	**Use**	**Associated Proteins**	**Ref**
Ag	Antimicrobial	Binds to -SH groups, albumin, metallothionein	[245]
Al	Unknown	Albumin	[176]
As	Biomethylation, enzyme inhibition, apoptosis	Pyruvate dehydrogenase (inhibits), arsenic methyltransferase, tubulin, actin, glucocorticoid receptor	[434]
B	Production of steroid hormones, regulates mRNA expression, protects against oxidative stress	Borate cotransporter	[383, 416]
Ba	Unknown	Phospholipase, EGF domains, calmodulin	[237]
Br	Cofactor	Peroxidasin	[300]
Ca	Cofactor in enzymes, attachment, motility, cell morphology, signal transduction, metabolic processes, replication	Annexins, calnexin, calreticulin, calbindins, troponin C, calmodulin, S-100 proteins	[38]
Cd	Irreversibly binds DNA	Metallothionein	[470]
Co	Cofactor in enzymes that use cobalamin (Vitamin B_{12})	Methionine aminopeptidase, methylmalonyl-CoA, prolidase, nitrile hydratase, glucose isomerase, bromoperoxidase	[231]
Cr	Increases insulin binding, induces DNA-protein binding	DNA, Cr-pep	[12, 154, 282]
Cu	Cofactor in proteins, aids in iron transport	Lysyl oxidase (LOX), ceruplasmin, copper oxidases, superoxide dismutase, tyrosinase, cytochrome c oxidase	[125, 214, 352]
I	Part of thyroid hormones, reducing agent	Thyroxine, triiodothyronine, thyroglobulin, sodium-iodide symporter	[96]
K	Membrane potential, volume control	Sodium-Potassium ATPase pump, K^+ channels, cell cycle progression, voltage-gated K^+ channels, cell proliferation	[197, 454]
F	Actin filament arrangement, decrease cellular protein concentration	Phosphatase, fluoride ion channel	[317, 453]

Continued on next page

Table 2.4: List of trace metals that are commonly included in chemically defined media. This table also lists their known use in cell functions and associated proteins in mammalian cells.

Metal	**Use**	**Associated Proteins**	**Ref**
Fe	Important electron acceptor in electron transport chain and oxygen transport, cofactor in many enzymes	Heme groups, Fe-S clutsers in proteins, cytochrome, ribonucleotide reductase, phenylalanine hydroxylase (PAH), phytanoyl-CoA hydroxylase	[62, 389, 490]
Ge	Antioxidant	Unknown	[492]
Li	Enhances stem cell proliferation, downregulates AQP2, mimics Wnt signaling	Inositol monophosphatase, GSK-3	[104, 255, 440, 494]
Mg	Energy requiring metabolism, protein synthesis, membrane integrity, high affinity for phosphates	Calmodulin, troponin, parvalbumin, S100, various phosphatases and kinases	[241, 237, 407]
Mn	Cofactor, antioxidant defense, glucose and lipid metabolism	Arginase, glutamine synthase, pyruvate carboxylase, super-oxide dismutase, transferrin	[70, 260]
Mo	Protein structure, cofactor, detoxifying excess sulphite, must be bound to pterin	Sulfite oxidase, xanthine dehydrogenase, aldehyde oxidase, nitrate reductase	[312, 313]
Na	Membrane Potential, fluid balance, glucose homeostasis, voltage-gated Na^+ channels	Sodium-Potassium ATPase pump, sodium-potassium channels, sodium cotransporters	[100, 530, 538]
Ni	Unknown	Albumin, a2-macroglobulin	[8, 177]
Rb	Substitute for on K^+ transport pathways	K^+ transporters	[33]
Se	Antioxidant, oxidative stress, cofactor, thyroid hormone production	Selenium-dependent glutathione peroxidases, thioredoxin reductases, selenoproteins	[192, 288, 306]
Si	Unknown	Silicon transporter (Slc34a2), aquaglyceroporins	[140, 395]
Sn	Electron transfer catalyst	DNA	[308]
Ti	Unknown	Plasma proteins	[239]
V	Biocatalyst of oxidation, mimics insulin and EGF, oxidizes NADH, regulates activity of cAMP and IP3, helps mibilize Ca^{+2}	Albumin	[237, 87, 426]
Zn	Cofactor in proteins, stabilizes cell membrane and DNA, replacement for insulin	Zinc finger proteins, superoxide dismutase, alcohol dehydrogenase, glutamic acid dehydrogenase, metallotheionein	[301, 509]
Zr	Upregulates BMP signaling pathway	Unknown	[71]

2.1.5 Vitamins

Vitamins are a vital part in any SFM formulation. Many of the vitamins listed in Table 2.5 cannot be synthesized in mammalian cells, although they are important cofactors or coenzymes in cellular processes. When vitamins were first being discovered, they were thought to be growth factors instead of cofactors for microorganisms due to their importance in media formulations [491]. Vitamins typically added in basal and SFM vary from millimolar to micromolar in concentration. SFM has higher concentrations of every vitamin, except ascorbic acid, pyridoxine, vitamin A and vitamin D2 (Figure 2.7).

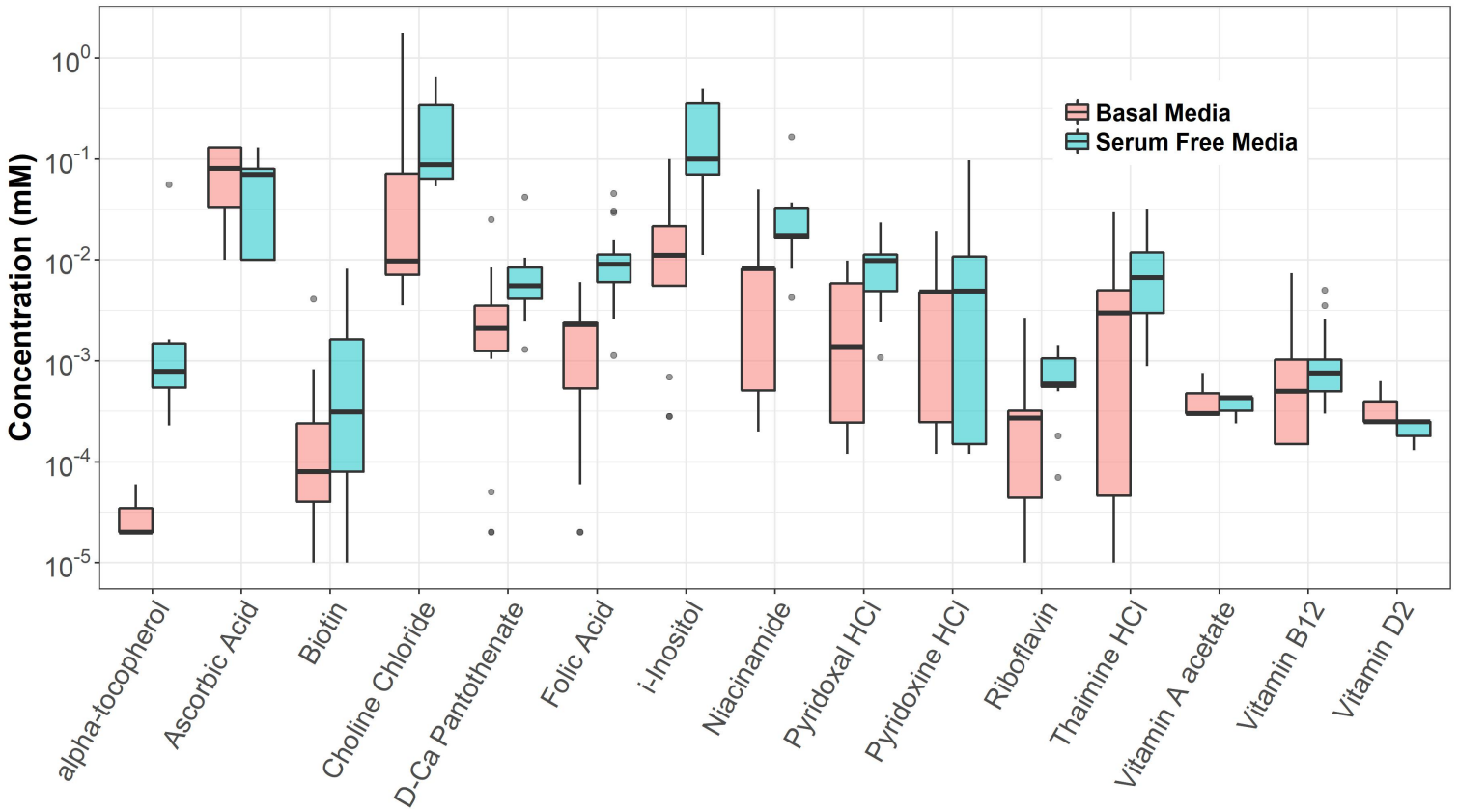

Figure 2.7: Vitamin concentrations in basal and serum-free mediums

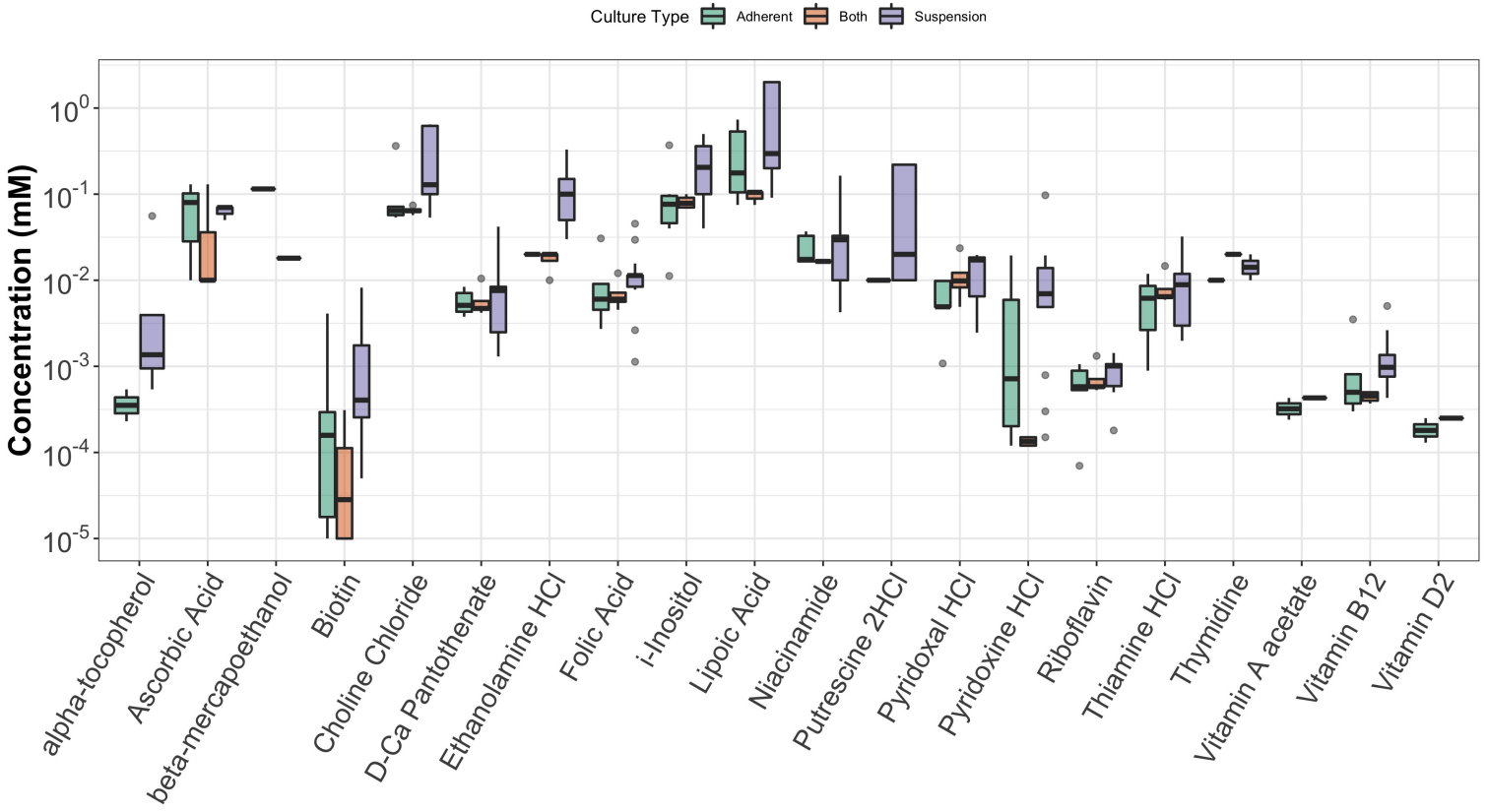

Figure 2.8: Vitamin concentrations in serum-free mediums. Teal coloured boxplots are media that support adherent growth, the pink colour represents media that support both adherent and suspension culture methods, and purple represents media that support suspension grwoth.

Vitamins as Antioxidants

Cultivating mammalian cells under 95% air and 5% CO_2 results in hyperoxia (excess oxygen compared to *in vivo* systems) of the medium. Historically, media have been designed so that cells can be cultured in incubators that use air (21% oxygen) instead of physiological conditions of about 5% oxygen, which would require a specialized incubator [307]. This increases the amount of reactive oxygen species (ROS) and free radicals in the medium [167]. Therefore, cell culture medium must be supplemented with antioxidant agents to prevent damage to other compounds in the medium and the cells. Various antioxidant substances such as glutathione, selenite, β-mercaptoethanol, and dithiothreitol are commonly added to media, along with vitamins C (water soluble) and E (lipid soluble) [279].

Vitamin C (ascorbic acid, $AscH_2$; ascorbate, $AscH^-$) is a water-soluble molecule that can be used as a reducing agent and donor antioxidant. It can form ascorbate radicals ($Asc^{\cdot-}$) and dehydroascorbic acid (DHA) by undergoing two consecutive one-electron oxidations [107, 444]. Vitamin C can be supplied as ascorbate, ascorbate-2-phosphate, L-ascorbic acid 2-phosphate sesquimagnesium salt hydrate, or DHA in the medium [261, 467]. However, DHA is unstable at physiological pH with a half-life of 5-15 minutes at 37 °C [46]. Therefore, ascorbate-2-phosphate and ascorbate are more commonly used, as they more stable and do not oxidize in the media or produce H_2O_2.

Vitamin E consists of eight fat-soluble compounds including α-, β-, γ-, δ-tocopherol, and α-, β-, γ-, δ-tocotrienol, which are synthesized by plant organisms [137]. α-tocopherol is the preferred form of vitamin E in culture medium because it is an essential component of cellular defense mechanisms against oxidants. Since α-tocopherol is fat-soluble, its site of antioxidant action is believed to be in hydrophobic regions in cell culture media and

cell membranes. There it scavenges lipid peroxyl radicals that can damage fatty acids and lipids.

Supplementation of cell culture medium with vitamins C and E prevents most of the defects caused by ROS including peroxidation of membrane phospholipids, and alteration of cellular molecules, such as lipids, proteins, and nucleic acids. However, vitamins are unstable in biological systems, and a renewed supply is required to protect cells against oxidative stress. Some vitamins can create a pro-oxidant effect when free transition metals are present in the culture medium [64]; therefore, the production of reactive intermediates must be considered when these vitamins are continuously added to the medium. For example, in an application of chemically defined medium to produce a monoclonal antibody, continuous supplementation of the medium with ascorbic acid as an antioxidant agent resulted in xylosone modification of the produced antibodies [78]. Xylosone contains a reactive carbonyl groups and modifies the antibody by forming either hemiaminal, or Schiff base products [78]. Xylosone is a highly reactive species generated by oxidative degradation of ascorbate. In addition to modification of the produced antibodies, this degraded form of vitamin C could potentially modify a myriad of other host cell proteins, which could impact cell viability.

Vitamin B Group

This group of water-soluble vitamins functions mostly as co-enzymes that are involved in energy production as well as the metabolism of lipids, proteins, carbohydrates, and nucleic acids. To function as co-enzymes, these vitamins must be in their active form within the cell to perform their corresponding activities. Therefore, it is necessary for a chemically defined medium to be supplemented with this group of vitamins.

Thiamine (vitamin B_1) is an essential co-enzyme involved in biomass generation, amino acid catabolism, and energy production. The most important function of thiamine is its role as a co-enzyme for pyruvate dehydrogenase, the enzyme that prepares pyruvate to enter the Krebs cycle [290]. It also functions as a coenzyme for transketolase, which is active in two steps of the pentose shunt, and therefore affecting nucleotide synthesis. Although thiamine is usually supplemented in the culture medium as thiamine hydrochloride, it must be phosphorylated before being taken up by cells. The most active form of this vitamin inside the cell is thiamine-diphosphate or thiamine pyrophosphate (TPP) [274].

Riboflavin (vitamin B_2) acts as an electron acceptor in the oxidative metabolism of carbohydrates, amino acids and fatty acids [482]. Recent studies show that riboflavin plays a role in the oxidative folding of proteins in the ER [289]. Upon cellular uptake, this vitamin is immediately phosphorylated to flavin mononucleotide (FMN) and then is further metabolized to flavin adenine dinucleotide (FAD), which are the two active co-enzyme forms of this vitamin [482].

Niacin (vitamin B_3), which is also known as nicotinamide or nicotinic acid, are used in the biosynthesis of NADPH and NADH [142] NAD^+ and NADH are crucial for energy generation and in regulating numerous enzymes of energy metabolism. On the hand, NADPH is essential in maintaining the antioxidant state and reductive biosynthesis inside the cell. Additionally, numerous enzymes use NAD^+ or $NADP^+$ as a substrate for post-translational modification of proteins and to synthesize small signaling molecules [199].

Pantothenic acid (vitamin B_5) is a precursor for production of CoA [256]. CoA acts as a carboxylic acid substrate carrier and supports many essential biochemical transformations, including the activities of the citric acid cycle, sterol biosynthesis, amino acid metabolism, and the synthesis and degradation of fatty acids and complex lipids [93, 533]. Pantothenic acid is usually supplied in the culture medium in the form of calcium-pantothenate but is

rapidly phosphorylated upon cellular uptake by pantothenate kinases. The production of phosphopantothenate is a key regulatory step of CoA biosynthesis.

Vitamin B_6 is the collective term for a family of six compounds including pyridoxine, pyridoxal, pyridoxamine, and their corresponding phosphorylated derivatives [369]. Vitamin B_6 is a coenzyme necessary for a large number of enzymes that are involved in amino acid, lipid or carbohydrate metabolic pathways. Recent evidence suggests that B_6 vitamins function as potent antioxidants, metal chelators, photosensitizers, and carbonyl scavengers [508]. Vitamin B_6 is usually supplied to the culture medium as pyridoxine hydrochloride or pyridoxal hydrochloride, but pyridoxal-5'-phosphatase (PLP) is the cofactor form of the vitamin the cell uses [213]. Recent studies showed that intracellular PLP levels do not change significantly when cells are cultured in medium containing different species of the vitamin, indicating that cells do not appear to have a preference of which species of Vitamin B_6 is supplemented in the medium [213].

Biotin (vitamin B_7 or vitamin H) functions as coenzyme for various carboxylases involved in metabolic pathways including gluconeogenesis, fatty acid biosynthesis and catabolism of assorted odd-chain fatty acids and branched chain amino acids [534]. It has also been reported that biotin is involved in the regulation of gene expression of specific membrane transporters and in the regulation of intracellular cyclic guanosine monophosphate (cGMP) levels [405]. Furthermore, the role of this vitamin in histone modification (via biotinylation) was also recently shown. This function may be important for cell proliferation and DNA repair. Since animal cells cannot synthesize this micronutrient, biotin is regularly supplemented to the growth medium as D-biotin isomers [534].

Folic acid (vitamin B_9) transfers one carbon unit from donor molecules to various intermediates in the synthesis of DNA and in biological methylation reactions, including the methylation of DNA, proteins, and phospholipids [540]. Therefore, it is implicated

in the regulation of gene expression, transcription, chromatin structure, genomic repair and genomic stability. The biologically active form of this vitamin is tetrahydrofolate (THF), which is activated as THF-polyglutamates inside the cell. Since this vitamin is not synthesized by mammalian cells, it must be provided by the culture medium and is usually provided in the cell culture medium as folic acid.

Cobalamin (vitamin B_{12}) consists of a corrinoid structure with cobalt in the center of the molecule [27]. There are only two forms of cobalamin that have biological activity as cofactors in enzymatic reactions. These are adenosylcobalamin (AdoCbl) and methylcobalamin (MeCbl) [391]. The AdoCbl is involved in isomerization of methylmalonyl-CoA to succinyl-CoA as a co-factor for the enzyme methylmalonyl-CoA mutase in mithochondria. The MeCbl functions as a cofactor in synthesis of methionine from homocysteine by the cytosolic enzyme methionine synthase [228]. Neither humans nor animals are able to synthesize cobalamin; therefore this vitamin must also be provided to the cell culture medium.

There are different studies on the effect of addition of vitamin B groups in the cell culture medium. Vitamin enrichment was reported to be necessary for formulating a serum-free medium able to support high cell density [442]. For a CHO cell line producing a recombinant antibody, the serum-free culture medium was supplemented with twelve water soluble vitamins (biotin, D-calcium pantothenate, choline chloride, cyanocobalamin, folic acid, i-inositol, niacinamide, pyridoxal·HCl, riboflavin, thaimine·HCl, ascorbic acid) and the researchers were able to obtain a higher maximum specific growth rate compared to basal medium [222]. They also showed that with the fortification of choline chloride and folic acid, specific antibody productivities were similar to that obtained from the basal protein-free medium; however the integrals of viable cell density were higher than the control, which resulted in increased final antibody concentrations. Thiamine fortification

of the medium has also shown higher antibody productivity; however, the negative effect of the vitamins on the quality of the product must also be considered for group B vitamins. Group B vitamins (especially vitamins B_2, B_6 and B_{12}) may also result in an undesired color of the final products, which is an attribute of product quality. There are various reports of red, pink and brown colors of the final products due to the presence of vitamin B_{12} [97]. For example, in a case study, Xu *et al.*, mentioned a brown color in the final formulated drug substances [516]. They revealed this brown color was caused by the cell culture medium containing high concentrations of iron and vitamin B_{12}. Iron caused yellowing through oxidizing tryptophan in the protein to form N-formylkynurenine and kynurenine products. A pink color was caused by residual vitamin B_{12} bound to the final drug substance, and the brown color was the result of the combinatory effect of yellow and pink colors. In another study, Vijayasankaran *et al.* showed that lowering the concentration of the group B vitamins in culture medium could result in 25% reduction in color intensity of the final formulated product [489].

Table 2.5: List of vitamins, their use and associated proteins for mammalian cells. (*indicates lipid soluble vitamin, ** indicates not a true vitamin, but included here because of their importance for growth)

Vitamin	**Use**	**Associated Proteins**	**Ref**
Ascorbic Acid (Vitamin C)	Cofactor in enzymes, antioxidant, reducing agent	Prolyl hydroxylase, ascorbate peroxidase	[19, 129, 167, 329, 336, 361]
Biotin (Vitamin B_7)	Cofactor in enzymes, precursor to biocytin	Acetyl-CoA Carboxylase (ACC), propionyl-CoA carboxylase, pyruvate carboxylase, β-methylcrotonyl-CoA carboxylase	[493, 534]
Choline Chloride**	Phospholipid head group	OCT1-3, CHT1, CTL1-5	[196]
Cobalamin (Vitamin B_{12})	Cofactor, recycling folate, regulation of homocysteine	Methyltransferases, methionine synthase, isomerases, reductive dehalogensases	[27, 228, 391]
Folate (Vitamin B_9)	Precursor for tetrahydrofolate, serine and glycine metabolism, histidine catabolism, thymidylate synthesis, methionine synthesis, purine synthesis	Folate receptors (FOLR1-3), γ-glutamyl-hydrolase, folylpolyglutamate synthetase	[228, 540]
ι-inositol** (myo-inositol)	Phospholipid precursor, cell signaling, insulin signaling	Inositol kinases, inositol 1-phosphatase	[61, 181, 186, 223]
Niacin (Niacinamide, Nicotinamide, Nicotinic acid, Vitamin B_3)	Precursor to NAD^+ and $NADP^+$, repair DNA damage, energy metabolism, inhibits specific kinases	Nicotinamide phosphoribosyltransferase, nicotinamide mononucleotide adenylyltransferase	[142, 318, 465]
D-Ca-Pantothenate (Vitamin B_5)	Precursor to CoA and proteins with a phosphopantetheine prosthetic group	Coenzyme A (CoASH or CoA), pantothenate kinases	[93, 256]
Pyridoxine, pyridoxal, pyridoxamine (Vitamin B_6)	Precursor to PLP and pyridoxamine-5-phosphate, protein folding chaperone, degradataion of amino acids, critical for epinephrine, dopamine and serotonin production	Phosphorylase, albumin, aminolevuliniv acid synthase	[302, 369]

Continued on next page

Table 2.5: List of vitamins, their use and associated proteins for mammalian cells. (*indicates lipid soluble vitamin, ** indicates not a true vitamin, but included here because of their importance for growth)

Vitamin	**Use**	**Associated Proteins**	**Ref**
Riboflavin (Vitamin B_2)	Precursor FAD and FMN, protects from oxidative stress and apoptosis	Flavin enzymes, flavin proteins, electron transfer flavoprotein, NADH-Coenzyme Q reductase, transporters SLC52A1-3, SLC25A32	[382, 482]
Thiamine (Vitamin B_1)	Precursor for TPP, catalyst in pentose and hexose monophosphate pathways, antioxidant	Pyruvate dehydrogenase complex, α-ketoglutarate dehydrogenase, transketolase, thiamin pyrophosphate 1, transporters SLC19A1-3	[274, 290]
*Vitamin A (Retinol)	Precursor for retinoids and carotenoids, antioxidant, cellular signaling (JAK2, STAT3/5)	Retinoic acid receptors, retinoic X receptors, retinoic binding protein, retinal dehydrogenases, transtheyretin, albumin, transporter STRA6	[183, 262, 349]
*Vitamin D (Calciferol)	Regulates Ca^{2+} and Cl^- channels, regulates gene transcription via vitamin D response elements in promoter regions, regulates parathyroid hormone secretion, insulin secretion, fibroblast growth factor	Vitamin D binding protein, vitamin D receptor, albumin, 25-hydroxylase (CYP2R1, CUP27B1)	[43]
*Vitamin E (α-tocopherol is the most studied member)	Antioxidant, plasma membrane repair and stabilizer	Chylomicrons, tocopherol binding proteins	[137, 191, 344]
*Vitamin K_1 (phylloquinone), *Vitamin K_2 (menaquinone), *Vitamin K_3 (menadione)	Cofactor for γ-carboxyglutamyl carbosylase	Vitamin K proteins (PRGP1, PRGP2), chylomicrons, γ-glutamylcarboxylase, Vitamin K reductases	[356, 431]

2.1.6 Purines and Pyridines

Purines and pyrimidines are aromatic organic compounds that are the nitrogenous bases for nucleotides. Purines consist of adenine, guanine, hypoxanthine, xanthine and uric acid. Cytosine, thymine and uracil are pyrimidines. The ability of cells to produce nucleotides from purines and pyrimidines is crucial for DNA and RNA synthesis, cell replication and protein production. Cells need to replicate their DNA to pass on genetic information to its daughter cells, and RNA to send information from the nucleus to the cytoplasm. Purines are not only used for DNA and RNA synthesis, but also the phosphorylation of proteins. ATP is used to transfer energy in the cell and donates a phosphate group to release energy that drives hundreds of reactions, ion transport, protein folding and movement within the cell [490]. Guanosine triphosphate (GTP) also participates in cellular reactions by causing conformational changes in proteins rendering them in the active or inactive state. When cells lack purines and pyrimidines in the media, they must make them from other compounds such as amino acids. This requires energy from the cell and diverts resources from other pathways, which can slow cell growth.

Most basal mediums contain hypoxanthine and thymidine in varying concentrations, and M-199 contains the highest amounts of purines and pyrimidines. Hypoxanthine is a versatile purine that can be converted into any of the other purines and is easily soluble in water, making it a good choice as a media additive [480]. Other purines and pyrimidines are supplemented into basal mediums through serum, yeast or plants extracts, which contain undefined amounts of these compounds. ATP, hypoxanthine, and guanine are purines that are in the highest abundance in cell culture, FBS and yeast extract [174, 275, 480]. Fenselau *et al.*, demonstrated that adding deoxyribo- or ribonucleosides to M-199 media increased cell growth of fetal bovine aortic endothelial cells [124]. The largest increase in

cell growth occurred when deoxycytidine and deoxyuridine were used together.

Although cells can make their own purines and pyrimidines from other sources, it is easier for the cell to acquire the purines/pyrimidines from the media rather than producing them through a biosynthetic pathway [436]. Work with CHO cells showed that adding hypoxanthine and thymidine (HT supplements) can increase the cell density in protein free media [34, 436].

2.1.7 Osmolarity

An important consideration in SFM design is the overall concentration of solute, referred to as the medium osmolarity or osmolality. The amount of solute determines the osmotic pressure of a solution, and the balance between intracellular osmotic pressure and that of the medium is important for cell health. Osmotic pressure imbalances impair the cells ability to maintain homeostasis, and negatively influences water flux and cell size [51]. Animal cell culture osmolality is typically kept between 260 and 320 mOsm/kg to mimic physiological conditions (human blood serum is approximately 290 mOsm/kg) [133], although optimal levels may vary between cell lines and types [500]. It is well established that both hypoosmotic [418] and the more commonly encountered hyperosmotic [20, 169, 360] conditions slow or halt cell growth. The degree to which cell growth is altered depends on the magnitude of deviation from physiological osmolarity and differs between cell types. An osmolality of 435 mOsm/kg has been shown to approximately halve growth rate in both CHO and hybridoma cell lines [101]. A separate study found that CHO cells were not significantly affected by osmolality increasing from 320 to 390 mOsm/kg, but further increases led to a sharp reduction in growth rate [240]. Hyperosmotic conditions are particularly an issue in fed-batch processes and processes requiring pH adjustments [171, 343],

which are common in industry. In some mammalian cell cultures, hyperosmotic media has been demonstrated to improve specific protein productivity [225, 360] and as such may be a desirable trait when designing production media. Specific productivity improvement may be coupled with the use of an osmoprotective additive in an effort to achieve both high growth and productivity. A variety of compounds have been demonstrated to act as strong osmoprotectants in hybridoma cell lines, including: glycine betaine, sarcosine, proline, glycine, and asparagine [101, 358]. Øyaas *et al.* demonstrated that glycine betaine was effective at mitigating hyperosmotic growth reduction while maintaining high antibody productivity in mouse hybridoma cells [358]. In CHO cells, the effect of glycine betaine on hyperosmotic protein production was shown to vary greatly between recombinant CHO cell lines [417]. This variation is due to glycine betaine reducing specific protein productivity while overcoming hyperosmotic stress. Kim *et al.* tested similar conditions for thrombopoietin (TPO) production in 23 recombinant CHO cell lines. Hyperosmotic conditions increased specific TPO productivity and glycine betaine acted as an osmoprotectant in all cell lines, however only 6 of the lines achieved a significant (greater than 40%) increase in maximum TPO titer compared to physiological controls [466].

Considering the relatively wide range of acceptable growth medium osmolarity, media design based on examples outlined in this review will likely not encounter osmotic stress related issues. However, osmolarity should be monitored and kept consistent to reduce potential batch-to-batch growth variability. Specific applications or operating conditions may require more careful consideration of culture osmolarity. In certain cases, osmoprotective compounds should be considered for use as media additives.

2.2 Summary

Overall, cell culture media are a complex mixture of compounds that interact with and influence each other as well as with the cells. The recent advances in media technology has allowed the creation of chemically defined media to reduce researchers dependence on undefined supplements that can vary from lot-to-lot. While serums and plant hydrolysates offer a convenient source of growth inducing compounds and proteins, the variability between batches can create undesirable outcomes, such as low yields and poor product quality. The benefit of having a chemically defined media is consistency, along with controlling the environment that the cells are cultured in to have reproducible results and high quality products.

This review offers a summary of the past five decades of media research along with descriptions of the more important components in media. We show what improvements have been made to basal media first created in the 1970's to replace serum, and compare suspension to adherent SFM formulations to highlight the key changes made to media to obtain a suspension phenotype. Altogether, this work provides a starting formulation in Appendix A for a chemically defined SFM such that researchers can modify and further improve media formulations.

Chapter 3

The Development of a Chemically Defined Media for Mammalian Cells in Suspension

3.1 Introduction

The single cell suspension phenotype is a sought after characteristic of biopharmaceutical production cell lines. Cells adapted for suspension growth can simplify scale-up and manufacturing workflows compared to anchorage-dependent cells. Further, since higher cell densities are often achieved with cells in suspension than in adherent culture, volumetric productivity may be improved. However, transitioning from an anchorage-dependent phenotype to single cell suspension can be incredibly challenging to achieve. Cell adhesion plays a crucial role in several cellular processes; cell adhesion molecules (CAMs) on the surface of the cell interact with other cells and the extracellular matrix (ECM) to detect

and respond to changes in the environment by directing signalling cascades within and between cells. These signalling cascades have important roles in cell proliferation, motility, contact inhibition, and apoptosis, and aberrant cell adhesion is linked with several disease processes including cancer [76, 68, 270, 335]. Nevertheless, these challenges have been overcome and many animal cell lines have been adapted to growth in suspension including HeLa [201], Madin-Darby canine kidney (MDCK) [487], human embryonic kidney (HEK293) [311], baby hamster kidney (BHK21) [487], Chinese hamster ovary (CHO) [165], and HepG2 [42]. Adaptation has traditionally involved modifying or completely changing the growth medium and gradually transitioning from static tflasks to shaker flasks over long periods of time.

Classical cell culture media is commonly comprised of a basal medium that is supplemented with animal serum such as fetal bovine (or calf) serum (FBS or FCS) or horse serum. The basal medium includes essential nutrients such as carbohydrates, amino acids, vitamins, and minerals, whereas the serum component consists of the aforementioned nutrients and proteins, growth factors, hormones, and other molecules important for cell proliferation [351]. Serum also contains components of the ECM such as vitronectin and fibronectin which are important binding partners of CAMs. Significantly, previous studies have suggested that these molecules can coat the walls of flasks and provide a support structure that cells can anchor themselves to [524, 452]. While this might be mitigated by siliconizing glass vessels prior to their use, this strategy is likely limited to lab bench scale experiments in research environments. Alternatively, reducing the amount of serum in the media has supported growth of cells in suspension in some cases; for example, HEK293 cells grown in a commercial medium developed for suspension culture and supplemented with 2% FCS were successfully adapted to suspension culture in spinner flasks and stirred-tank reactors (STRs) [311]. Large aggregates of cells ($>$ 200 cells/aggregate) were observed;

however, they were subsequently reduced to 5 cells/aggregate by reducing the FCS to 1%.

Despite the important contribution of serum components to cellular processes, several disadvantages have relegated serum-containing media as undesirable for manufacturing therapeutics; in addition to the cell aggregation in suspension, batch-to-batch variation and the poorly defined concentrations of bioactive components in serum can cause inconsistent cell growth [351]. Further, serum represents an important source of contamination with adventitious agents, and some constituents of serum may interact with other media additives to form toxic compounds [351]. As a result, development of suspension cell lines has largely been integrated with development of serum-free medium (SFM) formulations in parallel. As noted, however, serum contains important components that interact with CAMs, and their removal may impact important cellular processes. Design of experiments (DoEs) are commonly used to rapidly identify important factors for serum replacement in medium formulations [415, 535, 249]. Common designs include fractional factorials that can screen many compounds simultaneously whilst identifying interaction effects between compounds. This approach is faster than performing one-factor at a time experiments, however iterative experiments are often required to achieve an optimized medium formulation.

Previously, a SFM formulation developed through mixing various basal media and other components (e.g., HEPES, insulin, bovine serum albumin, serum replacement concentrate) supported growth of Vero cells in suspension, however they could only be grown as large aggregates [269]. More recently, van Wielink *et al.* attempted to use a commercial SFM medium (SFM4BHK21) that supported MDCK and BHK-21 suspension growth, but found that Vero cells would form small aggregates but not grow in suspension in this medium [487]. Nevertheless, research efforts devoted to developing suspension Vero cell lines continued, and very recent reports are beginning to show the importance of these efforts; an

in-house medium (IPT-AFM) was used to successfully adapt Vero cells to single cell suspension in 2019. These cells were also able to replicate rabies virus. Notably, a higher specific productivity was achieved for suspension Vero cells (3.75 ±1 fluorescent focus unit (FFU)/cell/day), compared to adherent Vero cells grown on microcarriers in IPT-AFM (2.5 ±0.8 FFU/cell/day) [415, 412]. Shen *et al.*, also recently reported a single cell suspension Vero cell line using a separately developed in-house medium (IHM03) and produced vesicular stomatitis virus (VSV) in a 3 L bioreactor [433]. They showed three times improved volumetric productivity for VSV production in suspension compared to Vero cells grown in Tflasks. Most recently, Lee *et al.*, reported that Vero cells were adapted to suspension over 150 days using OptiPRO™ SFM, and were permissive to infection with an adenovirus type 5 virus [248]. While these reports represent improvements for Vero cell-based vaccine manufacturing, the cells grew at approximately half the rate compared to serum-containing media, adding significant time to the bioprocess duration. Additionally, all the media formulations contained undefined plant hydrolysates or peptones, which also suffer from batch-to-batch variability and may lead to inconsistent product yield or quality [304]. A fully chemically defined medium formulation that is capable of supporting growth of Vero cells in single cell suspension would drastically improve vaccine manufacturing using Vero cells.

In this study, a chemically defined medium that supports the growth of adherent Vero cells was developed. Significantly, recombinant epidermal growth factor (rEGF) was an essential growth factor for Vero cells and the addition of trace metals was essential for cell growth and viability. Unexpectedly, Vero cells were able to adhere to non-treated Tflasks in the presence of typical calcium and magnesium concentrations (i.e., 1mM and 0.7 mM, respectively), whereas other cell lines (i.e., CHO-K1, MDCK and HEK293T) were successfully adapted to suspension in this formulation. This may suggest that the

underlying biology of the Vero cell may play a large role in its recalcitrance toward a single cell suspension phenotype. A 10× decrease of the concentration of calcium and magnesium was required to encourage anchorage-independence, however the growth of Vero cells in suspension was dramatically reduced. This is significant because, the development of a chemically defined medium formulation for Vero cells represents a large step toward improving Vero cell vaccine manufacturing bioprocesses.

3.2 Materials and methods

3.2.1 Cell culture

Vero (CCL81 n+51, ATCC) and CHO-K1 cells (gift from Dr. Pu Chen, University of Waterloo, Canada) were maintained in DMEM/F12 + 10% FBS + 4 mM GlutaMax, whereas MDCK and HEK293T cells (gifts from Dr. Matthew Miller, McMaster University, Canada) were maintained in DMEM + 10% FBS. All cell lines were maintained in a humidified, 5% CO_2 incubator at 37°C, and cells were passaged when the cells were 80-90% confluent. Cells were detached from the culture vessel by using TrypLE™ Select for 3-5 minutes and the trypsinization was stopped using defined soy bean trypsin inhibitor. The cells were pelleted at 100×g for 5 minutes, and then the supernatant was discarded and the cells were resuspended in the appropriate medium formulation. The cells were counted by diluting the cell sample 1:1 with trypan blue dye and counted using a Countess II. After taking the counts, the cells were seeded at the appropriate cell density, and placed into a clean T25 Tflask with a final volume of 5 mL.

Commercial cell lines (HEK293T, MDCK, and CHO-K1) were adapted to suspension medium (CDM2, CD CHO, 293 SFM II, or OptiPRO™ SFM) by first thawing the cells in

serum-containing medium for 3 passages, and then 25% of the serum-containing medium was replaced with suspension medium in tissue culture treated T flasks. The cells were grown in this 25% CDM2/ 75% serum-containing medium until they achieved their normal doubling time. Once this was accomplished the cells were adapted to 50% CDM2/50% serum-containing medium and cultured until they achieved their normal doubling time. This sequential reduction of serum in the medium was continued until the cells were in medium that contained 10% serum-containing medium and 90% suspension medium. The cells were then transferred to 125 mL shaker flasks with vented caps. The cells were then placed on an orbital shaker at 80 rpm at 300,000 cells/mL. Cells were allowed to grow to a density of 10^6 cells/mL and then they were passaged until their achieved a similar doubling time as their adherent phenotype. The amount of serum was further reduced until the cells were fully adapted to the serum-free suspension medium.

3.2.2 Media development

Unless otherwise stated, all compounds were obtained from Sigma-Aldrich. All media formulations used DMEM/F12 with 15 mM HEPES, without L-glutamine, L-leucine, L-lysine, L-methionine, $CaCl_2$, $MgCl_2$, $MgSO_4$, sodium bicarbonate, and phenol red as the base medium (catalogue #D9785, Sigma-Aldrich, USA).

Plackett-Burman design of experiments

To screen compounds, a Plackett-Burman style of experiment design was used with 24 media samples that tested 23 different compounds (example experimental layout in Table 3.1). To make the media, concentrated stock solutions of each compound were made using ultra pure MilliQ water. DMEM/F12 with 15 mM HEPES, without L-glutamine,

L-leucine, L-lysine, L-methionine, $CaCl_2$, $MgCl_2$, $MgSO_4$, sodium bicarbonate, and phenol red was made from a pre-mixed powder using ultra pure MilliQ water (< 18.2 MΩ-cm) in 1 L batches. 40 mL of each medium formulation was made by supplementing DMEM/F12 with the various compounds, without increasing the volume more than 10%.

Vero cells were adapted to the new media formulations over 28-90 days in treated T25 flasks, for Placket-Burman experiments #1-3, the experiments were stopped after they were cultured in 100% of the new medium formulation for approximately 3 passages. For Plackett-Burman experiment #4, once the cells were fully adapted (100% new medium formulation), they were then cultured in non-treated T25 flasks for an additional 90 days. After 180 days, the T flasks were slowly shaken (40 rpm) to dissociate cell aggregates. Media samples that were able to support viable cells were cultured and all others were discontinued.

3.2.3 Data Analysis

R (version 4.1.1) and RStudio were used to perform the data analysis along with the packages ggplot2, tidyverse and RColorBrewer. Briefly, cell count and viability data was exported as a CSV file from the Countess II, which also included timestamp and cell size data. The data was then loaded into the RStudio environment and the doubling time and growth rate were calculated using the following equations, where N is the cell number, t is time the count was acquired and the subscript 0 indicates the starting time, or cell number:

Growth Rate:

$$\mu = \frac{ln(N_t/N_0)}{(t - t_0)}$$

Doubling Time:

$$t_D = \frac{ln(2)(t - t_0)}{ln(N_t/N_0)}$$

Table 3.1: An example layout of a 23 factor (A-W) Plackett Burman experiment with 24 runs.

Run	**A**	**B**	**C**	**D**	**E**	**F**	**G**	**H**	**I**	**J**	**K**	**L**	**M**	**N**	**O**	**P**	**Q**	**R**	**S**	**T**	**U**	**V**	**W**
1	1	1	1	1	1	-1	1	-1	1	1	-1	-1	1	1	-1	-1	1	-1	1	-1	-1	-1	-1
2	-1	1	1	1	1	1	-1	1	-1	1	1	-1	-1	1	1	-1	-1	1	-1	1	-1	-1	-1
3	-1	-1	1	1	1	1	1	-1	1	-1	1	1	-1	-1	1	1	-1	-1	1	-1	1	-1	-1
4	-1	-1	-1	1	1	1	1	1	-1	1	-1	1	1	-1	-1	1	1	-1	-1	1	-1	1	-1
5	-1	-1	-1	-1	1	1	1	1	1	-1	1	-1	1	1	-1	-1	1	1	-1	-1	1	-1	1
6	1	-1	-1	-1	-1	1	1	1	1	1	-1	1	-1	1	1	-1	-1	1	1	-1	-1	1	-1
7	-1	1	-1	-1	-1	-1	1	1	1	1	1	-1	1	-1	1	1	-1	-1	1	1	-1	-1	1
8	1	-1	1	-1	-1	-1	-1	1	1	1	1	1	-1	1	-1	1	1	-1	-1	1	1	-1	-1
9	-1	1	-1	1	-1	-1	-1	-1	1	1	1	1	1	-1	1	-1	1	1	-1	-1	1	1	-1
10	-1	-1	1	-1	1	-1	-1	-1	-1	1	1	1	1	1	-1	1	-1	1	1	-1	-1	1	1
11	1	-1	-1	1	-1	1	-1	-1	-1	-1	1	1	1	1	1	-1	1	-1	1	1	-1	-1	1
12	1	1	-1	-1	1	-1	1	-1	-1	-1	-1	1	1	1	1	1	-1	1	-1	1	1	-1	-1
13	-1	1	1	-1	-1	1	-1	1	-1	-1	-1	-1	1	1	1	1	1	-1	1	-1	1	1	-1
14	-1	-1	1	1	-1	-1	1	-1	1	-1	-1	-1	-1	1	1	1	1	1	-1	1	-1	1	1
15	1	-1	-1	1	1	-1	-1	1	-1	1	-1	-1	-1	-1	1	1	1	1	1	-1	1	-1	1
16	1	1	-1	-1	1	1	-1	-1	1	-1	1	-1	-1	-1	-1	1	1	1	1	1	-1	1	-1
17	-1	1	1	-1	-1	1	1	-1	-1	1	-1	1	-1	-1	-1	-1	1	1	1	1	1	-1	1
18	1	-1	1	1	-1	-1	1	1	-1	-1	1	-1	1	-1	-1	-1	-1	1	1	1	1	1	-1
19	-1	1	-1	1	1	-1	-1	1	1	-1	-1	1	-1	1	-1	-1	-1	-1	1	1	1	1	1
20	1	-1	1	-1	1	1	-1	-1	1	1	-1	-1	1	-1	1	-1	-1	-1	-1	1	1	1	1
21	1	1	-1	1	-1	1	1	-1	-1	1	1	-1	-1	1	-1	1	-1	-1	-1	-1	1	1	1
22	1	1	1	-1	1	-1	1	1	-1	-1	1	1	-1	-1	1	-1	1	-1	-1	-1	-1	1	1
23	1	1	1	1	-1	1	-1	1	1	-1	-1	1	1	-1	-1	1	-1	1	-1	-1	-1	-1	1
24	-1	-1	-1	-1	-1	-1	-1	-1	-1	-1	-1	-1	-1	-1	-1	-1	-1	-1	-1	-1	-1	-1	-1

3.3 Results

3.3.1 Medium component screening using Plackett-Burman design of experiments

The Plackett-Burman DoE was selected for component screening experiments because it allows for the evaluation of the largest number of factors using the smallest number of possible formulations. Cell culture media and serum are very complex mixtures often contain over 90 compounds, and replacement of serum requires supplementation of many compounds simultaneously. The curated list of compounds and their appropriate concentrations compiled and described in Chapter 2 informed the Plackett-Burman design space. In total, 60 compounds in 96 different medium formulations were tested over four experiments. The compounds and the concentrations at low (-1) and high (+1) levels are listed next to the results of each Plackett-Burman experiment (Figures 3.1, 3.3, 3.5, and 3.7).

After Plackett-Burman experiment #1, cells were first grown in OptiPRO™ SFM, to reduce the adaptation time, and then adapted to the media formulations for the experiment. OptiPRO™ SFM is a serum-free medium that is commonly used to grow Vero cells and it is animal origin-free which makes it good for biomanufacturing.

Plackett-Burman DoE #1

The main effects plot and significant factors for DoE #1 are presented in Figure 3.1 and listed in Table 3.2, respectively. In this experiment, 17 of 22 factors were identified as significant ($p<0.1$); the non-significant factors were biotin, dexamethasone, the amino acids arginine and glutamine, and recombinant human serum albumin (rHSA). Moreover, recombinant epidermal growth factor (rEGF) was the most significantly positive factor,

whereas serine, cholesterol, and the vitamin C+ferric citrate combination were identified as negative factors with similar coefficient estimates (Table 3.2). The high levels of calcium+magnesium and selenite showed a slight improvement in viable cell density (VCD), while zinc, copper and the vitamin C+ferric citrate combination had negative effects overall. Calcium+magnesium had the second most significant positive impact on VCD, however reducing the concentration to $1/10^{\text{th}}$ of the typical level supplemented in DMEM/F12 medium drastically reduced cell viability and growth.

The growth factor supplements insulin, transferrin and selenite supplement (ITS) and rEGF showed positive effects. Significantly, data suggested that cells were unable to maintain viability without rEGF regardless of the overall medium formulation. This observation was supported by analysis of the main effects of the designed experiment, which identified rEGF as the most significant compound tested (Table 3.2). Therefore, it was included in all future experiments. Since ITS was a mixture of insulin, transferrin and selenite, it is unclear which of the individual compounds had a positive impact or if the impact was due to a combination of the three. The results also indicated that selenite (Na_2SeO_3) by itself had a positive effect, although the coefficient is smaller than ITS (16,033 versus 23,195, Table 3.2), which indicates that insulin and/or transferrin may have a positive contribution as well.

The addition of L-arginine and L-glutamine did not improve or have a significant impact on the VCD whereas L-serine and the non-essential amino acid supplement had significantly negative effects. The addition of different carbon sources such as galactose and pyruvate did have a positive effect.

Similar mixed results were seen with vitamins. Vitamin B_{12} had a significant negative impact, while α-tocopherol had a significant positive impact, and D-biotin had no significant impact. Vitamin C also appeared to have a negative effect, however it mixed with

ferric citrate, so the overall impact of each constituent was confounded.

Interestingly, there were mixed results depending on the type of lipid supplement that was used. The cholesterol concentrate (250x, Gibco™) had a negative impact whereas the chemically defined lipid supplement (100x, Millipore Sigma) showed a slight improvement in VCD. The formulation for the cholesterol concentrate by Gibco™ is unknown, and therefore the reason why the supplement had a negative impact on cell growth is unknown. The formulation for the chemically defined lipid supplement by Sigma is listed in Supplementary Table B.1. The supplement contains cholesterol, many of the fatty acids that were identified in Chapter 2 and Pluronic™ F-68; Pluronic™ F-68 was also found to have a significantly positive effect on the VCD of Vero cells.

Overall, this data supported inclusion of Chemically Defined Lipid Mixture 1 supplement, Pluronic™ F-68, pyruvate, and rEGF at their respective high levels in further medium formulations. Additionally, selenite, α-tocopherol, ethanolamine, and the high level of biotin appeared to improve VCD and as such were selected as candidates to be retested at different concentration levels.

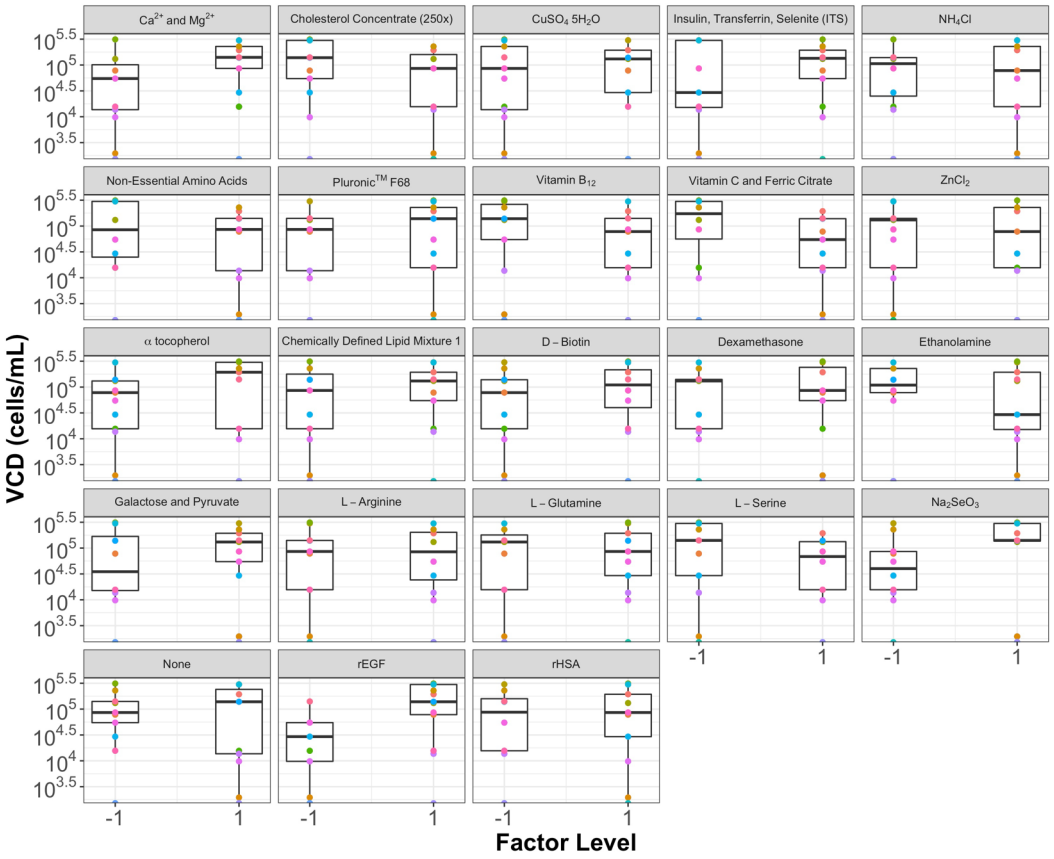

Compound		-1 (mM)	1 (mM)
L-Arginine		0.7	5.7
D- Biotin		0.00001	0.00011
Calcium + Magnesium	$CaCl_2$	0.1	1
	$MgCl_2$	0.03	0.3
	$MgSO_4$	0.18	1.8
Cholesterol Concentrate (250x)		5% (v/v)	15% (v/v)
$CuSO_4$ $5H_2O$		5.2×10^{-6}	0.00052
Dexamethasone		0	0.001
Ethanolamine HCl		0	0.023
Galactose + Pyruvate	Galactose	0	5
	Pyruvate	0.5	1.5
L-Glutamine		2.5	4
Insulin, Transferring and Selenite (ITS)		0	10% (v/v)
Chemically Defined Lipid Mixture 1		0	10% (v/v)
Non-Essential Amino Acids (NEAA)		0	10% (v/v)
NH_4Cl		0	4
None		0	0
Pluronic™ F68		0	0.02 % (w/v)
Recombinant Human Epidermal Growth Factor (rEGF)		0	0.00002
Recombinant Human Serum Albumin (rHSA)		0	0.0025 g/mL
Na_2SeO_3		0	0.0003
L-Serine		0.25	2.25
α-tocopherol acetate		1.2×10^{-5}	3.2×10^{-4}
Vitamin C + Ferric Citrate	Vitamin C	0	0.1
	Ferric Citrate	0	0.3
Vitamin B_{12}		0.0005	0.001
Zinc ($ZnCl_2$)		0.0015	0.0055

Figure 3.1: The results from the first Plackett-Burman media screening experiment. The concentrations for each component at the high (+1) and low (-1) levels are listed in the table and the viable cell density (VCD) is on the y-axis of each of the plots. Vero cells were adapted to the media over 14 days and then grown for another 14 days in the various media. The VCD is from day 28 of the experiment.

Table 3.2: List of significant (p<0.1) main effects of the first Plackett-Burman experiment.

	Coefficient Estimate	t value	Pr(> $\|t\|$)
(Intercept)	85412.5184	13.2616929	1.15E-17
rEGF	64408.7617	10.0005156	2.53E-13
Ca^{2+} and Mg^{2+}	33956.1451	5.27224789	3.17E-06
L-Serine	-31658.382	-4.9154825	1.07E-05
Vitamin C and Ferric Citrate	-29888.917	-4.640744	2.71E-05
Cholesterol Concentrate (250x)	-28226.806	-4.3826742	6.36E-05
ITS	23195.3042	3.60145102	0.00074863
Pluronic™ F-68	22067.8211	3.4263908	0.00126307
Chemically Defined Lipid Mix 1	16871.0418	2.61950566	0.01175218
Na_2SeO_3	16033.6804	2.48949159	0.01631041
α-tocopherol	14727.9863	2.28676118	0.02666185
NH_4Cl	13128.6021	2.03843058	0.04703624
Vitamin B_{12}	-13106.015	-2.0349235	0.04740159
$ZnCl_2$	-12785.832	-1.9852099	0.052851
Galactose and Pyruvate	11826.3978	1.83624203	0.0725194
Ethanolamine	11648.8161	1.80866956	0.07676845
$CuSO_4 \cdot 5H_2O$	-11463.922	-1.7799616	0.08141298
Non-Essential Amino Acids	-11166.734	-1.7338184	0.0893698

Plackett-Burman DoE #2

The second experiment focused on increasing the concentrations of amino acids, incorporating key trace metals such as molybdenum, nickel, selenium and vanadium, increasing glucose, and adding additional vitamins. Twenty-four formulations were used to screen 23 compounds listed in Figure 3.3. The calcium and magnesium levels were kept at 0.1 mM and 0.21 mM (respectively) to encourage suspension growth. All the formulations with the exception of Formula 8 stopped growing when the concentration of OptiPRO™ SFM was lower than 50% (Figure 3.2). The recipe for Formulation 8 is in Appendix B.

Significantly, after 40 days of culture only formulations 8 and 20 showed slight growth. Interestingly, the cells in Formulation 8 appeared to be partially in suspension (Figure 3.2). After 75 days, however, the Vero cells had adapted to adherent growth in the low calcium and magnesium conditions (Figure 3.4 left panel). To encourage adaptation to suspension growth, these cells were additionally sub-cultured to non-treated T25 flasks, and either shaken or allowed to remain static (Figure 3.4). The non-treated Tflasks prevented most of the cells from adhering to the surface of the flask, whereas the cells in the shaken Tflask remained detached from the surface. The cells formed aggregates in suspension but eventually stopped growing, and on day 97 the culture was stopped, since it had 44% viability and a cell density of 5.28×10^4 cells/mL.

The main effects plot is presented as Figure 3.3, but since the VCDs were so low, the statistical analysis did not find any significant components in the experiment. Of the 23 total compounds, only the addition of the amino acids aspartic acid and lysine appeared to have a positive effect on the VCD of the cells (Figure 3.3). The other amino acids (i.e., glutamic acid, glutamine, leucine and methionine) appeared to have a negative impact on the VCD. Trace metals (i.e., $NiSO_4$, $(NH_4)_6Mo_7O_{24}$, V_2O_5, and Na_2SeO_3) appeared to

have an overall positive impact on the VCD. Similarly, additional glucose appeared to have a positive impact on VCD for suspension cells, while ethanolamine at the high level had a negative impact on the VCD.

Taken together, this data demonstrates the importance of trace metals when replacing serum, and how crucial the quality of water is for media formulation.

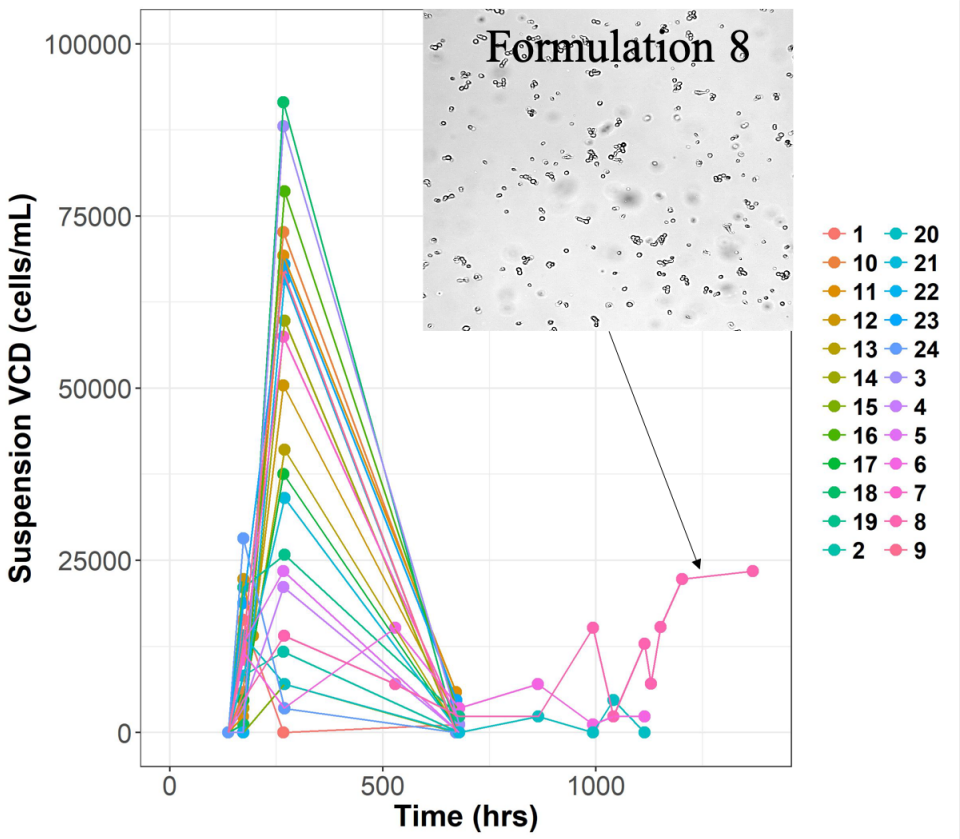

Figure 3.2: The viable cell counts for the second Plackett-Burman experiment. The viable suspension cells were tracked over 75 days. Vero cells were adapted to the media over 14 days and then grown for another 61 days in the various media. A 10x brightfield image of the cells grown in Formulation 8 is displayed in the top right corner to demonstrate the morphology of the cells on day 75.

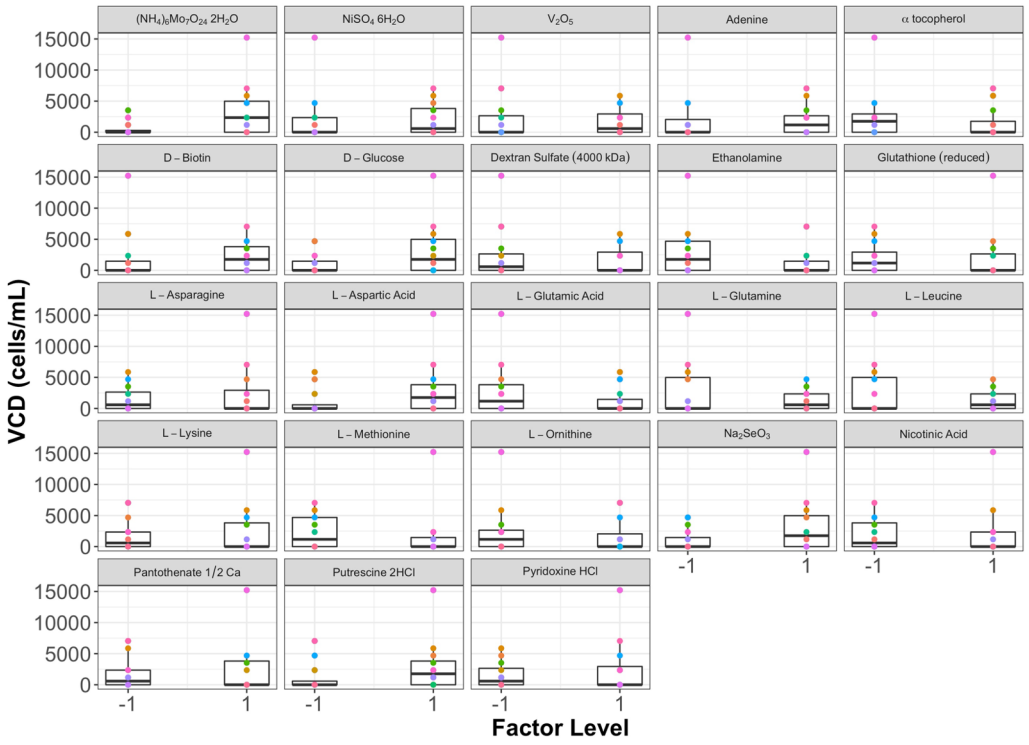

Compound	-1 (mM)	1 (mM)
D-Glucose	17.5	25
L-Glutamine	2.5	5
L-Ornithine HCl	0.3	0.65
L-Glutamic Acid	0.05	0.65
L-Leucine	0.5	2.81
L-Lysine HCl	0.5	2.74
L-Methionine	0.1	0.77
Pyridoxine HCl	0.00015	0.00079
L-Aspartic Acid	0.05	0.30
L-Asparagine H_2O	0.05	0.27
$NiSO_4$ $6H_2O$	$4.21x10^{-7}$	$9.26x10^{-7}$
$(NH_4)_6Mo_7O_{24}$ $4H_2O$	$1.00x10^{-6}$	$5.00x10^{-6}$
V_2O_5	$5.5x10^{-5}$	$7.5x10^{-6}$
Na_2SeO_3	$3.00x10^{-5}$	$3.00x10^{-4}$
Nicotinic Acid	0.00406	0.00162
D-Biotin	$1.43x10^{-5}$	$5.32x10^{-5}$
α-tocopherol acetate	0.000296	0.000381
Pantothenate ½ Calcium	0.0168	0.0621
Putrescine 2HCl	0.000503	0.00621
Adenine	0	0.00127
Ethanolamine HCl	0.022	0.041
Glutathione (reduced)	0	0.00325
Dextran Sulfate (4,000 kDa)	0	0.03 g

Figure 3.3: The results from the second Plackett-Burman media screening experiment. The concentrations for each component at the high (+1) and low (-1) levels are listed in the table and the viable cell density (VCD) for suspension cells is on the y-axis of each of the plots. Vero cells were adapted to the media over 14 days and then grown for another 14 days in the various media. The VCD is from day 28 of the experiment.

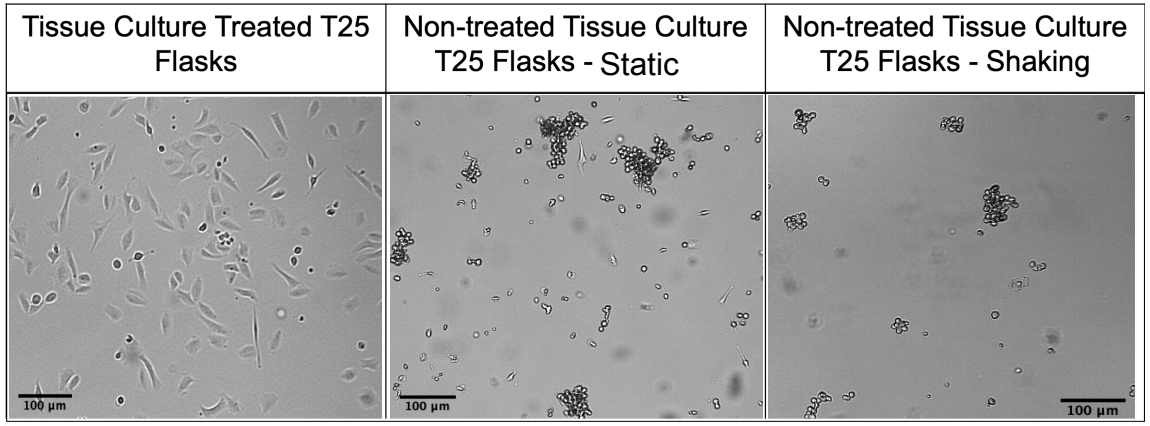

Figure 3.4: 10x brightfield images of Vero cells grown in Formulation 8, without OptiPRO™ SFM for 13 days in 3 different conditions after 83 days of culture (Tissue Culture Treated Tflask, Non-treated Tflask with static liquid, and Non-treated Tflask with shaking).

Plackett-Burman DoE #3

The basal medium formulation for DoE #3 is listed in Table B.3 and the goal of the this experiment was to further screen trace metals, amino acids and vitamins for more optimal concentrations that improves cell viability and proliferation. Hydrocortisone was also included. The main effects plot and significant factors for DoE #3 are presented in Figure 3.5 and listed in Table 3.3, respectively. Similar to DoE #1, 16 of 23 factors were identified as significant ($p<0.05$); the non-significant factors were the trace metals manganese and nickel, amino acids cysteine and ornithine, and vitamins α-tocopherol, pyridoxine, and hydrocortisone.

Small changes in concentration in trace metals had significant effects on the grow rate of cells, with all of the trace metals (except manganese and nickel) being identified as significant factors (Table 3.3). Increasing the level of molybdenum, metasilicate, and vanadium was negatively correlated with the growth rate, while increasing the amount of cobalt and nickel had a positive effect.

The coefficient estimates for the amino acids L-lysine and L-leucine were positive whereas and L-asparagine, L-methionine, and L-aspartic acid had negative coefficients (Table 3.3). Although L-cysteine was not identified as a significant factor, the main effect plot suggested that it had a negative effect on the growth rate of cells (Figure 3.5). Some of the amino acids had small changes in the concentrations between the high and low levels, but this small change reflected a large change in the cell growth rate. Additionally, there appears to be discrepancy between the statistical analysis of the results, compared to the trend that is plotted in Figure 3.5. For example, the main effect plot in Figure 3.5 for L-lysine appears to have a negative correlation, but the coefficient estimate in Table 3.3 is positive, whereas the opposite observation is true for L-methionine. The concentration

between the two levels of L-lysine and L-methionine are very small (0.02 and 0.05 mM, respectively). It is likely that the effect of these two amino acids could have interactions with other compounds, but we are unable to detect the effect of the interaction using this style of experiment.

The vitamins nicotinic acid, D-biotin, and vitamin B_{12} had an overall significantly positive effect on the growth rate of the cells. Figure 3.5 shows that pyridoxine had positive correlation between the concentration and the growth rate, although it is not significant. Only pantothenate hemicalcium had a significant and negative coefficient, all other vitamins were either not significant factors, or had a positive coefficient.

Glutathione acts as an antioxidant to prevent oxidative damage from the heavy metals, peroxides, free radicals and lipid peroxides. It appeared to have had a negative effect on the growth rate at the slightly higher concentration. Adenine also had a negative effect on the growth rate with a small increase in concentration between the two levels. This highlights the potential toxic effects of these compounds if they are supplemented in too high concentrations in the medium. On the other hand, the polyamine putrescine had a positive coefficient with the small increase. Finally, hydrocortisone did not prove to have an effect on the growth rate of the Vero cells and this compound was not investigated further.

Overall, this data supports the importance of trace metals, amino acids and vitamins in SFM, but highlights the narrow acceptable concentration range for some of the components. Additionally, with the finding that adenine had a significantly negative impact, different pyrimidines and nucleosides were tested in the next experiment. For the next study all of the compounds were included in the basal medium formulation at their most beneficial levels, with the exception of hydrocortisone which was not included in any further studies.

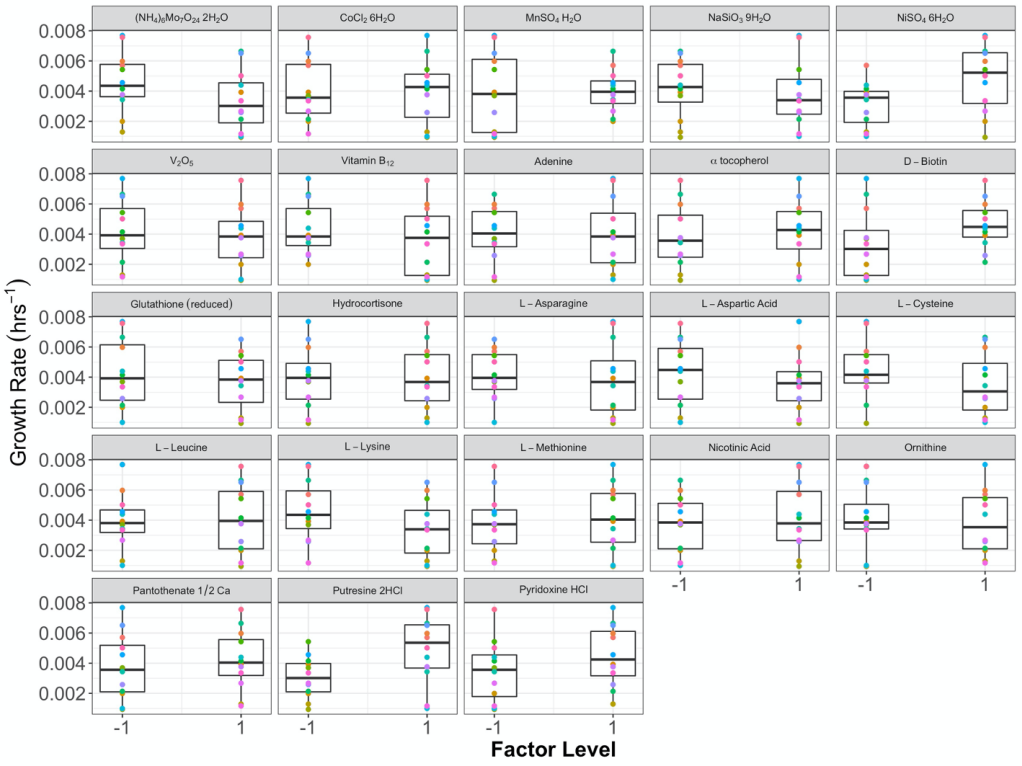

Compound	-1 (mM)	1 (mM)
$(NH_4)_6Mo_7O_{24}$ $2H_2O$	5.0 x 10^{-6}	5.5 x 10^{-6}
$CoCl_2$ $6H_2O$	4.2 x 10^{-6}	8.0 x 10^{-6}
$MnSO_4$ H_2O	0.9 x 10^{-6}	1 x 10^{-6}
$NaSiO_3$ $9H_2O$	54 x 10^{-6}	60 x 10^{-6}
$NiSO_4$ $6H_2O$	0.9 x 10^{-6}	1 x 10^{-6}
V_2O_5	5.5 x 10^{-6}	5.7 x 10^{-6}
Vitamin B_{12}	0.4 x 10^{-6}	4.0 x 10^{-6}
Adenine	1.3 x 10^{-3}	1.4 x 10^{-3}
α-tocopherol	3.8 x 10^{-4}	4.3 x 10^{-4}
D- Biotin	5.3 x 10^{-5}	5.9 x 10^{-5}
Glutathione (reduced)	3.3 x 10^{-3}	3.6 x 10^{-3}
Hydrocortisone	0	2.8 x 10^{-8}
L-Asparagine	0.27	0.53
L-Aspartic Acid	0.30	0.60
L- Cysteine	0.16	0.32
L-Leucine	0.45	0.48
L-Lysine	2.74	2.76
L-Methionine	0.12	0.17
Nicotinic Acid	4.1 x 10^{-3}	4.3 x 10^{-3}
Ornithine	0.65	0.72
Pantothenate ½ Calcium	0.046	0.051
Putrescine 2HCl	5.0 x 10^{-4}	5.2 x 10^{-4}
Pyridoxine HCl	1.5 x 10^{-4}	2.8 x 10^{-4}

Figure 3.5: The results from the third Plackett-Burman media screening experiment. The concentrations for each component at the high (+1) and low (-1) levels are listed in the table and the growth rate for adherent cells is on the y-axis of each of the plots. Vero cells were adapted to the media over 14 days and then grown for another 61 days in the various media. The growth rate is from day 75 of the experiment.

Table 3.3: List of significant ($p<0.052$) main effects of the third Plackett-Burman experiment.

	Coefficient Estimate	t value	$Pr(>\|\|t\|\|)$
(Intercept)	0.005314903	50.49294616	0
Nicotinic Acid	0.000604031	5.738453781	1.03E-08
Glutathione (reduced)	-0.000581601	-5.525355785	3.50E-08
$CoCl_2 \cdot 6H_2O$	0.000553965	5.262810543	1.49E-07
V_2O_5	-0.000451875	-4.292928181	1.81E-05
L-Asparagine	-0.000425822	-4.045422605	5.32E-05
Pantothenate $1/2Ca^{2+}$	-0.000422662	-4.015394688	6.04E-05
D-Biotin	0.000324982	3.087411608	0.002033071
$NaSiO_3 \cdot 9H_2O$	-0.000320125	-3.041268881	0.002371282
L-Methionine	-0.000309262	-2.938073049	0.003321682
L-Aspartic Acid	-0.000252022	-2.39427816	0.016699415
L-Lysine	0.000242251	2.30144346	0.021418334
Vitamin B_{12}	0.000229069	2.176210596	0.029598519
Adenine	-0.000227019	-2.156734099	0.031086484
Putresine·2HCl	0.000211976	2.013821687	0.044095874
L-Leucine	0.000207171	1.968181169	0.049116962
$(NH_4)_6Mo_7O_{24} \cdot 4H_2O$	-0.000204716	-1.944852615	0.05186352

Plackett-Burman DoE #4

Plackett-Burman DoE #4 included sodium bicarbonate, purines and pyrimidines, as well as more amino acids, trace metals, vitamins, and growth factors for supplementation. The concentration of sodium bicarbonate recommended by the manufacturer was 1.2 g/L, but this was assuming serum addition to the medium. For 5% incubators, serum-free medium should contain 2-2.2 g/L of sodium bicarbonate to provide the correct buffering capacity. Insulin-like growth factor 1 (IGF) was also added in an effort to increase the growth rate. The main effects plot and significant factors ($p<0.05$) for DoE #4 are presented in Figure 3.7 and listed in Table 3.4, respectively. In total, 11 of 23 compounds tested were identified as significant factors; the vitamins folic acid, thiamine, D-biotin, and α-tocopherol, amino acids methionine and tryptophan, and other components including cobalt chloride, choline chloride, putrescine, and myo-inositol significantly affected growth. Significantly, changes in cell morphology were observed in this experiment (Figure 3.6A); as cells were adapted to serum-free and low-calcium/magnesium conditions the cells had a more dendritic morphology. When the cells were moved into non-treated tissue culture flasks, many of the cells in the medium formulations formed aggregates and stopped growing. The size of the aggregates varied depending on the medium formulation, but could be broken up using a pipette. In an effort to obtain single cell suspensions, the T25 non-treated tissue culture flasks were placed on an orbital shaker at 40 rpm. In response to the shaking, the cells in many of the formulations formed tighter aggregates. Interestingly, cells in formulation 17 started to grow in small aggregates of approximately 1-10 cells. Formulations 11, 17 and 23 were able to be cultured for over 211 days, and Formulations 11 and 23 continued to grow in small aggregates, whereas the cells in Formulation 17 began to grow slowly as single cells. The complete recipes for Formulations 11, 17 and 23 are listed in Table B.4 Appendix B.

The approximate doubling time and growth rate for each of the formulations are shown in Figure 3.6B, C and D. There were two main groups of medium formulations, some with a doubling time greater than 1000 hours, and another group with a doubling time less than 750 hours. The compound that had the greatest influence on the doubling time was sodium bicarbonate. The sodium bicarbonate level for the slower growing group was 1.2 g/L, whereas the faster growing group contained 2.2 g/L sodium bicarbonate. Sodium bicarbonate was not detected as a significant compound in Table 3.4, but cobalt, folic acid, D-biotin, L-methionine, thiamine, L-tryptophan, myo-inositol, IGF, choline chloride, putrescine and α-tocopherol were identified as significant. Cobalt and tin had a negative effect on the growth rate, although tin did not have a significant effect. The purines (adenine, guanosine, and hypoxanthine) and pyrimidines (thymidine and uridine) showed no significant improvement. Figure 3.7 shows that there is a slight negative correlation between the factor level and the growth rate for the purines and pyrimidines that were supplemented, with the exception of uridine, which had a positive trend.

The additional vitamins (α-tocopherol, D-biotin, folic acid, and thiamine) also proved to have a significant positive correlation with the growth rate, with the exception of D-biotin which had a negative coefficient. The amino acids L-methionine and L-tryptophan were significant factors and were negatively correlated with the growth rate. Most of the amino acids had a negative correlation with the growth rate, except for L-arginine and L-threonine. Interestingly, IGF was identified as a significant component, but in the presence of IGF, there was a lower growth rate. The polyamine, putrescine, was added at much higher concentrations than previous experiments, and at the higher level, it proved to be detrimental to the growth rate of the Vero cells. Like putrescine, increasing the concentration of choline chloride in the cell culture media reduced the growth rate, while myo-inositol had the opposite effect (Table 3.4).

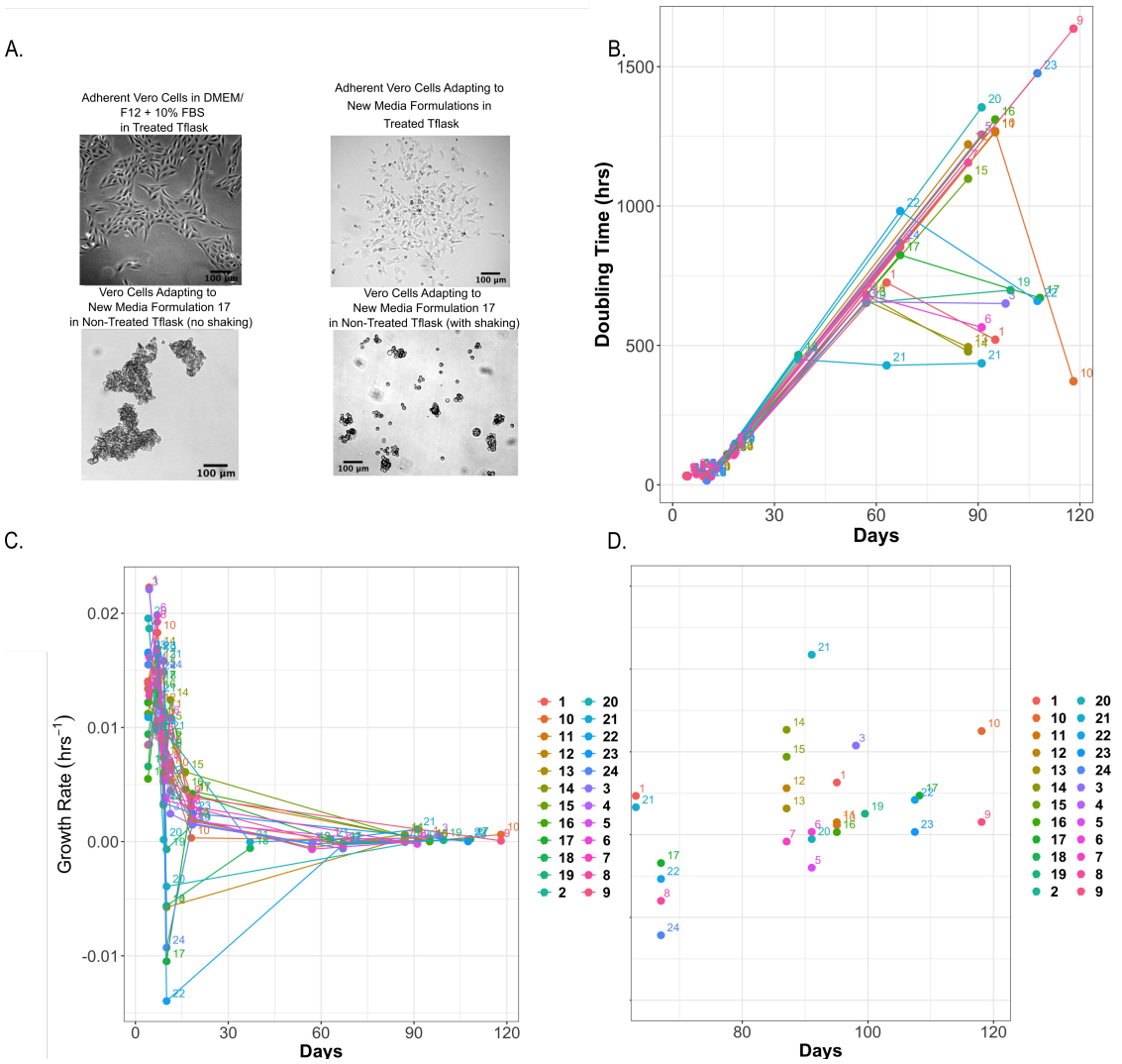

Figure 3.6: A. Brightfield images of Vero cells as they adapt to low-calcium and magnesium media over the course of 120 days. Vero cells grown in DMEM/F12 + 10% FBS is used as a reference for normal morphology, compared to the cells growing in the chemically defined media (top right image). Vero cells were unable to adhere to non-treated Tflasks in the chemically defined media, and with the addition of shaking (40 rpm, bottom right image) single cells and small aggregates were observed. B. The doubling time of Vero cells increased dramatically as they were adapted to the low-calcium and magnesium media over the course of 118 days. The shortest doubling time at the end of the experiment was approximately 20 days (500 hours). C. The growth rate of Vero cells as they adapted to the new medium formulations for PB4 over 118 days. D. A zoomed in image of the growth rate of the medium formulations between days 65 and 120.

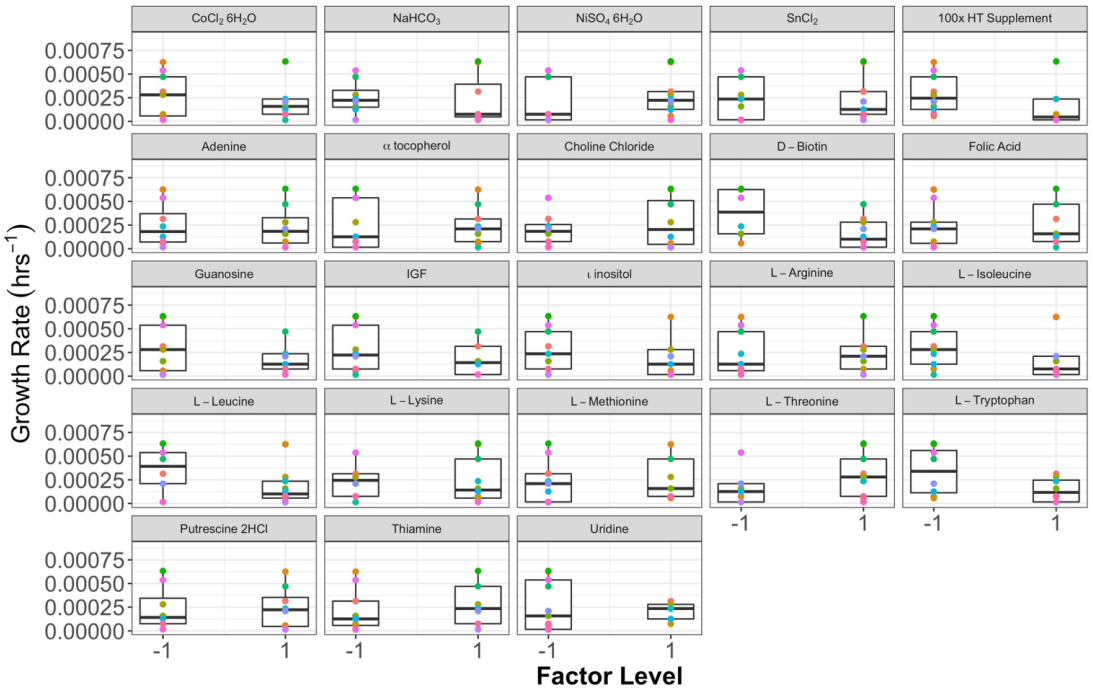

Compound		-1 (mM)	1 (mM)
$CoCl_2$ $6H_2O$		4.2×10^{-6}	12×10^{-6}
$NaHCO_3$		14.3	26.2
$NiSO_4$ $6H_2O$		3.7×10^{-6}	6.2×10^{-6}
$SnCl_2$ $7H_2O$		0	0.45×10^{-6}
100x HT Supplement	Hypoxanthine	0.1	0.2
	Thymidine	0.016	0.032
Adenine		2×10^{-3}	5.8×10^{-3}
α-tocopherol		5.4×10^{-4}	13.6×10^{-4}
Choline Chloride		0.06	0.10
D- Biotin		1.0×10^{-4}	3.8×10^{-4}
Folic Acid		6.0×10^{-3}	10.1×10^{-3}
Guanosine		2.5×10^{-3}	3.5×10^{-3}
Insulin-like Growth Factor (IGF)		0	1×10^{-5} g/L
ι-inositol		0.07	0.12
L- Arginine		0.70	1.11
L-Isoleucine		0.42	1.03
L-Leucine		0.76	2.14
L-Lysine		1.4	2.73
L-Methionine		0.67	1.34
L-Threonine		0.45	1.65
L-Tryptophan		0.04	0.51
Putrescine 2HCl		6.2×10^{-4}	95×10^{-4}
Thiamine		6.4×10^{-3}	7.1×10^{-3}
Uridine		5.1×10^{-4}	51×10^{-4}

Figure 3.7: The results from the last Plackett-Burman media screening experiment. The concentrations for each component at the high (+1) and low (-1) levels are listed in the table and the growth rate (hours^{-1}) for adherent cells is on the y-axis of each of the plots. Vero cells were adapted to the media over 12 days and then grown for another 168 days in the various media. The growth rate data is from day 83 of the experiment.

Table 3.4: List of significant ($p<0.05$) main effects of the last Plackett-Burman experiment.

	Coefficient Estimate	t value	$Pr(>\|t\|)$
(Intercept)	0.00025634	14.2163012	1.02E-23
$CoCl_2 \cdot 6H_2O$	-0.000198	-10.867093	1.73E-17
Folic Acid	0.00017295	9.5917951	5.39E-15
D-Biotin	-0.0001448	-8.0305767	6.54E-12
L-Methionine	-8.87E-05	-7.0344188	5.79E-10
Thiamine	0.00014192	5.62574325	2.56E-07
L-Tryptophan	-6.75E-05	-3.7016399	0.0003894
myo-inositol	6.24E-05	3.46048549	0.00086308
IGF	-5.56E-05	-3.0830861	0.00280062
Choline Chloride	-4.14E-05	-2.3717624	0.02007633
Putrescine·2HCl	-5.92E-05	-2.3447009	0.02149091
α-tocopherol	5.22E-05	2.03576477	0.04504293

Taken together this data suggests that the maximum concentration of certain compounds had been achieved and increasing the concentration proved toxic to the cells. Moving forward, folic acid, α-tocopherol, myo-inositol and thiamine were increased in the final medium formulation.

3.3.2 CDM2 medium formulation supports suspension growth of CHO, MDCK, and HEK293T cells and robust adherent growth of Vero cells

In light of the promising results from Plackett-Burman DoE #4, Formulation 17 was modified to increase the concentrations of Ca^{2+} and Mg^{2+} to 1 mM and 0.7 mM, respectively, and renamed Chemically Defined Medium 2 Adherent (CDM2-A), and the low calcium and magnesium version was renamed Chemically Defined Medium 2 Suspension (CDM2-S). Since Formulation 17 had drastically low levels of calcium and magnesium, this was found to inhibit the growth rate of other cell lines and it was increased to support robust proliferation of various cell lines. The CDM2-A formulation was then assessed for its ability to support growth in single cell suspension of other common mammalian cell lines (i.e., MDCK, CHO-K1, and HEK293T cells). Cells were sequentially adapted to CDM2-A or other appropriate commercial media as described in materials and methods.

Unsurprisingly, maximum cell density was achieved for HEK293T and CHO-K1 cells in their respective commercial media; HEK293T cells achieved 4.37×10^6 cells/mL in 293 SFM II media by day 6, whereas CHO-K1 cells grown in CD CHO with 1x anticlump, 1x HT supplement and 4 mM GlutaMax achieved a maximum cell density of 4.05×10^6 cells/mL after 7 days before the onset of stationary phase and eventual loss in cell viability was observed. Interestingly, HEK293T in the same CD CHO media grew to a cell density of 3.33×10^6 cells/mL by day 6, which was approximately 76% of the cell density supported by the 293 SFM II medium. Conversely, MDCK cells grew poorly in OptiPRO™ SFM, and failed to adapt to either CD CHO or 293 SFM II. CDM2-A, on the other hand, supported growth in suspension in all cases (Figure 3.8). For each cell line, maximum VCD was observed by day 4 in CDM2-A, after which cell viability dropped significantly, which can

be seen in the dramatic decrease in the VCD in Figure 3.8. However, by day 3, colour change of the pH-responsive dye phenol red in CDM2-A indicated a shift in the culture conditions to acidic pH, which may be a primary cause of this decrease. Notably, this drop in VCD did not occur with the commercial media. Nevertheless, cells grown in CDM2-A achieved maximum cell density of 1.80×10^6 cells/mL, 1.65×1^6 cells/mL, and 1.92×10^6 cells/mL for HEK293T, CHO-K1, and MDCK cells lines, respectively). This represents approximately 41% of the maximum cell density achieved in the respective commercial media formulated specifically for both HEK293T and CHO-K1 cells. Additionally, given the success of adapting three different continuous cell lines to CDM2-A, this may indicate that CDM2-A may support growth of a broad array of mammalian cell lines and offer an excellent formulation to serve as a baseline for optimization of CDM for other cell lines. Moreover, this highlighted the unique challenge Vero cells pose.

Buoyed by these results, the performance of Vero cells grown in CDM2-A was investigated. As the calcium and magnesium levels were increased compared to Formulation 17, it was expected that Vero cells would grow as adherent culture in CDM2-A. Significantly, the VCD of adherent (CDM2-A) grown cells was similar to that of the commercial CDM NutriVero Flex 10 at day 4, and higher than the undefined SFM OptiPRO™ SFM. Exhaustion of growth and 95% confluence was observed after 4 days for CDM2-A, at which point the medium was exchanged with fresh medium. Conversely, cells in OptiPRO™ SFM and NutriVero continued to grow after day 4 and after they reached 99% confluence, and the medium was exchanged when a colour change was observed (day 7 for OptiPro and days 4, 6, and 8 for NutriVero). Overall, the growth rate of Vero cells in OptiPRO™ SFM and NutriVero were 0.0197 hrs^{-1} and 0.0201 hrs^{-1}, respectively, while CDM2 was slightly (8%) slower at 0.0184 hrs^{-1}. Finally, the fastest growth rate of Vero cells was in DMEM/F12 + 10% FBS (0.0265 hrs^{-1}). This may indicate that all 3 SFM formulations (i.e., OptiPro,

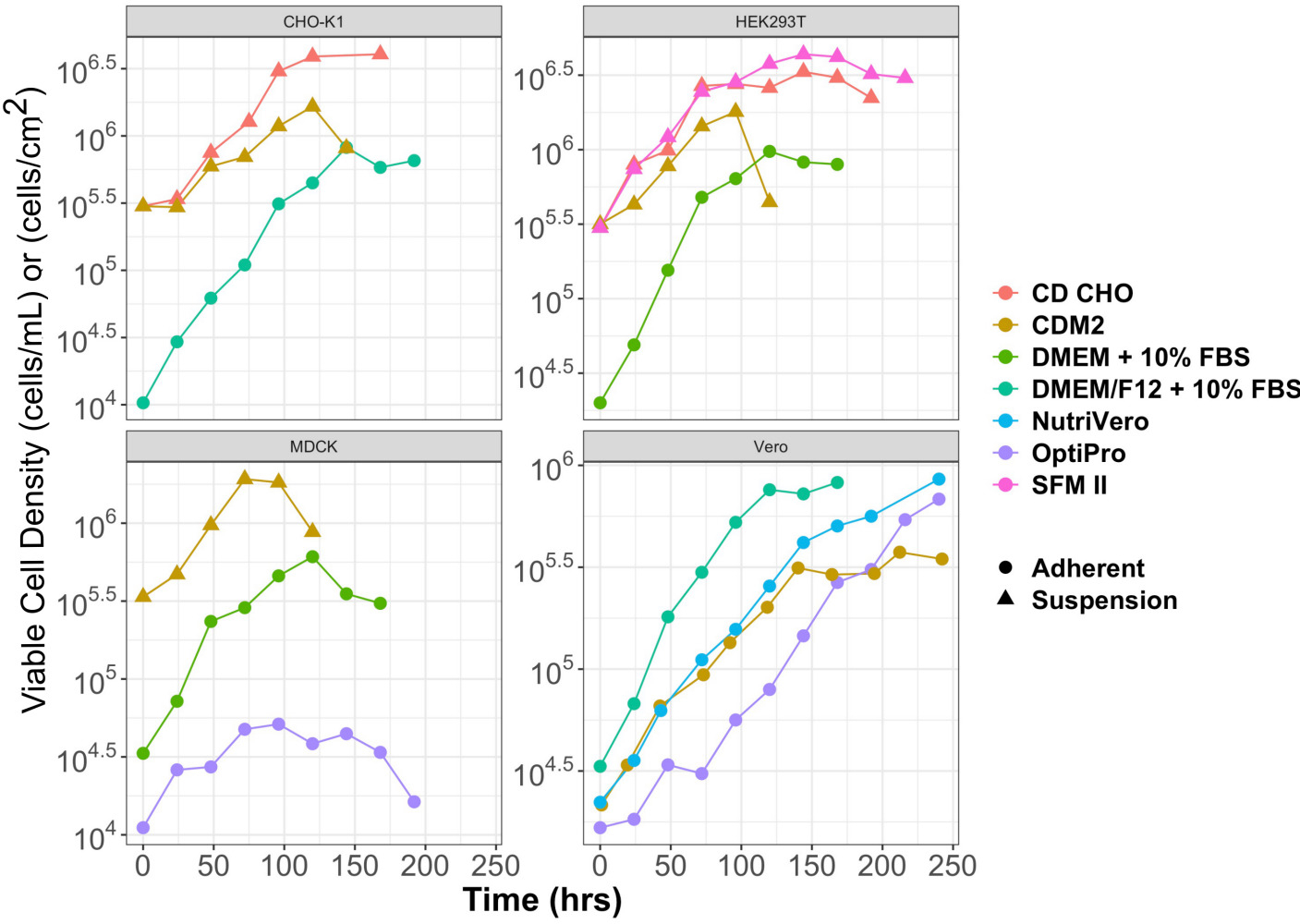

Figure 3.8: The chemically defined media that was formulated from the series of Plackett-Burman experiments was modified to include 1 mM Ca^{2+} and 0.7 mM Mg^{2+} (called CDM2-A) to support a higher growth rate in Vero cells. CHO-K1, HEK293T and MDCK cells were slowly adapted to CDM2-A from serum-containing basal media in static Tflasks. All three cell types were able to grow in suspension when they were fully adapted to CDM2-A and were cultured in 125 mL shake flasks. Vero cells remained adherent for all media formulations.

NutriVero Flex 10, and CDM2) require further development to identify growth-enhancing compounds that are supplied by serum. Nevertheless, these results indicate that CDM2-A is comparable for Vero cell adherent growth to commercial mediums currently on the market, and it can additionally be used to grow three other cells lines in suspension.

3.4 Discussion

The Vero cell line is one of the most widely accepted continuous cell lines by regulatory bodies responsible for the licensure of medicinal products. Since Jonas Salk produced an inactivated vaccine for poliomyelitis virus in the 1950s, the Vero cell has been used to propagate an incredible diversity of viruses in cell culture, and several Vero-produced vaccines have been approved for human use [30]. Despite this prominence, the development of efficient bioprocessing strategies for improving productivity of vaccine manufacturing using this platform has lagged behind other commercially important mammalian cell lines such as HEK293, CHO and MDCK, for which CDM formulations and cells adapted to suspension culture exist. Although at least one commercially-available CDM formulation for Vero cell culture is on the market (i.e., NutriVero Flex 10), this medium does not support growth of Vero cells in suspension. Rather, the majority of large scale bioprocesses for manufacturing vaccines using Vero cells rely on microcarrier technology, which requires several extra processing steps and leads to significantly increased bioprocess complexity and labour intensity [221]. Nevertheless, the successful adaptation of Vero cells to suspension culture using in-house SFM formulations have been recently reported [433, 412, 220]. However, low growth rates and formation of cell aggregates remain important issues requiring further scrutiny. Media development is expected to play a prominent role in the further improvement of the Vero cell platform.

In this work, a chemically defined medium formulation was developed that supported high viability and growth of Vero cells. Plackett-Burman-styled DoEs were utilized to screen 60 unique compounds in basal DMEM/F12 medium, and growth of Vero cells in suspension and as adherent cultures was investigated. Significantly, robust growth was observed for Vero cells grown as adherent culture in CDM2-A (i.e., CDM2-S with 1 mM Ca^{2+} and 0.7 mM Mg^{2+}), however significantly lower concentrations of the divalent cations were required to promote cell detachment. Unsurprisingly, this had a significantly negative impact on the growth rate of cells in suspension. Conversely, CDM2-A supported growth of HEK293T, CHO, and MDCK cells in suspension, indicating that the CDM2-A medium formulation is effective for growth of mammalian cells in suspension. This may also indicate that the unique underlying biology of the Vero cell may be playing a significant role in its resistance to growth in suspension.

Results from the screening experiments indicated that purines and pyrimidines (i.e., adenine, guanosine, uridine, hypoxanthine and thymidine) had no overall effect on the growth rate, with the exception of the HT supplement, which was supplemented at too high of a concentration and had a negative effect on the growth rate at the highest concentration that was supplemented. Alternatively, it was found that metals improved the growth rate of Vero cells. In addition to commonly supplemented metals such as calcium, magnesium, iron, copper and zinc, various trace metals were added to the medium formulation. Specifically, cobalt, manganese, molybdenum, silicate, selenite, nickel, tin, and vanadium were very beneficial for Vero cell growth. These trace metals are commonly found in serum, but are usually excluded from basal media (Table 2.4) [59, 326]. These trace metals were critical to achieving growth of Vero cells in a serum-free medium which was prepared with ultra pure water, although there was a narrow range of acceptable concentrations before the metals were toxic to cells. One of the drawbacks of adding metals to

protein-free media, is that metals are pro-oxidants and can lead to the oxidation of media if antioxidants or metal chelators are not present. Subsequently, antioxidants such as α-tocopherol (Vitamin E), ascorbic acid (Vitamin C), glutathione, citric acid, and pyruvate were added to the media. Each of these compounds were beneficial at high concentrations, with the exception of glutathione, which had a detrimental effect on cell growth at concentrations greater than 3.3 µM. Rourou *et al.* reported adding between 100-500 µM ferric citrate to their in-house media IPT-AFM, which also contained hydrolysates, improved Vero cell growth [415, 413]. Iron proved to be very toxic at higher concentrations (300 µM) in CDM2-A, even when various chelators were added to the chemically defined medium. Furthermore, the concentration used by Rourou *et al* was much higher than what is typically seen in serum-free media, which is approximately 18.6 µM (Chapter 2, Figure 2.5).

In addition to trace metals, vitamins also play a vital role in many different functions in the cell (various functions listed in Table 2.5). They can act as important coenzymes and need to be supplemented in media since cells are unable to synthesize them. These sets of experiments evaluated the effect of ascorbic acid, α-tocopherol, choline chloride, D-pantothenate 1/2 Ca^{2+}, D-biotin, folic acid, myo-inositol, nicotinic acid, pyridoxine, thiamine and vitamin B_{12}. All of the vitamins had a positive impact on cell growth at the concentrations that were tested.

Increasing the concentration of the amino acids had mixed effects on the growth rate for Vero cells. Increasing the concentration of the amino acids to levels that were identified in the review from Chapter 2 appeared to have negative effects on cell growth of Vero cells at the highest concentrations. Overall, the concentrations of arginine, aspartic acid, asparagine, cysteine, isoleucine, leucine, lysine, methionine, threonine were increased, but not to the concentrations that were found in the review of commercially available media

(Appendix A). Each of the amino acids has multiple functions in the cell, and their uses are interdependent of each other. Methionine and cysteine contain a thiol group and are used in protein synthesis. Methionine can be used to produce SAM which is used as a methyl donor for phospholipids, RNA and DNA methylation [491]. Cysteine can be used to generate glutathione, which is used to maintain the redox balance inside the cell [132, 299]. Isoleucine and leucine are branched amino acids that are used by the cell as building blocks for protein synthesis and fatty acids [106]. Lysine is used for protein synthesis, and is also a precursor for carnitine and L-pipecolic acid, which also play a role in fatty acid transport [283, 488]. Arginine is a versatile amino acid that can be used as a precursor for polyamines (putrescine, spermine, spermidine, citrulline, and ornithine). Ornithine and putrescine were also found to have a beneficial effect on Vero cell growth. Polyamines are associated with cell cycle progression and iron uptake [474, 448, 135]. Asparagine and aspartic acid are considered non-essential amino acids since mammalian cells can produce them and they do not need to be supplemented in cell culture media [109]. Although they are non-essential, it is easier for the cell to consume them instead of having to produce them, and their concentration levels influence cell growth and the transport of other amino acids into the cell.

Calcium and magnesium ions are important for cell adhesion proteins such as cadherins, which require a certain extracellular concentration (> 55 µM) of calcium to maintain the correct rigid conformation to remain active [385]. Cadherins are a family of transmembrane proteins that binds to other cadherins on the cell surface. This leads to an adhesive signal which creates a cascade of other signaling events by β-catenin [485]. Calcium is also involved in many cellular processes besides cell adhesion [272] such as cell signaling [38], enzyme activity, and apoptosis [354]. Healthy cells maintain a large concentration gradient between the cytosol (0.1 µM) and extracellular space (1-2 mM) ([273]. Magnesium is the second

(after potassium) most abundant cation inside the cell and ranges from 17-20 mM in most mammalian cells [407, 406]. Most of the magnesium is bound to various cellular structures, and only about 0.8-1.2 mM is free Mg^{2+} [407]. It is essential for the most basic functions in the cell, for example ATP requires magnesium to be biologically active. Overall, these divalent cations are crucial for many cellular processes besides cell adhesion.

As noted previously, to promote detachment of Vero cells from the Tflask, the concentration of calcium and magnesium had to be drastically reduced. Although this change was successful in maintaining the Vero cells in suspension, their growth rate was significantly affected; the doubling time increased for Vero cells grown adherently in CDM2 from 38 hours to approximately 500 hours in low calcium/magnesium CDM2, representing a more than 13 fold decrease in growth rate. Cell aggregation was reported for suspension Vero cells in previous studies; interestingly, complete elimination of calcium and magnesium contributed to aggregate removal and only decreased maximum cell density by approximately 10% compared to standard composition IPT-AFM, while reducing their concentration from 500 µM to 100 µM appeared to significantly improve both the growth rate and maximum cell density while maintaining growth as single cell suspension [412]. Conversely, our results indicated that reducing the total concentration of calcium and magnesium to 300 µM nearly halted growth entirely. Interestingly, Vero cells cultured adherently in IPT-AFM achieved a specific growth rate of 0.019 $hours^{-1}$ [415], while CDM2 supported a specific growth rate of 0.018 $hours^{-1}$. The similar performances of these media for adherent growth may indicate that components in the undefined plant hydrolysates in IPT-AFM could play an important role in growth in suspension. Along with the use of undefined plant hydrolysates in the IPT-AFM, significantly older Vero cells (thawed at n+131, compared to n+81 for this study) were used and the accumulation of genetic mutations over the additional 50 passages could have contributed to the robust growth of the suspension cells.

Conversely, the ability of CDM2 to support growth in suspension of HEK293T, CHO, and MDCK cells could indicate that calcium-dependent adhesion molecules such as cadherins and selectins may not play a large role in the ability of cells to grow in suspension, and rather something in the underlying biology of the Vero cell may be playing a significant role.

Finally, none of the animal component free (ACF) media formulations grew as fast as serum-containing DMEM/F12 with 10% FBS. This could suggest that some as-yet unidentified components remain missing from ACF media such as cell signaling molecules that are in low concentration, growth factors, or adhesion proteins that are missing from serum-free media. In this study growth factors rEGF, IGF and hydrocortisone were tested for their effect on Vero cell growth, but only rEGF proved to significantly improve cell growth which is aligned with previously reported medium formulation for Vero cells [415, 9]. A study conducted by Desai *et al.*, tracked the growth factors that were produced by Vero cells [99, 98]. They found that Vero cells excreted platelet derived growth factor (PDGF), interleukin 6 (IL-6) and leukemia inhibitory factor (LIF), but were unable to detect EGF or active TGF-β. Interestingly, Guo *et al.*, were only able to find epidermal growth factor receptors (EGFR) on Vero cells when they conducted a proteomic analysis of the membrane proteins [163]. It could be that due to the limited annotation of the Vero genome and surface proteins, that Vero cells possibly have receptors for PDGF, IL-6 and LIF, or that the EGFR in Vero cells can interact with many different ligands. Regardless, rEGF did stimulate proliferation of adherent Vero cells in the chemically defined media, but the literature suggests that other growth factors could be used in addition to, or to replace rEGF. Epidermal growth factor (EGF) is commonly added to chemically defined cell culture media because the EGF receptor (EGFR, also known as ErbB1) is expressed on almost all cell types. It is a mitogen for a variety of epidermal and epithelial cells and

enhances proliferation, cell survival, regulation of ion channels, calcium mediated signaling through the interaction and activation of several signaling pathways [21, 136, 371]. The recombinant human form of EGF is only 6.2 kDa and can be produced in *E. coli* which lends itself well to ACF media formulations with very low protein content [451]. Other growth factors that can be considered to stimulate EGFR signaling include transforming growth factor alpha (TGF-β), amphiregulin, betacellulin, heparin-binding epidermal growth factor, and epiregulin [21]. Plant hydrolysates have been known to mimic growth factor-like effects for many different cell types at low cost and are ACF, which makes them good alternatives to supplementing with individual growth factors [130, 424, 484].

3.5 Conclusion

In conclusion, a chemically defined media was developed that supports the growth of various mammalian cell lines in suspension. Vero cells, however, were unable to proliferate in suspension in this medium, although when the calcium and magnesium concentrations were increased, Vero cells grown adherently had a comparable doubling time to a commercial chemically defined media for Vero cells. This work offers a formulation for a medium to support the growth of Vero cells in a chemically defined, and ultra low protein environment that can decrease the batch-to-batch variability that traditional serum-containing media suffer from.

Chapter 4

Transcriptomics to Identify Differences in Gene Expression Between Adherent and Suspension Vero Cells

4.1 Introduction

Early improvements of animal cell culture processes were typically found through extensive iterative and empirical optimization of the culture mode (i.e., batch, fed-batch, or perfusion) and the accompanying culture parameters (i.e., nutrient content, pH, temperature, and dissolved oxygen). Similarly, the development of serum-free media (SFM) and chemically-defined media (CDM) formulations has improved both the overall consistency of cell growth and productivity [55]. In more recent years, the animal cell biotechnol-

ogy field has witnessed the development of sophisticated genetic engineering technologies, bioinformatics pipelines for whole genome sequencing, assembly, and annotation, as well as genome-scale reconstructions of cellular metabolism networks. Likewise, advancements in analytical tools and more sophisticated data processing and modelling approaches have added technologies such as transcriptomics, epigenomics, and glycomics to the 'omics' repertoire to complement already existing genomics, proteomics, and metabolomics data sets [455]. Together, these technologies have enabled the development of a multitude of new, engineered production hosts and platforms with improved or completely novel properties. They have also allowed for deeper investigation of cellular function and observation of the underlying changes the cell is experiencing in different environments. The use of 'omics technologies has had a particular impact on the observation of cellular processes during adaptation to both SFM and growth in single cell suspension. For example, proteomics-based investigation of the adaptation of MDCK cells first to SFM and then to growth in suspension revealed over 90% of the changes in the proteome were identified after serum removal, and were related to cytoskeletal structure, genetic information processing, and cellular metabolism [229]. The switch to suspension growth caused differential expression of myosin proteins and proteins linked to tumorigenicity and oncogenic networks. Myosin proteins are ATPases that move along actin filaments and convert ATP energy into mechanical energy [273], and they play important roles in cytokinesis and cytoskeleton-membrane interactions [273]. Similarly, transcriptomics has been used to probe the underlying gene expression differences between adherent and suspension phenotypes for cell lines such as CHO-K1, HeLa, MDCK, BHK-21 and HEK293 [201, 252, 285, 76, 102, 372]. For example, the *siat7e* gene was identified as being up-regulated in suspension HeLa cells, whereas the *lama4* was downregulated in these cells compared to cells grown as adherent culture [201]. The *siat7e* gene encodes a type II membrane glycosylating sialyltransferase and differen-

tially expressed sialylated glycans are associated with the anoikis resistance of metastatic tumors [428]. The *lama4* gene, on the other hand, encodes the Lamanin 4α protein, which is a member for the laminin family of glycoproteins. It is also associated with metastatic breast tumors [410]. Interestingly, expression of *siat7e* enabled robust growth in suspension of MDCK cells [76]. Moreover, the *siat7e*-expressing cells were able to successfully replicate Influenza B virus, and the specific production of hemagglutinin was approximately 20 times higher than the specific production from the parental, adherent, MDCK cells. Importantly, the MDCK-*siat7e* suspension cell line was not more tumorigenic in mice compared to the parental cell line [77]. In a separate study, 5 down-regulated and 3 up-regulated genes were identified in CHO-K1 cells that were adapted in protein-free media to growth in suspension [252]. Among these, the *igfbp4* and *aqp1* genes were identified as being critical down-regulated genes for the suspension phenotype. Subsequently, CHO-K1 cell lines with disrupted *igfbp4*, *aqp1*, *fos*, *sulf2*, and *nr4a1* genes were developed. Of these mutants, only the single knock outs of *igfbp1* or *aqp1* reduced the adaptation time to suspension by 54% compared to the wildtype cell line. The *igfbp4* gene encodes the insulin-like growth factor binding protein, and *aqp1* codes for an aquaporin which functions as a molecular water channel in the cell. Interestingly, the *aqp1* gene is also a potential cancer marker that may promote metastasis and progression of cancer [477]. Finally, whole transcriptome sequencing of suspension and adherent BHK-21 and CHO-K1 cell lines identified four candidate genes (*papbc1*, *lars*, *glul*, and *pfn1*) that may be important for modulating the anchorage-dependent phenotype. The *papbc1* gene was subsequently targeted for down-regulation using RNA interference, which triggered anchorage-independent growth [91].

The chemically defined medium formulation, CDM2, reported in Chapter 3 supported robust growth of Vero cells as adherent culture, however their growth rate in suspension was drastically reduced. Despite this, CDM2 supported growth of MDCK, HEK293T, and

CHO-K1 cells in suspension, indicating that the medium itself is effective at supporting suspension growth of mammalian cells. Therefore, the purpose of this work was to investigate the transcriptomic differences between adherent and suspension phenotypes of Vero cells cultured in CDM2. We performed RNA-seq analysis to identify key genes and pathways that were differentially expressed in our suspension Vero cells, and this data provided insight as to why these cells had poor growth characteristics.

4.2 Materials and Methods

4.2.1 RNA-seq Analysis

Vero cells were maintained in DMEM/F12 + 10% FBS, Formula 17 (described in Appendix B, and referred to as CDM2-S), and Formula 17 + 1 mM calcium and 0.7 mM magnesium (CDM2-A). Cell samples were collected for RNA extraction from approximately $3x10^5$ cells to 10^6 cells. The RNA was extracted using a Total RNA Tissue Kit (Roche) and samples were stored at -80°C following extraction. cDNA libraries were prepared and sequenced at the Centre for Applied Genomics, Sick Kids Hospital, Toronto, Canada. mRNA was isolated and cDNA libraries were constructed with using the NEBNext kit for stranded poly(A) mRNA library preparation. The quality of the libraries was monitored using a Bioanalyzer-2100 (Agilent Technologies, USA). Only libraries with an RNA integrity number (RIN) value of at least 7.0 were submitted for sequencing on the Illumina HiSeq2500 sequencing platform. The sequenced reads were received in FASTQ format with >15 Million paired end reads of 125-bp length per sample. The read quality was controlled with FastQC v3 [14] before and after trimming. The reads were trimmed from 3 termini with a k-mer size of 23 using BBduk [54]. Reads were aligned with STAR aligner

v2.6.0 [103] to the Vervet-AGM genome assembly 43 (ChlSab1.1: GCA_000409795.2) from Ensembl release 96.1. The gene expression level was quantified with RSEM v1.3.1 [258] with default settings. The quantified reads for each gene per sample were then further analyzed in RStudio (RStudio Team, 2016) with the package edgeR [402]. EdgeR identified the differentially expressed genes for the two comparisons of adherent against suspension, or control against suspension samples. These contrasts tested for the differences caused by the adaptation to the chemically defined media and adaptation of the cells to suspension culture. For pathway analysis, the Vervet-AGM gene annotations from Ensembl were changed to human homologs with HGNC symbols annotation using biomaRt [110].

4.2.2 Gene set enrichment analysis

Gene set enrichment analysis (GSEA) was performed as described by Subramanian *et al.* [459]. Briefly, the gene list from edgeR was ordered by the -log10(p-values) multiplied with the sign of the log fold-change. The first tested gene sets were from biological processes from Gene Ontology (GO) [22]. The enrichment results for GO sets were visualized in Cytoscape [445] with the package Enrichment map [320]. The enrichment scores were calculated with default settings in GSEA. For the enrichment map, a false discovery rate (FDR) threshold of 5% was applied to filter the enriched gene set list, and the overlap of the gene sets was calculated with a combination of Jaccard and Overlap similarity coefficients of 20 to 80 and a threshold of 0.6. To obtain tissue type specific gene sets, RNA-seq data from Human Protein Atlas (HPA) [483] from 35 tissues were analyzed with TissueEnrich [200], which assigns genes to gene sets as enriched when their expression is five times higher than in any other tissue in the data set. Similarly, specific gene sets were defined for nephron segments based on a previous study [251]. The 15 segments include the glomerulus (G), S1

proximal tubule (S1), S2 proximal tubule (S2), S3 proximal tubule (S3), long descending limb in outer medulla (LDLOM), long descending limb in inner medulla (LDLIM), thin ascending limb (tAL), medullary thick ascending limb (mTAL), cortical thick ascending limb (cTAL), distal convoluted tubule (DCT), connecting tubule (CNT), cortical collecting duct (CCD), outer medullary collecting duct (OMCD) and inner medullary collecting duct (IMCD). For the GSEA of both sets, the minimum identified number of genes were set to five. Transcription factor target gene sets from GTEx [17] were tested for enrichment to identify regulatory patterns in the data sets. The gene sets contain 1607 transcription factors, each with 300 target genes. The GSEA was performed with default settings.

4.2.3 Housekeeping gene expression for quality control

A Pearson correlation of housekeeping genes was performed for all samples against all samples based on the assumption that housekeeping genes should be relatively invariant in healthy cells. Housekeeping genes were defined based on the investigation Eisenberg, *et al.* [117] with 3122 housekeeping genes identified as expressed in our RNA-seq data. The correlation was calculated with the R package corrplot [501]. A positive expression correlation of $r > 0.90$ between samples is indicative for biologically intact samples.

4.2.4 RNA-seq heatmaps

Heatmaps were generated with the package heatmap3 [537]. The weighted trimmed mean of M values (TMM) standardized, normalized $\log_2$ counts per million (CPM) gene list were filtered with an FDR threshold of 0.1%. The Pearson distance matrix was calculated and clustered by an agglomerative hierarchical clustering algorithm with the complete-linkage method.

4.2.5 Visualization

Graphs were generated with ggplot2 [504]. The cell cycle pathways from KEGG (pathway hsa04110) was rendered with the R package pathview [280].

4.3 Results

4.3.1 RNA-seq analysis of Vero cell adaptation to CDM as adherent and suspension culture

To analyze the transcriptome dynamics of Vero cells during adaptation to CDM and suspension culture, RNA-seq analysis was completed for Vero cells cultured in 3 different conditions; 1) Vero cells grown adherently in basal medium (DMEM/F12) supplemented with 10% FBS (Cont), 2) Vero cells grown adherently in SFM that was developed in the previous chapter (i.e., CDM2-A) with the same calcium and magnesium concentrations as DMEM/F12 (Adh), or 3) Vero cells grown in suspension in CDM2-S with low calcium and magnesium (Sus). RNA sequencing was performed on mRNA isolated from four aliquots from the same flask of each treatment and aligned with the genome of the African Green monkey (*Chlorocebus sabaeus*). Cells that were in suspension were adpted over 209 days, while the cells grown adherently had been cultured for 64 days. The Vero cells that were cultured in suspension had a very low growth rate (0.000235 hr^{-1} for Formulation 17) compared to the adherently grown cells (0.018 hr^{-1}), but maintained a high viability (Figure 4.1). Formulation 17 was cultured for 209 days and was subsequently renamed CDM2-S. Vero cells grown in DMEM/F12 + 10% FBS had a growth rate of 0.026 hr^{-1}, and Vero cells grown in CDM2 as adherent culture had a growth rate of 0.018 hr^{-1} (data not shown). Over 96% of the reads for each sample were uniquely aligned and 11,135 genes were considered expressed by filtering for genes that were expressed with at least 1 count per million (CPM) in all four samples. These genes were then mapped using homologs to the *Homo sapiens*' cellular pathways in the Ensembl database.

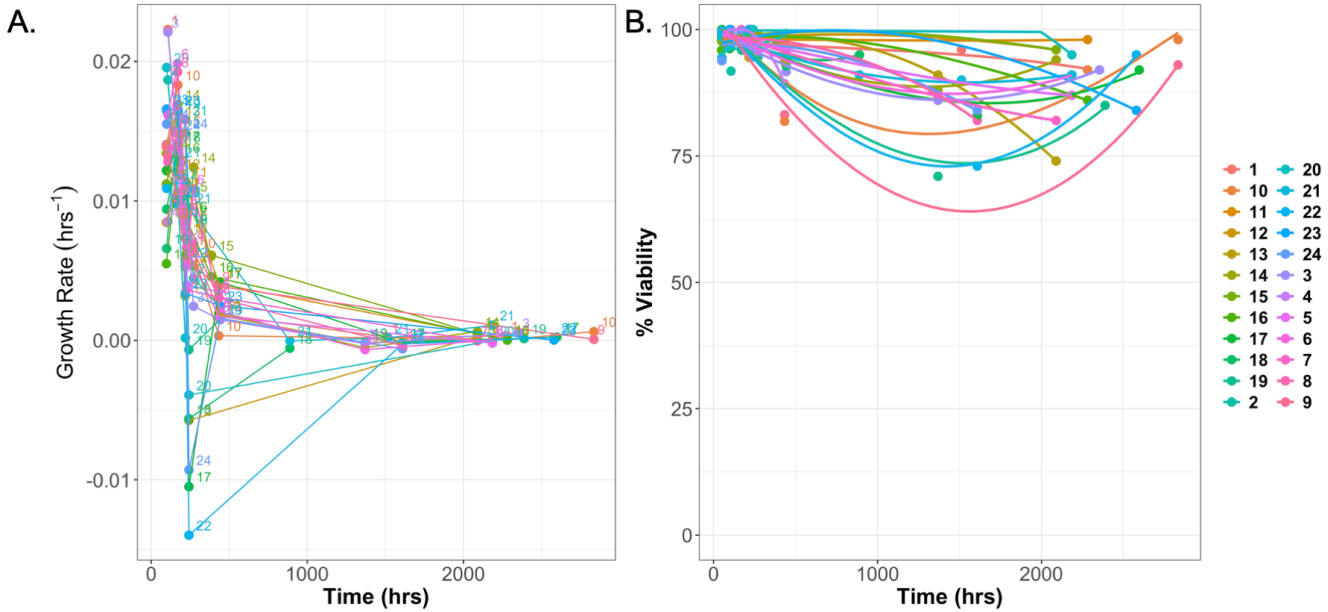

Figure 4.1: **A.** The growth rate of Vero cells adapted to various medium formulations grown over 105 days with low calcium and magnesium concentrations to encourage single cell suspension. **B.** The viability of the cells from each medium formulation over time as the cells adapted to the new media. Each formulation is represented by a number (1-24) and as indicated by the number on the plot and with a different color.

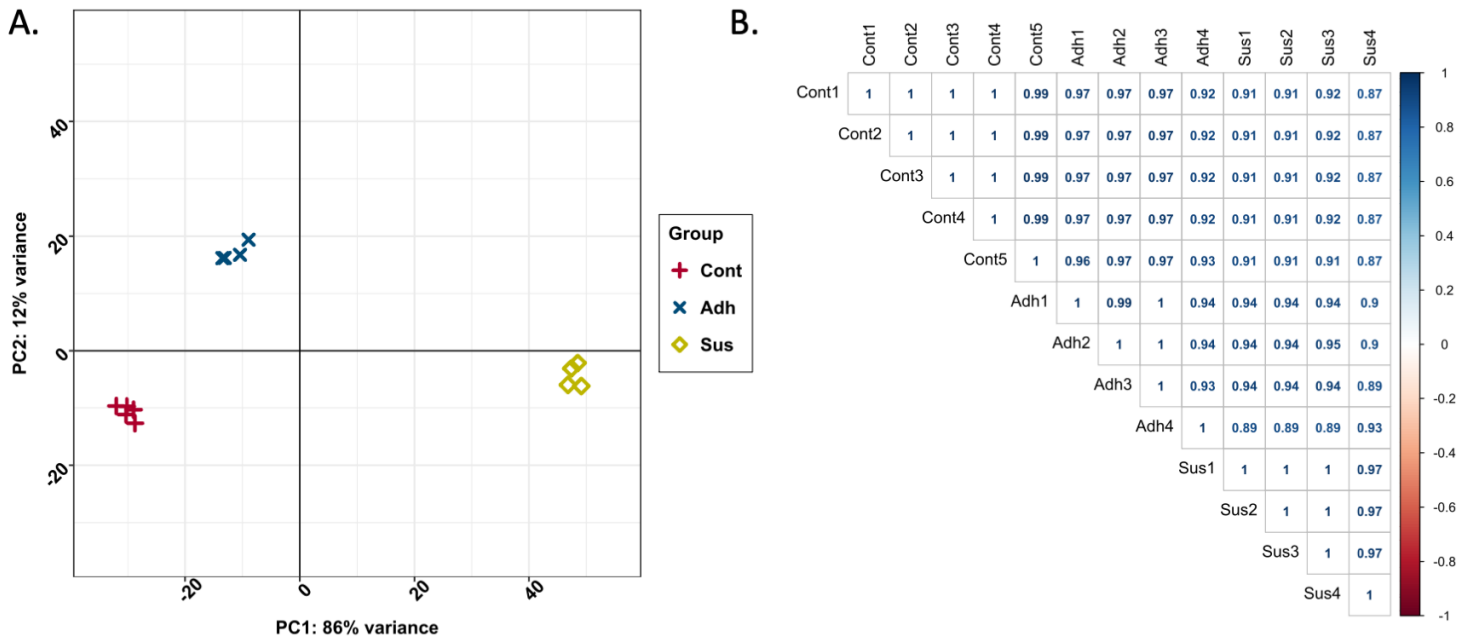

Figure 4.2: Analysis of RNA-seq data variance. **A.** A two-dimensional plot of principal component analysis (PCA) for all 13 samples of the 500 most variable genes. Each symbol represents one sample. Group affiliation is shown in the legend on the right side. **B.** Pearson's correlation between all samples for 3122 detected housekeeping genes. Correlation coefficients r values are annotated and colour coded according to the legend on the right side of the figure. Vero cells grown adherently in basal medium (DMEM/F12) supplemented with 10% FBS are labeled 'Cont', 'Adh' is Vero cells grown adherently in CDM2 with the same calcium and magnesium concentrations as DMEM/F12 are and 'Sus' are Vero cells grown in suspension in CDM2.

Variability between the data sets was analyzed using principle component analysis (PCA) of the top 500 most variable genes, and a Pearson correlation of expressed housekeeping genes (Figure 4.2). The PCA plot illustrates the clear separation between culture conditions and tight clustering of the replicate samples. PC1 accounts for 86% of the variance and PC2 accounts for an additional 12%. While the PCA plot emphasizes intergroup variability, the Pearson's correlation analysis (Figure 4.2B) shows the intragroup variation with a correlation value of $r > 0.87$, indicating that each condition had similar expression levels of housekeeping genes [232].

4.3.2 Changes in Regulation of Proliferation and Apoptosis

A gene set enrichment analysis (GSEA) was conducted to identify differentially expressed genes within the gene sets. An enrichment map of the significant (False discovery rate (FDR) threshold of 5%) down-regulated GO-terms in suspension cells compared to adherent Vero cells grown in CDM2-A, are shown associated with their biological processes in Figure 4.3. Gene sets that are related in their biological function cluster together and overlap in associated genes. Overall, 151 gene sets were significantly down-regulated and 91 were significantly up-regulated (Figure 4.3). Most down-regulated gene sets were related to cell cycle regulation, mitosis, DNA-replication and DNA organization and therefore, have a high degree of overlap in their assigned genes. Furthermore, genes involved in inflammatory processes, fluid shear stress, cell migration and endothelial barrier were up-regulated indicating a stress response during cell adaption to growth in suspension. In contrast, gene sets related to regulation of programmed cell death were not detected as either differentially regulated.

In light of these results, genes specifically associated with DNA replication, the cell

cycle, and regulation of apoptosis were investigated further. To illustrate, genes were mapped to the cell cycle phase associated with their function (Figure 4.4A) and the full KEGG pathway cell cycle map (Figure C.1). Overall, 103 genes were identified in the KEGG cell cycle pathway, and 36% were detected as significantly different between the Sus and Adh groups with a FDR threshold of 0.1%. The majority of the genes that were down-regulated are associated with DNA replication, chromosome formation, centrosome maturation, and spindle assembly. These genes are essential to the progress through S phase and M phase. A table of each gene and its description can be found in Appendix C. Although the GSEA did not identify gene networks associated with apoptosis as being differentially expressed, the possibility that the low growth rate of suspension Vero cells could be due to apoptosis remained. Therefore, the expression pattern of positive regulatory (GO:0043065) and negative regulatory (GO:0043066) gene sets of apoptotic processes from gene biology were summarized in Figure 4.4B. Overall, the average expression is more variable for suspension Vero cell samples than for adherent Vero cell samples. Suspension cells had an log fold-change range from -9.5 to +14 for pro-apoptotic genes and -9.5 to +11 for anti-apoptotic genes, while adherent Vero cell's log fold-change ranged from -4.8 to +5 for anti-apoptotic genes and -5 to +4.8 for pro-apoptotic genes. The average log fold-change was approximately zero for adherent samples for both pro- and anti-apoptotic sets, and for suspension samples it was slightly positive for both sets. Therefore, based on this data, it does not appear that Vero cells in suspension had up-regulated pro-apoptotic genes compared to the adherent Vero cells grown in CDM2, although there are several genes (pro- and anti-apoptotic) that are significantly up- and down-regulated. For example the suspension Vero cells up-regulated the anti-apoptotic genes *lrp2*, *tmigd1*, and *tox3* and pro-apoptotic gene *tnfsf10*. The gene *tnfsf10* encodes for the tumor necrosis factor ligand superfamily 10, which is a cytokine that binds to TNFRSF10/TRAILR to induce

apoptosis specifically in tumor cells and transformed cells [505]. The *lrp2* gene codes for the low-density lipoprotein receptor-related protein 2, which mediates the renal uptake of many different lipoproteins, leptin, anti-apoptotic proteins and metal-binding proteins through endocytosis [205, 227]. The *tmigd1* gene codes for the transmembrane and immunoglobulin domain-containing protein 1, which protects renal cells from oxidative cell injury and promotes cell survival [16]. The *tox3* gene protects against cell death by inducing anti-apoptotic (estrogen-responsive or BCL-2 promoters) and repressing pro-apoptotic transcripts. Taken together, this data suggests that the cells are expressing anti-apoptotic genes related to renal cells, but also up-regulating the expression of tumor necrosis factor that will specifically induce apoptosis in transformed cells. This, along with the knowledge that the cells have arrested their cell cycle, leads to the possibility that the suspension Vero cells could be reverting back to a renal phenotype.

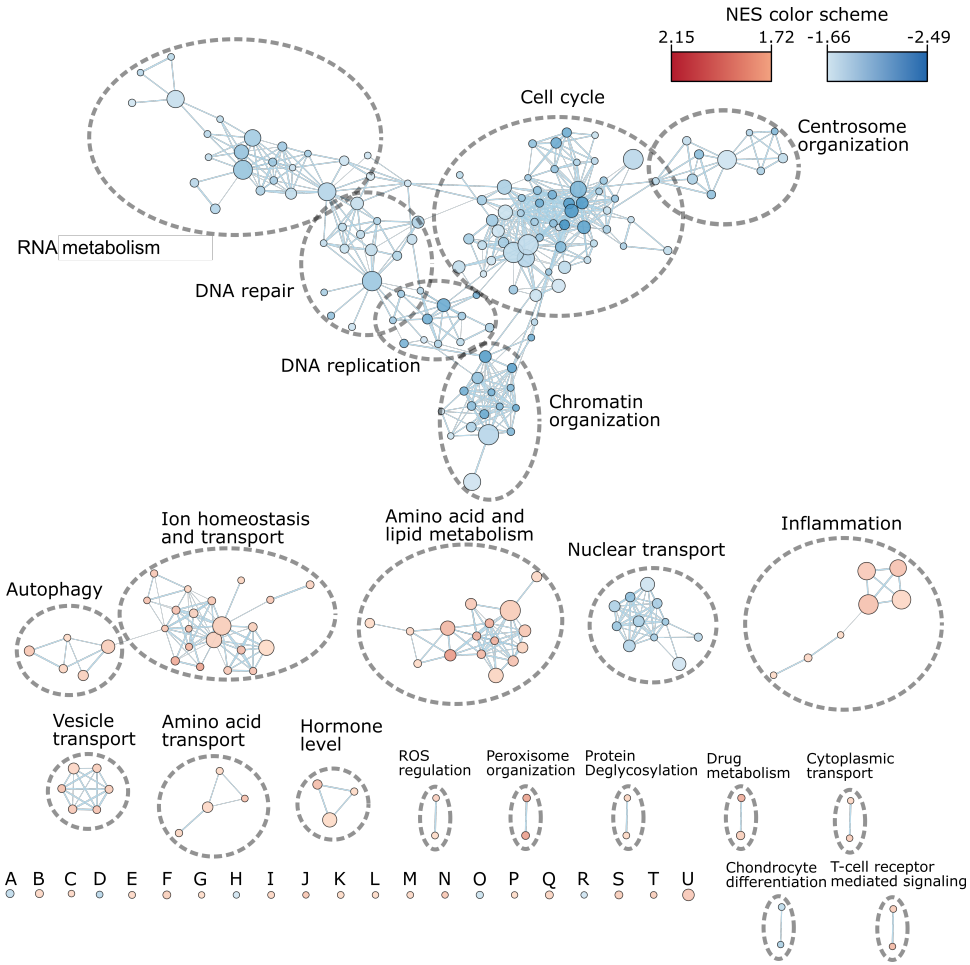

Figure 4.3: Enrichment map for significant down-regulated GO-terms in biological processes for the comparison of Sus against Adh (threshold at FDR of 0.05). The size of the node is proportional to the number of identified genes annotated to the GO-term. The thickness of edges represents the level of overlap between the GO-terms. A: DNA templated transcription termination, B: Aerobic respiration, C: Response to increased oxygen levels, D: Protein peptidyl prolyl isomerization, E: Cofactor transport, F: positive regulation of inflammatory response,G: Cellular response to fluid shear stress, H: Regulation of ubiquitin protein ligase activity, I: Establishment of endothelial barrier, J: Hyperosmotic response, K: Regulation of protein oligomerization, L: Excitatory synapse assembly, M: Regulation of calcineurin mediated signaling, N: Modified amino acid transport, O: Cell migration involved in sprouting angiogenesis, P: Low density lipoprotein receptor particle metabolic process, Q: Endosome organization, R: Pyrimidine nucleotide triphosphate biosynthetic process, S: Water soluble vitamin metabolic process, T: Collagen catabolic process, U: Drug metabolic process. NES: Normalized enrichment score.

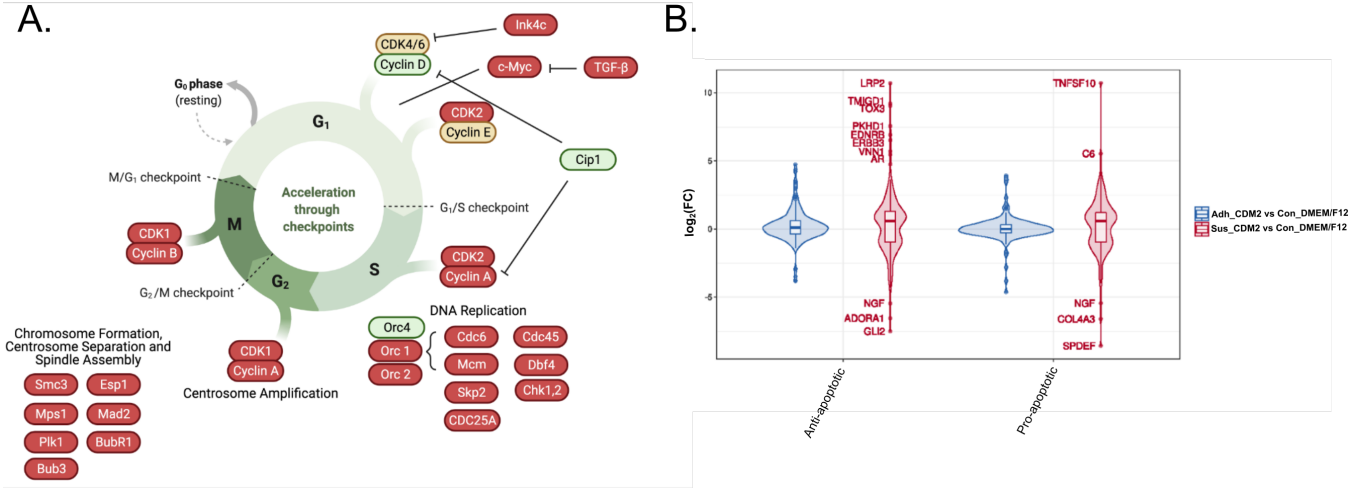

Figure 4.4: Expression regulation of cell cycle related genes in relation to the interphase cycle using BioRender. Genes that were identified as differentially expressed in the KEGG cell cycle pathway are mapped onto a cell cycle image with their respective proteins. Up-regulated genes between Sus and Adh are highlighted in green and down-regulated genes are in red. G1: Gap phase 1 of the cell cycle, G1/S: Gap 1 to synthesis transition phase, S: synthesis phase, G2: Gap phase 2, G2/M: Gap2 to mitosis transition phase, M: mitosis phase.**B.** Log fold-change for genes linked to anti- or pro-apoptosis according to Gene Ontology. The comparison of the expression levels between Vero cells grown adherently in CDM2 to the control group (DMEM/F12 + 10% FBS) for apoptosis related genes is shown in blue and the comparison of the suspension Vero cells compared to the control group is shown in red.

4.3.3 Up-regulation of Kidney Related Genes

Since the cells were not proliferating, tissue profiles for enriched genes from the human protein atlas (HPA, available from http://www.proteinatlas.org) were screened to identify if the changes in the suspension cells were tissue specific [483]. The HPA contains expression profiles of human genes for 44 different human tissues. Interestingly, the genes most associated with the kidney expression profile showed the highest degree of up-regulation (Figure 4.5). The kidney profile from HPA contained 53 genes of which 25 were identified in the data set and 22 contributed to the enrichment score. Additionally, 17 genes were identified as associated with liver tissue expression profile of which 12 contributed to the enrichment score. However, the liver profile from HPA contains 242 enriched genes, and only 17 genes from this set were expressed by the suspension Vero cells. This suggests that the suspension Vero cells were expressing relatively more kidney-specific genes than liver-associated genes. Additionally, Vero cells were originally derived from kidney tissue, therefore further analysis was conducted on kidney-related genes.

The 25 genes from the kidney profile were further shown in the mean-difference (MD) plot in Figure 4.6. With the exceptions of *slc13a1*, *npr3* and *lhx1*, all genes were significantly up-regulated with an FDR < 0.001. The strongest up-regulation in suspension cells was seen for renal tubule associated genes such as transmembrane transporters *slc6a18* [408], *slc7a13* [337] and flavin-containing monooxygenase *fmo1* [348] and with an log fold-change > 9 compared to the adherent samples (see Supplementary Table C.2 for the function of each gene, or associated protein). Additionally, 12 of these genes are identified as being specific for renal tubule according to HPA (red points in Figure 4.6). This suggests that the cells are up-regulating genes which are specifically important for renal tubule cell functions like reabsorption, fluid flow, shear forces and secretion of particular compounds

from the blood.

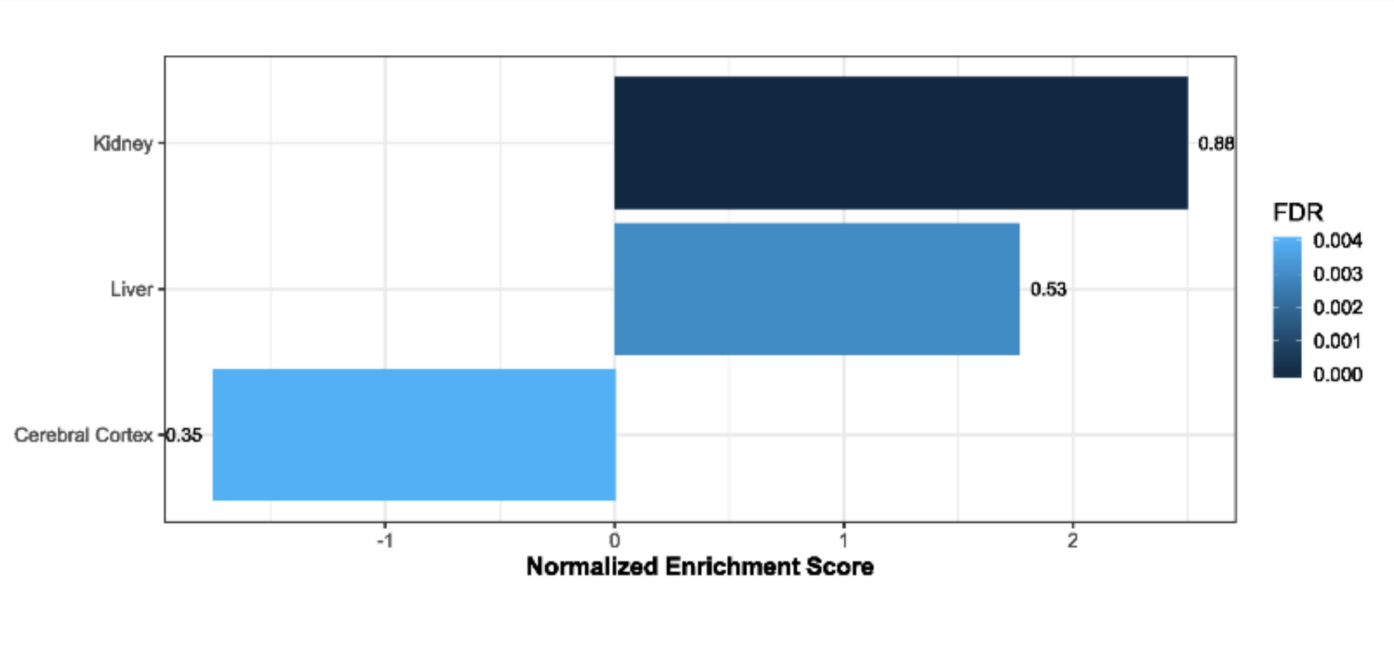

Figure 4.5: Kidney related type of suspension cells. HPA tissue related gene set enrichment analysis of Sus_CDM2 samples compared to Adh_CDM2 samples (FDR < 0.05). Tissue profiles were developed with the package TissueEnrich. Only tissue enriched genes were selected for the profiles, and only profiles with size of at least 5 specific genes were considered for the analysis. The proportion of the genes related to that profile and contributing to the enrichment scores are annotated at the side of the bars. The coloring of the bars depicts the FDR values according to the legend on the right side of the figure.

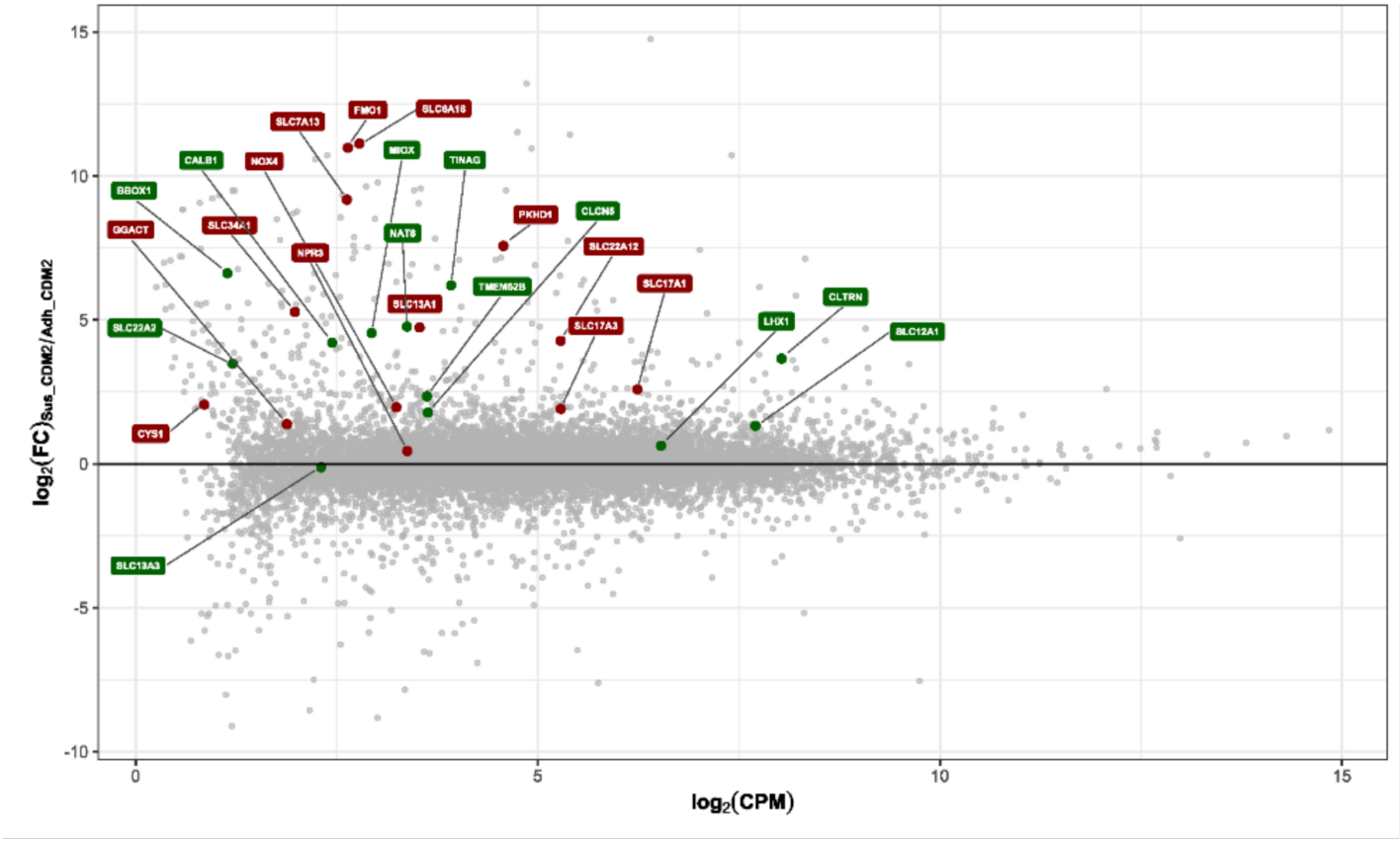

Figure 4.6: Kidney related type of suspension cells. Mean Difference plot of identified kidney enriched genes with log fold-change and log(CPM) values. Red labels are specifically to identify renal tubules, and the green labels represent the genes that are associated with the whole kidney according to Human Protein Atlas database, respectively.

4.3.4 Membrane Transporters

Based on the genes that were identified using the HPA analysis, transporters appeared to be up-regulated as an entire group. Figure 4.7 shows three heatmaps that demonstrate the up-regulation of various transporter families such as solute carriers, vacuolar-type ATPases (V-ATPases), and ATP-binding cassette (ABC)-transporters. It appears that the Vero suspension cells over-expressed most transporters compared to the adherent cells grown in CDM2-A and DMEM/F12+10% FBS, with the exception of a few that are listed in Supplementary Table C.3. Figure 4.7A lists the gene names that were differentially expressed, and colouring has been added to show if the transporter is associated with the transport of amino acids, bicarbonate ions, small ions, organic ions or other. Interestingly, some of the transporters that were not up-regulated by suspension cells are responsible for glucose, phosphate, amino acid, thiamine transport, depend on calcium, sodium, or borate. This supports the idea that suspension cells are not growing because of the down-regulated glucose uptake. Only one of the significantly up-regulated transporters (i.e., *slc2a13*) transports glucose, while four glucose related transporters were down-regulated (i.e., *slc2a1*, *slc2a10*, *slc2a14*, and *slc37a3*), which indicates that the adherent Vero cells are taking up more glucose compared to suspension cells (4.7A).

Figure 4.7C shows the differentially expressed ATP-binding cassette (ABC) transporter genes. ABC transporters use the energy from hydrolysing ATP to transport compounds across different membranes in the cell. The up-regulation of ABC transporters (specifically *abcc1*) is associated with multidrug resistance in cancer cells [401]. Like with the V-ATPases, most of these transporters are up-regulated (except of *abcb10*). The *abcb10* gene is associated with protection from oxidative stress in the mitochondria [263]. Figure 4.8 shows a diagram of the location of significantly up-regulated membrane transporters on

the basolateral or apical side of the cells and their target molecules. Given the kidney-like nature of the cells, Figure 4.8 suggests the placement of the membrane transporters on either the lumen facing side, or the blood facing side of the cell. This demonstrates the potential efforts of the Vero cells to filter the medium to achieve some version of homeostasis while being cultured in CDM2-S.

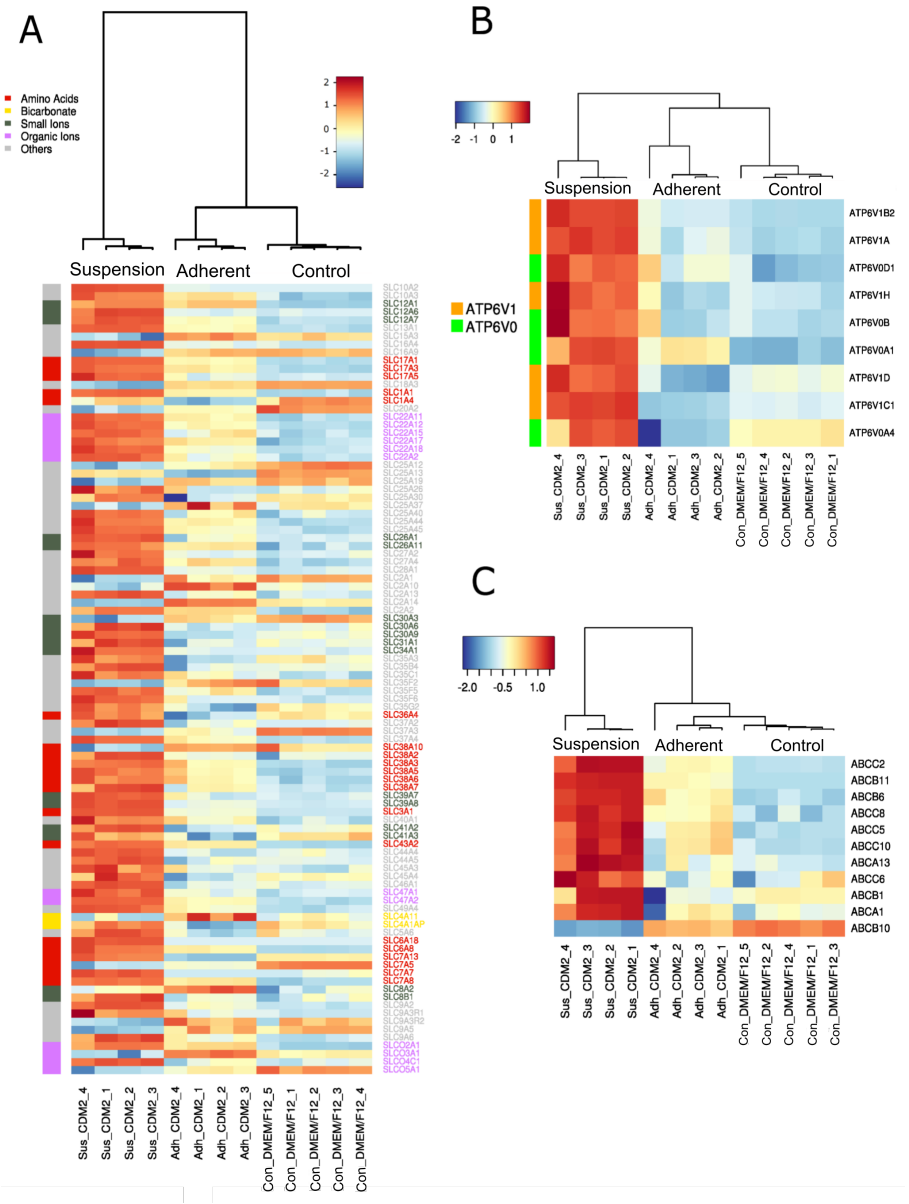

Figure 4.7: Heatmaps of differentially expressed membrane transporters (FDR < 0.001). The x-axis shows the samples, and the y-axis represents the HGNC symbols. The colouring of the heatmap represents the standardized, normalized expression log(CPM) values according to the legend at the top left side of each heatmap. **A.** Heatmap of differentially regulated solute carrier. **B.** Heatmap of differentially regulated subunits of V-type proton ATP (ATP6V). **C.** Heatmap of differentially regulated ATP-binding cassette (ABC)-transporters. The name of each gene has colouring overlaid on the text to show if the transporter is associated with the transport of amino acids (red), bicarbonate ions (yellow), small ions (dark green), organic ions (pink) or other (grey). Control is Vero cells grown in DMEM/F12+10% FBS and Adherent is Vero cells grown in CDM2-A.

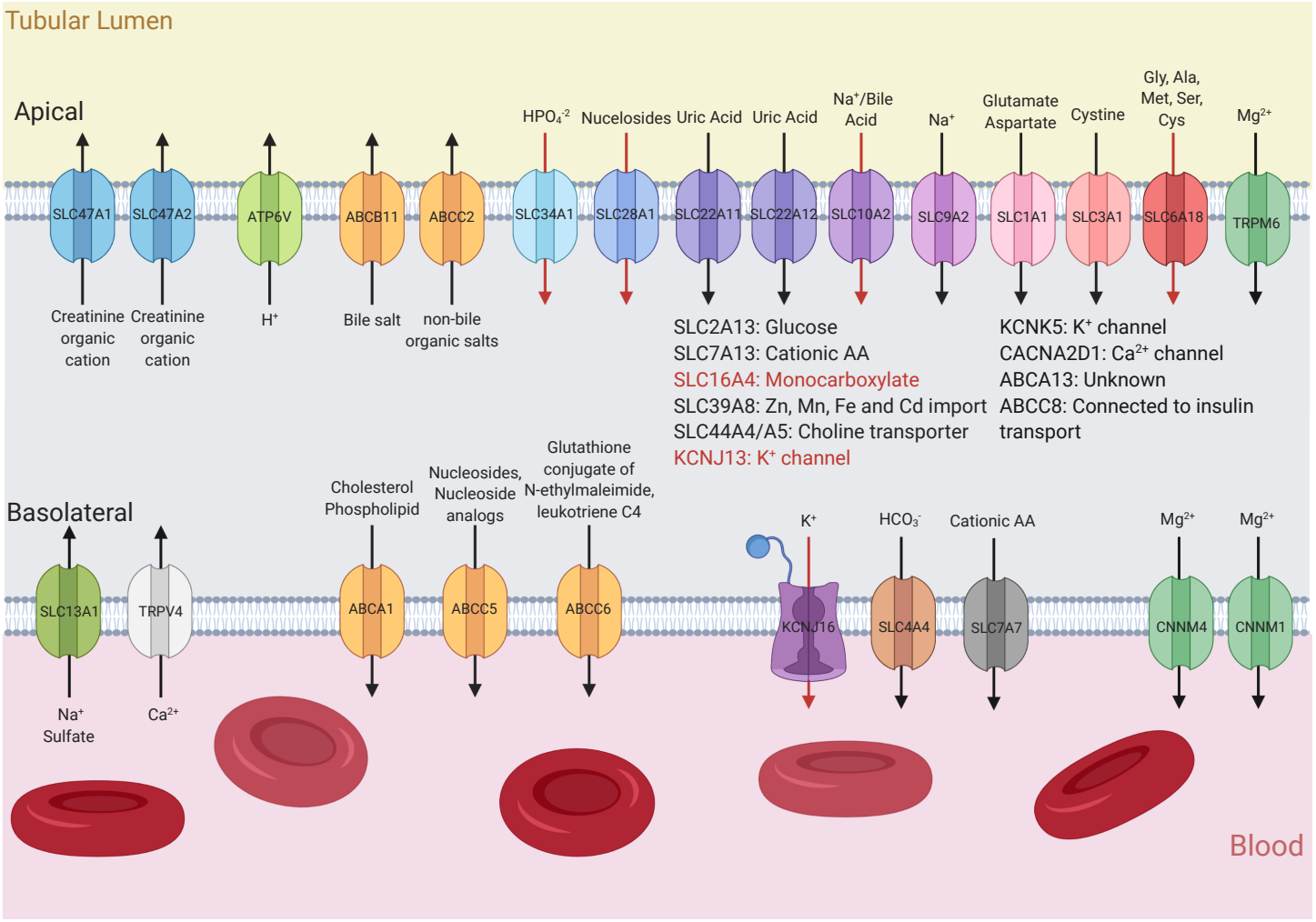

Figure 4.8: A scheme of the significantly up-regulated membrane transporters with the target molecules and the direction of transport in a nephron. The transporters whose location are unknown are mentioned in the center of the image. Red colored arrows or gene names indicate an log fold-change > 5. Image created using *BioRender.com*.

4.3.5 Up-regulation of Cell Adhesion Genes

In previous experiments from this work, suspension Vero cells grew as aggregates, which is consistent with a previous report in which Vero cells were cultured in SFM as aggregates [269]. To investigate cell adhesion further, genes encoding cell adhesion molecules (CAMs) (i.e., CAMs involved in cell-cell adhesion or adhesion with the extracellular matrix) were analyzed. Figure 4.9 shows the normalized expression level in $\log_2$CPM of various claudins (*cldn*), *vcam1*, and integrin β_2 (*itgb2*) genes in the three different groups of Vero cells. Vero cells grown in CDM2-S had higher expression of *cldn1*, *cldn2*, *cldn10*, *vcam1* and *itgb2* compared to cells grown in DMEM/F12+10% FBS. Vero cells grown in CDM2-A specifically up-regulated *cldn15* as compared to the other conditions, and down-regulated *cldn4* and *cldn12*. Conversely, suspension Vero cells up-regulated almost all the adhesion molecules with the exception of *cldn15*. Claudin 15 is permeable for small cations and water, and is present in many different types of tissues where tight junctions are required such as the small intestines, colon segments, but it is not present in the kidney tubules [409].

4.3.6 Up-regulation of Fatty Acid β-Oxidation

Genes associated with fatty acid β-oxidation were heavily up-regulated in suspension Vero cells compared to the adherent phenotype. In total, 35 genes associated with fatty acid β-oxidation were identified, and 29 of those were up-regulated in suspension Vero cells (Figure 4.10). Figure 4.11 shows a diagram of the proteins that were up-regulated in suspension Vero cells and where they are located in the cell for fatty acid degradation through the mitochondria. Suspension Vero cells up-regulated all of the genes in Figure 4.10 except *tgfb1*, *crot*, *acsl3*, *lipg* and *lipe*. Interestingly, many of the same fatty acid

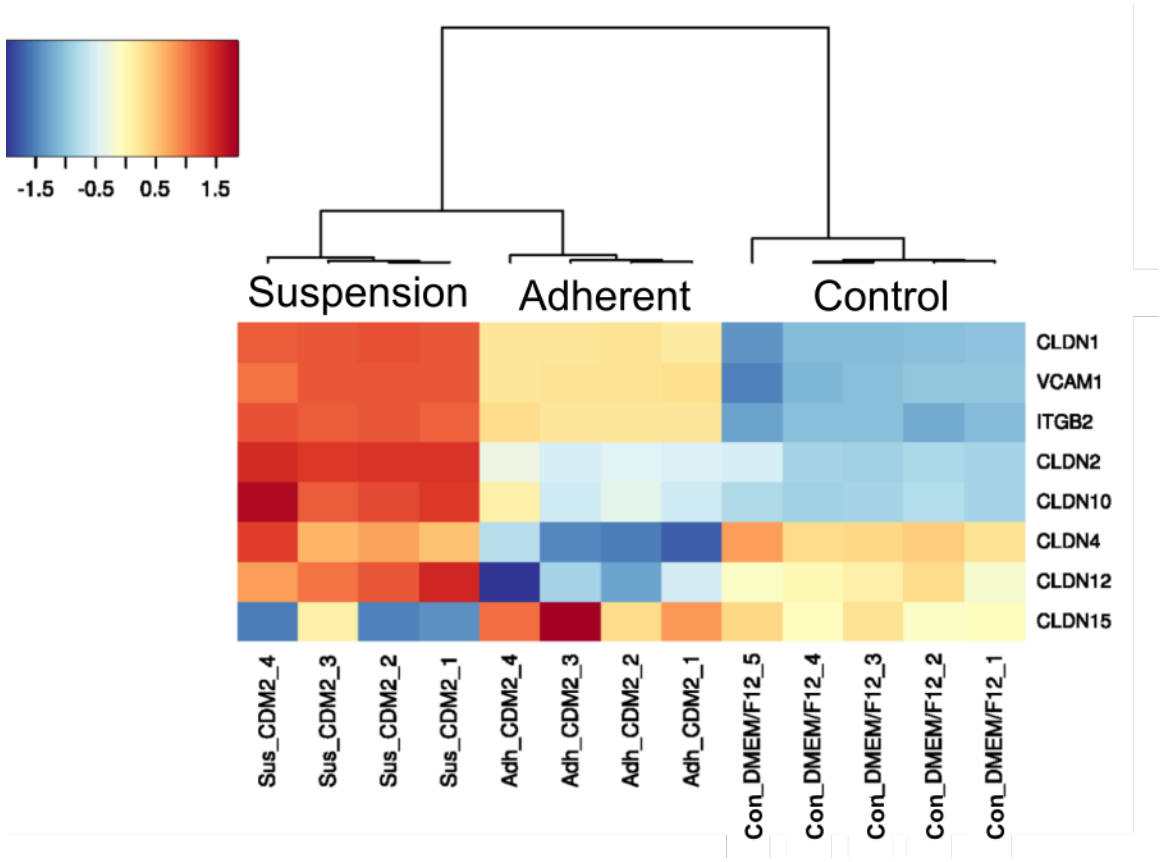

Figure 4.9: Heat map of tight junctions associated claudins (FDR < 0.001). The x-axis shows the samples and the y-axis represents the HGNC symbols. The colouring of the heatmap represents the standardized, normalized expression $\log_2$CPM values according to the legend at the top left side of each heatmap. Control is Vero cells grown in DMEM/F12+10% FBS and Adherent is Vero cells grown in CDM2-A.

β-oxidation associated genes that were down-regulated by suspension Vero cells were up-regulated in Vero cells grown adherently in CDM2-A. Specifically, the only up-regulated genes in the Adh group were *tgfb1*, *acsl3*, *lipg*, *mgll* and *lipe*. Table 4.1 lists the genes that were differentially expressed between suspension and adherently grown Vero cells in CDM2-A. The genes *acsl3*, *lipg*, and *lipe* are associated with the cellular process of breaking down lipids into fatty acids and are up-regulated in both the Con and Adh Vero cells groups, but down-regulated in the Sus Vero cells. The *tgfb1* gene was highly expressed in Adh Vero cells and it encodes for the transforming growth factor β1. This growth factor was not supplied in CDM2 and these cells were still able to proliferate. Conversely, *tgfb1* was not highly expressed in suspension cells. The *tgfb1* gene is associated with cell growth and epithelial-mesenchymal transition (EMT) that allows epithelial cells to take on a mesenchymal phenotype such as decreased cell adhesion, loss of polarity and tight junctions [172].

Table 4.1: List of differentially expressed genes between adherent and suspension Vero cells grown in CDM2-A and CDM2-S. All information was acquired from UniProt.

Gene Name	**Protein Name**	**Function**	**Ref.**
acsl3	Long-chain-fatty-acid-CoA ligase 3	Acyl-CoA synthetases (ACSL) activates long-chain fatty acids for both synthesis of cellular lipids, and degradation via beta-oxidation. Required for the incorporation of fatty acids into phosphatidylcholine, the major phospholipid located on the surface of VLDL (very low density lipoproteins). Has mainly an anabolic role in energy metabolism.	[526, 340]
crot	Peroxisomal carnitine O-octanoyltransferase	Catalyzes the reversible transfer of fatty acyl groups between CoA and L-carnitine in the peroxisome and mitochondria. CROT has an affinity for medium-chain fatty acids (between 6 and 12 carbons)	[247]
lipe	Hormone-sensitive lipase	Lipase with broad substrate specificity, catalyzing the hydrolysis of triacylglycerols (TAGs), diacylglycerols (DAGs), monoacylglycerols (MAGs), cholesteryl esters and retinyl esters	[185, 10, 138, 404]
lipg	Endothelial lipase	Exerts both phospholipase and triglyceride lipase activities.	[203, 303, 184]
mgll	Monoglyceride lipase	Converts monoacylglycerides to free fatty acids and glycerol. It also regulates the levels of fatty acids that serve as signaling molecules and promotes cancer cell migration, invasion and tumor growth.	[422, 346]
tgfb1	Transforming growth factor β-1 proprotein	Multifunctional protein that regulates the growth and differentiation of various cell types and is involved in various processes, such as normal development, immune function, microglia function and responses to neurodegeneration. It can induce epithelial-mesenchymal transition (EMT) and cell migration in various cell types.	[224, 193]

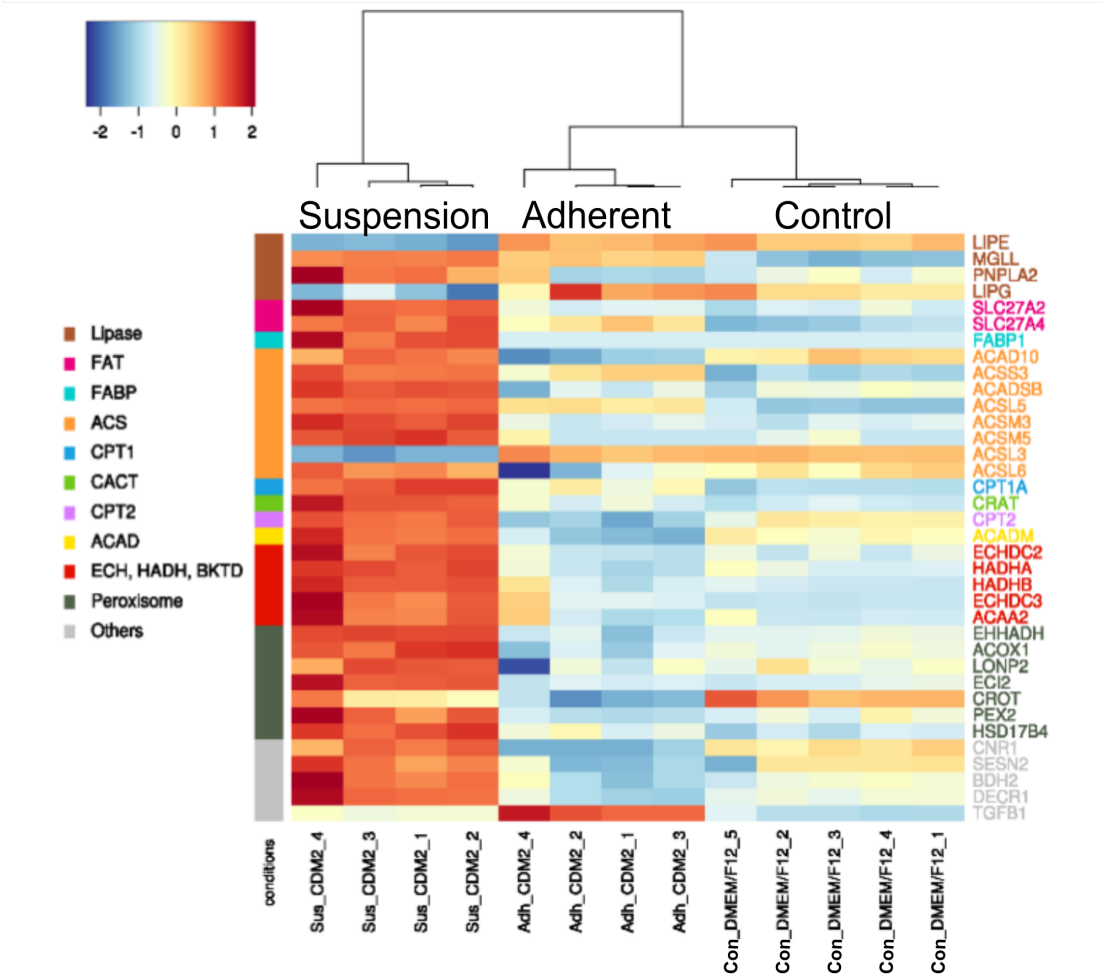

Figure 4.10: Up-regulation of fatty acid beta oxidation related genes (GO:0006635). A heatmap of differentially regulated genes. The x-axis shows the samples and the y-axis represents the HGNC symbols. Colouring of the samples is the same as in Figure 4.11. The colouring of the heatmap represents the standardized, normalized expression $\log_2$CPM values according to the legend at the top left side of each heatmap.

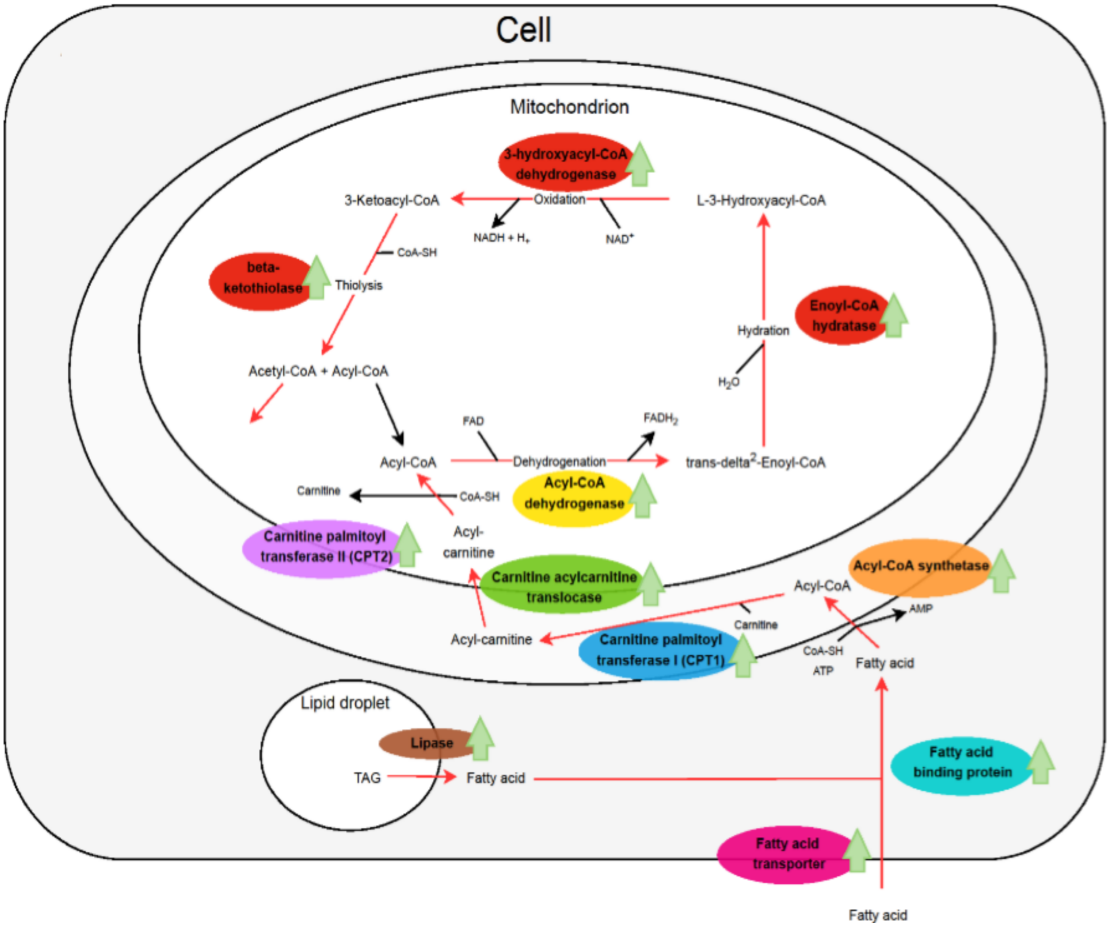

Figure 4.11: Up-regulation of fatty acid beta oxidation related genes (GO:0006635). Diagram of fatty acid beta oxidation with the main reactions and enzymes in mitochondria. Green arrows label significant up-regulation of at least one gene in that reaction group with an FDR threshold of 0.001. Red arrows emphasize the fatty acid and derivatives flow through the process until Acetyl-CoA.

4.4 Discussion

In recent years, 'omics technologies have been leveraged to improve animal cell culture processes by allowing observation and subsequent elucidation of underlying cellular processes in response to different environments. Transcriptomics involves the analysis of gene expression levels in order to identify how various cellular processes such as metabolism, cell signalling, apoptosis, or cell proliferation are regulated as the cell responds to its environment. This information can be used to identify and understand the role of genes or gene pathways that are important for development or function of different tissues and specific phenotypes, or important in disease processes and drug resistance [455]. It has also proven valuable for identifying differences in gene expression profiles between suspension and adherent cell phenotypes [201, 252]. Significantly, gene targets identified through this approach have been disrupted or introduced using genetic engineering techniques to enable the development of new suspension-adapted cell lines or accelerate the adaptation process of the same cell type [76, 252]. The major goal of this work was to use transcriptomics (i.e., RNA-seq) to identify key differences between suspension and adherent Vero cells in an effort to understand the underlying cellular processes that contribute to the recalcitrance of Vero cells to growth in suspension in CDM2-S medium. Significantly, our data suggested that suspension Vero cells displayed gene expression profiles more similar to kidney tissue-specific patterns than Vero cells cultured adherently in either DMEM/F12 + 10% FBS or CDM2-A. Genes associated with cell growth, membrane transporters, cell-cell adhesion proteins and fatty acid β-oxidation were notably differentially expressed.

Progression through the cell cycle requires expression of genes involved in DNA replication and condensation, spindle formation, and centrosome separation. Cyclin-dependent kinases (CDKs) and cyclins promote cell cycle transitions by positive feedback loops [40]

and were down-regulated in the suspension cells compared to the adherent culture (Figure 4.4). Specifically, cyclin A binds CDK2 and CDK1 to initiate progression through the G1/S phase and G2/M phase, respectively, and is therefore required for the onset of DNA replication and mitosis Figure 4.4 [72]. Cdk1 is associated with the G2/M checkpoint, and modulating the the centrosome cycle [496]. All three of these proteins were down-regulated in suspension cells compared to adherent cells. On the other hand, the Cdk interacting protein 1 (CIP1) was up-regulated. The CIP1 protein inhibits Cdk activity by binding to cyclin/Cdk complexes (particularly cyclin A-E/Cdk2, cyclin D/Cdk4-6 and cyclin A-B/Cdk1 heterodimers) [49]. This further prohibits the cells from progressing through the cell cycle. Furthermore, other genes that influence DNA-replication in the S phase were also down-regulated, such as *cdc6* [350], *cdc45* [468], *skp2* [362], *dbf4* [394] and genes associated with the MCM complex [481]. This implies that there was reduced DNA synthesis in the suspension Vero cells. Interestingly, *chk1* and *chk2* were also down-regulated, although they are responsible for arresting cell growth when there is DNA damage [92]. Since there was little DNA being synthesized, there was little use for cells to produce proteins to check for DNA damage. The genes associated with the G2/M phase transition were also down-regulated; Cdc25a activates CDK2 and CDK1 [265, 471]. Other genes such as *smc3* [134], *mps1* [216], *esp1* [81], *plk1* [496], *mad2* [430] also participate in the G2 and M phases by influencing chromosome segregation, spindle formation and centrosome separation and duplication. The specific role of each gene can be found in Supplementary Table C.1 in Appendix C. During M phase, the less abundant Bub3 and Bubr1 proteins are part of the spindle checkpoint function, specifically inhibiting the anaphase-promoting complex or cyclosome [460]. Down regulation of these key cell cycle genes is consistent with senescence of the suspension Vero cells.

Despite the very low growth rate, Vero cells cultured in CDM2-S in suspension main-

tained high viability (> 80%) after 105 days (Figure 4.1). To ensure that the slow growth rate was not due to programmed cell death (i.e., apoptosis), the RNA-seq data was explored to identify differentially expressed genes associated with apoptotic pathways. The highest up-regulated log fold-change for anti-apoptotic genes were *lrp2*, *pkhd1* and *tmigd1* (Figure 4.4B). These genes have been shown to protect renal cells from apoptosis [16, 67, 284]. On the other hand, the pro-apoptotic *tnfsf10* gene, which has been shown to trigger apoptosis in renal cells, was up-regulated. Interestingly, *tnfsf10*-mediated apoptosis appears to be especially important in high glucose environments (30 mM glucose); CDM2-S contains 25 mM glucose [276, 32]. This may be consistent with the idea that apoptosis does play a role in the low observed growth rate of the suspension Vero cells. Conversely, the expression of common apoptogenic genes (i.e., *bax*, *bak1*, and *bad*) and anti-apoptotic genes (i.e., *mcl1* and *bcl-2l2*) were similar between suspension and adherent cells. Interestingly, the anti-apoptotic *bcl-2* [66] gene was up-regulated in suspension Vero cells relative to the adherent cultures. Overall, the wide range in expressional changes in both pro- and anti-apoptosis genes does not indicate definitively that the low proliferation rate of CDM2-S grown Vero cells was due to apoptosis. However, it is impossible to discount this possibility entirely, as several anti- and pro-apoptotic genes were differentially regulated, suggesting that the cells in CDM2-S may have been experiencing some kind of stress, and apoptosis may have a role.

Overall, the down-regulation of several cell-cycle genes supports the possibility that the suspension Vero cells had arrested their growth, rather than the cell culture having a high rate of apoptosis. To overcome cell quiescence, key genes can be up-regulated such as *c-myc* [49], *bcl-2* [23], or the addition of growth stimulating growth factors such as transforming growth factor beta (TGF-β) [172]. The *c-myc* gene is associated with tumor progression and was down-regulated in suspension Vero cells. It has been shown that the

expression of *c-myc* in quiescent cells caused them to re-enter the cell cycle and begin to proliferate [49]. Interestingly, in non-cancerous cells TGF-β will cause the down-regulation of *c-myc* and stop cell proliferation [49]. Although, once the cancerous phenotype is already established, TGF-β will not stop the cells from proliferating, but will allow cells to become mesenchymal-like, such as being more motile, and reducing their dependence on adhesion factors, which allows cancers to metastasize [170].

The epithelial-mesenchymal transition (EMT) is a process by which epithelial cells undergo biochemical changes (i.e., loss of cell apical-basal polarity and cell-cell adhesion; reorganization of the cytoskeleton; and changed cell shape/morphology) to assume a mesenchymal cell phenotype (i.e., gain enhanced migratory and invasiveness capacity; increased production of ECM components; and multipotency). Mesenchymal cells, and by extension the EMT, are important for wound healing, tissue regeneration, and organ fibrosis processes [208]. On the other hand, the reverse process (i.e., mesenchymal-epithelial transition; MET) is critical for the development of tissues and organs; MET is well-studied for its role in kidney development, and is marked by increased expression of cell polarity-related cell surface molecules, assembly of junctional complexes and tight junctions, along with the organization of organelles and cytoskeletal structures [375, 208]. Markers of mesenchymal transition include N-cadherin, vimentin, fibronectin, and β1 and β3 integrins, whereas MET in kidney tissue is driven by genes such as paired box 2 (*pax2*), bone morphogenetic protein 7 (*bmp7*), and Wilms tumor 1 (*wt1*) [208]. The phenotypic plasticity of EMT also means that cells can express both types of markers simultaneously; for example, some types of cells can assume some mesenchymal traits whilst maintaining most of their epithelial traits [208, 105, 242]. Therefore, this process is most aptly considered as a continuum of cell differentiation states; full, terminal differentiation (i.e., epithelial cells organized as epithelium and exerting tissue-specific function) is at one end and fully realized phenotypic

plasticity is at the other. Moreover, although differential expression of epithelial-specific or mesenchymal-specific genes is important, regulation of EMT/MET is also dependent on several other factors: extracellular signals such as juxtacrine and paracrine signalling from macrophages and fibroblasts within the stroma; autocrine signalling such as TGF-β; extensive changes in the splicing of mRNAs to generate diverse protein isoforms; and micro-RNA-mediated control of translation all contribute to EMT progression [105, 208, 242]. It is pertinent to note that the contribution of the latter two factors in particular may be difficult to ascertain by transcriptomics alone. Nevertheless, the sum total of the RNA-seq dataset suggests that suspension Vero cells in CDM2-S displayed higher expression of genes associated with epithelial cells compared to the adherent Vero cultures (Supplementary Figures D.5 and D.6 in Appendix D).

Vero cells cultured in CDM2-S showed up-regulation of genes encoding CAMs, specifically those associated with tight junctions called claudins. Claudins are a family of transmembrane proteins that are important components of tight junctions, which allow epithelial and endothelial cells to form connected cell 'sheets' to provide a barrier to prevent water and other small molecules from passing between cells, and maintain cell polarity. To promote single cell suspension, CDM2-S had low amounts of calcium and magnesium to prevent calcium-dependent CAMs from properly functioning; many CAMs (i.e., cadherins, integrins, and selectins) require calcium or magnesium cofactors for proper function, however, claudins and vascular adhesion molecules (VCAM-1) do not have this requirement [335, 217, 7]. Moreover, along with up-regulation of the aforementioned MET genes *pax2* and *bmp7*, genes encoding fibronectin (*fn1*), N-cadherin (*cdh2*), and β1 integrin (*itgb1*) were downregulated. Additionally, the transforming growth factor-β (*tgfb1*), which plays a central role in inducing EMT in kidney tissue [105], was also significantly downregulated, possibly indicating that suspension Vero cells are undergoing MET [242]. Conversely,

the epithelial marker E-cadherin (*cdh1*) was also significantly downregulated in CDM2-S-grown cells. Further, expression of vimentin (*vim*) and several matrix metalloproteinases (e.g., *mmp1*, *mmp10*, *mmp14*, and *mmp27*), which enhance ECM protein degradation, were significantly up-regulated compared to control cells [208]. Significantly, the *mmp1* gene was up-regulated in anchorage-independent *siat7e*- and oncogenic and EMT-inducing gene *ras*-expressing MDCK cells, and overexpression of *mmp1* in parental MDCK cells reduced cellular adhesion [437, 296, 75]. These seemingly contradictory results highlight the dynamic nature and complicated underlying biology of EMT. Finally, it is important to note that many of the same expression patterns were also observed for CDM2-A-grown Vero cells, perhaps indicating that a medium formulation with higher levels of calcium and magnesium may yet support growth of Vero cells in suspension.

For many types of carcinomas, growth factors can be added to the medium such as hepatocyte growth factor (HGF), epidermal growth factor (EGF), platelet-derived growth factor (PDGF), and TGF-β to induce EMT promoting transcription factors [208]. In the CDM2-A/S medium formulations, only rEGF was present at 20 ng/mL, whereas in other in-house media that were used by Rourou *et al.* and Shen *et al.* to support Vero growth in suspension contained undefined plant hydrolysates or peptones [412, 433]. Soy hydrolysates have been shown to replace autocrine growth factors in single-cell suspension medium for CHO cells [518], and peptides derived from soy protein or wheat gluten can mimic growth or survival factors for mouse hybridoma ME-760 cells [130]. As such, supplementation of additional growth factors to the CDM2 medium may stimulate growth and induce EMT.

Finally, the RNA-seq data could suggest that the Vero cells cultured in CDM2-S are undergoing terminal differentiation (i.e., exerting kidney tissue-specific function). The data indicated that genes encoding membrane transporter proteins were up-regulated in suspension cells compared to adherent cells. Specifically, the cells appear to want to im-

port uric acid (using up-regulated SLC22A11 and SLC22A12 transporters)and nucleosides (SLC28A1) from the tubular lumen side into the cell. Additionally they appear to be wanting to export nucleosides and nucleoside analogs (ABCC5) into the blood stream. Interestingly, nucleotide and nucleoside signalling has been implicated in the regulation of the EMT process; the human equilibrative nucleoside transporter 1 (ENT1; *slc29a1*) gene reportedly has a protective role in maintaining the epithelial phenotype [293]. This receptor, as well as the sodium/nucleoside cotransporter *slc28a1* gene were significantly up-regulated in suspension Vero cells. Urate is a waste product from the metabolism of purines (adenine, guanosine, xathine, hypoxanthine) or nucleosides, and the normal blood urea levels for African Green monkeys ranges from 10-11 mg/dL [421]. Here it appears that the Vero cells could be attempting to regulate blood urate levels since none was supplemented in the CDM2-A/S media formulation. In addition to up-regulation of several amino acid transporters, several genes encoding solute transporter proteins were also up-regulated. Interestingly, 5 of these had sodium as a target, whereas 4 transported metals such as iron, zinc and calcium. Moreover, trace metals are extremely important in SFM formulations as they act as cofactors in many integral enzymes. The cells could be attempting to import more of the metals for proper enzyme function. Similarly, V-ATPases were up-regulated in suspension Vero cells compared to the adherent phenotype. These types of pumps are used by the cells to create an ion gradient across the plasma membrane to maintain the pH balance inside the cell and in endosomes and lysosomes [365, 457]. In the epithelial cells of the kidney's proximal tubule, V-ATPases help maintain the pH balance of blood and lower pH in urine [365]. Further, it was found that significant up-regulation of V-ATPases (subunits B2, E and c) and high levels of TGF-β1 resulted in the EMT of rat proximal tubular epithelial cells [63]. It is possible that the addition of TFG-β could cause suspension Vero cells to become more mesenchymal-like and increase their prolif-

eration rate. Finally, gene pathways associated with fatty acid β-oxidation (FAO) were significantly up-regulated in suspension Vero cells compared to Vero cells that were grown adherently (Adh and Con). Previous studies have suggested that proliferating or cancerous cells will preferentially utilize glycolysis for energy metabolism rather than fatty acid β-oxidation, whereas quiescent endothelial and kidney epithelial cells use fatty acid oxidation for energy generation and regenerate NADPH [209, 419, 392, 31, 441]. Interestingly, recent studies have provided evidence that FAO is required for the maintenance of endothelial identity; induction of the endothelial-mesenchymal transition triggers inhibition of FAO in endothelial cells [515, 277]. Further, inhibited or altered FAO has been associated with various kidney disorders, including kidney fibrosis and chronic kidney disease, further implicating the importance of FAO in terminally differentiated kidney epithelial cells [277, 190, 211, 31]. Therefore, this data supports the idea that suspension Vero cells are becoming quiescent kidney cells by shifting their metabolism from using glucose, to using fatty acid β-oxidation. Notably, this observation may also provide evidence that the suspension Vero cells are still metabolically active and not apoptotic.

Overall, this work provides clues of why the suspension Vero phenotype has been so difficult to achieve, and possible genes to increase the growth rate of the cells.

4.5 Conclusions

Transcriptomics is a powerful tool for eliciting a deeper understanding of how cells react to their environment on a genetic level, and helps elucidate some of the phenotypic changes that occur within the cell. Overall, the RNA-seq data here demonstrated that suspension Vero cells became quiescent rather than apoptotic, and that genes associated with cell-cycle progression were down-regulated whereas genes associated with fatty acid β-oxidation were

up-regulated. The differentially expressed genes in both these pathways suggested that the suspension Vero cells were quiescent, but still metabolically active. In addition to the arrest of growth, suspension Vero cells up-regulated kidney tissue-associated genes. Suspension Vero cells specifically up-regulated genes associated with solute membrane transporters and proteins that form tight junctions which is important for the epithelial barrier and function of the tubule of the kidney for filtering blood. These kidney-like Vero cells also had higher expression of epithelial-associated genes rather than mesenchymal-associated genes compared to the adherent phenotype, which indicates that the suspension cells could have undergone MET. In order to overcome the low growth rate, genes associated with the EMT should be up-regulated or growth factors that promote the transition should be added to the medium.

Chapter 5

Improvement of Chemically Defined Media Using Transcriptomics

5.1 Introduction

Traditionally, media development has relied on techniques such as liquid chromatography (LC), nuclear magnetic resonanace (NMR), or mass spectrometry (MS) to identify and quantify media components that are depleted or consumed during cell culture. These techniques look at the metabolic profiles of the cells at specific timepoints of when the samples were taken. This provides researchers with snapshots of the concentrations of various compounds in the media, and the production or consumption of the compounds can be tracked over time. LC can detect amino acid concentrations in the micromolar range, and has also been adapted to take in-line measurements of cell culture processes [146, 246]. One of the drawbacks of using LC is that it requires a standard curve of pure substances to be made for each compound of interest to be run before running samples.

Additionally, only certain classes of compounds can be detected in a single measurement because of poor separation of compounds, which is determined based on the column and detector set up. Similarly, NMR can also detect relatively high concentrations of compounds in the micromolar range, but the number of compounds that can be detected in a single measurement is far greater than with LC since NMR uses the unique resonance frequency of a compound instead of it's elution time from a chromatography column. Like LC, NMR cell culture media sample preparation involves filtering the sample and spiking in an internal standard, but there is no need to create a standard curve for every compound of interest. Compounds can be profiled based on their known resonances which can be found on NMR profiling softwares (for example Chenomx) or from online databases (Human Metabolome Database, https://hmdb.ca/) [291]. However, NMR instruments are complex and require extensive and specialized training to obtain high quality results and peak profiling is still done by hand which is laborious and time-consuming. When detection of compounds present in very low concentrations is required, MS is often used. This device can acquire huge amounts of data, but requires complex sample preparation and can only measure compounds with similar chemical and physical properties at a time. These instruments are extremely expensive and also requires extensive expertise to operate and to process the data. MS has the additional benefit of being used for proteomic work since it can also measure changes in the cell's proteome as they adapt from adherent to suspension culture. Kluge *et al.*, studied the stepwise adaptation of MDCK cells from adherent growth with serum-containing media (SCM), to serum-free media (SFM) and suspension growth [229]. They found that most of the changes in the proteome were associated with serum-deprivation, cytoskeletal restructuring, genetic information processing, or cellular metabolism [229].

Another method used to measure changes that occur in cell populations as they adapt

from adherent to suspension growth is transcriptomics. Various expression pathways can be probed to identify up-regulated or down-regulated genes using this technology. Particularly, this has been used to measure the different expression patterns in stem cells, cancer pathways, identifying biomarkers, and understanding the expression patterns governing different phenotypes [278]. RNA sequencing (RNA-seq) has become the most popular method to gather transcriptomic data with 8,083 publications in 2020 (PubMed), because of the low background noise, speed and depth of the data that can be collected with this technique. Given the vast amount of transcriptomic information that can be collected by RNA-seq, metabolic pathways can also be probed to identify changes in the cell's gene expression as it adapts from adherent to suspension culture.

Historically, the change from adherent-dependent growth to suspension growth was accomplished by adapting the cells to SFM and then transitioning the cells on to a shaking platform, or stirred tank reactor [229]. Research has focused on time-consuming media development of SFM by screening thousands of compounds to produce suspension cell lines. Although, this is changing as more genetic information is becoming available for a plethora of different cell lines. Since 2007, transcriptomics has been used to study the underlying changes in gene expression while adapting various cells lines to suspension growth by mechanical shaking. Jaluria *et al.*, used DNA microarrays to identify two key genes (*siat7e* and *lama4*) that influenced HeLa cell adhesion [201]. They found that overexpressing *siat7e* and reducing the expression of *lama4* reduced cellular adhesion in HeLa cells [201]. Subsequently, in 2009 Chu *et al.* overexpressed *siat7e* in MDCK cells to produce an anchorage-independent culture that was capable of producing high titers (40,690 HAU/mL) of Influenza B/Victoria/504/2000 strain [76]. *Siat7e* (ST6GGALNAC5, ST6 N-acetylgalactosaminide α-2,6-sialyltransferase 5) is a human sialyltransferase that plays a role in forming the ganglioside GD1α which rests on the cell's surface and inhibits cell

adhesion [469, 173]. This was a pivotal study that showed the ability to insert a gene that is not known to be oncogenic to promote suspension growth without interfering with virus production. A similar study was then conducted in 2016 by Lee *et al.* where they adapted CHO-K1 cells to suspension [252]. They used RNA-seq to identify two key down-regulated genes (*igfbp4* and *aqp1*) associated with the suspension phenotype, and verified the effect using the CRISPR/Cas9 system by deleting the genes from adherent CHO-K1 cells which resulted in a 54% reduced adaptation time [252]. While all of these studies provided key insights on genes that are associated with adaptation to the suspension phenotype, applying this information to other cell lines would require genetic engineering of other cell lines, and the genes identified from the aforementioned research are not guaranteed to work for all cell types.

Alternatively, researchers can use the transcriptome data not only to identify genes that are differentially expressed between the two phenotypes, but can look more specifically look at differentially expressed genes associated with metabolic pathways. For many in industry, it is more amenable to make changes in the media rather than genetically engineering different cell lines, since these edited cell lines will have to be requalified to meet regulatory requirements by the Food and Drug Administration (FDA) and European Medicines Agency (EMA) [123]. By using transcriptomics, researchers can see how the cell changes the expression levels of mRNA in relation to metabolic pathways as they adapt from adherent to suspension growth. This information can provide more detail on the nutritional needs of the cells and guide researchers on how to improve their media formulations, for adherent or suspension cells. Given the increased accessibility and reduction in cost of conducting experiments, transcriptomics provides complementary information to MS and NMR analyses by giving better insight on low-concentration components that could be missing from the media and that cells are compensating for by overexpression of

certain genes.

Here, we used RNA-seq data from adherent and suspension Vero cells to improve a chemically defined media formulation. Metabolic pathways that were up-regulated in Vero cells maintained in suspension culture were identified. Subsequently, Plakett-Burman design of experiments were used to screen the effect of supplementation of these identified growth factors, polyamines, vitamins and steroids. Supplementation of several components, including progesterone, β-estradiol, prostaglandin E_2, and vitamin A had positive effects on growth rate. Thus, RNA-seq may be a valuable tool for guiding cell culture media development by identifying molecules the cell may require direct supplementation.

5.2 Materials and Methods

5.2.1 Cell Culture and Media Development

Vero cells (CCL81 n+51, ATCC, USA) were thawed from liquid nitrogen and maintained in DMEM/F12 (Corning, USA) + 10% FBS (Hyclone, USA) + 4 mM GlutaMax™ (Gibco, USA) in a humidified, 5% CO_2 incubator at 37°C. Cells were passaged every 2-3 days to keep confluence below 90%. Unless otherwise stated, all compounds were obtained from Sigma-Aldrich. The media formulation that was developed in Plackett-Burman Experiment 4 in Chapter 3 was used as the base media and the additional compounds were added to this medium formulation. Cell adaption to the SFM was performed over 4 passages by replacing 25% of DMEM/F12 + 10% FBS + 4 mM GlutaMax™ with the SFM. Once the cells were adapted to the SFM they were seeded on to tissue-culture treated 6-well plates. Each day for 10 days, 1 mL media sample was taken and stored in a -80°C freezer and cells were washed twice with Ca^{2+}-, Mg^{2+}-free D-PBS and detached with TrypLE™

for 3-5 minutes. The cells were resuspended in a final volume of 1 mL and a cell count was performed using a Countess II Automated Cell Counter, using trypan blue to stain for dead cells.

Plackett-Burman

To screen compounds, a Plackett-Burman style of experiment design was used with 8 media samples that tested 7 different compounds. To make the media, concentrated stock solutions of each compound were made using ultra pure MiliQ water. DMEM/F12 base with 15 mM HEPES, without L-glutamine, L-leucine, L-lysine, L-methionine, $CaCl_2$, $MgCl_2$, $MgSO_4$, sodium bicarbonate, and phenol red was made from powder using ultra pure MiliQ water in 1 L batches. 40 mL of each media sample was made by supplementing DMEM/F12 with the various compounds, without increasing the volume more than 10%.

5.2.2 RNA-seq Analysis

The RNA-seq analysis was completed as previously described in Chapter 4. In brief, Vero cells were maintained in DMEM/F12 + 10% FBS, Formula 17 (described in Appendix B), and Formula 17 + 1 mM calcium and 0.7 mM magnesium. The RNA was extracted using a Total RNA Tissue Kit and samples were stored at -80°C following extraction. cDNA libraries were prepared and sequenced at the Centre for Applied Genomics, Sick Kids Hospital, Toronto, Canada. The read quality was controlled with FastQC v3 [14] before and after trimming. The reads were trimmed from 3 termini with a k-mer size of 23 using BBduk [54]. Reads were aligned with STAR aligner v2.6.0 [103] to the Vervet-AGM genome assembly 43 (ChlSab1.1: GCA_000409795.2) from Ensembl release 96.1. The gene expression level was quantified with RSEM v1.3.1 [258] with default settings. The

quantified reads for each gene per sample were then further analyzed in RStudio (RStudio Team, 2016) with the package edgeR [402]. EdgeR identified the differentially expressed genes for the two comparisons of adherent against suspension, or control against suspension samples. These contrasts tested for the differences caused by the adaption to the chemically defined media and adaptation of the cells to suspension culture. For pathway analysis, the Vervet-AGM gene annotations from Ensembl were changed to human homologs with HGNC symbols annotation using BioMart [110].

5.2.3 NMR Analysis

The procedure that was used in this research has previously been described by Sokolenko *et al.* [446]. In brief, 630 µL of cell culture supernatant was spiked with 70 µL of an internal standard internal NMR standard composed of 99.9% D2O with 5 mM 2,2-dimethyl-2-silapentane-5-sulfonate (DSS) serving as a chemical shape indicator (CSI) and 0.2% w/v sodium azide (NaN_3) to inhibit bacterial growth (Chenomx Inc., Edmonton, Canada). The solution was vortexed, and 700 L was pipetted into a 5 mm NMR tube (NE-UL5-7, New Era Enterprises Inc., Vineland, NJ) for scanning.

NMR spectra were acquired using the first increment of a nuclear Overhauser effect spectroscopy (NOESY) pulse sequence with a 1 s presaturation pulse (10 ms relaxation delay, 990 ms water suppression), 100 ms mixing time, and a 4 s acquisition time on a Bruker Avance 600.13 MHz spectrometer with a triple resonance probe (TXI 600). Following acquisition, spectra were imported into Chenomx NMR Suite 8.4 (Chenomx Inc., Edmonton, Canada). Phase and baseline corrections were carried out manually. Line asymmetry correction was performed automatically on each sample by the software based on a manual comparison of ideal and observed DSS peaks. Compounds were quantified by hand us-

ing the softwares built-in 600 MHz compound library by comparison to a known amount of DSS as the internal standard (see http://www.chenomx.com/ for more information on targeted profiling).

The data was then exported as a CSV file and the plots were generated using the R programming language.

5.2.4 Visualization

Graphs were generated with ggplot2 [504]. The cell cycle pathways from KEGG (pathway hsa04110) was rendered with the R package pathview [280].

5.3 Results

5.3.1 NMR Metabolite Analysis

The medium formulation that was developed in Chapter 3 was compared to 2 commercially available ACF media (NutriVero Flex 10 and OptiPro™ SFM). NutriVero Flex 10 is an ACF, chemically defined media designed for adherent Vero cells, and OptiPRO™ SFM is a SFM and ACF medium that contains very low amounts of protein (< 7.5 µg/mL). Vero cells were grown in the three SFM, for 10 days and the media was refreshed when its color changed from red to orange, which indicates a drop in pH. Daily medium samples were collected and analyzed using NMR to identify depleted media components.

Over the course of 10 days, cells grown in CDM2 continued to grow exponentially for approximately 6 days, and they were unable to achieve a cell density higher than 350,000 cells/cm^2, despite subsequent media exchanges (indicated by arrows in Figure 5.1). This trend of the cells plateauing after 6 days could also be seen with DMEM/F12 + 10% FBS, although the maximum cell density was 820,000 cells/cm^2. NutriVero Flex 10 was able to attain a similar maximum cell density (850,000 cells/cm^2) as DMEM/F12 + 10%FBS, but the cells required 10 days and three media exchanges, whereas the serum-containing media was able to achieve the maximum cell density in 6 days and only required 2 media exchanges. OptiPRO™ SFM did not perform as well, reaching a maximum cell density of 680,00 cells/cm^2 over 10 days, and required one media exchange on day 7. The doubling times also reflected this difference between the three different media, as seen in Table 5.1, although none of them performed as well as serum-containing DMEM/F12 (26.2 h). NutriVero Flex 10 had the shortest doubling time (34.5 h) of all the SFM.

Analysis of metabolite differences between the three different media (Figures 5.2 and

5.3), indicated several key differences between the formulations. Figure 5.2 shows the glucose consumption and lactate production of the cells, along with the consumption of pyruvate and citrate. CDM2 had the highest initial concentration of glucose (25 mM). Vero cells in CDM2 consumed 8.4 mM of glucose in the first 4 days of culture, and produced 12.4 mM lactate. NutriVero Flex 10 had a similar consumption of glucose during the first 4 days of 9.6 mM glucose (starting with 15 mM glucose), and had a higher conversion of glucose to lactate by producing 18.3 mM. Interestingly, the glucose concentration for OptiPRO™ SFM did not start to decrease until after day 3, but lactate accumulation was observed during this period. The starting glucose concentration in OptiPRO™ SFM was 22.4 mM, and by day 7 it had decreased to 11.4 mM (change of 11 mM over 4 days), and the amount of lactate produced was 15.2 mM. Table 5.1 lists the different lactate to glucose conversion rates, along with the production of biomass per mole of glucose for the cells grown in the three animal component-free media. NutriVero Flex 10 had the highest conversion of glucose to lactate, but also produced the highest number of cells from a mole of glucose which may indicate that the Vero cells were using another carbon source which is not disclosed in the product literature. CDM2 and OptiPRO™ SFM performed similarly in terms of glucose conversion to lactate and biomass, although Figure 5.1 shows that OptiPRO™ SFM achieved higher cell densities than CDM2.

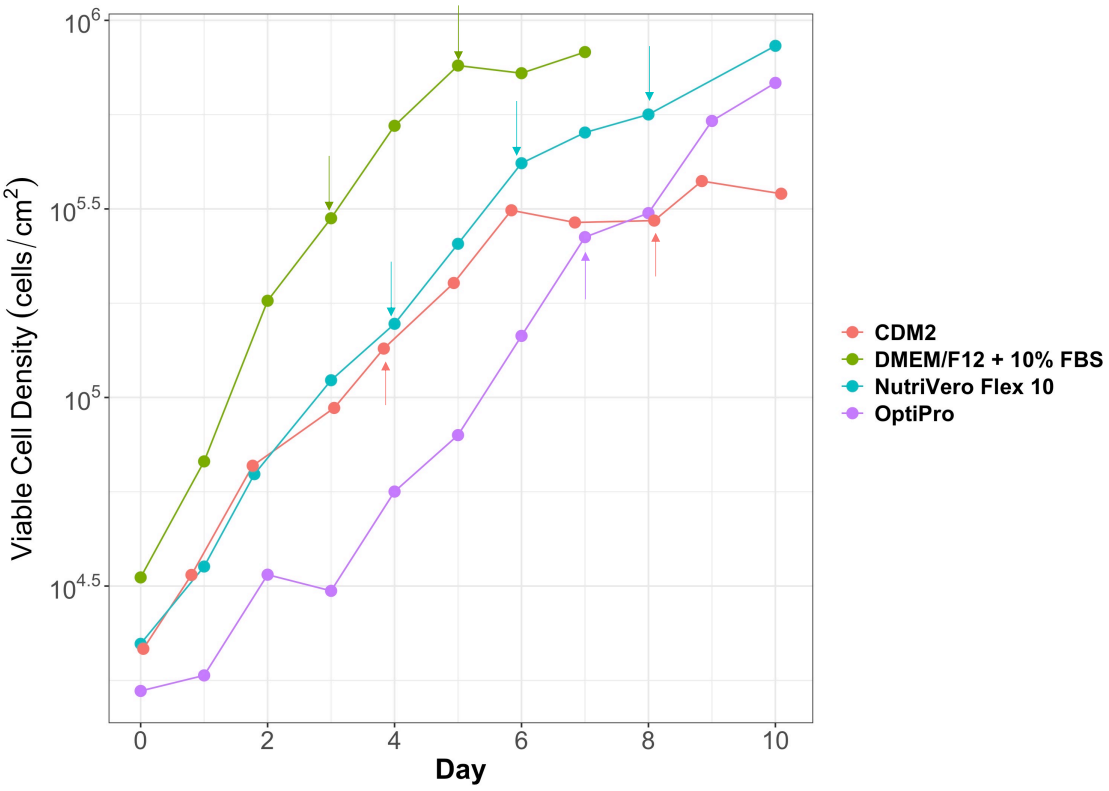

Figure 5.1: Vero cells were adapted from DMEM/F12 + 10% FBS into three different serum-free and animal origin-free media (CDM2, OptiPRO™ SFM, and NutriVero Flex 10). The cells were cultured over 10 days without being passaged, but the media was refreshed as indicated by the arrows. Each colour represents a different media formulation that Vero cells were cultured in and one replicate was taken per sample.

Table 5.1: The doubling times and conversion ratio of glucose to lactate of Vero cells grown in DMEM/F12 + 10% FBS, CDM2, NutriVero Flex 10, or OptiPRO™ SFM. The doubling time was calculated from the exponential growth phase of the adherent cell culture. $Y_{Lactate/Glucose}$ is the ratio of the lactate concentration that had accumulated since day 0, to the day the media was refreshed (media was refreshed on day 4 for cells grown in NutriVero Flex 10 and CDM2, and on day 7 for cells grown in OptiPRO™ SFM).

Media	**Doubling Time (h)**	$\mathbf{Y_{(Lactate/Glucose)}}$	$\mathbf{Y_{(10^8\ cell/Glucose\ (M))}}$
DMEM/F12 + 10% FBS	26.2	N.D.	N.D.
CDM2	38.0	1.5	1.22
NutriVero Flex 10	34.5	1.9	1.26
OptiPRO™ SFM	35.2	1.4	1.19

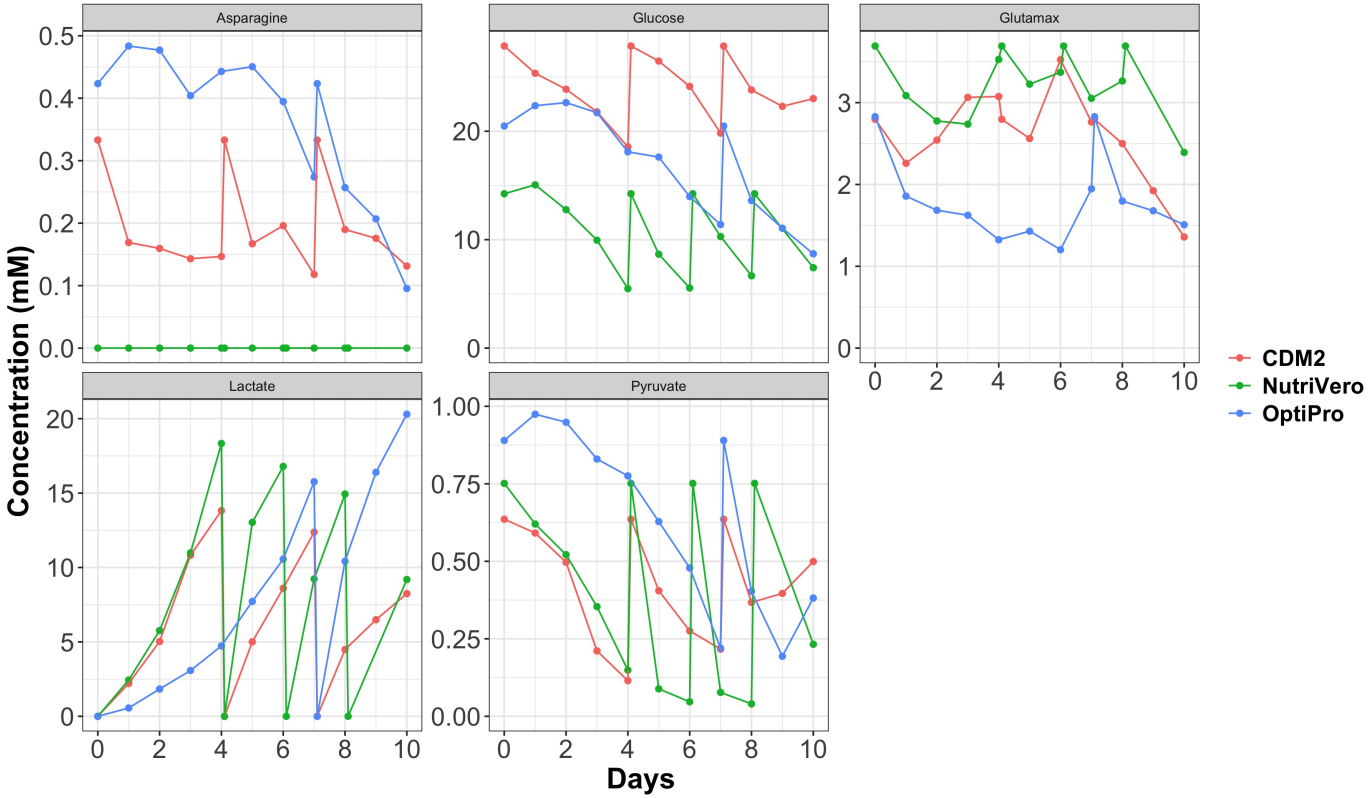

Figure 5.2: Media samples were collected from Vero cells being cultured in either CDM2, NutriVero Flex 10 or OptiPRO™ SFM for 10 days. The metabolites were analyzed using NMR, and specifically compounds that have large changes (glucose, lactate, citric acid and pyruvate) are shown here.

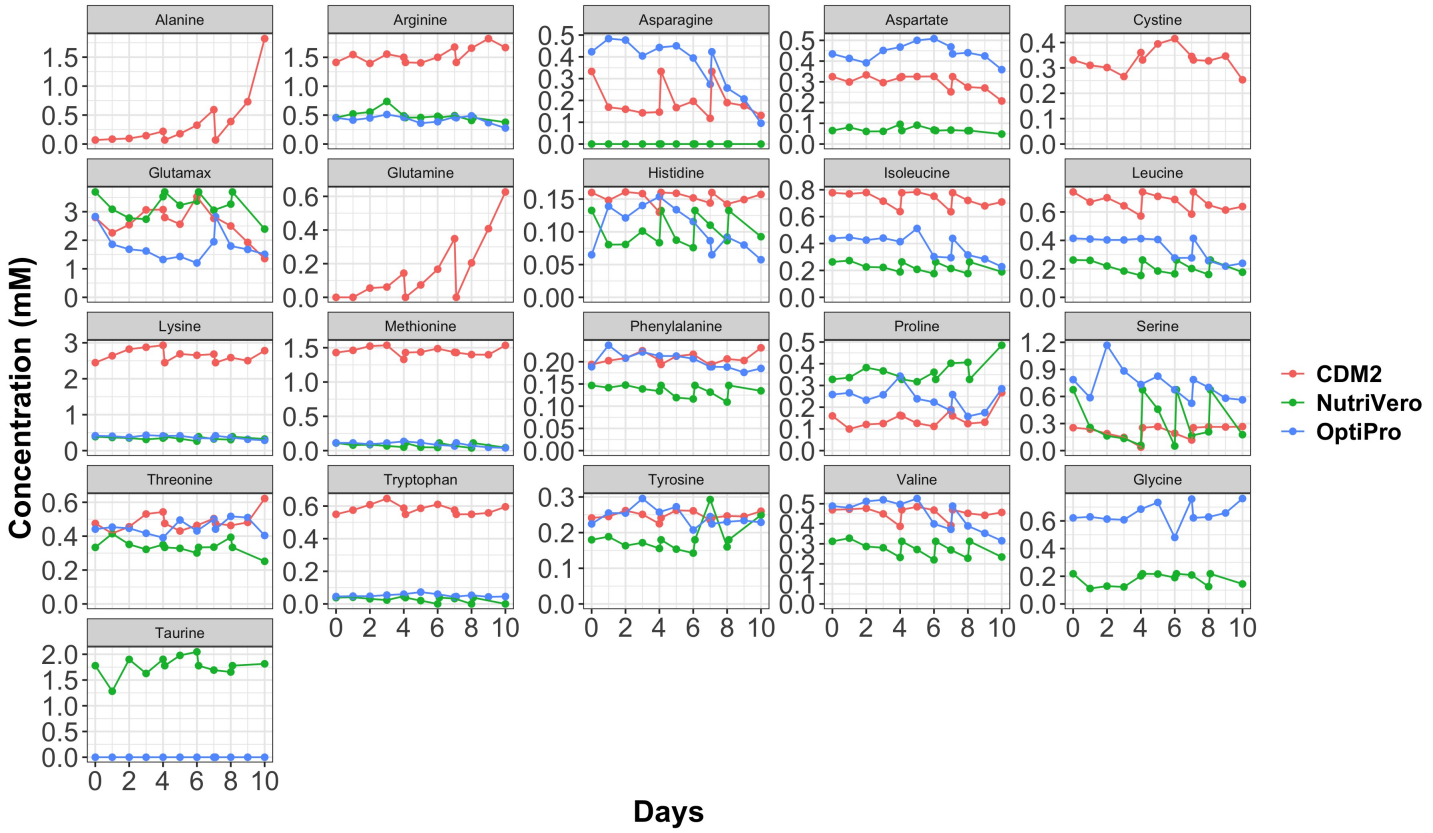

Figure 5.3: Media samples were collected from Vero cells being cultured in either CDM2, NutriVero Flex 10 or OptiPRO™ SFM for 10 days. The metabolites were analyzed, and amino acids that can be profiled by NMR are shown here.

Table 5.2: The conversion ratios of asparagine, GlutaMax™, or pyruvate to biomass of Vero cells grown in CDM2, NutriVero Flex 10, or OptiPRO™ SFM. $Y_{10^8 \text{ cells/Carbon Source}}$ is the ratio of the change in the cell concentration divided by the change in the concentration of the compound over the first 4 days of culture.

Media	$Y_{(10^8 \text{ cell/Asparagine (M)})}$	$Y_{(10^8 \text{ cell/GlutaMax™ (M)})}$	$Y_{(10^8 \text{ cell/Pyruvate (M)})}$	$Y_{(10^8 \text{ cell/All Carbon Sources (M)})}$
CDM2-A	60.8	78.3	21.7	1.12
NutriVero Flex 10	0	73.6	20.1	1.17
OptiPRO™ SFM	131.0	7.14	23.4	1.10

In addition to glucose, cells can also use asparagine, GlutaMax™ and pyruvate as a carbon source [379]. Table 5.2 lists the yield coefficients for the various carbon sources that Vero cells could use to proliferate. Regardless of the media that Vero cells are in, they appeared to all produce the same amount of biomass per mole of pyruvate that was consumed. A larger difference can be seen for the use of GlutaMax™, where Vero cells grown in the chemically defined media (NutriVero Flex 10 or CDM2) appear not to consume as much GlutaMax™ in OptiPRO™ SFM (Figure 5.2). The largest difference can be seen in the asparagine to biomass yield coefficient. NutriVero Flex 10 did not have detectable levels of asparagine in the media, and therefore the yield coefficient is 0. Cells in OptiPRO™ SFM consumed 0.09 mM of asparagine, whereas cells in CDM2 consumed 0.17 mM of asparagine within the first 24 hours of culture (Figure 5.2).

NutriVero Flex 10 and CDM2-A had very similar concentration profiles for pyruvate consumption over the first 4 days of culture. After the media was refreshed on day 4, cells grown in NutriVero Flex 10 appeared to consume all of the pyruvate in a single day, while cells in CDM2-A consumed less pyruvate each time after the media was exchanged. OptiPRO™ SFM initially contained more pyruvate than the other two media formulations, but the Vero cells appeared not to consume any pyruvate, glucose, or asparagine for the first

2 days, possibly because the cells were using GlutaMax their main carbon source. After the OptiPRO™ SFM media was refreshed on day 7, most of the pyruvate was consumed within 2 days. Since OptiPRO™ SFM contains undefined plant proteins, it is possible that the cells were consuming peptides that were not profiled using NMR.

Along with the carbons sources, NMR was also used to measure the concentration of various amino acids present in the three different media (Figure 5.3). For the initial concentrations of amino acids such as phenylalanine, threonine, tyrosine, and valine, their concentration did not differ from those listed in the DMEM/F12 formulation. CDM2-A contained much higher concentrations of arginine, cystine, isoleucine, leucine, lysine, methionine, and tryptophan compared to the other two media. NutriVero Flex 10 was the only formulation that contained taurine and also contained the highest concentration of proline. OptiPRO™ SFM had higher concentrations of asparagine and aspartate, although this formulation does contain undefined plant hydrolysates that likely contains extra amino acids in peptide form, among other things such as carbohydrates, lipids, trace metals, and vitamins [398, 322].

There are several amino acids that do not appear to be consumed during culture such as arginine, lysine, methionine, proline, threonine, tryptophan, tyrosine, and taurine. Furthermore, analysis of metabolites prior to refreshing the media showed that the only amino acid that was completely depleted was serine. An experiment was conducted with increased concentration of serine in CDM2-A, but it did not result in an increased cell density or growth rate (data not shown).

5.3.2 Using Transcriptomic Data to Identify Up-Regulated Metabolic Pathways

Using the data set that was collected when comparing the Vero suspension cells to adherent cells grown in CDM2-A, we took a different approach to analyzing the data. Instead of trying to identify key genes associated with the suspension phenotype that were up- or down-regulated, we looked at entire pathways of up-regulated genes. From these up-regulated pathways, three main pathways associated with cell proliferation stood out; fatty acid degradation, retinol metabolism, and steroid hormone biosynthesis. From Figure 5.4, it can be seen that many of the genes associated with fatty acid degradation are up-regulated, which demonstrates that it's possible that the Vero cells were catabolizing fatty acids to produce more coenzyme A, which feeds into the citrate cycle. The specific gene names and functions are listed in Appendix D.1.

The retinol metabolism was also up-regulated, although there were two genes that were drastically down-regulated in the pathway (*aldh1s*, *bcmo1*, *ugt2b7*). These genes are involved in the production of 9-cisretinoate, and converting β-carotene to all-trans-retinal, and *ugt2b7* is theoretically involved in the retinol metabolism (Figure 5.5). Retinol, also known as Vitamin A, was not originally supplemented in CDM2-A, but the RNA-seq data demonstrated that the Vero cells were attempting to produce retinol-containing compounds.

The last important pathway that was identified from the RNA-seq data, is the steroid hormone biosynthesis pathway (Figure 5.6). Progesterone, estrogen, androsterone, and testosterone are all part of this pathway. Suspension Vero cells up-regulated 6 genes (*hsd17b1*, *ugt*, *cyp1a1*, *E1.1.149*, *srd5a1*, *hsd17b2*) that were associated with proteins that are part of synthesizing C-18, C-19, and C-21 steroids, and down-regulated 3 genes

(*E1.1.1.51*, *comt*, and *akr1c2*). The genes are for various dehydrogenases, a glucuronosyltranserase, a catechol O-methyltransferase, and cytochrome p450. The glucuronosyltransferase protein (*2.4.1.17* in Figure 5.6) appears multiple times in the pathway, but is mainly concentrated in the C-18 steroids, which contain the main estrogen molecules.

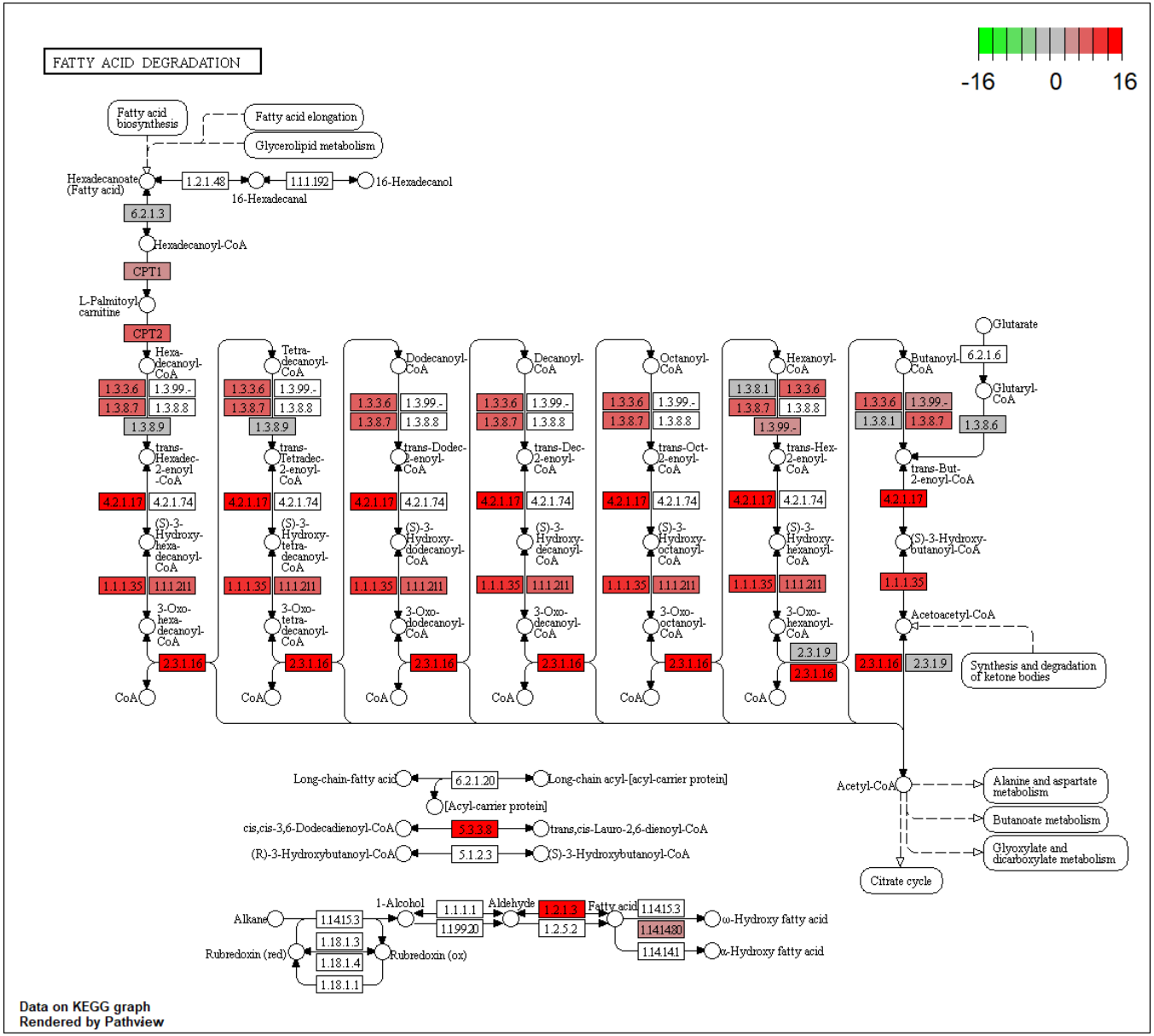

Figure 5.4: The expression of genes associated with fatty acid degradation in suspension compared to adherent Vero cells grown in CDM2-S media. Genes that are differentially expressed are highlighted in green (down-regulated) and red (up-regulated) to demonstrate the changes in suspension cells compared to adherent cells using the Pathview package.

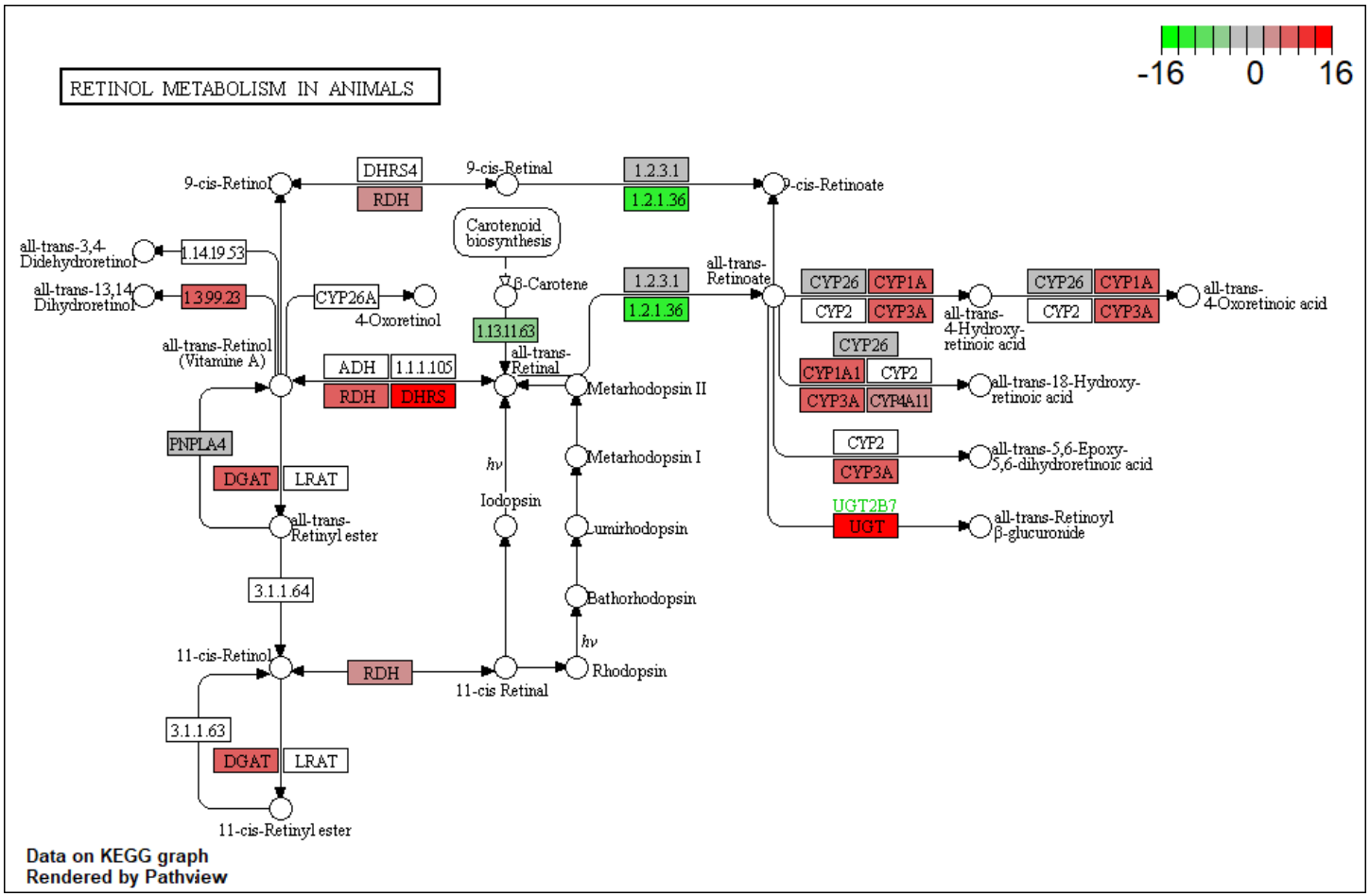

Figure 5.5: The expression of genes associated with retinol metabolism in suspension compared to adherent Vero cells grown in CDM2-S media. Genes that are differentially expressed are highlighted in green (down-regulated) and red (up-regulated) to demonstrate the changes in suspension cells compared to adherent cells using the Pathview package.

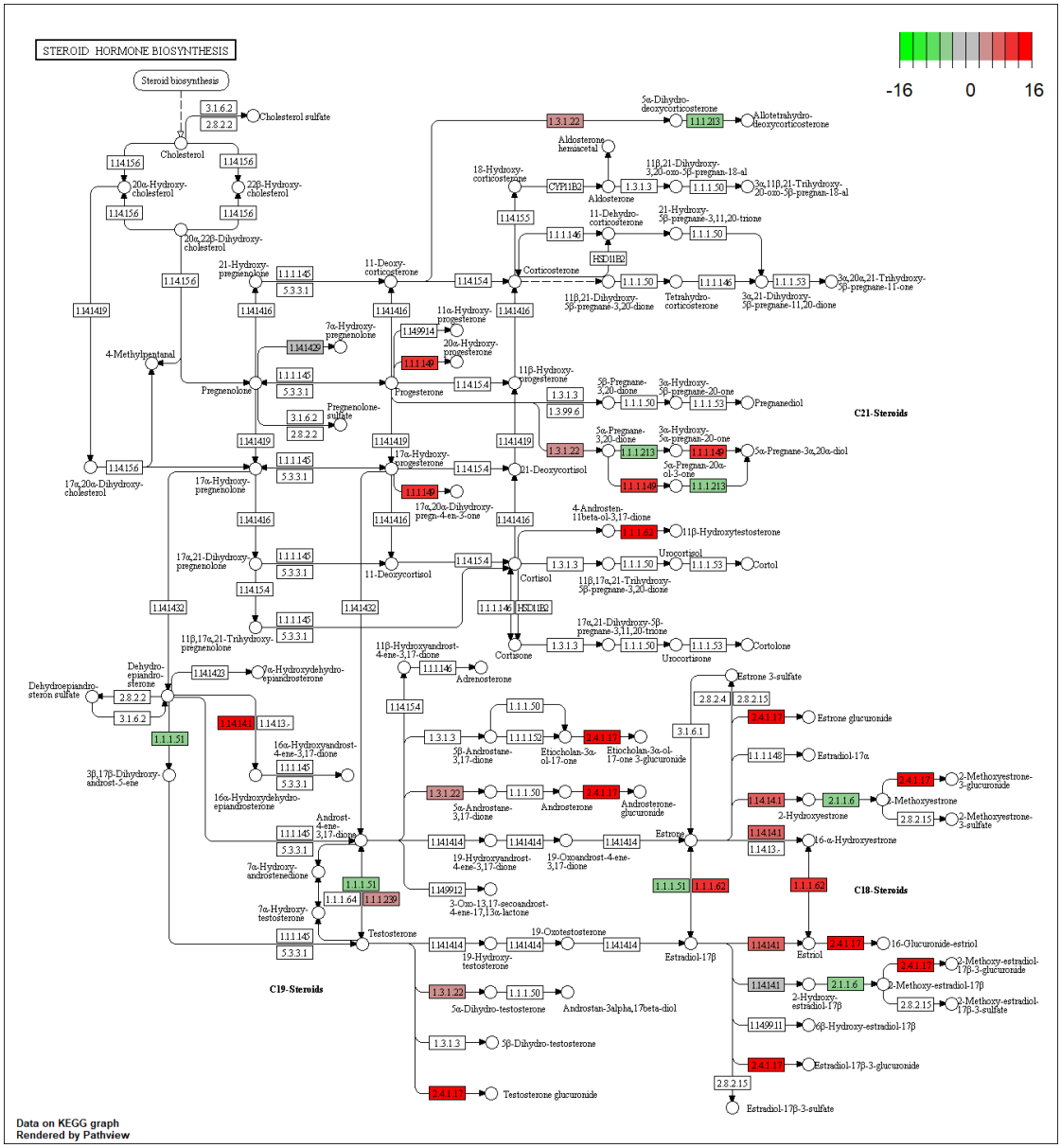

Figure 5.6: The expression of genes associated with steroid hormone biosynthesis in suspension compared to adherent Vero cells grown in CDM2-S media. Genes that are differentially expressed are highlighted in green (down-regulated) and red (up-regulated) to demonstrate the changes in suspension cells compared to adherent cells using the Pathview package.

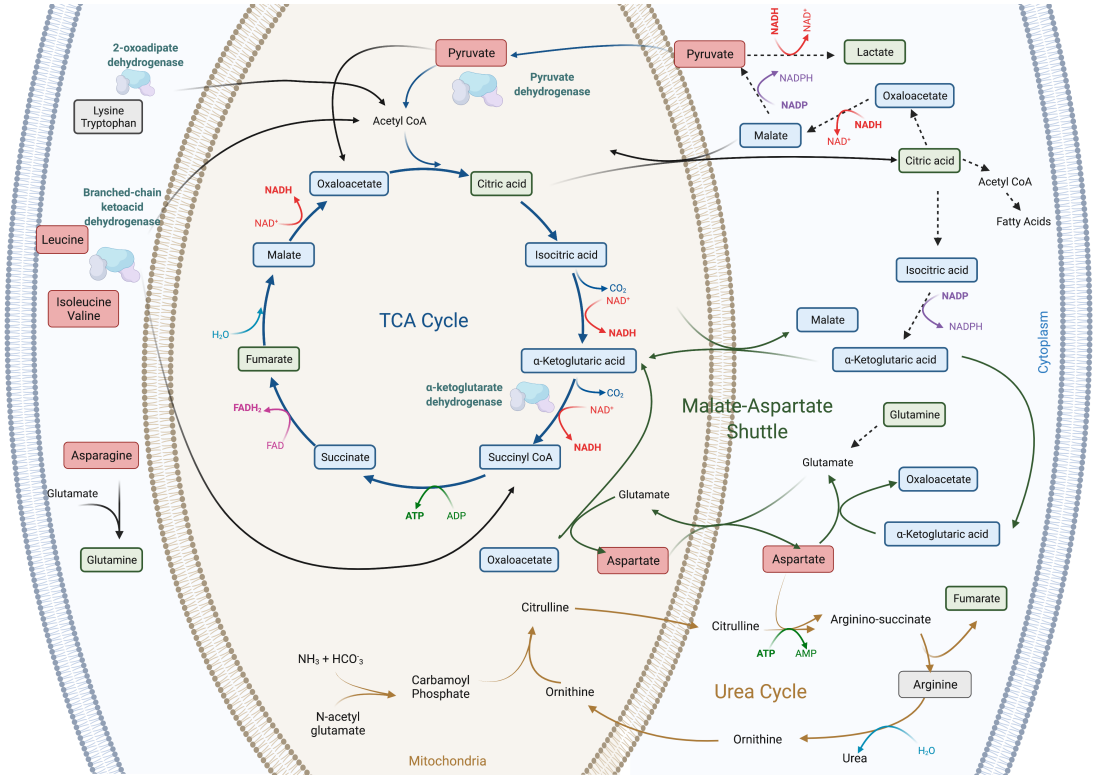

Figure 5.7: A map of the TCA cycle, the urea cycle and the malate-aspartate shuttle. The compounds that were identified by NMR as depleted in the extracellular space are outlined in red, and the compounds that accumulated are outlined in green. The TCA cycle has arrows marked in dark blue to show the pathway, the urea cycle is dark yellow and the malate-aspartate shuttle is in dark green. The names of the dehydrogenase enzymes are marked in teal.

5.3.3 Design of Experiments to Test Media Components

Based on the results from the NMR, RNA-seq and literature review, compounds were chosen to improve the growth rate of Vero cells in CDM2-A. To accomplish this, three Plackett-Burman experiments were conducted to screen 21 compounds each at 2 levels. Using the NMR data, it was observed that many of the compounds that were produced or consumed in large quantities were related to the tricarboxylic acid cycle (TCA), urea cycle, and the malate-aspartate shuttle (Figure 5.7).

The first experiment consisted of testing progesterone, which was identified using RNA-seq analysis, through the up-regulation of the steroid biosynthesis pathway. Citric acid and lipoic acid were also chosen based on the accumulation/consumption of metabolites associated with the TCA using the NMR analysis. Lipoic acid was added since it is an important cofactor for dehydrogenases that create products that feed into the TCA cycle, and citric acid was chosen as a chelator for ferric ions in the media as well as being a precursor for fatty acids in the cell (Figure 5.7). Aurintricarboxylic acid (ATA) and oleoyl-L-lysophosphastidic acid (LPA) were added based on a literature search for growth inducing compounds [149, 319, 39]. Niacinamide was also identified through the literature, and the analysis of various media formulations in Chapter 2. Povidone was identified as a surfactant, in addition to Pluronic F68™, to reduce any shear forces the cells may have experienced. Overall, citric acid, ATA, and lipoic acid did not have a significant impact on cell growth rate at the concentrations tested, whereas LPA had a large negative effect on the growth rate (Figure 5.8). Niacinamide and povidone had slightly positive effects on cell growth rate. Progesterone had the largest positive effect on the growth rate, which confirmed the RNA-seq data.

The next Plackett-Burman experiment focused on adding metals, antioxidants, and growth-enhancing compounds (Figure 5.9). With the hypothesis that citrate may have been accumulating in the medium to chelate metal ions, ferric citrate was added to increase the amount of chelated iron in the media. L-Ascorbic acid 2-phosphate sesquimagnesium salt hydrate (Mg Ascorbic Acid) was added as an antioxidant to help reduce any oxidative stress caused by unchelated metal ions in the protein-free media. $ZnCl_2$ was added to increase the amount of zinc in the media to match the concentrations that are more commonly seen in SFM (Figure 2.6). Growth enhancing compounds included GlutaMax, the polyamines spermidine and spermine, and basic fibroblast growth factor (bFGF).

Ferric citrate had the largest positive effect, while zinc, and spermidine also had slightly positive effects. The addition of 6 mM versus 4 mM GlutaMax did not have a significant improvement, and neither did the addition of ascorbic acid or spermine. Surprisingly, bFGF had a negative effect on the cell growth rate.

The last Plackett-Burman experiment added different steroids, carnitine, and retinyl acetate that were identified from the RNA-seq data (Figure 5.10). Oxaloacetate was chosen based on the NMR data that showed there may be an imbalance in the malate-aspartate shuttle, and oxaloacetate can be used to supply more α-ketoglutaric acid in the TCA cycle (Figure 5.7). Since spermidine showed some promise for enhancing growth, and the concentration of arginine in CDM2-A was relatively high compared to the other two commercial Vero cell media, citrulline was also tested. Arginine is used by the cell to make polyamines, but also citrulline, and to prevent the cell from consuming arginine to produce citrulline, it was added directly the medium to supply the cell with an exogenous source [498]. Para-aminobenzoic acid (PABA) was also identified through literature as a commonly added media component as a vitamin-like compound (called Vitamin B_X) since it has a similar structure to folate. PABA and carnitine had negative effects on the cell growth rate, while citrulline and oxaloacetate only had slightly positive effects. Retinyl acetate and β-estradiol, and prostaglandin E_2 all had large positive effects on the growth rate of Vero cells. All of these compounds were identified using the RNA-seq data.

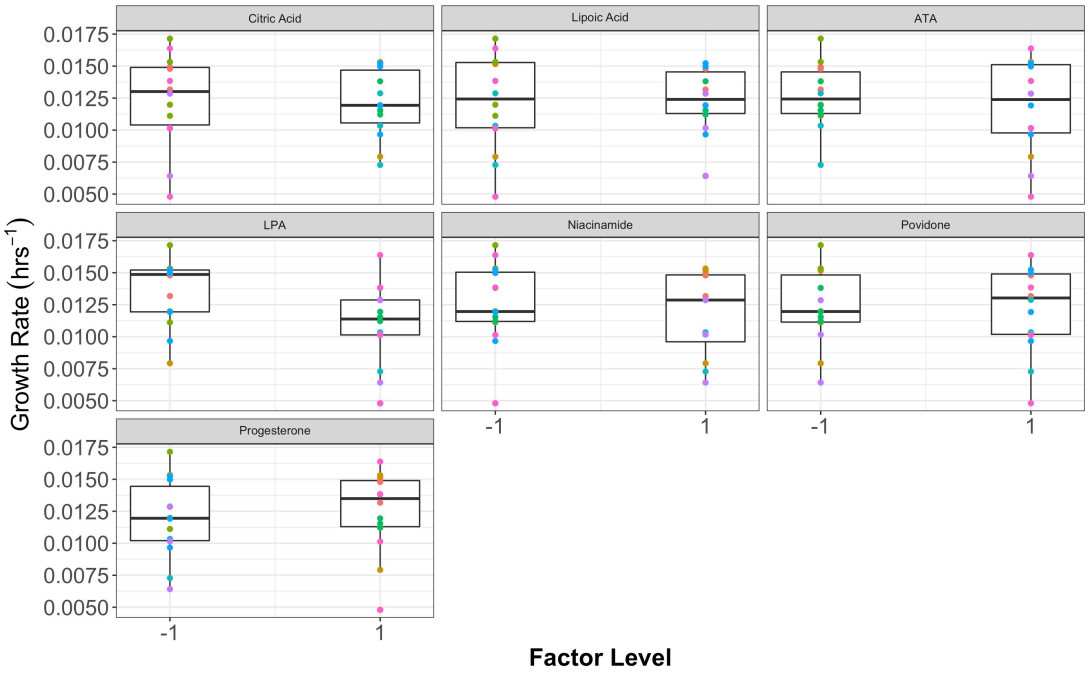

Compound	-1 (mM)	1 (mM)
Aurintricarboxylic Acid	0	0.003
Citric Acid	0	0.1
Lipoic Acid	5.1 x 10^{-4}	9.7 x 10^{-4}
oleoyl-L-alpha-lysophosphastidic acid (LPA)	0	0.002
Niacinamide	0.016	0.025
Povidone	0	100 mg/L
Progesterone	0	1.3 x 10^{-5}

Figure 5.8: The results from the first Plackett-Burman media screening experiment using components identified through RNA-seq, NMR and a literature search. The concentrations for each component at the high (+1) and low (-1) levels are listed in the table and the growth rate for adherent Vero cells was calculated while the cells were 100% in the new media formulation for 3 passages. Each formulation was numbered 1 through 8 and is represented by a different colour in the plot.

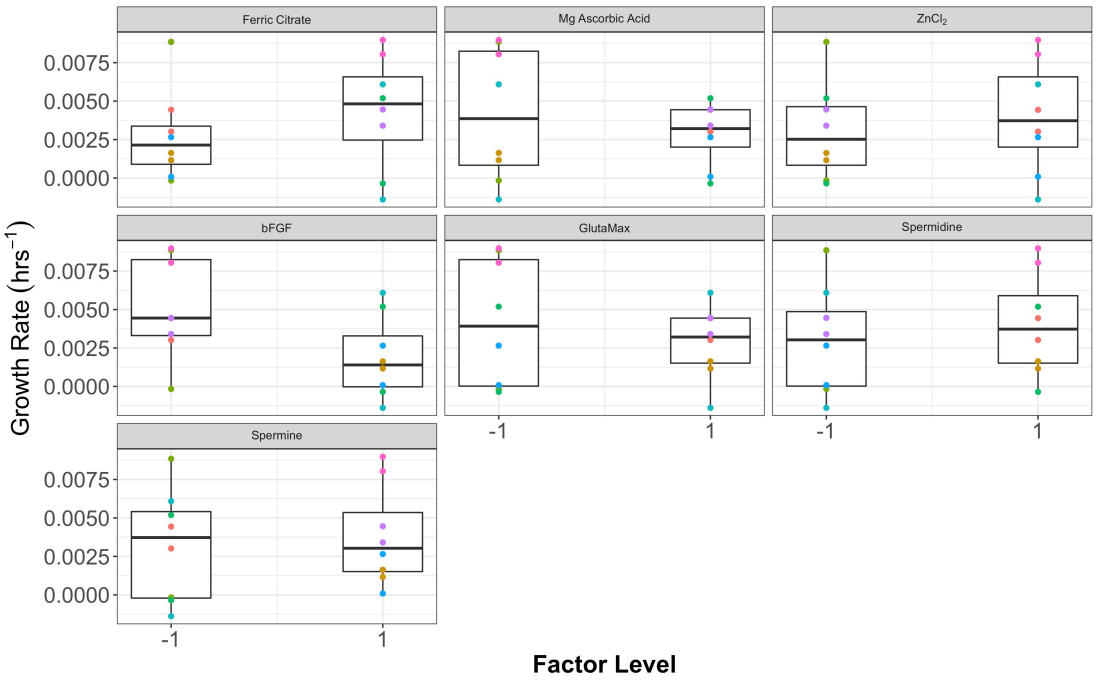

Compound	-1 (mM)	1 (mM)
basic Fibroblast Growth Factor (bFGF)	0	10 ng/mL
Ferric Citrate	0	0.03
GlutaMax	4	6
Mg Ascorbic Acid	0	0.01
Spermine	0	0.002
Spermidine	0	0.002
$ZnCl_2$	0	0.0036

Figure 5.9: The results from the second Plackett-Burman media screening experiment using components identified through RNA-seq, NMR and a literature search. The concentrations for each component at the high (+1) and low (-1) levels are listed in the table and the growth rate for adherent Vero cells was calculated while the cells were 100% in the new media formulation for 2 passages. Each formulation was numbered 1 through 8 and is represented by a different colour in the plot.

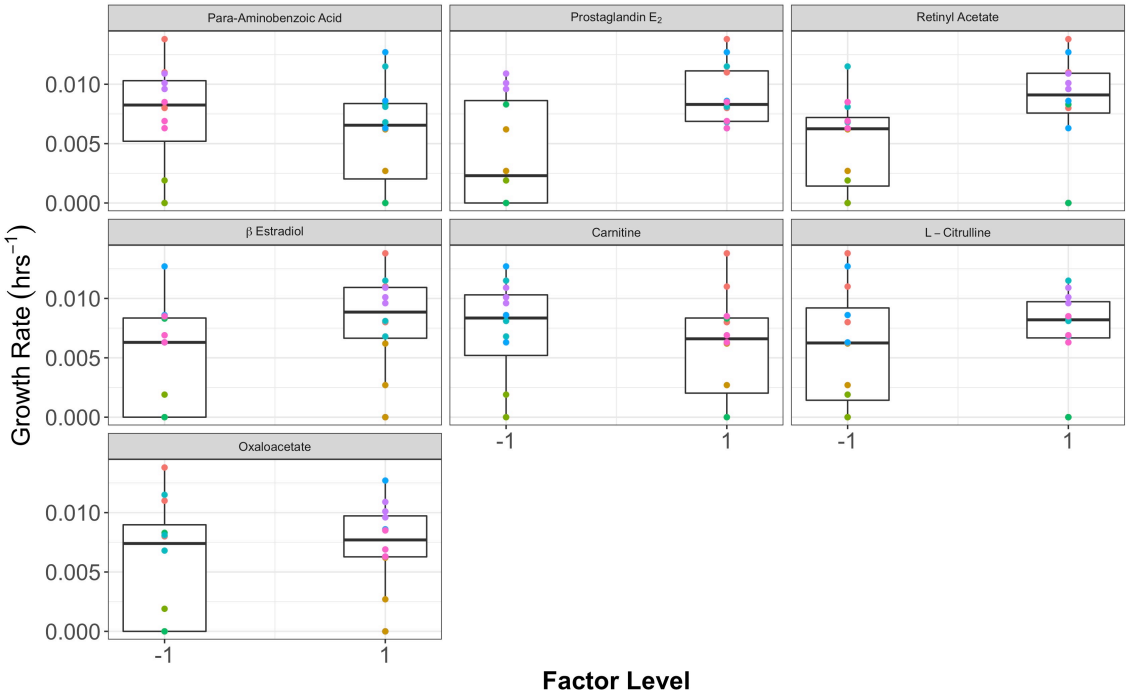

Compound	-1 (mM)	1 (mM)
β-estradiol	0	1 x 10^{-5}
Carnitine	0	1 x 10^{-3}
Citrulline	0	0.02
Oxaloacetate	0	0.02
Para-aminobenzoic acid (PABA)	0	1.5 x 10^{-4}
Prostaglandin E_2	0	2.8 x 10^{-5}
Retinyl acetate	0	2.4 x 10^{-4}

Figure 5.10: The results from the last Plackett-Burman media screening experiment using components identified through RNA-seq, NMR and a literature search. The concentrations for each component at the high (+1) and low (-1) levels are listed in the table and the growth rate for adherent Vero cells was calculated while the cells were 100% in the new media formulation for 3 passages. Each formulation was numbered 1 through 8 and is represented by a different colour in the plot.

Table 5.3: The formulation differences between CDM2, CDM3 and CDM4.

Compound	**CDM2 (g/L)**	**CDM3(g/L)**	**CDM4 (g/L)**
Lipoic Acid	0.000105	0.0002	0.0002
Progesterone	-	0.0032	0.0032
Spermine	-	0.00202	0.0005
Spermidine	-	0.0014	0.0007
Ferric Citrate	-	0.0005	0.0005
$ZnCl_2$	0.000432	0.000922	0.000922
β-Estradiol	-	-	0.00000272
Prostaglandin E_2	-	-	0.00001
L-Citrulline	-	-	0.0037
Retinyl Acetate	-	-	0.00008

To test the improvements made through these Plackett-Burman experiments, new media formulations were made based off the results from the three Plackett-Burman experiments (called CDM3 and CDM4, respectively). The goal of this experiment was to calculate the improvement in growth rate with the addition of the new media components. Table 5.3 lists the iterative improvements made to the original CDM2 formulation after each Plackett-Burman experiment, and table 5.4 shows the doubling time for each of the formulations for adherent Vero cells. The final formulation for CDM4 is listed in Appendix E. The concentrations of spermine and spermidine were reduced between CDM3 and CDM4 since the concentrations that were tested in Figure 5.9 were high compared to what is reported in literature [194].

Table 5.4: The doubling times of Vero cells grown in DMEM/F12 + 10% FBS, CDM2, CDM3, CDM4, NutriVero Flex 10, or OptiPRO™ SFM. The doubling time was calculated from the exponential growth phase of the adherent cell culture.

Media	**Doubling Time (hr)**
DMEM/F12 + 10% FBS	26.2
CDM2	38.0
CDM3	41.5
CDM4	32.1
NutriVero Flex 10	34.5
OptiPRO™ SFM	35.2

5.4 Discussion

RNA-seq is a more cost effective approach in obtaining vast amounts of data about a cell's transcriptome compared to more traditional methods and has given researchers insight into the dynamically changing cellular signals. It has been used for disease profiling, studying human pathogens, studying cellular changes in response to their environment, and annotating gene functions [278]. Part of studying cellular responses to changes in environment includes studying cell's reaction to different culture media and type of culturing method (adherent versus suspension) [436, 252]. Conversely, more traditional methods of metabolite analysis have been historically used to design cell culture media, these mainly consist of measuring intracellular and extracellular compounds that are consumed or produced during cell culture [266]. Methods like NMR, LC and MS allow for the identification of compounds at various concentrations, and have been used to improve cell culture media by supplementing or removing compounds to improve growth or protein production [399].

NMR is an excellent tool to detect various compounds in a single measurement at relatively high concentrations (micromolar), but for complex mixtures, it can be difficult to deconvolute different spectra leading to mislabeling and misquantifying compounds [446]. This limits NMR from being able to accurately detect compounds that are in very small quantities, such as growth factors, steroids, vitamins and polyamines. Recent advances have developed a LC-MS high-throughput method to quantify 93 different amino acids, nucleic acids, vitamins, sugars and other relevant compounds in a single assay [464]. Even with the recent advances with LC-MS, which can measure very small amounts (picomolar and femtomolar range) of compounds, to quantify compounds accurately, one will need to have a targeted approach where the compounds of interest are previously decided and a calibration curve is created. Alternatively, an untargeted LC-MS approach will allow the user to identify a wider range of compounds, but it is more difficult to quantify the compounds, and identify different classes of compounds in a single run [400]. RNA-seq can offer additional insights of the cell's nutritional needs by probing the cell's transcriptome to identify genes or entire pathways that are up-regulated that are related to the cell's metabolism. Here we identified extracellular metabolites using NMR, and also used RNA-seq data to probe up-regulated pathways in Vero cells. RNA-seq data allowed us to see how the cell was compensating for compounds that were missing from the media by the upregulation of certain genes that were associated with various pathways. Different compounds were selected based on the NMR results, the RNA-seq data, and through literature search. These compounds were then tested in three consecutive Plackett-Burman experiments to improve the growth rate of adherent Vero cells.

For the NMR study, Vero cells were grown adherently in three separate SFM; OptiPRO™ SFM, NutriVero Flex 10 and CDM2 media that was developed in-house. NutriVero Flex 10 and CDM2 are both chemically defined, animal component-free media

formulations that support the adherent growth of Vero cells [50]. OptiPRO™ SFM is animal component-free but it contains very low amounts of plant hydrolysate (< 7.5 µg/mL) [69, 150]. Although it is not chemically defined, OptiPRO™ SFM was chosen as well because it is commonly used in industry to produce vaccines using Vero cells [145, 69, 248, 531]. The cells were cultured for 10 days, with daily cell counts and media samples taken for NMR analysis. Vero cells grown in CDM2 had a longer doubling time (38 hours) than NutriVero Flex10 (34.5 hours), but after some iterative improvements identified through Plackett-Buman experiments, the doubling time was reduced to 32 hours which is a 16% decrease in doubling time. From the NMR data it was observed that Vero cells grown in all three different culture media consumed most of the pyruvate in the media, and had similar yield coefficients for glucose and pyruvate to cell biomass. While there were minimal differences in the yield coefficients for glucose and pyruvate, there were larger differences for the amount of lactate that was produced per mole of glucose that was consumed. Petiot *et al.*, grew Vero cells in an animal component-free media that contains undefined protein extracts and studied Vero cell metabolism [380, 379]. They found that Vero cells converted most of their glucose to lactate ($Y_{Lactate/Glucose}$ of 1.7) and that most cultures reached a maximum of 18.5 mM lactate which is similar to what was observed for Vero cells grown in OptiPRO™ SFM and NutriVero Flex 10 (20.3 mM and 18.3 mM, respectively). They also found that lowering the starting glucose concentration to 11 mM, the $Y_{Lactate/Glucose}$ increased to 2.2 [380]. A similar trend was seen with NutriVero Flex 10 contained the lowest amount of glucose (approximately 15 mM) and produced the most lactate per unit of glucose (1.9). For all three of the medium formulations, it was found that most of the glucose was converted to lactate, although none of the yields were greater than the maximal theoretical yield of 2.

In addition to studying the carbon metabolism, amino acids were profiled to study

any trends between the three media formulations. For all the media formulations, cells consumed L-serine, and L-isoleucine, L-leucine and L-valine at high cell densities ($>$ 130,000 cells/cm^2). L-isoleucine, L-leucine and L-valine are branched-chain amino acids that are catabolized by the cell to make products that enter the TCA cycle [175]. L-isoleucine can be degrated to propionyl-CoA and acetyl-CoA, L-leucine can be catabolized into acetoacetae and acetyl-CoA, and L-valine can be used to form propionyl-CoA [5]. From this, compounds to be tested in subsequent Plackett-Burman experiments would focus on supplementing compounds related to the TCA cycle. These compounds included citric acid, lipoic acid, GlutaMax™, and oxaloacetate.

From the RNA-seq data, genes associated with fatty acid degradation, retinol metabolism, and steroid hormone biosynthesis were found to be up-regulated. In taking a closer look at the genes that were up-regulated for fatty acid degradation, many of the genes were also associated with enzymes that are involved in the catabolism of leucine, isoleucine and valine (acyl-CoA dehydrogenase medium chain, enoyl-CoA hydratase, short chain 1, enoyl-CoA hydratase and 3-hydroxyacyl CoA dehydrogenase, hydroxyacyl-CoA dehydrogenase trifunctional multienzyme complex subunit alpha, acetyl-CoA acyltransferase 2, acyl-CoA dehydrogenase family member 8, aldehyde dehydrogenase 2 family member) [5, 495]. This finding is supported by the NMR profiles for the branched-chain amino acids. In terms of the cells upregulating genes associated with fatty acid degradation (*cpt1* and *cpt2*), a literature search found that carnitine palmitoyltransferase 1 is a rate limiting enzyme for the transport of fatty acids into the mitochondria [211]. The role of this enzyme is to conjugate fatty acids to carnitine, which is not present in the media [488]. Carnitine can be made endogenously by the cell, but we identified it as a potential key media component that could potentially boost the growth rate if it was directly supplied to the cell. Unfortunately, the addition of carnitine did not improve the growth rate of Vero cells, indicating

that the cells were most likely able to produce enough carnitine, and this was not the rate limiting step.

The other pathway that was up-regulated was retinol metabolism. Retinol is crucial for cell growth, and oxidative phosphorylation in the mitochondria, and self-renewal of stem cells [122, 4, 219]. It is commonly found in chemically defined cell culture media, but at higher concentrations ($>$ 3 µM), it can prevent cell proliferation [238]. Retinoids work through binding to nuclear receptors known as retinoic acid receptors (RAR) and retinoid X receptors (RXR) that have over 532 direct and indirect regulatory targets [26]. Given retinol's broad range of targets, and upregulation of genes associated with the retinol metabolism pathway, it was also added to the list of compounds to be tested. The addition of retinyl acetate to CDM2 had a positive effect of the cell's growth rate at a concentration of 0.00024 mM. This concentration could potentially be increased in further experiments, since the median concentration in SFM media is 0.00032 mM and 0.00043 mM (for adherent and suspension cultures, respectively) (Appendix A).

The final pathway that was upregualted in Vero cells was steroid hormone biosynthesis. CDM2 only contained recombinant epidermal growth factor (rEGF) and did not contain any other hormones to stimulate growth. Many of the genes associated with the creation of various forms of estradiol and progesterone are up-regulated according to the RNA-seq dataset. These hormones were tested in the Plackett-Burman experiments and were both found to have a positive effect on the growth rate. Additionally, prostaglandin E_2 also had a positive effect on the growth rate of Vero cells. This hormone was identified using the RNA-seq data, where the genes associated with the KEGG Phospholipase D signaling pathway were up-regulated (Appendix D Figure D.1). Specifically, Vero cells were upregulating the gene associated with the G protein-coupled receptors (GPCR) which is a family of receptors that can bind a wide variety of ligands including glutamate, prostaglandins,

platelet-activating factor, and many others [95].

In general, the compounds identified using RNA-seq analysis had a positive effect on the cell growth rate, with the exception of carnitine which had a slightly negative effect. The compounds identified using NMR did not have positive effects, with most of the compounds resulting in slightly negative effects, but not significant. The compounds identified through a literature search had a wide range of effects with ferric citrate having the largest positive effect, and LPA having a large negative effect on cell growth rate. None of the polyamines had a drastic effect on the cell growth rate, although there is a large body of evidence that suggests polyamines are important for cell growth and are included in many commercial media [50, 243, 474]. Investigation of other concentrations and/or polyamines may be pertinent given the body of evidence in the literature of positive effect of polyamine compounds [374, 353].

Although some of the compounds were found to not improve the growth rate of Vero cells in CDM2, they will still be included in the final formulation. The Plackett-Burman styled experiments that were conducted during this work are not able to detect interactions between compounds which may have proven to be significantly positive. The advantage of using a Plackett-Burman is to screen many different factors in the fewest possible runs, but only the main effects of the factors can be quantified. Many trace metals are beneficial at very small quantities, but if they are not chelated or are in high concentrations, they create reactive oxygen species that are harmful to cells. Further investigation of the compounds that were found not to have a positive effect on the growth rate, may find positive interactions with other compounds, or the concentration can be modified to find a more optimal range for the cell.

Overall, when it comes to identifying compounds of interest to improve the media formulation, the RNA-seq data provided the best insights, and then the compounds identified

through a literature search provided the second best set of compounds to test. Unfortunately the compounds that were identified from the NMR data did not improve the cell culture media, possibly because NMR is unable to detect small quantities of key compounds such as vitamins, trace metals and growth factors.

5.5 Conclusions

In conclusion, we used NMR metabolite data, along with RNA-seq transcriptomic data to improve the growth rate of Vero cells in an animal component-free chemically defined medium. Through RNA-seq analysis we identified retinyl acetate, progesterone, β-estradiol and prostaglandin E_2 as growth enhancing compounds. The NMR metabolite analysis did not result in the addition of any compounds that improved the growth rate, although they did not reduce the growth rate either. Using the compounds identified through RNA-seq, NMR and a literature review, the doubling time of Vero cells was reduced from 38 hours to 32.1 hours, which is better than the animal component-free commercially available media currently on the market today. This work demonstrates an additional use for RNA-seq data to enhance medium development to complement more traditional methods such as NMR, LC and MS.

Chapter 6

Original Contributions and Recommendations

6.1 Original Contributions

6.1.1 Serum-Free Media Formulations Database

In Chapter 2 of this thesis, a review of the available basal (i.e., requiring supplementation with serum) and complete, serum-free media formulations for the growth of continuous cell lines (e.g., MDCK, CHO, Vero, HEK293) that were disclosed in patents and journal articles was conducted. A total of 14 basal and 25 serum-free media, for which complete formulations were disclosed, were included in the review. The focus of this analysis was centered on 2 main factors: 1. to compare basal and serum-free formulations to identify important components required to replace serum; and 2. to compare the differences between adherent and suspension serum-free media formulations. Increasing the concen-

tration of fatty acids, cholesterol, amino acids, trace metals, and vitamins, in addition to supplementation with growth factors and other proteins and purine/pyrimidine nitrogenous bases were identified as critical components to replace serum. Moreover, formulations for suspension cultures were enriched compared to adherent formulations. Overall, formulations to support suspension culture had higher concentrations of fatty acids, amino acids, trace metals, and vitamins. The median values for the serum-free adherent and suspension formulations are listed in Appendix A, and may be useful as an initial formulation for developing other serum-free medium formulations.

6.1.2 Chemically Defined Media Formulation for Suspension Vero Cells

Chapter 3 reported the major contribution of this thesis: a chemically defined media formulation that could support Vero cells in suspension. Design of Experiments was employed to iteratively develop a medium formulation capable of supporting the transition of Vero cells from adherent to suspension culture. The screening experiments rapidly identified the importance of trace metals, rEGF, lipids, high glucose, α-tocopherol, and other vitamins in the serum-free formulation. However, the Vero cells were able to adhere to the tissue-culture treated flasks when 1 mM of calcium and 0.7 mM of magnesium were present in the medium, and therefore their concentrations were reduced to promote anchorage-independence. After adaptation to the low-calcium/magnesium formulations the cells were moved to non-treated flasks. In non-treated flasks under static conditions, large cell aggregates were observed, but with gentle shaking (40 rpm) aggregates in two of the medium formulations supported single cell suspension. Vero cells in suspension had a very slow growth rate (< 0.00075 hr^{-1}) in CDM2-S medium. In light of this result,

HEK293T, CHO-K1 and MDCK cells were adapted to the novel medium CDM2-A to give some indication whether the low growth rate was likely due to the medium formulation itself or if it was specific to Vero cells. Each of these cell lines have been adapted to growth in single cell suspension previously. All of the cell lines were able to successfully adapt to suspension culture in CDM2-A and reached maximum cell densities between 1.7×10^6 to 1.9×10^6. This is less than the maximum cell densities achieved using commercial media which obtained approximately 4×10^6 cells/mL, but overall this indicated that CDM2-A could support suspension growth in multiple cells lines that it was not necessarily designed for.

6.1.3 RNA-seq Analysis Comparing Suspension to Adherent Vero Cells

Chapter 4 reported the findings of using RNA-seq to probe the transcriptional differences between Vero cells grown as adherent cultures in DMEM/F12 + 10% FBS or CDM2-A, and in suspension in modified CDM2-S (low calcium and magnesium) to attempt to identify underlying genetic reasons for the low growth rate in suspension. Through comparing the transcriptomes of Vero cells grown in the different conditions, it was found that Vero cells grown in single cell suspension had greatly down-regulated genes associated with cell cycle progression, and up-regulated genes associated with kidney tissue. These genes included membrane transporters and cell-cell adhesion molecules which are important for the epithelial barrier and filtering of the blood which is a key function for renal tubule cells. In addition to up-regulating the aforementioned sets of genes, the suspension Vero cells also had up-regulated fatty acid β-oxidation genes which demonstrates that even though the cells were not proliferating, they were still metabolically active. It was hypothesized that

certain genes could be overexpressed in suspension Vero cells to allow them to proliferate again such as *c-myc*, *blc-2*, or genes associated with the mesenchymal phenotype. Also additional growth factors could be added to the medium such as PDGF, HGF or TGF-β.

6.1.4 Using RNA-seq Data to Improve Media Formulations

Chapter 5 demonstrated an increase the growth rate of Vero cells cultured in CDM2-A and compared the performance of this novel formulation to commercially available media. In addition to conducting a literature search to identify candidate compounds that have previously improved the growth rate of mammalian cells, the supernatant of cell cultures were analyzed using NMR, and further analysis of the RNA-seq dataset was conducted to identify gene pathways involved in metabolism and utilization of growth factors to elucidate specific molecules that may be amenable to further supplementation. NMR-based metabolite measurements were performed on Vero cells grown adherently in two commercially available media (NutriVero Flex 10 and OptiPRO™ SFM) and CDM2-A. This analysis identified potential bottlenecks in the TCA cycle in cells cultured in CDM2-A, but it did not show large differences between CDM2-A and the commercially available media formulations. Next, the RNA-seq data was used to map upregulated metabolic pathways in Vero cells to identify compounds that the cells were attempting to produce themselves. Through this analysis, Vitamin A, β-estradiol and prostaglandin E_2 were identified as potential candidates to improve the growth rate. All three of these compounds had a positive impact on the growth rate. After three Plackett-Burman experiments, the doubling time of Vero cells grown in the novel chemically defined medium (i.e., CDM4) was reduced from 38 hours to 32.1 hours, and the cells were able to grown faster than in the other two commercially available mediums (doubling times of 34.5 and 35.2 hours).

6.2 Recommendations and future prospects

1. As described in this thesis, Vero cells can adapt to suspension culture through the modification of the cell culture medium. Media formulations are normally not disclosed due to intellectual property implications for commercialization of the product. This has created an extremely large gap in the available knowledge of media development to the extent that publicly disclosed formulations have not improved significantly since the 1970s. Indeed, the recently reported suspension Vero cell formulations reported by Rourou *et al.* and Shen *et al.* were only described as 'in-house' formulations and the complete formulation was not described [412, 433]. By using the medium formulation that is described in this work, researchers can use this as a basal formulation to culture Vero, CHO-K1, MDCK and HEK293T cells in suspension. In addition, using a strategy of screening medium components using a design of experiments approach and obtaining concentration ranges from a curated list through the literature review, the medium can be further improved for each specific cell line. Future research focusing on suspension Vero cell medium should consider additional steroids to improve the growth rate and metal chelators to reduce the potential reactive oxygen species. Researchers should also focus on the potential of a protein-free medium if rEGF can be removed, while supplementing with steroids, polyamines, and prostaglandins to maintain the growth rate of Vero cells. In addition to improving the growth rate, the medium should be tested for how well viruses can be produced by Vero cells. Since Vero cells are mainly used to produce vaccines, this is an essential function of Vero cells and is an important metric for biomanufacturing.

2. Moreover, this work not only used design of experiments to screen components for the medium, but using the results from RNA-seq proved to be a very valuable tool

to probe the metabolic pathways of Vero cells for compounds that were missing from the medium. Although there is limited RNA-seq data for Vero cells, there is more data available for HEK293T and CHO cell lines and this data can be revisited to study the differentially expressed genes associated with a variety of metabolic and signalling pathways [252, 73, 443, 527]. Specific pathways that look at a variety of vitamins, the TCA cycle, and ligands for growth receptors [305]. If the formulations for the chemically defined mediums are known, transcriptomic changes in the cells can be mapped to the different compounds that are available in the medium.

3. Through this work it was determined that solely modifying the cell culture medium did not obtain a robustly growing suspension Vero cell culture. It is likely that genetic changes must occur in the cell for Vero cells to sustain growth in suspension. To improve the RNA-seq database for Vero cells and to elucidate the genes associated with the suspension phenotype, the cells lines that were developed by Rourou *et al.* and Shen *et al.* should also be analyzed using transcriptomics. This work will not only add to the genetic understanding of Vero cells, but it will follow the work that has been done using other commercial cell lines (CHO-K1 [252], HeLa [201], and MDCK [229]), where the transcriptomic and proteomic differences between the two culture methods have been compared. When candidate genes have been identified, the Vero cells can be transduced using a lentiviral vector with the gene of interest, and then the time to attain a suspension phenotype can be measured.

References

[1] Advanced DMEM/F12 Formulation.

[2] Ferric and Ferrous Iron in Cell Culture.

[3] 41350 - NCTC - 135 Medium, 2016.

[4] R. AcinPerez, B. Hoyos, F. Zhao, V. Vinogradov, D. A. Fischman, R. A. Harris, M. Leitges, N. Wongsiriroj, W. S. Blaner, G. Manfredi, and U. Hammerling. Control of oxidative phosphorylation by vitamin A illuminates a fundamental role in mitochondrial energy homoeostasis. *The FASEB Journal*, 24(2):627–636, 2010.

[5] M. M. Adeva-Andany, L. López-Maside, C. Donapetry-García, C. Fernández-Fernández, and C. Sixto-Leal. Enzymes involved in branched-chain amino acid metabolism in humans. *Amino Acids*, 49(6):1005–1028, 2017.

[6] A. Agil, C. J. Fuller, and I. Jialal. Susceptibility of plasma to ferrous iron/hydrogen peroxide-mediated oxidation: Demonstration of a possible Fenton reaction. *Clinical Chemistry*, 41(2):220–225, 1995.

[7] B. Alberts, J. Melorose, R. Perroy, and S. Careas. *Molecular Biology of the Cell*, volume 1. 2015.

[8] M. Alfano and C. Cavazza. Structure, function, and biosynthesis of nickel-dependent enzymes. *Protein Science*, (January):1071–1089, 2020.

[9] R. Alfano, A. Pennybaker, P. Halfmann, and C. Y. Huang. Formulation and production of a blood-free and chemically defined virus production media for VERO cells. *Biotechnology and Bioengineering*, 117(11):3277–3285, 2020.

[10] Y. B. Ali, F. Carrière, R. Verger, S. Petry, G. Muller, and A. Abousalham. Continuous monitoring of cholesterol oleate hydrolysis by hormone-sensitive lipase and other cholesterol esterases. *Journal of Lipid Research*, 46(5):994–1000, 2005.

[11] C. Altamirano, C. Paredes, J. J. Cairo, and F. Godia. Improvement of CHO Cell Culture Medium Formulation: Simulrtaneous Substitution of Glucose and Glutamine. *Biotechnology Progress*, 16:69–75, 2000.

[12] J. M. Anderson. Multinucleated Giant Cells. *Current opinion in hematology*, 7:40–47, 2000.

[13] R. L. Anderson, K. W. Minton, G. C. Li, and G. M. Hahn. Temperature-induced homeoviscous adaptation of chinese hamster ovary cells. *BBA - Biomembranes*, 641(2):334–348, 1981.

[14] S. Andrews. FastQC: A quality control tool for high throughput sequence data, 2010.

[15] E. Anggård. Ethanol, essential fatty acids and prostaglandins. *Pharmacology, biochemistry, and behavior*, 18 Suppl 1:401–407, 1983.

[16] E. Arafa, P. A. Bondzie, K. Rezazadeh, R. D. Meyer, E. Hartsough, J. M. Henderson, J. H. Schwartz, V. Chitalia, and N. Rahimi. TMIGD1 Is a Novel Adhesion Molecule

That Protects Epithelial Cells from Oxidative Cell Injury. *American Journal of Pathology*, 185(10):2757–2767, 2015.

[17] K. G. Ardlie, D. S. DeLuca, A. V. Segrè, T. J. Sullivan, T. R. Young, E. T. Gelfand, C. A. Trowbridge, J. B. Maller, T. Tukiainen, M. Lek, L. D. Ward, P. Kheradpour, B. Iriarte, Y. Meng, C. D. Palmer, T. Esko, W. Winckler, J. N. Hirschhorn, M. Kellis, D. G. MacArthur, G. Getz, A. A. Shabalin, G. Li, Y. H. Zhou, A. B. Nobel, I. Rusyn, F. A. Wright, T. Lappalainen, P. G. Ferreira, H. Ongen, M. A. Rivas, A. Battle, S. Mostafavi, J. Monlong, M. Sammeth, M. Melé, F. Reverter, J. M. Goldmann, D. Koller, R. Guigó, M. I. McCarthy, E. T. Dermitzakis, E. R. Gamazon, H. K. Im, A. Konkashbaev, D. L. Nicolae, N. J. Cox, T. Flutre, X. Wen, M. Stephens, J. K. Pritchard, Z. Tu, B. Zhang, T. Huang, Q. Long, L. Lin, J. Yang, J. Zhu, J. Liu, A. Brown, B. Mestichelli, D. Tidwell, E. Lo, M. Salvatore, S. Shad, J. A. Thomas, J. T. Lonsdale, M. T. Moser, B. M. Gillard, E. Karasik, K. Ramsey, C. Choi, B. A. Foster, J. Syron, J. Fleming, H. Magazine, R. Hasz, G. D. Walters, J. P. Bridge, M. Miklos, S. Sullivan, L. K. Barker, H. M. Traino, M. Mosavel, L. A. Siminoff, D. R. Valley, D. C. Rohrer, S. D. Jewell, P. A. Branton, L. H. Sobin, M. Barcus, L. Qi, J. McLean, P. Hariharan, K. S. Um, S. Wu, D. Tabor, C. Shive, A. M. Smith, S. A. Buia, A. H. Undale, K. L. Robinson, N. Roche, K. M. Valentino, A. Britton, R. Burges, D. Bradbury, K. W. Hambright, J. Seleski, G. E. Korzeniewski, K. Erickson, Y. Marcus, J. Tejada, M. Taherian, C. Lu, M. Basile, D. C. Mash, S. Volpi, J. P. Struewing, G. F. Temple, J. Boyer, D. Colantuoni, R. Little, S. Koester, L. J. Carithers, H. M. Moore, P. Guan, C. Compton, S. J. Sawyer, J. P. Demchok, J. B. Vaught, C. A. Rabiner, and Lockhart. The Genotype-Tissue Expression (GTEx) pilot analysis: Multitissue gene regulation in humans. *Science*, 348(6235):648–660, 2015.

[18] C. T. Armstrong, P. E. Mason, J. L. Anderson, and C. E. Dempsey. Arginine side chain interactions and the role of arginine as a gating charge carrier in voltage sensitive ion channels. *Scientific Reports*, 6(August 2015):1–10, 2016.

[19] O. Arrigoni and M. C. De Tullio. Ascorbic acid: Much more than just an antioxidant. *Biochimica et Biophysica Acta - General Subjects*, 1569(1-3):1–9, 2002.

[20] T. Arsenijevic, A. Vujovic, F. Libert, A. O. De Beeck, A. Hébrant, S. Janssens, F. Grégoire, A. Lefort, N. Bolaky, J. Perret, L. Caspers, F. Willermain, and C. Delporte. Hyperosmotic stress induces cell cycle arrest in retinal pigmented epithelial cells. *Cell Death and Disease*, 4(6), 2013.

[21] C. L. Arteaga and J. A. Engelman. ERBB Receptors: From Oncogene Discovery to Basic Science to Mechanism-Based Cancer Therapeutics. *Cancer Cell*, 25(3):282–303, 2014. mar.

[22] M. Ashburner, C. A. Ball, J. A. Blake, D. Botstein, H. Butler, J. M. Cherry, A. P. Davis, K. Dolinski, S. S. Dwight, J. T. Eppig, M. A. Harris, D. P. Hill, L. Issel-Tarver, A. Kasarskis, S. Lewis, J. C. Matese, J. E. Richardson, M. Ringwald, G. M. Rubin, and G. Sherlock. Gene ontology: Tool for the unification of biology. *Nature Genetics*, 25(1):25–29, 2000.

[23] K. Astley and M. Al-Rubeai. The role of Bcl-2 and its combined effect with p21CIP1 in adaptation of CHO cells to suspension and protein-free culture. *Applied Microbiology and Biotechnology*, 78(3):391–399, 2008.

[24] ATCC. The sodium bicarbonate-carbon dioxide system, 2014.

[25] A. Atfi, K. LePage, P. Allard, A. Chapdelaine, and S. Chevalier. Activation of a Serine/Threonine Kinase Signaling Pathway by Transforming Growth Factor Type b. 92(December):12110–12114, 1995.

[26] J. E. Balmer and R. Blomhoff. Gene expression regulation by retinoic acid. *Journal of Lipid Research*, 43(11):1773–1808, 2002.

[27] R. Banerjee and S. W. Ragsdale. The Many Faces of Vitamin B 12 : Catalysis by Cobalamin-Dependent Enzymes . *Annual Review of Biochemistry*, 72(1):209–247, 2003.

[28] A. Banjac, T. Perisic, H. Sato, A. Seiler, S. Bannai, N. Weiss, P. Kölle, K. Tschoep, R. D. Issels, P. T. Daniel, M. Conrad, and G. W. Bornkamm. The cystine/cysteine cycle: a redox cycle regulating susceptibility versus resistance to cell death. *Oncogene*, 27(11):1618–1628, 2007. mar.

[29] S. Bannai and N. Tateishi. Role of membrane transport in metabolism and function of glutathione in mammals. *The Journal of Membrane Biology*, 89(1):1–8, 1986. feb.

[30] P. N. Barrett, W. Mundt, O. Kistner, and M. K. Howard. Vero cell platform in vaccine production: moving towards cell culture-based viral vaccines. *Expert review of vaccines*, 8(5):607–18, 2009.

[31] A. Bataille, P. Galichon, N. Chelghoum, B. M. Oumoussa, M. J. Ziliotis, I. Sadia, S. Vandermeersch, N. Simon-Tillaux, D. Legouis, R. Cohen, Y. C. Xu-Dubois, M. Commereuc, E. Rondeau, S. Le Crom, and A. Hertig. Increased Fatty Acid Oxidation in Differentiated Proximal Tubular Cells Surviving a Reversible Episode of Acute Kidney Injury. *Cellular Physiology and Biochemistry*, 47(4):1338–1351, 2018.

[32] S. M. Baumgartner-Parzer, L. Wagner, M. Pettermann, J. Grillari, A. Gessl, and W. Waldhäusl. High-glucose-triggered apoptosis in cultured endothelial cells. *Diabetes*, 44(11):1323–1327, 1995.

[33] F. X. Beck, A. Dorge, E. Blumner, G. Giebisch, and K. Thurau. Cell rubidium uptake: A method for studying functional heterogeneity in the nephron. *Kidney International*, 33(3):642–651, 1988.

[34] T. Beckmann, T. Thüte, C. Heinrich, H. Büntemeyer, and T. Noll. Proteomic and metabolomic characterization of CHO DP-12 cell lines with different high passage histories. *BMC Proceedings*, 5(Suppl 8):P92, 2011.

[35] R. Beery, M. Haimsohn, N. Wertheim, R. Hemi, U. Nir, A. Karasik, H. Kanety, and A. Geier. Activation of the insulin-like growth factor 1 signaling pathway by the antiapoptotic agents aurintricarboxylic acid and Evans blue. *Endocrinology*, 142(7):3098–3107, 2001.

[36] Z. Bercovich, Z. Snapir, A. Keren-Paz, and C. Kahana. Antizyme affects cell proliferation and viability solely through regulating cellular polyamines. *Journal of Biological Chemistry*, 286(39):33778–33783, 2011.

[37] J. Berg, J. Tymoczko, and L. Stryer. Fatty Acid Metabolism. In W. Freeman, editor, *Biochemistry*, chapter 22. New York, 5 edition, 2002.

[38] M. J. Berridge, M. D. Bootman, and H. L. Roderick. Calcium signalling: Dynamics, homeostasis and remodelling. *Nature Reviews Molecular Cell Biology*, 4(7):517–529, 2003.

[39] K. Bertheussen. Growth of cells in a new defined protein-free medium. *Cytotechnology*, 11(3):219–231, 1993.

[40] A. Besson, S. F. Dowdy, and J. M. Roberts. CDK Inhibitors: Cell Cycle Regulators and Beyond. *Developmental Cell*, 14(2):159–169, 2008.

[41] N. Bhagavan and C.-E. Ha. Protein and Amino Acid Metabolism. In *Essentials of Medical Biochemistry*, pages 227–268. Elsevier, 2015.

[42] R. T. Biaggio, M. S. Abreu-Neto, D. T. Covas, and K. Swiech. Serum-free suspension culturing of human cells: adaptation, growth, and cryopreservation. *Bioprocess and Biosystems Engineering*, 38(8):1495–1507, 2015.

[43] D. Bikle. *Vitamin D: Production, Metabolism, and Mechanisms of Action*, volume 25. 2000.

[44] K. Birsoy, T. Wang, W. W. Chen, E. Freinkman, M. Abu-Remaileh, and D. M. Sabatini. An Essential Role of the Mitochondrial Electron Transport Chain in Cell Proliferation Is to Enable Aspartate Synthesis. *Cell*, 162(3):540–551, 2015.

[45] C. W. Boone, N. Mantel, T. D. Caruso, E. Kazam, and R. E. Stevensont. Quality control stuies on fetal bovine serum used in tissue culture. *In Vitro*, 7(3):174–189, 1972.

[46] H. Borsook, H. W. Davenport, C. E. P. Jeffreys, and R. C. Warner. The oxidation of ascorbic acid and its reduction in vitro and in vivo. *Journal of Biological Chemistry*, 117(1):237–279, 1937.

[47] J. J. Boza, D. Moënnoz, C. E. Bournot, S. Blum, I. Zbinden, P. A. Finot, and O. Ballèvre. Role of glutamine on the de novo purine nucleotide synthesis in Caco-2 cells. *European Journal of Nutrition*, 39(1):38–46, 2000.

[48] R. A. Bozym, F. Chimienti, L. J. Giblin, G. W. Gross, I. Korichneva, Y. Li, S. Libert, W. Maret, M. Parviz, C. J. Frederickson, and R. B. Thompson. Free zinc ions outside a narrow concentration range are toxic to a variety of cells in vitro. *Experimental Biology and Medicine*, 235(6):741–750, 2010.

[49] G. Bretones, M. D. Delgado, and J. León. Myc and cell cycle control. *Biochimica et Biophysica Acta - Gene Regulatory Mechanisms*, 1849(5):506–516, 2015.

[50] R. Brill, D. Fiorentini, B. van der Wijden, B. Monica, G. van Eikenhorst, E. Rodrigues, Y. E. Thomassen, A. Lugari, M. Lau, and E. Schulze. 4Cell ® NutriVero Flex 10 Medium. *BioProcess Online*, pages 1–7, 2020.

[51] C. Brocker, D. C. Thompson, and V. Vasiliou. The role of hyperosmotic stress in inflammation and disease. *BioMolecular Concepts*, 3(4):345–364, 2012.

[52] H. P. Broquist. Lysine-Pipecolic Acid Metabolic Relationships in Microbes and Mammals. *Annual Review of Nutrition*, 11(1):435–448, 1991.

[53] M. Burnette, T. Brito-Robinson, J. Li, and J. Zartman. An inverse small molecule screen to design a chemically defined medium supporting long-term growth of Drosophila cell lines. *Molecular BioSystems*, 10(10):2713–2723, 2014.

[54] B. Bushnell. BBMap, 2015.

[55] M. Butler. Animal cell cultures: Recent achievements and perspectives in the production of biopharmaceuticals. *Applied Microbiology and Biotechnology*, 68(3):283–291, 2005.

[56] M. Butler and J. Berry. Serum-free medium for growth of anchorage-dependant mammalian cells. (WO 98/04680), 1998.

[57] M. Butler, A. Burgener, M. Patrick, M. Berry, D. Moffatt, N. Huzel, N. Barnabe, and K. Coombs. Application of a serum-free medium for the growth of Vero cells and the production of reovirus. *Biotechnology Progress*, 16(5):854–858, 2000.

[58] M. Butler, N. Huzel, N. Barnabe, T. Gray, and L. Bajno. Linoleic acid improves the robustness of cells in agitated cultures. *Cytotechnology*, 30(1-3):27–36, 1999.

[59] E. M. Butt, T. C. Gilmour, S. L. Didio, and S. Mariano. Trace metal levels in human serum and blood. *Archives of Environmental Health*, 8(1):52–57, 1964.

[60] L. A. Byers, L. Diao, J. Wang, P. Saintigny, L. Girard, M. Peyton, L. Shen, Y. Fan, U. Giri, P. K. Tumula, M. B. Nilsson, J. Gudikote, H. Tran, R. J. Cardnell, D. J. Bearss, S. L. Warner, J. M. Foulks, S. B. Kanner, V. Gandhi, N. Krett, S. T. Rosen, E. S. Kim, R. S. Herbst, G. R. Blumenschein, J. J. Lee, S. M. Lippman, K. K. Ang, G. B. Mills, W. K. Hong, J. N. Weinstein, I. I. Wistuba, K. R. Coombes, J. D. Minna, and J. V. Heymach. An EpithelialMesenchymal Transition Gene Signature Predicts Resistance to EGFR and PI3K Inhibitors and Identifies Axl as a Therapeutic Target for Overcoming EGFR Inhibitor Resistance. *Clinical Cancer Research*, 19(1):279–290, 2013. jan.

[61] H. Cabrera-Cruz, L. Oróstica, F. Plaza-Parrochia, I. Torres-Pinto, C. Romero, and M. Vega. The insulin-sensitizing mechanism of myo-inositol is associated with AMPK activation and GLUT-4 expression in human endometrial cells exposed to a PCOS environment. *American Journal of Physiology - Endocrinology and Metabolism*, 318(2):E237–E248, 2020.

[62] G. Cairo, F. Bernuzzi, and S. Recalcati. A precious metal: Iron, an essential nutrient for all cells. *Genes Nutrition*, 1(1):25–40, 2006.

[63] X. Cao, Q. Yang, J. Qin, S. Zhao, X. Li, J. Fan, W. Chen, Y. Zhou, H. Mao, and X. Yu. V-ATPase promotes transforming growth factor-β-induced epithelial-mesenchymal transition of rat proximal tubular epithelial cells. *American Journal of Physiology - Renal Physiology*, 302(9):1121–1132, 2012.

[64] A. Carr and B. Frei. Does vitamin C act as a prooxidant under physiological conditions? *The FASEB Journal*, 13(9):1007–1024, 1999.

[65] L. M. Carrillo-Cocom, T. Genel-Rey, D. Araíz-Hernández, F. López-Pacheco, J. López-Meza, M. R. Rocha-Pizaña, A. Ramírez-Medrano, and M. M. Alvarez. Amino acid consumption in naïve and recombinant CHO cell cultures: producers of a monoclonal antibody. *Cytotechnology*, 67(5):809–820, 2015.

[66] E. M. Carrington, Y. Zhan, J. L. Brady, J. G. Zhang, R. M. Sutherland, N. S. Anstee, R. L. Schenk, I. B. Vikstrom, R. B. Delconte, D. Segal, N. D. Huntington, P. Bouillet, D. M. Tarlinton, D. C. S. Huang, A. Strasser, S. Cory, M. J. Herold, and A. M. Lew. Anti-apoptotic proteins BCL-2, MCL-1 and A1 summate collectively to maintain survival of immune cell populations both in vitro and in vivo. *Cell Death and Differentiation*, 24(5):878–888, 2017.

[67] C. Caruso-Meves, A. A. S. Pinheiro, H. Cai, J. Souza-Menezes, and W. B. Guggino. PKB and megalin determine the survival or death of renal proximal tubule cells. *Proceedings of the National Academy of Sciences of the United States of America*, 103(49):18810–18815, 2006.

[68] U. Cavallaro and G. Christofori. Cell adhesion and signalling by cadherins and Ig-CAMs in cancer. *Nature Reviews Cancer*, 4(2):118–132, 2004.

[69] A. Chen, S. L. Poh, C. Dietzsch, E. Roethl, M. L. Yan, and S. K. Ng. Serum-free microcarrier based production of replication deficient influenza vaccine candidate virus lacking NS1 using Vero cells. *BMC biotechnology*, 11(1):81, 2011.

[70] P. Chen, J. Bornhorst, and M. Aschner. Manganese metabolism in humans. *Frontiers in bioscience (Landmark edition)*, 23:1655–1679, 2018.

[71] Y. Chen, S. I. Roohani-Esfahani, Z. F. Lu, H. Zreiqat, and C. R. Dunstan. Zirconium ions up-regulate the BMP/SMAD signaling pathway and promote the proliferation and differentiation of human osteoblasts. *PLoS ONE*, 10(1):1–17, 2015.

[72] T. Chibazakura, K. Kamachi, M. Ohara, S. Tane, H. Yoshikawa, and J. M. Roberts. Cyclin A Promotes S-Phase Entry via Interaction with the Replication Licensing Factor Mcm7. *Molecular and Cellular Biology*, 31(2):248–255, 2011.

[73] C. L. Chin, J. B. Goh, H. Srinivasan, K. I. Liu, A. Gowher, R. Shanmugam, H. L. Lim, M. Choo, W. Q. Tang, A. H. M. Tan, T. Nguyen-Khuong, M. H. Tan, and S. K. Ng. A human expression system based on HEK293 for the stable production of recombinant erythropoietin. *Scientific Reports*, 9(1):1–16, 2019.

[74] S. S. Chou, M. S. Clegg, T. Y. Momma, B. J. Niles, J. Y. Duffy, G. P. Daston, and C. L. Keen. Alterations in protein kinase C activity and processing during zinc-deficiency-induced cell death. *The Biochemical journal*, 383(Pt 1):63–71, 2004.

[75] C. Chu, D. P. Bottaro, M. J. Betenbaugh, and J. Shiloach. Stable ectopic expression of ST6GALNAC5 induces autocrine MET activation and anchorage-independence in MDCK Cells. *PLoS ONE*, 11(2):1–17, 2016.

[76] C. Chu, V. Lugovtsev, H. Golding, M. Betenbaugh, and J. Shiloach. Conversion of MDCK cell line to suspension culture by transfecting with human siat7e gene and its application for influenza virus production. *PNAS*, 2009.

[77] C. Chu, V. Lugovtsev, A. Lewis, M. Betenbaugh, and J. Shiloach. Production and antigenic properties of influenza virus from suspension MDCK-siat7e cells in a bench-scale bioreactor. *Vaccine*, 28(44):7193–7201, 2010.

[78] C. Chumsae, P. Hossler, H. Raharimampionona, Y. Zhou, S. McDermott, C. Racicot, C. Radziejewski, and Z. S. Zhou. When Good Intentions Go Awry: Modification of a Recombinant Monoclonal Antibody in Chemically Defined Cell Culture by Xylosone, an Oxidative Product of Ascorbic Acid. *Analytical Chemistry*, 87(15):7529–7534, 2015.

[79] V. C. Ciccarone, D. Gruber, and S. Bennett. Cell Culture Medium for Cell Growth and Transfection. (US 2003/0096414 A1), 2018.

[80] J. Cinatl. Protein-free culture of Vero cells: a substrate for replication of human pathogenic viruses. *Cell Biology International*, 17(9):885–896, 1993. sep.

[81] R. Ciosk, W. Zachariae, C. Michaelis, A. Shevchenko, M. Mann, and K. Nasmyth. An ESP1/PDS1 complex regulates loss of sister chromatid cohesion at the metaphase to anaphase transition in yeast. *Cell*, 93(6):1067–1076, 1998.

[82] D. E. Clapham. Calcium Signaling. *Cell*, 131(6):1047–1058, 2007.

[83] M. J. V. Clausen and H. Poulsen. Sodium/Potassium Homeostasis in the Cell. In A. Sigel, H. Sigel, and R. Sigel, editors, *Metal Ions in Life Sciences*, chapter 12, pages 41–67. 2013.

[84] W. Cleveland and E. Bernard. Protein-Free Culture Medium. (US 4767704 A), 1988.

[85] M. Coppolino, C. Leung-Hagesteijn, S. Dedhar, and J. Wilkins. Inducible Interaction of Integrin alpha (2) beta (1) with Calreticulin. *Journal of Biological Chemistry*, 270(39):23132, 1995.

[86] M. G. Coppolino, M. J. Woodside, N. Demaurex, S. Grinstein, R. St-Arnaud, and S. Dedhar. Calreticulin is essential for integrin-mediated calcium signalling and cell adhesion. *Nature*, 386(6627):843–847, 1997. apr.

[87] J. Costa Pessoa, E. Garribba, M. F. A. Santos, and T. Santos-Silva. Vanadium and proteins: Uptake, transport, structure, activity and function. *Coordination Chemistry Reviews*, 301-302:49–86, 2015.

[88] T. G. Cross, D. Scheel-Toellner, N. V. Henriquez, E. Deacon, M. Salmon, and J. M. Lord. Serine/threonine protein kinases and apoptosis. *Experimental Cell Research*, 256(1):34–41, 2000.

[89] J. J. R. da Silva and R. J. P. Williams. *The Biological Chemistry of the Elements: The Inorganic Chemistry of Life*. OUP Oxford, 2001.

[90] M. G. Daelli. Vero Cell Line Adapted to Grow in Suspension. (US 2007/0111309 A1), 2007.

[91] X. Dai, Y. Miao, P. Han, X. Zhang, S. Yang, Q. Lv, and D. Hua. Pabpc1 enables cells with the suspension cultivation feature. *ACS Synthetic Biology*, 10(2):309–317, 2021.

[92] Y. Dai and S. Grant. Targeting Chk1 in the replicative stress response. *Cell Cycle*, 9(6):1025–1030, 2010. mar.

[93] L. E. Dansie, S. Reeves, K. Miller, S. P. Zano, M. Frank, C. Pate, J. Wang, and S. Jackowski. Physiological roles of the pantothenate kinases. *Biochemical Society Transactions*, 42(4):1033–1036, 2014.

[94] U. N. Das. Nutrients, essential fatty acids and prostaglandins interact to augment immune responses and prevent genetic damage and cancer. *Nutrition (Burbank, Los Angeles County, Calif.)*, 5(2):106–10.

[95] A. P. Davenport, C. C. Scully, C. de Graaf, A. J. Brown, and J. J. Maguire. Advances in therapeutic peptides targeting G protein-coupled receptors. *Nature Reviews Drug Discovery*, 19(6):389–413, 2020.

[96] A. De La Vieja and P. Santisteban. Role of iodide metabolism in physiology and cancer. *Endocrine-Related Cancer*, 25(4):R225–R245, 2018.

[97] G. E. Derfus, J. Dizon-Maspat, J. T. Broddrick, A. C. Velayo, J. D. Toschi, R. T. Santuray, S. K. Hsu, C. M. Winter, R. Krishnan, and A. Amanullah. Red colored IgG4 caused by vitamin B12from cell culture media combined with disulfide reduction at harvest. *mAbs*, 6(3):679–688, 2014.

[98] N. Desai and J. Goldfarb. Co-cultured human embryos may be subjected to widely different microenvironments: Pattern of growth factor/cytokine release by Vero cells during the co-culture interval. *Human Reproduction*, 13(6):1600–1605, 1998.

[99] N. N. Desai and J. M. Goldfarb. Growth factor/cytokine secretion by a permanent human endometrial cell line with embryotrophic properties. *Journal of Assisted Reproduction and Genetics*, 13(7):546–550, 1996.

[100] S. U. Devaskar and M. M. Mueckler. The mammalian glucose transporters. *Pediatric Research*, 31(1):1–13, 1992.

[101] V. M. DeZengotita, L. R. Abston, A. E. Schmelzer, S. Shaw, and W. M. Miller. Selected amino acids protect hybridoma and CHO cells from elevated carbon dioxide and osmolality. *Biotechnology and Bioengineering*, 78(7):741–752, 2002.

[102] V. Dill, F. Pfaff, A. Zimmer, M. Beer, and M. Eschbaumer. Adherent and suspension baby hamster kidney cells have a different cytoskeleton and surface receptor repertoire. *PLoS ONE*, 16(6 June):1–15, 2021.

[103] A. Dobin, C. A. Davis, F. Schlesinger, J. Drenkow, C. Zaleski, S. Jha, P. Batut, M. Chaisson, and T. R. Gingeras. STAR: Ultrafast universal RNA-seq aligner. *Bioinformatics*, 29(1):15–21, 2013.

[104] B. T. Dong, G. J. Tu, Y. X. Han, and Yi-Chen. Lithium enhanced cell proliferation and differentiation of mesenchymal stem cells to neural: Cells in rat spinal cord. *International Journal of Clinical and Experimental Pathology*, 8(3):2473–2483, 2015.

[105] A. Dongre and R. A. Weinberg. New insights into the mechanisms of epithelialmesenchymal transition and implications for cancer. *Nature Reviews Molecular Cell Biology*, 20(2):69–84, 2019. feb.

[106] H. Dorai, S. K. Yun, D. Ellis, C. A. Kinney, C. Lin, D. Jan, G. Moore, and M. J. Betenbaugh. Expression of anti-apoptosis genes alters lactate metabolism of Chinese Hamster ovary cells in culture. *Biotechnology and Bioengineering*, 103(3):592–608, 2009.

[107] J. Du, J. J. Cullen, and G. R. Buettner. Ascorbic acid: Chemistry, biology and the treatment of cancer. *Biochimica et Biophysica Acta - Reviews on Cancer*, 1826(2):443–457, 2012.

[108] T. M. Duarte, N. Carinhas, L. C. Barreiro, M. J. T. Carrondo, P. M. Alves, and A. P. Teixeira. Metabolic responses of CHO cells to limitation of key amino acids. *Biotechnology and Bioengineering*, 111(10):2095–2106, 2014.

[109] R. Dulbecco and G. Freeman. Plaque production by the polyoma virus. *Virology*, 8(3):396–397, 1959. jul.

[110] S. Durinck, Y. Moreau, A. Kasprzyk, S. Davis, B. De Moor, A. Brazma, and W. Huber. BioMart and Bioconductor: A powerful link between biological databases and microarray data analysis. *Bioinformatics*, 21(16):3439–3440, 2005.

[111] J. Dyachok, S. Earnest, E. N. Iturraran, M. H. Cobb, and E. M. Ross. Amino acids regulate mTORC1 by an obligate two-step mechanism. *Journal of Biological Chemistry*, 291(43):22414–22426, 2016.

[112] H. Eagle. Propagation in a Fluid Medium of a Human Epidermoid Carcinoma, Strain KB. *Experimental Biology and Medicine*, 89(3):362–364, 1955. jul.

[113] H. Eagle. Amino Acid Metabolism in Mammalian Cell Cultures. *Science*, 130(3373):432–437, 1959. aug.

[114] H. Eagle, V. I. Oyama, M. Levy, and R. Fleischman. The growth response of mammalian cells in tissue culture to L-glutamine and L-glutamic acid. *The Journal of Biological Chemistry*, 218(218):607–616, 1956.

[115] H. J. Ehrlich, G. Berezuk, S. Fritsch, G. Aichinger, J. Singer, D. Portsmouth, M. K. Hart, W. El-Amin, O. Kistner, and P. N. Barrett. Clinical development of a Vero cell culture-derived seasonal influenza vaccine. *Vaccine*, 30(29):4377–4386, 2012.

[116] D. J. Eide. Zinc transporters and the cellular trafficking of zinc. *Biochimica et Biophysica Acta - Molecular Cell Research*, 1763(7):711–722, 2006.

[117] E. Eisenberg and E. Y. Levanon. Human housekeeping genes, revisited. *Trends in Genetics*, 29(10):569–574, 2013.

[118] A. Enomoto, N. Kido, M. Ito, N. Takamatsu, and K. Miyagawa. Serine-Threonine Kinase 38 is regulated by Glycogen Synthase Kinase-3 and modulates oxidative stress-induced cell death. *Free Radical Biology and Medicine*, 52(2):507–515, 2012.

[119] B. Eppler and R. Dawson. Cytoprotective role of taurine in a renal epithelial cell culture model. *Biochemical Pharmacology*, 63(6):1051–1060, 2002.

[120] D. A. Epstein, R. Monsell, J. Horwitz, S. Lenk, S. Ozturk, and C. Marsh. Chemically Defined Media Compositions. (US 2006/0094113 A1), 2006.

[121] E. O. Erra, H. H. Askling, L. Rombo, J. Riutta, S. Vene, S. Yoksan, L. Lindquist, S. H. Pakkanen, E. Huhtamo, O. Vapalahti, and A. Kantele. A Single Dose of Vero Cell-Derived Japanese Encephalitis (JE) Vaccine (Ixiaro) Effectively Boosts Immunity in Travelers Primed With Mouse Brain-Derived JE Vaccines. *Clinical Infectious Diseases*, 55(6):825–834, 2012. sep.

[122] L. Favennec and M. J. Cals. The Biological Effects of Retinoids on Cell Differentiation and Proliferation. *Clinical Chemistry and Laboratory Medicine*, 26(8):479–490, 1988.

[123] FDA. Guidance for Industry Cell Characterization and Qualification of Cell Substrates and Other Biological Materials Used in the Production of Viral Vaccines for Infectious Disease Indications. *FDA Guidance for Industry*, (February):1–50, 2010.

[124] A. Fenselau, D. Kaiser, and K. Wallis. Nucleoside requirements for the in vitro growth of bovine aortic endothelial cells. *Journal of Cellular Physiology*, 108(3):375–384, 1981.

[125] R. A. Festa and D. J. Thiele. Copper: An essential metal in biology. *Current Biology*, 21(21):R877–R883, 2011. nov.

[126] R. P. Field. Animal Cell Culture. (US 6593140 B1), 2003.

[127] D. C. Fish, J. P. Dobbs, and J. M. Elliott. Effect of Osmotic Pressure, Na+-K+ Ratio and Medium Concentration on Enzyme-Activity and Growth of L Cells in Suspension Culture. *In Vitro-Journal of the Tissue Culture Association*, 9(2):108–113, 1973.

[128] J.-P. Fonta, P. Ducommun, and V. Deparis. Serum-Free Culture for the production of recombinant gonadotropins. (US 8093052 B2), 2006.

[129] T. Franceschi. The Role of Ascorbic Acid in the Hydroxylation of Peptide-Bound Proline. *Nutrition Reviews*, 37(1):26–28, 1979. apr.

[130] F. Franek, O. Hohenwarter, and H. Katinger. Plant protein hydrolysates: Preparation of defined peptide fractions promoting growth and production in animal cells cultures. *Biotechnology Progress*, 16(5):688–692, 2000.

[131] N. M. Frazzati-Gallina, R. L. Paoli, R. M. Mourão-Fuches, S. A. C. Jorge, and C. A. Pereira. Higher production of rabies virus in serum-free medium cell cultures on microcarriers. *Journal of Biotechnology*, 92(1):67–72, 2001.

[132] J. H. Freedman, M. R. Ciriolo, and J. Peisach. The role of glutathione in copper metabolism and toxicity. *Journal of Biological Chemistry*, 264(10):5598–5605, 1989.

[133] R. I. Freshney. *Culture of Animal Cells: A Manual of Basic Technique and Specialized Applications*. John Wiley Sons, 7 edition, 2015.

[134] H. Fujita, Y. Yoshino, and N. Chiba. Regulation of the centrosome cycle. *Molecular and Cellular Oncology*, 3(2):1–7, 2016.

[135] F. Gaboriau, A. Kreder, N. Clavreul, J. P. Moulinoux, J. G. Delcros, and G. Lescoat. Polyamine modulation of iron uptake in CHO cells. *Biochemical Pharmacology*, 67(9):1629–1637, 2004.

[136] M. Gaestel. MAPKAP kinases - MKs - Two's company, three's a crowd. *Nature Reviews Molecular Cell Biology*, 7(2):120–130, 2006.

[137] F. Galli, A. Azzi, M. Birringer, J. M. Cook-Mills, M. Eggersdorfer, J. Frank, G. Cruciani, S. Lorkowski, and N. K. Özer. Vitamin E: Emerging aspects and new directions. *Free Radical Biology and Medicine*, 102(June 2016):16–36, 2017.

[138] J. Gao and M. Simon. Identification of a novel keratinocyte retinyl ester hydrolase as a transacylase and lipase. *Journal of Investigative Dermatology*, 124(6):1259–1266, 2005.

[139] J. Garcia-Bermudez, L. Baudrier, K. La, X. G. Zhu, J. Fidelin, V. O. Sviderskiy, T. Papagiannakopoulos, H. Molina, M. Snuderl, C. A. Lewis, R. L. Possemato, and K. Birsoy. Aspartate is a limiting metabolite for cancer cell proliferation under hypoxia and in tumours. *Nature Cell Biology*, 20(7):775–781, 2018.

[140] A. P. Garneau, G. A. Carpentier, A. A. Marcoux, R. Frenette-Cotton, C. F. Simard, W. Rémus-Borel, L. Caron, M. Jacob-Wagner, M. Noël, J. J. Powell, R. Bélanger, F. Côté, and P. Isenring. Aquaporins mediate silicon transport in humans. *PLoS ONE*, 10(8):1–15, 2015.

[141] M. M. Gaschler and B. R. Stockwell. Lipid peroxidation in cell death. *Biochemical and Biophysical Research Communications*, 482(3):419–425, 2017.

[142] V. Gasperi, M. Sibilano, I. Savini, and M. V. Catani. Niacin in the central nervous system: An update of biological aspects and clinical applications. *International Journal of Molecular Sciences*, 20(4):1–26, 2019.

[143] M. Gawalitzek, S. Luo, and C. T. Bevilacqua. Production Of Proteins In Glutamine-free Cell Culture Media. (US 9714293 B2), 2018.

[144] Y. Genzel, C. Dietzsch, E. Rapp, J. Schwarzer, and U. Reichl. MDCK and Vero cells for influenza virus vaccine production: A one-to-one comparison up to lab-scale bioreactor cultivation. *Applied Microbiology and Biotechnology*, 88(2):461–475, 2010.

[145] Y. Genzel, M. Fischer, and U. Reichl. Serum-free influenza virus production avoiding washing steps and medium exchange in large-scale microcarrier culture. *Vaccine*, 24(16):3261–3272, 2006.

[146] Y. Genzel, S. König, and U. Reichl. Amino acid analysis in mammalian cell culture media containing serum and high glucose concentrations by anion exchange chromatography and integrated pulsed amperometric detection. *Analytical Biochemistry*, 335(1):119–125, 2004. dec.

[147] Y. Genzel and U. Reichl. Continuous cell lines as a production system for influenza vaccines. *Expert review of vaccines*, 8(12):1681–1692, 2009.

[148] Y. Genzel, J. B. Ritter, S. König, R. Alt, and U. Reichl. Substitution of glutamine by pyruvate to reduce ammonia formation and growth inhibition of mammalian cells. *Biotechnology Progress*, 21(1):58–69, 2005.

[149] F. G. Giancotti and E. Ruoslahti. Integrin Signaling. *Science*, 285(5430):1028–1032, 1999.

[150] Gibco. OptiPRO SFM. Technical report, 2014.

[151] A. P. Gilmore. Anoikis. *Cell Death and Differentiation*, 12:1473–1477, 2005. nov.

[152] A. B. Glassman, R. S. Rydzewski, and C. E. Bennett. Trace metal levels in commercially prepared tissue culture media. *Tissue & cell*, 12(4):613–617, 1980.

[153] S. Goetghebeur and W. S. Hu. Cultivation of anchorage-dependent animal cells in microsphere-induced aggregate culture. *Applied Microbiology and Biotechnology*, 34(6):735–741, 1991.

[154] B. J. Goldstein, L. Zhu, R. Hager, A. Zilbering, Y. Sun, and J. B. Vincent. Enhancement of post-receptor insulin signaling by trivalent chromium in hepatoma cells is associated with differential inhibition of specific protein-tyrosine phosphatases. *Journal of Trace Elements in Experimental Medicine*, 14(4):393–404, 2001.

[155] R. G. Gonzalez, R. S. Haxo, and T. Schleich. Mechanism of Action of Polymeric Aurintricarboxylic Acid, a Potent Inhibitor of Protein-Nucleic Acid Interactions. *Biochemistry*, 19(18):4299–4303, 1980.

[156] N. E. Good, G. D. Winget, W. Winter, T. N. Connolly, S. Izawa, and R. M. M. Singh. Hydrogen Ion Buffers for Biological Research. *Biochemistry*, 5(2):467–477, 1966.

[157] S. Gorfien, B. Paul, J. Walowitz, R. Keem, W. Biddle, and D. Jayme. Growth of NS0 cells in protein-free, chemically defined medium. *Biotechnology progress*, 16(5):682–687, 2000.

[158] S. F. Gorfien, R. M. Fike, G. P. Godwin, J. L. Dzimian, D. A. Epstein, D. Gruber, D. McClure, P. J. Price, J. L. Dzimian, D. A. Epstein, D. Gruber, D. McClure, and P. J. Price. Serum-free mammalian cell culture medium, and uses thereof. (US 2006/0148074 A1), 1998.

[159] M. Gregoire, M. Rejean, M. A. Quilliam, and D. Gravel. On auxotrophy for pyrimidines of respiration-deficient chick embryo cells. *European Journal of Biochemistry*, 142(1):49–55, 1984. jul.

[160] M. K. Gregory, H. W. King, P. A. Bain, R. A. Gibson, D. R. Tocher, and K. A. Schuller. Development of a fish cell culture model to investigate the impact of fish oil replacement on lipid peroxidation. *Lipids*, 46(8):753–764, 2011.

[161] W. Gregory Hamilton and R. G. Ham. Clonal growth of Chinese hamster cell lines in protein-free media. *In Vitro*, 13(9):537–547, 1977.

[162] L. Grillberger, M. Reiter, W. Mundt, F. Dorner, L. Gillberger, M. Reiter, W. Mundt, F. Dorner, L. Grillberger, M. Reiter, W. Mundt, F. Dorner, L. Gillberger, M. Reiter, W. Mundt, and F. Dorner. Animal Protein-Free Media for Cultivation of Cells. (US 2006/0094104 A1), 2010.

[163] D. Guo, Q. Zhu, H. Zhang, and D. Sun. Proteomic analysis of membrane proteins of vero cells: exploration of potential proteins responsible for virus entry. *DNA and Cell Biology*, 33(1):20–8, 2014.

[164] J. M. C. Gutteridge. Lipid peroxidation and antioxidants as biomarkers of tissue damage. *Clinical Chemistry*, 41(12 SUPPL.):1819–1828, 1995.

[165] R. Haldankar, J. J. Kopchick, and D. Ridgway. Stable production of a human growth hormone antagonist from CHO cells adapted to serum-free suspension culture. *Biotechnology Progress*, 15(3):336–346, 1999.

[166] D. Hallengärd, M. Kakoulidou, A. Lulla, B. M. Kümmerer, D. X. Johansson, M. Mutso, V. Lulla, J. K. Fazakerley, P. Roques, R. Le Grand, A. Merits, and P. Liljeström. Novel attenuated Chikungunya vaccine candidates elicit protective immunity in C57BL/6 mice. *Journal of virology*, 88(5):2858–2866, 2014.

[167] B. Halliwell. Cell culture, oxidative stress, and antioxidants: Avoiding pitfalls. *Biomedical Journal*, 0(0):0, 2014.

[168] R. G. Ham. Clonal Growth of Mammalian Cells in a Chemically Defined, Synthetic Medium. *Proceedings of the National Academy of Sciences of the United States of America*, 53(3002):288–293, 1965.

[169] Y. K. Han, Y.-G. Kim, J. Y. Kim, and G. M. Lee. Hyperosmotic stress induces autophagy and apoptosis in recombinant Chinese hamster ovary cell culture. *Biotechnology and Bioengineering*, 105(6):n/a–n/a, 2010.

[170] Z. Han, D. Kang, Y. Joo, J. Lee, G.-h. Oh, S. Choi, S. Ko, S. Je, H. J. Choi, and J. J. Song. TGF-β downregulation-induced cancer cell death is finely regulated by the SAPK signaling cascade. *Experimental Molecular Medicine*, 50(12):1–19, 2018. dec.

[171] M. A. Hanson, X. Ge, Y. Kostov, K. A. Brorson, A. R. Moreira, and G. Rao. Comparisons of Optical pH and Dissolved Oxygen Sensors With Traditional Electrochemical Probes During Mammalian Cell Culture. *Biotechnology and Bioengineering*, 97(4):833–841, 2007.

[172] Y. Hao, D. Baker, and P. ten Dijke. TGF-β-Mediated Epithelial-Mesenchymal Transition and Cancer Metastasis. *International Journal of Molecular Sciences*, 20(11):2767, 2019. jun.

[173] A. Harduin-Lepers, D. C. Stokes, W. F. Steelant, B. Samyn-Petit, M. A. Krzewinski-Recchi, V. Vallejo-Ruiz, J. P. Zanetta, C. Augé, and P. Delannoy. Cloning, expression and gene organization of a human Neu5Ac alpha 2-3Gal beta 1-3GalNAc alpha 2,6-sialyltransferase: hST6GalNAcIV. *The Biochemical Journal*, 352 Pt 1:37–48, 2000. nov.

[174] A. R. Harkness, R. J. Simmonds, P. Gough, P. K. Priscott, and J. A. Squire. Purine base and nucleoside, cytidine and uridine concentrations in foetal calf and other sera. *Biochemical Society Transactions*, 8(1):139–139, 1980. feb.

[175] A. E. Harper, R. H. Miller, and K. P. Block. Branched-chain amino acid metabolism. *Annual review of nutrition*, 4:409–454, 1984.

[176] M. K. Hasan, S. Alam, J. Mirkovic, and M. F. Hossain. Screening of Human Proteins for Fluoride and Aluminum Binding. *Bioinformation*, 14(02):68–74, 2018. feb.

[177] R. P. Hausinger and R. P. Hausinger. Animal Nickel Metabolism. *Biochemistry of Nickel*, pages 221–269, 1993.

[178] A. Health, P. Health, and C. Division. Polio Vaccine : IMOVAX Polio (Vero Cell Origin). *Alberta Health*, pages 4–6, 2017.

[179] M. G. V. Heiden, L. C. Cantley, C. B. Thompson, P. Mammalian, C. Exhibit, and A. Metabolism. Understanding the Warburg Effect : Cell Proliferation. *Science*, 324(May):1029, 2009.

[180] N. E. Hellman, S. Kono, G. M. Mancini, A. J. Hoogeboom, G. J. De Jong, and J. D. Gitlin. Mechanisms of copper incorporation into human ceruloplasmin. *Journal of Biological Chemistry*, 277(48):46632–46638, 2002.

[181] S. A. Henry, M. L. Gaspar, and S. A. Jesch. The response to inositol: Regulation of glycerolipid metabolism and stress response signaling in yeast. *Chemistry and Physics of Lipids*, 180:23–43, 2014.

[182] R. Hernández-Benítez, G. Ramos-Mandujano, and H. Pasantes-Morales. Taurine stimulates proliferation and promotes neurogenesis of mouse adult cultured neural stem/progenitor cells. *Stem Cell Research*, 9(1):24–34, 2012.

[183] H. Herschel Conaway, P. Henning, and U. H. Lerner. Vitamin a metabolism, action, and role in skeletal homeostasis. *Endocrine Reviews*, 34(6):766–797, 2013.

[184] K. I. Hirata, H. L. Dichek, J. A. Cioffi, S. Y. Choi, N. J. Leeper, L. Quintana, G. S. Kronmal, A. D. Cooper, and T. Quertermous. Cloning of a unique lipase from endothelial cells extends the lipase gene family. *Journal of Biological Chemistry*, 274(20):14170–14175, 1999.

[185] L. S. Holst, D. Langin, H. Mulder, H. Laurell, J. Grober, A. Bergh, H. W. Mohrenweiser, G. Edgren, and C. Holm. Molecular cloning, genomic organization, and expression of a testicular isoform of hormone-sensitive lipase. *Genomics*, 35(3):441–447, 1996.

[186] B. J. Holub. Metabolism and Function of myo -Inositol and Inositol Phospholipids. *Annual Review of Nutrition*, 6(1):563–597, 1986. jul.

[187] A. Hönscheid, S. Dubben, L. Rink, and H. Haase. Zinc differentially regulates mitogen-activated protein kinases in human T cells. *Journal of Nutritional Biochemistry*, 23(1):18–26, 2012.

[188] D. W. Horne, V. Tanphaichitr, and H. P. Broquist. Role of Lysine in Carnitine Biosynthesis in Neurospora crassa. *J Biol Chem*, 246(13):4373–4376, 1971.

[189] W. House. 11710 - Glasgow's MEM, 1964.

[190] S. M. Houten, S. Violante, F. V. Ventura, and R. J. Wanders. The Biochemistry and Physiology of Mitochondrial Fatty Acid β-Oxidation and Its Genetic Disorders. *Annual Review of Physiology*, 78:23–44, 2016.

[191] A. C. Howard, A. K. McNeil, and P. L. McNeil. Promotion of plasma membrane repair by vitamine E. *Nature Communications*, 2(1):1–8, 2011.

[192] Z. Huawei. Selenium as an essential micronutrient: Roles in cell cycle and apoptosis. *Molecules*, 14(3):1263–1278, 2009.

[193] C. Hwangbo, N. Tae, S. Lee, O. Kim, O. K. Park, J. Kim, S. H. Kwon, and J. H. Lee. Syntenin regulates TGF-β1-induced Smad activation and the epithelial-to-mesenchymal transition by inhibiting caveolin-mediated TGF-β type i receptor internalization. *Oncogene*, 35(3):389–401, 2016.

[194] L. J. Ignarro, G. M. Buga, L. H. Wei, P. M. Bauer, G. Wu, and P. del Soldato. Role of the arginine-nitric oxide pathway in the regulation of vascular smooth muscle cell proliferation. *Proc Natl Acad Sci U S A*, 98(7):4202–4208, 2001.

[195] E. Ikonen. Cellular cholesterol trafficking and compartmentalization. *Nature Reviews Molecular Cell Biology*, 9(2):125–138, 2008.

[196] M. Inazu. Functional expression of choline transporters in the blood-brain barrier. *Nutrients*, 11(10), 2019.

[197] J. Iorio, G. Petroni, C. Duranti, and E. Lastraioli. Potassium and Sodium Channels and the Warburg Effect: Biophysical Regulation of Cancer Metabolism. *Bioelectricity*, 1(3):188–200, 2019.

[198] N. N. Iscove and F. Melchers. Complete replacement of serum by albumin, transferrin, and soybean lipid in cultures of lipopolysaccharide-reactive B lymphocytes. *Journal of Experimental Medicine*, 147(3):923–933, 1978.

[199] E. L. Jacobson, H. Kim, M. Kim, and M. K. Jacobson. *Niacin: Vitamin and Antidyslipidemic Drug*, pages 37–47. Springer Netherlands, Dordrecht, 2012.

[200] A. Jain and G. Tuteja. TissueEnrich: Tissue-specific gene enrichment analysis. *Bioinformatics (Oxford, England)*, 35(11):1966–1967, 2019.

[201] P. Jaluria, M. Betenbaugh, K. Konstantopoulos, B. Frank, and J. Shiloach. Application of microarrays to identify and characterize genes involved in attachment dependence in HeLa cells. *Metabolic Engineering*, 9(3):241–251, 2007. may.

[202] A. Janowski and N. Sadlej. Complexes of Aurintricarboxylic Acid with Rare Earth Metal Ions - Luminescence Properties and Energy Transfer. *Journal of Luminescence*, 3:198–202, 1970.

[203] M. Jaye, K. J. Lynch, J. Krawiec, D. Marchadier, C. Maugeais, K. Doan, V. South, D. Amin, M. Perrone, and D. J. Rader. A novel endothelial-derived lipase that modulates HDL metabolism. *Nature Genetics*, 21(4):424–428, 1999.

[204] B. Jiang, Y. Wang, and R. I. Glass. Does a monovalent inactivated human rotavirus vaccine induce heterotypic immunity? Evidence from animal studies. *Human Vaccines and Immunotherapeutics*, 9(8):1634–1637, 2013.

[205] T. Jobst-Schwan, K. X. Knaup, R. Nielsen, T. Hackenbeck, M. Buettner-Herold, P. Lechler, S. Kroening, M. Goppelt-Struebe, U. Schloetzer-Schrehardt, B. G. Fürnrohr, R. E. Voll, K. Amann, K. U. Eckardt, E. I. Christensen, and M. S. Wiesener. Renal uptake of the antiapoptotic protein survivin is mediated by megalin at the apical membrane of the proximal tubule. *American Journal of Physiology - Renal Physiology*, 305(5):734–744, 2013.

[206] M. L. Johansen, L. K. Bak, A. Schousboe, P. Iversen, M. Sørensen, S. Keiding, H. Vilstrup, A. Gjedde, P. Ott, and H. S. Waagepetersen. The metabolic role of isoleucine in detoxification of ammonia in cultured mouse neurons and astrocytes. *Neurochemistry International*, 50(7-8):1042–1051, 2007.

[207] C. J. Jong, J. Azuma, and S. Schaffer. Mechanism underlying the antioxidant activity of taurine: Prevention of mitochondrial oxidant production. *Amino Acids*, 42(6):2223–2232, 2012.

[208] R. Kalluri and R. A. Weinberg. The basics of epithelial-mesenchymal transition. *Journal of Clinical Investigation*, 120(5):1786–1786, 2010. may.

[209] J. Kalucka, L. Bierhansl, N. V. Conchinha, R. Missiaen, I. Elia, U. Brüning, S. Scheinok, L. Treps, A. R. Cantelmo, C. Dubois, P. de Zeeuw, J. Goveia, A. Zecchin, F. Taverna, F. Morales-Rodriguez, A. Brajic, L.-C. Conradi, S. Schoors, U. Harjes, K. Vriens, G.-A. Pilz, R. Chen, R. Cubbon, B. Thienpont, B. Cruys, B. W. Wong, B. Ghesquière, M. Dewerchin, K. De Bock, X. Sagaert, S. Jessberger, E. A.

Jones, B. Gallez, D. Lambrechts, M. Mazzone, G. Eelen, X. Li, S.-m. Fendt, and P. Carmeliet. Quiescent Endothelial Cells Upregulate Fatty Acid β-Oxidation for Vasculoprotection via Redox Homeostasis. *Cell Metabolism*, 28(6):881–894.e13, 2018. dec.

[210] E. S. Kandel and N. Hay. The regulation and activities of the multifunctional serine/threonine kinase Akt/PKB. *Experimental Cell Research*, 253(1):210–229, 1999.

[211] H. M. Kang, S. H. Ahn, P. Choi, Y. A. Ko, S. H. Han, F. Chinga, A. S. D. Park, J. Tao, K. Sharma, J. Pullman, E. P. Bottinger, I. J. Goldberg, and K. Susztak. Defective fatty acid oxidation in renal tubular epithelial cells has a key role in kidney fibrosis development. *Nature Medicine*, 21(1):37–46, 2015.

[212] S. Kang, J. Mullen, L. P. Miranda, and R. Deshpande. Utilization of tyrosine- and histidine-containing dipeptides to enhance productivity and culture viability. *Biotechnology and Bioengineering*, 109(9):2286–2294, 2012.

[213] H. Kanouchi, M. Shibuya, S. Tsukamoto, Y. Fujimura, H. Tachibana, K. Yamada, and T. Oka. Comparisons of uptake and cell surface binding among pyridoxal, pyridoxine, and pyridoxamine in RAW264.7 cells. *Nutrition*, 26(6):648–652, 2010.

[214] J. H. Kaplan and S. Lutsenko. Copper transport in mammalian cells: Special care for a metal with special needs. *Journal of Biological Chemistry*, 284(38):25461–25465, 2009.

[215] J. H. Kaplan and E. B. Maryon. How Mammalian Cells Acquire Copper: An Essential but Potentially Toxic Metal. *Biophysical Journal*, 110(1):7–13, 2016.

[216] C. Kasbek, C. H. Yang, and H. A. Fisk. Mps1 as a link between centrosomes and genomic instability. *Environmental and Molecular Mutagenesis*, 50(8):654–665, 2009.

[217] A. M. Katz, D. Rosenthal, and D. N. Sauder. Cell Adhesion Molecules. *International Journal of Dermatology*, 30(3):153–160, 1991. mar.

[218] R. Kenerson. Cell Culture Medium Comprising Transition Metals or Trace Elements. (WO 2006/004728 A2), 2005.

[219] J. S. Khillan. Vitamin A/retinol and maintenance of Pluripotency of stem cells. *Nutrients*, 6(3):1209–1222, 2014.

[220] S. Kiesslich, G. N. Kim, C. F. Shen, C. Y. Kang, and A. A. Kamen. Bioreactor production of rVSV-based vectors in Vero cell suspension cultures. *Biotechnology and Bioengineering*, 118(7):2649–2659, 2021.

[221] S. Kiesslich, J. P. Vila-Chã Losa, J.-F. F. Gélinas, and A. A. Kamen. Serum-free production of rVSV-ZEBOV in Vero cells: Microcarrier bioreactor versus scale-X hydro fixed-bed. *Journal of Biotechnology*, 310(October 2019):32–39, 2020. feb.

[222] D. Y. Kim, J. C. Lee, H. N. Chang, and D. J. Oh. Effects of supplementation of various medium components on Chinese hamster ovary cell cultures producing recombinant antibody. *Cytotechnology*, 47(1-3):37–49, 2005.

[223] E. Kim, H. Ahn, M. G. Kim, H. Lee, and S. Kim. The expanding significance of inositol polyphosphate multikinase as a signaling hub. *Molecules and Cells*, 40(5):315–321, 2017.

[224] J. H. Kim, S. Ham, Y. S. Lee, G. Y. Suh, and Y. S. Lee. TTC3 contributes to TGF-β 1 -induced epithelialmesenchymal transition and myofibroblast differentiation, potentially through SMURF2 ubiquitylation and degradation. *Cell Death and Disease*, 10(2), 2019.

[225] N. S. Kim and G. M. Lee. Response of recombinant Chinese hamster ovary cells to hyperosmotic pressure: Effect of Bcl-2 overexpression. *Journal of Biotechnology*, 95(3):237–248, 2002.

[226] A. F. Kisselev, Z. Songyang, and A. L. Goldberg. Why does threonine, and not serine, function as the active site nucleophile in proteasomes? *Journal of Biological Chemistry*, 275(20):14831–14837, 2000.

[227] R. B. Klassen, K. Crenshaw, R. Kozyraki, P. J. Verroust, L. Tio, S. Atrian, P. L. Allen, and T. G. Hammond. Megalin mediates renal uptake of heavy metal metallothionein complexes. *American Journal of Physiology-Renal Physiology*, 287(3):F393–F403, 2004. sep.

[228] G. G. Klee. Cobalamin and Folate Evaluation: Measurement of Methylmalonic Acid and Homocysteine vs Vitamin B12 and Folate. *Clinical Chemistry*, 46(8):1277–1283, 2000. aug.

[229] S. Kluge, D. Benndorf, K. Scharfenberg, E. Rapp, and U. Reichl. Monitoring changes in proteome during stepwise adaptation of a MDCK cell line from adherence to growth in suspension. *Vaccine*, 33(35):4269–4280, 2015.

[230] A. Knedler and R. G. Ham. Optimized medium for clonal growth of human microvascular endothelial cells with minimal serum. *In Vitro Cellular Developmental Biology*, 23(7):481–491, 1987. jul.

[231] M. Kobayashi and S. Shimizu. Cobalt proteins. *European Journal of Biochemistry*, 261(1):1–9, 1999.

[232] C. M. Koch, S. F. Chiu, M. Akbarpour, A. Bharat, K. M. Ridge, E. T. Bartom, and D. R. Winter. A Beginner ' s Guide to Analysis of RNA Sequencing Data. *Am J Respir Cell Mol Biol*, 59(2):145–157, 2018.

[233] K. Kolell, J. Padilla-Zamudio, B. Schuchhardt, S. Gilliland, B. McNorton, S. Luo, and K. Etchberger. Virus Production in Vero Cells Using a Serum-Free Medium. *Cell Technology for Cell Products*, pages 583–585, 2007.

[234] I. M. Kolthoff and A. I. Medalia. The Reaction between Ferrous Iron and Peroxides. I. Reaction with Hydrogen Peroxide in the Absence of Oxygen. *Journal of the American Chemical Society*, 71(11):3777–3783, 1949.

[235] G. J. Kontoghiorghes. 2-Hydroxypyridine-N-oxides: Effective new chelators in iron mobilisation. *BBA - General Subjects*, 924(1):13–18, 1987.

[236] A. S. Krall, S. Xu, T. G. Graeber, D. Braas, and H. R. Christofk. Asparagine promotes cancer cell proliferation through use as an amino acid exchange factor. *Nature Communications*, 7:1–13, 2016.

[237] R. H. Kretsinger, V. N. Uversky, and E. A. Permyakov, editors. *Encyclopedia of Metalloproteins*. Number Ii. Springer New York, New York, NY, 2013.

[238] J. Kubilus, R. Rand, and H. P. Baden. Effects of Retinoic Acid and Other Retinoids on the Growth and Differentiation of 3T3 Supported Human Keratinicytes. *In Vitro*, 17(9):786–795, 1981. may.

[239] M. Kulkarni, A. Flašker, M. Lokar, K. Mrak-Poljšak, A. Mazare, A. Artenjak, S. Čučnik, S. Kralj, A. Velikonja, P. Schmuki, V. Kralj-Iglič, S. Sodin-Semrl, and A. Iglič. Binding of plasma proteins to titanium dioxide nanotubes with different diameters. *International Journal of Nanomedicine*, 10:1359–1373, 2015.

[240] N. Kurano, C. Leist, F. Messi, S. Kurano, and A. Fiechter. Growth behavior of Chinese hamster ovary cells in a compact loop bioreactor: 1. Effects of physical and chemical environments. *Journal of Biotechnology*, 15(1-2):101–111, 1990.

[241] M. Laires, C. Monteiro, and M. Bicho. Role of cellular magnesium in health and human disease. *Frontiers in Bioscience*, 9(1-3):262, 2004.

[242] S. Lamouille, J. Xu, and R. Derynck. Molecular mechanisms of epithelial-mesenchymal transition. *Nature Reviews Molecular Cell Biology*, 15(3):178–196, 2014.

[243] G. Landau, Z. Bercovich, M. H. Park, and C. Kahana. The role of polyamines in supporting growth of mammalian cells is mediated through their requirement for translation initiation and elongation. *Journal of Biological Chemistry*, 285(17):12474–12481, 2010.

[244] A. N. Lane and T. W. M. Fan. Regulation of mammalian nucleotide metabolism and biosynthesis. *Nucleic Acids Research*, 43(4):2466–2485, 2015.

[245] A. B. G. Lansdown. A Pharmacological and Toxicological Profile of Silver as an Antimicrobial Agent in Medical Devices. *Advances in Pharmacological Sciences*, 2010(9):1–16, 2010.

[246] T. M. Larson, M. Gawlitzek, H. Evans, U. Albers, and J. Cacia. Chemometric evaluation of on-line high-pressure liquid chromatography in mammalian cell cultures: Analysis of amino acids and glucose. *Biotechnology and Bioengineering*, 77(5):553–563, 2002.

[247] F. Le Borgne, A. Ben Mohamed, M. Logerot, E. Garnier, and J. Demarquoy. Changes in carnitine octanoyltransferase activity induce alteration in fatty acid metabolism. *Biochemical and Biophysical Research Communications*, 409(4):699–704, 2011. jun.

[248] D. K. Lee, J. Park, and D. W. Seo. Suspension culture of vero cells for the production of adenovirus type 5. *Clinical and Experimental Vaccine Research*, 9(1):48–55, 2020.

[249] G. M. Lee, E. J. Kim, N. S. Kim, S. K. Yoon, Y. H. Ahn, J. Y. Song, G. Min, E. Jung, N. Soo, and S. Kwan. Development of a serum-free medium for the production of erythropoietin by suspension culture of recombinant Chinese hamster ovary cells using a statistical design. *Journal of Biotechnology*, 69:85–93, 1999.

[250] H. C. Lee, Y. T. Yen, W. Y. Chen, B. A. Wu-Hsieh, and S. C. Wu. Dengue type 4 live-attenuated vaccine viruses passaged in Vero cells affect genetic stability and dengue-induced hemorrhaging in mice. *PLoS ONE*, 6(10), 2011.

[251] J. W. Lee, C. L. Chou, and M. A. Knepper. Deep sequencing in microdissected renal tubules identifies nephron segment-specific transcriptomes. *Journal of the American Society of Nephrology*, 26(11):2669–2677, 2015.

[252] N. Lee, J. Shin, J. H. Park, G. M. Lee, S. Cho, and B.-K. Cho. Targeted Gene Deletion Using DNA-Free RNA-Guided Cas9 Nuclease Accelerates Adaptation of CHO Cells to Suspension Culture. *ACS Synthetic Biology*, 5(11):1211–1219, 2016. nov.

[253] A. Leibovitz. Preparation of medium L-15. *Tissue Culture Association Manual*, 3(2):557–559, 1977.

[254] C. Leist, P. Meissner, and J. Schmidt. Improved Cell Culture Medium. 2013.

[255] R. H. Lenox and L. Wang. Molecular basis of lithium action: Integration of lithium-responsive signaling and gene expression networks. *Molecular Psychiatry*, 8(2):135–144, 2003.

[256] R. Leonardi and S. Jackowski. Biosynthesis of Pantothenic Acid and Coenzyme A. *EcoSal Plus*, 2(2):1–28, 2007.

[257] C. Y. Leung-Hagesteijn, K. Milankov, M. Michalak, J. Wilkins, and S. Dedhar. Cell attachment to extracellular matrix substrates is inhibited upon downregulation of expression of calreticulin, an intracellular integrin alpha-subunit-binding protein. *Journal of cell science*, 107 (Pt 3:589–600, 1994.

[258] B. Li and C. N. Dewey. RSEM: accurate transcript quantification from RNA-Seq data with or without a reference genome. *BMC Bioinformatics*, 12(1):323, 2011.

[259] L. Li, L. Song, X. Liu, X. Yang, X. Li, T. He, N. Wang, S. Yang, C. Yu, T. Yin, Y. Wen, Z. He, X. Wei, W. Su, Q. Wu, S. Yao, C. Gong, and Y. Wei. Artificial Virus Delivers CRISPR-Cas9 System for Genome Editing of Cells in Mice. *ACS Nano*, 11(1):95–111, 2017.

[260] L. Li and X. Yang. The Essential Element Manganese, Oxidative Stress, and Metabolic Diseases: Links and Interactions. *Oxidative Medicine and Cellular Longevity*, 2018:7580707, 2018.

[261] Z. Li, J. Wu, L. Wang, W. Han, J. Yu, X. Liu, Y. Wang, Y. Zhang, G. Feng, W. Li, G. N. Stacey, Q. Gu, B. Hu, L. Wang, Q. Zhou, and J. Hao. Generation of qualified clinical-grade functional hepatocytes from human embryonic stem cells in chemically defined conditions. *Cell Death Disease*, 10(10):763, 2019. oct.

[262] M. Lidén and U. Eriksson. Understanding retinol metabolism: Structure and function of retinol dehydrogenases. *Journal of Biological Chemistry*, 281(19):13001–13004, 2006.

[263] M. Liesa, W. Qiu, and O. S. Shirihai. Mitochondrial ABC transporters function: The role of ABCB10 (ABC-me) as a novel player in cellular handling of reactive oxygen species. *Biochimica et Biophysica Acta (BBA) - Molecular Cell Research*, 1823(10):1945–1957, 2012. oct.

[264] C. K. Lim, T. Takasaki, A. Kotaki, and I. Kurane. Vero cell-derived inactivated West Nile (WN) vaccine induces protective immunity against lethal WN virus infection in mice and shows a facilitated neutralizing antibody response in mice previously immunized with Japanese encephalitis vaccine. *Virology*, 374(1):60–70, 2008.

[265] D. Lim, K. M. X. Jocelyn, G. W. C. Yip, and B. H. Bay. Silencing the Metallothionein-2A gene inhibits cell cycle progression from G1- to S-phase involving ATM and cdc25A signaling in breast cancer cells. *Cancer Letters*, 276(1):109–117, 2009.

[266] W. L. Ling. Development of protein-free medium for therapeutic protein production in mammalian cells: recent advances and perspectives. *Pharmaceutical Bioprocessing*, 3(3):215–226, 2015.

[267] S. J. Lippard. Free Copper Ions in the Cell? *Science*, 284(5415):748–749, 1999. apr.

[268] G. Litwack. Membrane Transport. In *Human Biochemistry*, chapter 18, pages 553–589. 2018.

[269] J. Litwin. The growth of Vero cells in suspension as cell-aggregates in serum-free media. *Cytotechnology*, 10(2):169–174, 1992.

[270] G. Liu, Y. Jiang, P. Wang, R. Feng, N. Jiang, X. Chen, H. Song, and Z. Chen. Cell adhesion molecules contribute to Alzheimer's disease: Multiple pathway analyses of two genome-wide association studies. *Journal of Neurochemistry*, 120(1):190–198, 2012.

[271] M. Lobigs, M. Pavy, R. A. Hall, P. Lobigs, P. Cooper, T. Komiya, H. Toriniwa, and N. Petrovsky. An inactivated Vero cell-grown Japanese encephalitis vaccine formulated with Advax, a novel inulin-based adjuvant, induces protective neutralizing antibody against homologous and heterologous flaviviruses. *Journal of General Virology*, 91(6):1407–1417, 2010. jun.

[272] H. Lodish, A. Berk, and S. Zipurksy. Intracellular Ion Environment and Membrane Electric Potential. In *Molecular Cell Biology*, chapter 15.4. W.H. Freeman, 4 edition, 2000.

[273] H. Lodish, A. Berk, S. Zipursky, P. Matsudaira, D. Baltimore, and J. Darnel. Cell-Cell Adhesion and Communication. In *Molecular Cell Biology*, volume 29, chapter 22.1, pages 126–128. W.H. Freeman, New York, New York, 4 edition, 2000.

[274] D. Lonsdale. A review of the biochemistry, metabolism and clinical benefits of thiamin(e) and its derivatives. *Evidence-based Complementary and Alternative Medicine*, 3(1):49–59, 2006.

[275] H. S. Loring, J. L. Fairley, and H. L. Seagran. The purine and pyrimidine composition of yeast ribonucleic acid. *The Journal of Biological Chemistry*, 197(2):823–30, 1952. may.

[276] C. Lorz. Trail and kidney disease. *Frontiers in Bioscience*, Volume(14):3740, 2009.

[277] S. Lovisa and R. Kalluri. Fatty Acid Oxidation Regulates the Activation of Endothelial-to-Mesenchymal Transition. *Trends in Molecular Medicine*, 24(5):432–434, 2018.

[278] R. Lowe, N. Shirley, M. Bleackley, S. Dolan, and T. Shafee. Transcriptomics technologies. *PLoS Computational Biology*, 13(5):1–23, 2017.

[279] J. M. Lü, P. H. Lin, Q. Yao, and C. Chen. Chemical and molecular mechanisms of antioxidants: Experimental approaches and model systems. *Journal of Cellular and Molecular Medicine*, 14(4):840–860, 2010.

[280] W. Luo and C. Brouwer. Pathview: An R/Bioconductor package for pathway-based data integration and visualization. *Bioinformatics*, 29(14):1830–1831, 2013.

[281] R. S. MacDonald. The Role of Zinc in Growth and Cell Proliferation. *The Journal of Nutrition*, 130(5):1500S–1508S, 2000. may.

[282] A. MacFie, E. Hagan, and A. Zhitkovich. Mechanism of DNA-protein cross-linking by chromium. *Chemical Research in Toxicology*, 23(2):341–347, 2010.

[283] L. Magtanong, P. J. Ko, and S. J. Dixon. Emerging roles for lipids in non-apoptotic cell death. *Cell Death and Differentiation*, 23(7):1099–1109, 2016.

[284] W. Mai, D. Chen, T. Ding, I. Kim, S. Park, S.-y. Cho, J. S. F. Chu, D. Liang, N. Wang, D. Wu, S. Li, P. Zhao, R. Zent, and G. Wu. Inhibition of Pkhd1 Impairs Tubulomorphogenesis of Cultured IMCD Cells. *Molecular Biology of the Cell*, 16(9):4398–4409, 2005. sep.

[285] M. Malm, R. Saghaleyni, M. Lundqvist, M. Giudici, V. Chotteau, R. Field, P. Varley, D. Hatton, L. Grassi, T. Svensson, M. Uhlen, J. Nielsen, and J. Rockberg. Evolution

from adherent to suspension systems biology of HEK293 cell line development. *bioRxiv*, page 2020.01.29.924894, 2020.

[286] N. Mandal, D. Bhattacharjee, J. K. Rout, A. Dasgupta, G. Bhattacharya, C. Sarkar, and P. K. Gangopadhyaya. Effect of Copper on l-Cysteine/l-Cystine Influx in Normal Human Erythrocytes and Erythrocytes of Wilson's Disease. *Indian Journal of Clinical Biochemistry*, 31(4):468–472, 2016.

[287] S. Mandal, A. Mandal, H. E. Johansson, A. V. Orjalo, and M. H. Park. Depletion of cellular polyamines, spermidine and spermine, causes a total arrest in translation and growth in mammalian cells. *Proceedings of the National Academy of Sciences*, 110(6):2169–2174, 2013.

[288] E. Mangiapane, A. Pessione, and E. Pessione. Selenium and Selenoproteins: An Overview on Different Biological Systems. *Current Protein Peptide Science*, 15(6):598–607, 2014. jun.

[289] K. C. Manthey, Y. C. Chew, and J. Zempleni. Riboflavin Deficiency Impairs Oxidative Folding and Secretion of Apolipoprotein B-100 in HepG2 Cells, Triggering Stress Response Systems. *The Journal of Nutrition*, 135(5):978–982, 2005.

[290] S. Manzetti, J. Zhang, and D. Van Der Spoel. Thiamin function, metabolism, uptake, and transport. *Biochemistry*, 53(5):821–835, 2014.

[291] J. L. Markley, R. Brüschweiler, A. S. Edison, H. R. Eghbalnia, R. Powers, D. Raftery, and D. S. Wishart. The future of NMR-based metabolomics. *Current Opinion in Biotechnology*, 43:34–40, 2017.

[292] D. Marreiro, K. Cruz, J. Morais, J. Beserra, J. Severo, and A. de Oliveira. Zinc and Oxidative Stress: Current Mechanisms. *Antioxidants*, 6(2):24, 2017.

[293] A. S. Martínez-Ramírez, M. Díaz-Muñoz, A. Butanda-Ochoa, and F. G. Vázquez-Cuevas. Nucleotides and nucleoside signaling in the regulation of the epithelium to mesenchymal transition (EMT). *Purinergic Signalling*, 13(1):1–12, 2017.

[294] J. P. Mather and P. E. Roberts. Media. In *Introduction to Cell and Tissue Culture*, pages 41–62. Springer US, Boston, MA, 2007.

[295] J. P. Mather and M. C. Tsao. Method for culturing Chinese hamster ovary cells to improve production of recombinant proteins. (US 5122469 A), 1992.

[296] R. A. Mathias, B. Wang, H. Ji, E. A. Kapp, R. L. Moritz, H. J. Zhu, and R. J. Simpson. Secretome-based proteomic profiling of Ras-transformed MDCK cells reveals extracellular modulators of epithelial-mesenchymal transition. *Journal of Proteome Research*, 8(6):2827–2837, 2009.

[297] D. A. Mattos, M. V. Silva, L. P. Gaspar, and L. R. Castilho. Increasing Vero viable cell densities for yellow fever virus production in stirred-tank bioreactors using serum-free medium. *Vaccine*, 33(35):4288–4291, 2015.

[298] F. R. Maxfield and D. Wüstner. Intracellular cholesterol transport. *Journal of Clinical Investigation*, 110(7):891–898, 2002. oct.

[299] J. M. May, Z. chao Qu, and X. Li. Requirement for GSH in recycling of ascorbic acid in endothelial cells. *Biochemical Pharmacology*, 62(7):873–881, 2001.

[300] A. S. McCall, C. F. Cummings, G. Bhave, R. Vanacore, A. Page-Mccaw, and B. G. Hudson. Bromine is an essential trace element for assembly of collagen IV scaffolds in tissue development and architecture. *Cell*, 157(6):1380–1392, 2014.

[301] K. A. McCall, C.-c. Huang, and C. A. Fierke. Function and Mechanism of Zinc Metalloenzymes. *The Journal of Nutrition*, 130(5):1437S–1446S, 2000.

[302] D. B. McCormick. Vitamin B6 transport and metabolism: Clues for delivery of bioactive compounds. *Biochemistry of Vitamin B6 and PQQ*, pages 311–317, 1994.

[303] M. G. McCoy, G. S. Sun, D. Marchadier, C. Maugeais, J. M. Glick, and D. J. Rader. Characterization of the lipolytic activity of endothelial lipase. *Journal of Lipid Research*, 43(6):921–929, 2002.

[304] N. McGillicuddy, P. Floris, S. Albrecht, and J. Bones. Examining the sources of variability in cell culture media used for biopharmaceutical production. *Biotechnology Letters*, 40(1):5–21, 2018.

[305] C. McInnes and B. D. Sykes. Growth factor receptors: structure, mechanism, and drug discovery. *Biopolymers*, 43(5):339–66, 1997.

[306] W. L. McKeehan, W. G. Hamilton, and R. G. Ham. Selenium is an essential trace nutrient for growth of WI-38 diploid human fibroblasts. *Proceedings of the National Academy of Sciences of the United States of America*, 73(6):2023–2027, 1976.

[307] S. R. McKeown. Defining normoxia, physoxia and hypoxia in tumours - Implications for treatment response. *British Journal of Radiology*, 87(1035):1–12, 2014.

[308] J. R. N. McLean, D. H. Blakey, G. R. Douglas, and J. G. Kaplan. The effect of stannous and stannic (tin) chloride on DNA in Chinese hamster ovary cells. *Mutation Research Letters*, 119(2):195–201, 1983.

[309] W. T. McQuilkin, V. J. Evans, and W. R. Earle. The adaptation of additional lines of NCTC clone 929(strain L) cells to chemically defined protein-free medium NCTC 109. *Journal of the National Cancer Institute*, 19(5):885–907, 1957. nov.

[310] J. Medina, V. Guillot, E. Totain, M. Rouleau, R. Sodoyer, C. Moste, and I. Legastelois. Vero/CHOK1, a novel mixture of cell lines that is optimal for the rescue of influenza A vaccine seeds. *Journal of Virological Methods*, 196:25–31, 2014.

[311] P. Meissner, H. Pick, A. Kulangara, P. Chatellard, K. Friedrich, and F. M. Wurm. Transient gene expression: Recombinant protein production with suspension-adapted HEK293-EBNA cells. *Biotechnology and Bioengineering*, 75(2):197–203, 2001.

[312] R. R. Mendel. The Molybdenum Cofactor. *Journal of Biological Chemistry*, 288(19):13165–13172, 2013. may.

[313] R. R. Mendel and F. Bittner. Cell biology of molybdenum. *Biochimica et Biophysica Acta - Molecular Cell Research*, 1763(7):621–635, 2006.

[314] R. Z. Mendonça, S. J. Arrózio, M. M. Antoniazzi, J. M. C. Ferreira, and C. A. Pereira. Metabolic active-high density Vero cell cultures on microcarriers following apoptosis prevention by galactose/glutamine feeding. *Journal of Biotechnology*, 97(1):13–22, 2002. jul.

[315] R. Z. Mendonça and C. A. Pereira. High density Vero cell culture on microcarriers in a cell bioreactor. *Bioprocess Engineering*, 12(6):279–282, 1995.

[316] R. Z. Mendonça, C. A. Pereira, R. Z. Medonça, and C. A. Pereira. Cell metabolism and medium perfusion in VERO cell cultures on microcarriers in a bioreactor. *Bioprocess Engineering*, 18(3):213–218, 1998.

[317] A. Mendoza-Schulz, C. Solano-Agama, L. Arreola-Mendoza, B. Reyes-Márquez, O. Barbier, L. M. Del Razo, and M. E. Mendoza-Garrido. The effects of fluoride on cell migration, cell proliferation, and cell metabolism in GH4C1 pituitary tumour cells. *Toxicology Letters*, 190(2):179–186, 2009.

[318] Y. Meng, Z. Ren, F. Xu, X. Zhou, C. Song, V. Y. F. Wang, W. Liu, L. Lu, J. A. Thomson, and G. Chen. Nicotinamide Promotes Cell Survival and Differentiation as Kinase Inhibitor in Human Pluripotent Stem Cells. *Stem Cell Reports*, 11(6):1347–1356, 2018.

[319] J. J. Meredith, S. I. M. Winitz, J. M. Lewis, S. Hess, X.-d. Ren, M. W. Renshaw, and M. A. Schwartz. The Regulation of Growth and Intracellular Signaling by Integrins. *Endocrine Reviews*, 17(3):207–220, 1996. jun.

[320] D. Merico, R. Isserlin, O. Stueker, A. Emili, and G. D. Bader. Enrichment map: A network-based method for gene-set enrichment visualization and interpretation. *PLoS ONE*, 5(11), 2010.

[321] O. W. Merten, R. Wu, E. Couve, and R. Crainic. Evaluation of the serum-free medium MDSS2 for the production of poliovirus on vero cells in bioreactors. *Cytotechnology*, 25(1-3):35–44, 1997.

[322] J. F. Michiels, J. Barbau, S. De Boel, S. Dessy, S. N. Agathos, and Y. J. Schneider. Characterisation of beneficial and detrimental effects of a soy peptone, as an additive for CHO cell cultivation. *Process Biochemistry*, 46(3):671–681, 2011.

[323] W. L. Miller. Steroid hormone synthesis in mitochondria. *Molecular and Cellular Endocrinology*, 379(1-2):62–73, 2013.

[324] L. Miller-Fleming, V. Olin-Sandoval, K. Campbell, and M. Ralser. Remaining Mysteries of Molecular Biology: The Role of Polyamines in the Cell. *Journal of Molecular Biology*, 427(21):3389–3406, 2015.

[325] G. Minotti and S. D. Aust. The requirement for iron (III) in the initiation of lipid peroxidation by iron (II) and hydrogen peroxide. *Journal of Biological Chemistry*, 262(3):1098–1104, 1987.

[326] A. Mohammed Nawi, S. F. Chin, and R. Jamal. Simultaneous analysis of 25 trace elements in micro volume of human serum by inductively coupled plasma mass spectrometry (ICP-MS). *Practical Laboratory Medicine*, 18(February 2019):e00142, 2020.

[327] B. J. Montagnon. Polio and rabies vaccines produced in continuous cell lines: a reality for Vero cell line. *Developments in biological standardization*, 70:27–47, 1989.

[328] B. J. Montagnon, B. Fanget, and J. C. Vincent-Falquet. Industrial-Scale Production of Inactivated Poliovirus Vaccine Prepared by Culture of Vero Cells on Microcarrier. *Clinical Infectious Diseases*, 6(Supplement 2):S341–S344, 1984. may.

[329] V. Montecinos, P. Guzmán, V. Barra, M. Villagrán, C. Muñoz-Montesino, K. Sotomayor, E. Escobar, A. Godoy, L. Mardones, P. Sotomayor, C. Guzmán, O. Vásquez, V. Gallardo, B. Van Zundert, M. R. Bono, S. A. Oñate, M. Bustamante, J. G. Cárcamo, C. I. Rivas, and J. C. Vera. Vitamin C is an essential antioxidant that enhances survival of oxidatively stressed human vascular endothelial cells in the presence of a vast molar excess of glutathione. *Journal of Biological Chemistry*, 282(21):15506–15515, 2007.

[330] G. E. Moore and L. K. Woods. Culture media for human cells-RPMI 1603, RPMI 1634, RPMI 1640 and GEM 1717. *Tissue Culture Association Manual*, 3(1):503–509, 1977.

[331] M. Morales-Ruiz, D. Fulton, G. Sowa, L. R. Languino, Y. Fujio, K. Walsh, W. C. Sessa, and S. Elizabeth'. Vascular Endothelial Growth Factor-Stimulated Actin Reorganization and Migration of Endothelial Cells Is Regulated via the Serine/Threonine Kinase Akt. *Circulation Research*, 86(8):892–896, 2000. apr.

[332] J. F. Morgan, M. Elizabeth Campbell, and H. J. Morton. The nutrition of animal tissues cultivated in vitro. i. a survey of natural materials as supplements to synthetic medium 199. *Journal of the National Cancer Institute*, 16(2):557–567, 1955.

[333] S. M. Morris. Enzymes of arginine metabolism. *The Journal of Nutrition*, 134(July):2743S–2747S; discussion 2765S–2767S, 2004.

[334] H. J. Morton. A survey of commercially available tissue culture media. *In Vitro*, 6(2):89–108, 1970.

[335] S. A. Mousa. Cell adhesion molecules: Potential therapeutic diagnostic implications. *Molecular Biotechnology*, 38(1):33–40, 2008.

[336] S. Murad, D. Grove, K. A. Lindberg, G. Reynolds, A. Sivarajah, and S. R. Pinnell. Regulation of collagen synthesis by ascorbic acid. *Proceedings of the National Academy of Sciences*, 78(5):2879–2882, 1981.

[337] S. Nagamori, P. Wiriyasermkul, M. E. Guarch, H. Okuyama, S. Nakagomi, K. Tadagaki, Y. Nishinaka, S. Bodoy, K. Takafuji, S. Okuda, J. Kurokawa, R. Ohgaki, V. Nunes, M. Palacín, and Y. Kanai. Novel cystine transporter in renal proximal

tubule identified as a missing partner of cystinuria-related plasma membrane protein rBAT/SLC3A1. *Proceedings of the National Academy of Sciences of the United States of America*, 113(3):775–780, 2016.

[338] K. Nagira, T. Hara, M. Hayashida, K. Osada, M. Shiga, K. Sasamoto, K. Kina, and H. Murakami. Development of a protein-free medium with iron salts replacing transferrin for a human-human hybridoma. *Bioscience, Biotechnology and Biochemistry*, 59(4):743–745, 1995. apr.

[339] A. T. Nahapetian, J. N. Thomas, and W. G. Thilly. Optimization of environment for high density Vero cell culture: effect of dissolved oxygen and nutrient supply on cell growth and changes in metabolites. *Journal of Cell Science*, 81:65–103, 1986.

[340] K. Nakahara, A. Ohkuni, T. Kitamura, K. Abe, T. Naganuma, Y. Ohno, R. A. Zoeller, and A. Kihara. The Sjögren-Larsson Syndrome Gene Encodes a Hexadecenal Dehydrogenase of the Sphingosine 1-Phosphate Degradation Pathway. *Molecular Cell*, 46(4):461–471, 2012.

[341] P. Newsholme, J. Procopio, M. M. Ramos Lima, T. C. Pithon-Curi, and R. Curi. Glutamine and glutamate - Their central role in cell metabolism and function. *Cell Biochemistry and Function*, 21(1):1–9, 2003.

[342] F. H. Nielsen. Ultra Trace Elements in Nutrition. *Annual Reviews Nutrition*, 4:21–41, 1984.

[343] A. W. Nienow. Reactor engineering in large scale animal cell culture. *Cytotechnology*, 50(1-3):9–33, 2006.

[344] E. Niki. Role of vitamin E as a lipid-soluble peroxyl radical scavenger: in vitro and in vivo evidence. *Free Radical Biology and Medicine*, 66:3–12, 2014. jan.

[345] K. Nilausen. Role of fatty acids in growth-promoting effect of serum albumin on hamster cells in vitro. *Journal of Cellular Physiology*, 96(1):1–13, 1978. jul.

[346] D. K. Nomura, J. Z. Long, S. Niessen, H. S. Hoover, S.-W. Ng, and B. F. Cravatt. Monoacylglycerol Lipase Regulates a Fatty Acid Network that Promotes Cancer Pathogenesis. *Cell*, 140(1):49–61, 2010. jan.

[347] S. Norouzi, J. Adulcikas, S. S. Sohal, and S. Myers. Zinc stimulates glucose oxidation and glycemic control by modulating the insulin signaling pathway in human and mouse skeletal muscle cell lines. pages 1–15, 2018.

[348] R. M. Novick, A. M. Mitzey, M. S. Brownfield, and A. A. Elfarra. Differential localization of flavin-containing monooxygenase (FMO) isoforms 1, 3, and 4 in rat liver and kidney and evidence for expression of FMO4 in mouse, rat, and human liver and kidney microsomes. *Journal of Pharmacology and Experimental Therapeutics*, 329(3):1148–1155, 2009.

[349] N. Noy. Vitamin A Transport and Cell Signaling by the Retinol-Binding Protein Receptor STRA6. In *Subcell Biochem.*, volume 81, pages 77–93. 2016.

[350] M. Oehlmann, A. J. Score, and J. J. Blow. The role of Cdc6 in ensuring complete genome licensing and S phase checkpoint activation. *Journal of Cell Biology*, 165(2):181–190, 2004.

[351] R. O'Flaherty, A. Bergin, E. Flampouri, L. M. Mota, I. Obaidi, A. Quigley, Y. Xie, and M. Butler. Mammalian cell culture for production of recombinant proteins: A review of the critical steps in their biomanufacturing. *Biotechnology Advances*, 43(May):107552, 2020.

[352] Y. Ogra, A. Tejima, N. Hatakeyama, M. Shiraiwa, S. Wu, T. Ishikawa, A. Yawata, Y. Anan, and N. Suzuki. Changes in intracellular copper concentration and copper-regulating gene expression after PC12 differentiation into neurons. *Scientific Reports*, 6(June):1–9, 2016.

[353] S. M. Oredsson. Polyamine dependence of normal cell-cycle progression. *Biochemical Society Transactions*, 31(2):366–370, 2003.

[354] S. Orrenius, B. Zhivotovsky, and P. Nicotera. Regulation of cell death: The calcium-apoptosis link. *Nature Reviews Molecular Cell Biology*, 4(7):552–565, 2003.

[355] N. Osada, A. Kohara, T. Yamaji, N. Hirayama, F. Kasai, T. Sekizuka, M. Kuroda, and K. Hanada. The genome landscape of the african green monkey kidney-derived vero cell line. *DNA research : an international journal for rapid publication of reports on genes and genomes*, 21(6):673–683, 2014.

[356] T. R. Osborne. *A role for vitamin K-dependent proteins in ubiquitination and signal transduction*. PhD thesis, University of Washington, 2005.

[357] J. E. Osorio, J. N. Brewoo, S. J. Silengo, J. Arguello, I. R. Moldovan, M. Tary-Lehmann, T. D. Powell, J. A. Livengood, R. M. Kinney, C. Y. H. Huang, and D. T. Stinchcomb. Efficacy of a tetravalent chimeric dengue vaccine (DENVax) in cynomolgus macaques. *American Journal of Tropical Medicine and Hygiene*, 84(6):978–987, 2011.

[358] K. Øyaas, T. E. Ellingsen, N. Dyrset, and D. W. Levine. Hyperosmotic hbridoma cell cultures: Increased monoclonal antibody production with addition of glycine betaine. *Biotechnology and Bioengineering*, 44(8):991–998, 1994. oct.

[359] S. S. Ozturk. Engineering challenges in high density cell culture systems. *Cytotechnology*, 22(1-3):3–16, 1996.

[360] S. S. Ozturk, C. Maintenance, G. Laboratories, and P. Systems. Effect of Medium Osmolarity on Hybridoma Growth, Metabolism, and Antibody Production. *Biotechnology and Bioengineering*, 37(April):989–993, 1991.

[361] H. Padh. Cellular functions of ascorbic acid. *Biochemistry and Cell Biology*, 68(10):1166–1173, 1990.

[362] M. Pagano. Control of DNA synthesis and mitosis by the Skp2-p27-Cdk1/2 axis. *Molecular Cell*, 14(4):414–416, 2004.

[363] C. Paillet, G. Forno, R. Kratje, and M. Etcheverrigaray. Suspension-Vero cell cultures as a platform for viral vaccine production. *Vaccine*, 27(46):6464–6467, 2009.

[364] C. Paillet, G. Forno, N. Soldano, R. Kratje, and M. Etcheverrigaray. Statistical optimization of influenza H1N1 production from batch cultures of suspension Vero cells (sVero). *Vaccine*, 29(41):7212–7217, 2011.

[365] S. Pamarthy, A. Kulshrestha, G. K. Katara, and K. D. Beaman. The curious case of vacuolar ATPase: Regulation of signaling pathways. *Molecular Cancer*, 17(1):1–9, 2018.

[366] X. Pan, M. Streefland, C. Dalm, R. H. Wijffels, and D. E. Martens. Selection of chemically defined media for CHO cell fed-batch culture processes. *Cytotechnology*, 69(1):39–56, 2017.

[367] A. Parampalli, K. Eskridge, L. Smith, M. M. Meagher, M. C. Mowry, and A. Subramanian. Developement of serum-free media in CHO-DG44 cells using a central composite statistical design. *Cytotechnology*, 54(1):57–68, 2007.

[368] R. Parker, L. Castor, and E. McCulloch. Altered Cell Strains In Continuous Culture: A General Survey In Special Publications of the New York Academy of Sciences. pages 303–313. New York Academy of Sciences, 1957.

[369] M. Parra, S. Stahl, and H. Hellmann. Vitamin B6 and Its Role in Cell Metabolism and Physiology. *Cells*, 7(7):84, 2018.

[370] A. Parthasarathy, P. J. Cross, R. C. J. Dobson, L. E. Adams, M. A. Savka, and A. O. Hudson. A Three-Ring circus: Metabolism of the three proteogenic aromatic amino acids and their role in the health of plants and animals. *Frontiers in Molecular Biosciences*, 5(APR):1–30, 2018.

[371] R. L. Patterson, D. B. Van Rossum, N. Nikolaidis, D. L. Gill, and S. H. Snyder. Phospholipase C-γ: Diverse roles in receptor-mediated calcium signaling. *Trends in Biochemical Sciences*, 30(12):688–697, 2005.

[372] S. Pech, M. Rehberg, R. Janke, D. Benndorf, Y. Genzel, T. Muth, A. Sickmann, E. Rapp, and U. Reichl. Tracking changes in adaptation to suspension growth for MDCK cells: cell growth correlates with levels of metabolites, enzymes and proteins. *Applied Microbiology and Biotechnology*, 105(5):1861–1874, 2021.

[373] A. E. Pegg. Regulation of ornithine decarboxylase. *Journal of Biological Chemistry*, 281(21):14529–14532, 2006.

[374] A. E. Pegg and P. P. McCann. Polyamine metabolism and function. *American Journal of Physiology-Cell Physiology*, 243(5):C212–C221, 1982. nov.

[375] D. Pei, X. Shu, A. Gassama-Diagne, and J. P. Thiery. Mesenchymalepithelial transition in development and reprogramming. *Nature Cell Biology*, 21(1):44–53, 2019. jan.

[376] T. Peled, E. Landau, J. Mandel, E. Glukhman, N. R. Goudsmid, A. Nagler, and E. Fibach. Linear polyamine copper chelator tetraethylenepentamine augments long-term ex vivo expansion of cord blood-derived CD34+cells and increases their engraftment potential in NOD/SCID mice. *Experimental Hematology*, 32(6):547–555, 2004.

[377] S. Pereira, H. F. Kildegaard, and M. R. Andersen. Impact of CHO Metabolism on Cell Growth and Protein Production: An Overview of Toxic and Inhibiting Metabolites and Nutrients. *Biotechnology Journal*, 13(3):1–13, 2018.

[378] C. M. Perusich, S. Goetghebeur, and W.-S. Hu. Virus Production in Microscphere-Induced Aggregate Culture of Animal Cells. *Biotechology Techniques*, 5(2):145–148, 1991.

[379] E. Petiot, F. Fournier, C. Gény, H. Pinton, and A. Marc. Rapid screening of serum-free media for the growth of adherent vero cells by using a small-scale and non-invasive tool. *Applied Biochemistry and Biotechnology*, 160(6):1600–1615, 2010.

[380] E. Petiot, E. Guedon, F. Blanchard, C. Gény, H. Pinton, and A. Marc. Kinetic characterization of vero cell metabolism in a serum-free batch culture process. *Biotechnology and Bioengineering*, 107(1):143–153, 2010. may.

[381] M. J. Petris. The SLC31 (Ctr) copper transporter family. *Pflugers Archiv European Journal of Physiology*, 447(5):752–755, 2004.

[382] J. T. Pinto and A. J. L. Cooper. From Cholesterogenesis to Steroidogenesis: Role of Riboflavin and Flavoenzymes in the Biosynthesis of Vitamin D. *Advances in Nutrition*, 5(2):144–163, 2014.

[383] L. Pizzorno. Nothing Boring about Boron. *Integrative Medicine*, 14(4):35, 2015. feb.

[384] K. Plante, E. Wang, C. D. Partidos, J. Weger, R. Gorchakov, K. Tsetsarkin, E. M. Borland, A. M. Powers, R. Seymour, D. T. Stinchcomb, J. E. Osorio, I. Frolov, and S. C. Weaver. Novel chikungunya vaccine candidate with an ires-based attenuation and host range alteration mechanism. *PLoS Pathogens*, 7(7), 2011.

[385] A. Prasad and S. Pedigo. Calcium-dependent stability studies of domains 1 and 2 of epithelial cadherin. *Biochemistry*, 44(42):13692–13701, 2005.

[386] P. Price, S. Gorfien, D. Danner, and M. Plavsic. Animal Cell Culture Media Comprising non-animal or plant derived nutrients. (US 2004/0171152 A1), 2004.

[387] P. J. Price, S. F. Gorfien, and D. Danner. Animal Cell Culture Media Comprising Plant-Derived Nutrients. (WO 98/15614), 1996.

[388] E. Prus, T. Peled, and E. Fibach. The effect of tetraethylenepentamine, a synthetic copper chelating polyamine, on expression of CD34 and CD38 antigens on normal and leukemic hematopoietic cells. *Leukemia and Lymphoma*, 45(3):583–589, 2004.

[389] S. Puig, L. Ramos-Alonso, A. M. Romero, and M. T. Martínez-Pastor. The elemental role of iron in DNA synthesis and repair. *Metallomics*, 9(11):1483–1500, 2017.

[390] E. Qin, H. Shi, L. Tang, C. Wang, G. Chang, Z. Ding, K. Zhao, J. Wang, Z. Chen, M. Yu, B. Si, J. Liu, D. Wu, X. Cheng, B. Yang, W. Peng, Q. Meng, B. Liu, W. Han, X. Yin, H. Duan, D. Zhan, L. Tian, S. Li, J. Wu, G. Tan, Y. Y. Li, Y. Y. Li, Y. Liu,

H. Liu, F. Lv, Y. Zhang, X. Kong, B. Fan, T. Jiang, S. Xu, X. Wang, C. Li, X. Wu, Y. Deng, M. Zhao, and Q. Zhu. Immunogenicity and protective efficacy in monkeys of purified inactivated Vero-cell SARS vaccine. *Vaccine*, 24(7):1028–1034, 2006.

[391] E. V. Quadros. Advances in the understanding of cobalamin assimilation and metabolism. *British Journal of Haematology*, 148(2):195–204, 2010. jan.

[392] C. Quijano, L. Cao, M. M. Fergusson, H. Romero, J. Liu, S. Gutkind, I. I. Rovira, R. P. Mohney, E. D. Karoly, and T. Finkel. Oncogene-induced senescence results in marked metabolic and bioenergetic alterations. *Cell Cycle*, 11(7):1383–1392, 2012. apr.

[393] T. D. Rae, P. J. Schmidt, R. A. Pufahl, V. C. Culotta, and T. V. O'Halloran. Undetectable Intracellular Free Copper: The Requirement of a Copper Chaperone for Superoxide Dismutase. *Science*, 284(5415):805–808, 1999. apr.

[394] M. D. Ramer, E. S. Suman, H. Richter, K. Stanger, M. Spranger, N. Bieberstein, and B. P. Duncker. Dbf4 and Cdc7 proteins promote DNA replication through interactions with distinct Mcm2-7 protein subunits. *Journal of Biological Chemistry*, 288(21):14926–14935, 2013.

[395] S. Ratcliffe, R. Jugdaohsingh, J. Vivancos, A. Marron, R. Deshmukh, J. F. Ma, N. Mitani-Ueno, J. Robertson, J. Wills, M. V. Boekschoten, M. Müller, R. C. Mawhinney, S. D. Kinrade, P. Isenring, R. R. Bélanger, and J. J. Powell. Identification of a mammalian silicon transporter. *American Journal of Physiology - Cell Physiology*, 312(5):C550–C561, 2017.

[396] M. Reiter, W. Mundt, F. Dorner, L. Grillberger, and A. Mitterer. Medium for the Protein-Free and Serum-Free Cultivation of Cell. (US 2003/0203448 A1), 2003.

[397] K. R. H. Repke. The Role of the Na+/K+ Pump in Normal and Cancer Cell Proliferation. In *Biomembranes*, pages 160–176. Springer Berlin Heidelberg, Berlin, Heidelberg, 1988.

[398] J. Richardson, B. Shah, P. V. Bondarenko, P. Bhebe, Z. Zhang, M. Nicklaus, and M. C. Kombe. Metabolomics analysis of soy hydrolysates for the identification of productivity markers of mammalian cells for manufacturing therapeutic proteins. *Biotechnology Progress*, 31(2):522–531, 2015.

[399] F. V. Ritacco, Y. Wu, and A. Khetan. Cell culture media for recombinant protein expression in Chinese hamster ovary (CHO) cells: History, key components, and optimization strategies. *Biotechnology Progress*, 34(6):1407–1426, 2018.

[400] L. D. Roberts, A. L. Souza, R. E. Gerszten, and C. B. Clish. Targeted Metabolomics. *Current Protocols in Molecular Biology*, 98(1):1–34, 2012. apr.

[401] R. W. Robey, K. M. Pluchino, M. D. Hall, A. T. Fojo, S. E. Bates, and M. M. Gottesman. Revisiting the role of ABC transporters in multidrug-resistant cancer. *Nature Reviews Cancer*, 18(7):452–464, 2018. jul.

[402] M. D. Robinson, D. J. McCarthy, and G. K. Smyth. edgeR: A Bioconductor package for differential expression analysis of digital gene expression data. *Bioinformatics*, 26(1):139–140, 2009.

[403] M. E. Rodrigues, A. R. Costa, M. Henriques, J. Azeredo, and R. Oliveira. Comparison of commercial serum-free media for CHO-K1 cell growth and monoclonal antibody production. *International Journal of Pharmaceutics*, 437(1-2):303–305, 2012.

[404] J. A. Rodriguez, Y. Ben Ali, S. Abdelkafi, L. D. Mendoza, J. Leclaire, F. Fotiadu, G. Buono, F. Carrière, and A. Abousalham. In vitro stereoselective hydrolysis of di-

acylglycerols by hormone-sensitive lipase. *Biochimica et Biophysica Acta - Molecular and Cell Biology of Lipids*, 1801(1):77–83, 2010.

[405] R. Rodriguez-Melendez and J. Zempleni. Regulation of gene expression by biotin. *The Journal of Nutritional Biochemistry*, 14(12):680–690, 2003. dec.

[406] A. Romani and A. Scarpa. Regulation of cell magnesium. *Archives of biochemistry and biophysics*, 298(1):1–12, 1992. oct.

[407] A. M. P. Romani. Cellular magnesium homeostasis. *Archives of Biochemistry and Biophysics*, 512(1):1–23, 2011. aug.

[408] E. Romeo, M. H. Dave, D. Bacic, Z. Ristic, S. M. R. Camargo, J. Loffing, C. A. Wagner, and F. Verrey. Luminal kidney and intestine SLC6 amino acid transporters of B 0AT-cluster and their tissue distribution in Mus musculus. *American Journal of Physiology - Renal Physiology*, 290(2):376–383, 2006.

[409] R. Rosenthal, D. Günzel, J. Piontek, S. M. Krug, C. Ayala-Torres, C. Hempel, D. Theune, and M. Fromm. Claudin-15 forms a water channel through the tight junction with distinct function compared to claudin-2. *Acta Physiologica*, 228(1):1–15, 2020.

[410] J. B. Ross, D. Huh, L. B. Noble, and S. F. Tavazoie. Identification of molecular determinants of primary and metastatic tumour re-initiation in breast cancer. *Nature Cell Biology*, 17(5):651–664, 2015. may.

[411] H.-P. Roth and M. Kirchgeßner. Influence of Alimentary Zinc Deficiency on the Concentration of Growth Hormone (GH), Insulin-Like Growth Factor I (IGF-I) and Insulin in the Serum of Force-Fed Rats. *Hormone and Metabolic Research*, 26(09):404–408, 1994. sep.

[412] S. Rourou, M. Ben Zakkour, and H. Kallel. Adaptation of Vero cells to suspension growth for rabies virus production in different serum free media. *Vaccine*, 37(47):6987–6995, 2019. nov.

[413] S. Rourou, A. Van Der Ark, S. Majoul, K. Trabelsi, T. Van Der Velden, and H. Kallel. A novel animal-component-free medium for rabies virus production in Vero cells grown on Cytodex 1 microcarriers in a stirred bioreactor. *Applied Microbiology and Biotechnology*, 85(1):53–63, 2009.

[414] S. Rourou, A. van der Ark, T. van der Velden, and H. Kallel. A microcarrier cell culture process for propagating rabies virus in Vero cells grown in a stirred bioreactor under fully animal component free conditions. *Vaccine*, 25(19):3879–3889, 2007.

[415] S. Rourou, A. van der Ark, T. van der Velden, and H. Kallel. Development of an animal-component free medium for vero cells culture. *Biotechnology Progress*, 25(6):1752–1761, 2009.

[416] I. Routray and S. Ali. Boron inhibits apoptosis in hyperapoptosis condition: Acts by stabilizing the mitochondrial membrane and inhibiting matrix remodeling. *Biochimica et Biophysica Acta - General Subjects*, 1863(1):144–152, 2019.

[417] J. S. Ryu, T. K. Kim, J. Y. Chung, and G. M. Lee. Osmoprotective effect of glycine betaine on foreign protein production in hyperosmotic recombinant Chinese hamster ovary cell cultures differs among cell lines. *Biotechnology and Bioengineering*, 70(2):167–175, 2000.

[418] J. S. Ryu and G. M. Lee. Effect of hypoosmotic stress on hybridoma cell growth and antibody production. *Biotechnology and Bioengineering*, 55(3):565–570, 1997.

[419] J. Sabbatinelli, F. Prattichizzo, F. Olivieri, A. D. Procopio, M. R. Rippo, and A. Giuliani. Where Metabolism Meets Senescence: Focus on Endothelial Cells. *Frontiers in Physiology*, 10(December):1–17, 2019. dec.

[420] J. M. Samet, B. J. Dewar, W. Wu, and L. M. Graves. Mechanisms of Zn2+ induced signal initiation through the epidermal growth factor receptor. *Toxicology and Applied Pharmacology*, 191(1):86–93, 2003.

[421] E. M. Scallan, S. H. Sample, A. M. Beierschmitt, and R. M. Palmour. Hematologic and biochemical RIs for an aged population of captive African Green monkeys (Chlorocebus aethiops sabaeus). *Veterinary Clinical Pathology*, 46(3):430–435, 2017.

[422] L. Scalvini, D. Piomelli, and M. Mor. Monoglyceride lipase: Structure and inhibitors. *Chemistry and Physics of Lipids*, 197:13–24, 2016. may.

[423] S. W. Schaffer, C. Ju Jong, R. Kc, and J. Azuma. Physiological roles of taurine in heart and muscle. *Journal of Biomedical Science*, 17(SUPPL. 1):1–8, 2010.

[424] E. J. Schlaeger. The protein hydrolysate, Primatone RL, is a cost-effective multiple growth promoter of mammalian cell culture in serum-containing and serum-free media and displays anti-apoptosis properties. *Journal of Immunological Methods*, 194(2):191–199, 1996.

[425] M. Schneider, I. W. Marison, and U. Von Stockar. The importance of ammonia in mammalian cell culture. *Journal of Biotechnology*, 46(3):161–185, 1996.

[426] G. N. Schrauzer. The Discovery of the Essential Trace Elements: An Outline of the History of Biological Trace Element Research. *Biochemistry of the Essential Ultratrace Elements*, pages 17–31, 1984.

[427] M. Schröder, K. Matischak, and P. Friedl. Serum- and protein-free media formulations for the Chinese hamster ovary cell line DUKXB11. *Journal of Biotechnology*, 108(3):279–292, 2004.

[428] M. J. Schultz, A. F. Swindall, and S. L. Bellis. Regulation of the metastatic cell phenotype by sialylated glycans. *Cancer and Metastasis Reviews*, 31(3-4):501–518, 2012. dec.

[429] S. Sergeant and W. T. Johnson. Iron and copper requirements for proliferation and differentiation of a human promyelocytic leukemia cell line (HL60). *Journal of Cellular Physiology*, 163(3):477–485, 1995.

[430] J. V. Shah and D. W. Cleveland. Waiting for Anaphase. *Cell*, 103(7):997–1000, 2000.

[431] M. J. Shearer and P. Newman. Recent trends in the metabolism and cell biology of vitamin K with special reference to vitamin K cycling and MK-4 biosynthesis. *Journal of Lipid Research*, 55(3):345–362, 2014. mar.

[432] R. Sheets. History and Characterization of the Vero Cell Line. *Open session FDA*, pages 1–12, 2000.

[433] C. F. Shen, C. Guilbault, X. Li, S. M. Elahi, S. Ansorge, A. Kamen, and R. Gilbert. Development of suspension adapted Vero cell culture process technology for production of viral vaccines. *Vaccine*, 37(47):6996–7002, 2019. nov.

[434] S. Shen, X. F. Li, W. R. Cullen, M. Weinfeld, and X. C. Le. Arsenic binding to proteins. *Chemical Reviews*, 113(10):7769–7792, 2013.

[435] K. Shibuya, M. Atsumi, S. Tsunakawa, K. Nogaki, T. R. Fletcher, K. Imada, K. Lydersen, and B. K. Dersen. Serum-free medium for culturing animal cells. (WO 00/03000), 2002.

[436] S. Shridhar, G. Klanert, N. Auer, I. Hernandez-Lopez, M. M. Kańduła, M. Hackl, J. Grillari, N. Stralis-Pavese, D. P. Kreil, and N. Borth. Transcriptomic changes in CHO cells after adaptation to suspension growth in protein-free medium analysed by a species-specific microarray. *Journal of Biotechnology*, 257:13–21, 2017.

[437] P. Shukla, C. Vogl, B. Wallner, D. Rigler, M. Müller, and S. Macho-Maschler. High-throughput mRNA and miRNA profiling of epithelial-mesenchymal transition in MDCK cells. *BMC Genomics*, 16(1):1–19, 2015.

[438] N. Shyh-Chang, J. W. Locasale, C. A. Lyssiotis, Y. Zheng, R. Y. Teo, S. Ratanasirintrawoot, J. Zhang, T. Onder, J. J. Unternaehrer, H. Zhu, J. M. Asara, G. Q. Daley, and L. C. Cantley. Influence of threonine metabolism on S-adenosylmethionine and histone methylation. *Science (New York, N.Y.)*, 339(6116):222–6, 2013. jan.

[439] Y. Sidorenko, A. Wahl, M. Dauner, Y. Genzel, and U. Reichl. Comparison of metabolic flux distributions for MDCK cell growth in glutamine- and pyruvate-containing media. *Biotechnology Progress*, 24(2):311–320, 2008.

[440] A. K. Silva, H. Yi, S. H. Hayes, G. M. Seigel, and A. S. Hackam. Lithium chloride regulates the proliferation of stem-like cells in retinoblastoma cell lines: A potential role for the canonical went signaling pathway. *Molecular Vision*, 16(January):36–45, 2010.

[441] N. Simon and A. Hertig. Alteration of fatty acid oxidation in tubular epithelial cells: From acute kidney injury to renal fibrogenesis. *Frontiers in Medicine*, 2(AUG):1–8, 2015.

[442] M. S. Sinacore, D. Drapeau, and S. R. Adamson. Adaptation of Mammalian Cells to Growth in Serum-Free Media. *Molecular Biotechnology*, 15(3):249–258, 2000.

[443] A. Singh, H. F. Kildegaard, and M. R. Andersen. An Online Compendium of CHO RNA-Seq Data Allows Identification of CHO Cell Line-Specific Transcriptomic Signatures. *Biotechnology Journal*, 13(10):1–11, 2018.

[444] N. Smirnoff. Ascorbic acid metabolism and functions: A comparison of plants and mammals. *Free Radical Biology and Medicine*, (November 2017):1–14, 2018.

[445] M. E. Smoot, K. Ono, J. Ruscheinski, P. L. Wang, and T. Ideker. Cytoscape 2.8: New features for data integration and network visualization. *Bioinformatics*, 27(3):431–432, 2011.

[446] S. Sokolenko, E. J. Blondeel, N. Azlah, B. George, S. Schulze, D. Chang, and M. G. Aucoin. Profiling convoluted single-dimension proton NMR spectra: A plackett-burman approach for assessing quantification error of metabolites in complex mixtures with application to cell culture. *Analytical Chemistry*, 86(7):3330–3337, 2014.

[447] E. Somogyi, U. Petersson, K. Hultenby, and M. Wendel. Calreticulin - An endoplasmic reticulum protein with calcium-binding activity is also found in the extracellular matrix. *Matrix Biology*, 22(2):179–191, 2003.

[448] M. Spearman, S. Chan, V. Jung, V. Kowbel, M. Mendoza, V. Miranda, and M. Butler. Components of yeast (Sacchromyces cervisiae) extract as defined media additives

that support the growth and productivity of CHO cells. *Journal of Biotechnology*, 233:129–142, 2016.

[449] A. A. Spector and H.-Y. Kim. Discovery of essential fatty acids. *Journal of Lipid Research*, 56(1):11–21, 2015.

[450] A. A. Spector and M. A. Yorek. Membrane lipid composition and cellular function. *Journal of Lipid Research*, 26(9):1015–1035, 1985.

[451] S. Sriwidodo, T. Subroto, I. Maksum, N. Wathoni, T. Rostinawati, H. Ulya, and I. Putri. Optimization of secreted recombinant human epidermal growth factor production using pectate lyase B from Escherichia coli BL21(DE3) by central composite design and its production in high cell density culture. *Journal of Pharmacy And Bioallied Sciences*, 11(8):562, 2019.

[452] J. G. Steele, G. Johnson, and P. A. Underwood. Role of serum vitronectin and fibronectin in adhesion of fibroblasts following seeding onto tissue culture polystyrene. *Journal of Biomedical Materials Research*, 26(7):861–884, 1992.

[453] R. B. Stockbridge, L. Kolmakova-Partensky, T. Shane, A. Koide, S. Koide, C. Miller, and S. Newstead. Crystal structures of a double-barrelled fluoride ion channel. *Nature*, 525(7570):548–551, 2015.

[454] J. R. Stockigt. Potassium Metabolism. *Anaesthesia and Intensive Care*, 5(4):317–325, 1977. nov.

[455] G. Stolfa, M. T. Smonskey, R. Boniface, A. B. Hachmann, P. Gulde, A. D. Joshi, A. P. Pierce, S. J. Jacobia, and A. Campbell. CHO-Omics Review: The Impact of Current and Emerging Technologies on Chinese Hamster Ovary Based Bioproduction. *Biotechnology Journal*, 13(3):1–14, 2018.

[456] L. L. Stoll and A. A. Spector. Changes in serum influence the fatty acid composition of established cell lines. *In Vitro*, 20(9):732–8, 1984. sep.

[457] L. Stransky, K. Cotter, and M. Forgac. The function of v-atpases in cancer. *Physiological Reviews*, 96(3):1071–1091, 2016.

[458] E. A. Struys and C. Jakobs. Metabolism of lysine in alpha-aminoadipic semialdehyde dehydrogenase-deficient fibroblasts: Evidence for an alternative pathway of pipecolic acid formation. *FEBS Letters*, 584(1):181–186, 2010.

[459] A. Subramanian, P. Tamayo, V. K. Mootha, S. Mukherjee, B. L. Ebert, M. A. Gillette, A. Paulovich, S. L. Pomeroy, T. R. Golub, E. S. Lander, and J. P. Mesirov. Gene set enrichment analysis: a knowledge-based approach for interpreting genome-wide expression profiles. *Proceedings of the National Academy of Sciences of the United States of America*, 102(43):15545–15550, 2005.

[460] V. Sudakin, G. K. T. Chan, and T. J. Yen. Checkpoint inhibition of the APC/C in HeLa cells is mediated by a complex of BUBR1, BUB3, CDC20, and MAD2. *Journal of Cell Biology*, 154(5):925–936, 2001.

[461] D. A. Suhy, K. D. Simon, D. I. H. Linzer, and T. V. O'Halloran. Metallothionein is part of a zinc-scavenging mechanism for cell survival under conditions of extreme zinc deprivation. *Journal of Biological Chemistry*, 274(14):9183–9192, 1999.

[462] L. B. Sullivan, D. Y. Gui, A. M. Hosios, L. N. Bush, E. Freinkman, and M. G. Vander Heiden. Supporting Aspartate Biosynthesis Is an Essential Function of Respiration in Proliferating Cells. *Cell*, 162(3):552–563, 2015.

[463] L. B. Sullivan, A. Luengo, L. V. Danai, L. N. Bush, F. F. Diehl, A. M. Hosios, A. N. Lau, S. Elmiligy, S. Malstrom, C. A. Lewis, and M. G. Vander Heiden. Aspartate is an

endogenous metabolic limitation for tumour growth. *Nature Cell Biology*, 20(July):1, 2018.

[464] Z. Sun, Q. Ji, A. R. Evans, M. J. Lewis, J. Mo, and P. Hu. High-throughput LC-MS quantitation of cell culture metabolites. *Biologicals*, 61(August):44–51, 2019.

[465] D. Surjana, G. M. Halliday, and D. L. Damian. Role of nicotinamide in DNA damage, mutagenesis, and DNA repair. *Journal of Nucleic Acids*, 2010, 2010.

[466] Tae Kyung Kim, Joon Soo Ryu, Joo Young Chung, Min Soo Kim, and M. L. Gyun. Osmoprotective effect of glycine betaine on thrombopoietin production in hyperosmotic Chinese hamster ovary cell culture: Clonal variations. *Biotechnology Progress*, 16(5):775–781, 2000.

[467] S. Takamizawa, Y. Maehata, K. Imai, H. Senoo, S. Sato, and R. I. Hata. Effects of ascorbic acid and ascorbic acid 2-phosphate, a long-acting vitamin C derivative, on the proliferation and differentiation of human osteoblast-like cells. *Cell Biology International*, 28(4):255–265, 2004.

[468] D. Y. Takeda and A. Dutta. DNA replication and progression through S phase. *Oncogene*, 24(17):2827–2843, 2005.

[469] T. Taki, D. Ishikawa, M. Ogura, M. Nakajima, and S. Handa. Ganglioside gd1α functions in the adhesion of metastatic tumor cells to endothelial cells of the target tissue. *Cancer Research*, 57(10):1882–1888, 1997.

[470] M. J. Tamás, B. Fauvet, P. Christen, and P. Goloubinoff. Misfolding and aggregation of nascent proteins: a novel mode of toxic cadmium action in vivo. *Current Genetics*, 64(1):177–181, 2018.

[471] K. Tamura, R. L. Rice, P. Wipf, and J. S. Lazo. Dual G1 and G2/M phase inhibition by SC-$\alpha\alpha\delta$9, a combinatorially derived Cdc25 phosphatase inhibitor. *Oncogene*, 18(50):6989–6996, 1999.

[472] X.-H. Tang and N. F. Shay. Biochemical and Molecular Action of Nutrients Zinc Has an Insulin-Like Effect on Glucose Transport Mediated by Phosphoinositol-3-Kinase and Akt in 3T3-L1 Fibroblasts and Adipocytes 1. (December 2000):1414–1420, 2001.

[473] F. Tapia, D. Vázquez-Ramírez, Y. Genzel, and U. Reichl. Bioreactors for high cell density and continuous multi-stage cultivations: options for process intensification in cell culture-based viral vaccine production. *Applied Microbiology and Biotechnology*, 100(5):2121–2132, 2016.

[474] T. J. Thomas and T. J. Thomas. Polyamines in cell growth and cell death: molecular mechanisms and therapeutic applications. *Cellular and Molecular Life Sciences*, 58:244–258, 2001.

[475] Y. E. Thomassen, O. Rubingh, R. H. Wijffels, L. A. van der Pol, and W. A. M. Bakker. Improved poliovirus D-antigen yields by application of different Vero cell cultivation methods. *Vaccine*, 32(24):2782–2788, 2014.

[476] Y. E. Thomassen, G. van Eikenhorst, L. A. van der Pol, and W. A. M. Bakker. Platform Technology for Viral Vaccine Production: Comparison Between Attached and Suspension Vero Cells. In N. Jenkins, editor, *Proceedings of the 21st Annual Meeting of the European Society for Animal Cell Technology (ESACT), Dublin, Ireland, June 7-10, 2009*, pages 723–727. Springer Netherlands, Dordrecht, 2012.

[477] L. Tie, N. Lu, X.-Y. Pan, Y. Pan, Y. An, J.-W. Gao, Y.-H. Lin, H.-M. Yu, and X.-J. Li. Hypoxia-induced Up-regulation of Aquaporin-1 Protein in Prostate Cancer Cells

in a p38-dependent Manner. *Cellular Physiology and Biochemistry*, 29(1-2):269–280, 2012.

[478] M. Tiwari, M. Parida, S. R. Santhosh, M. Khan, P. K. Dash, and P. V. L. Rao. Assessment of immunogenic potential of Vero adapted formalin inactivated vaccine derived from novel ECSA genotype of Chikungunya virus. *Vaccine*, 27(18):2513–2522, 2009. apr.

[479] K. Trabelsi, S. Rourou, H. Loukil, S. Majoul, and H. Kallel. Comparison of various culture modes for the production of rabies virus by Vero cells grown on microcarriers in a 2-l bioreactor. *Enzyme and Microbial Technology*, 36(4):514–519, 2005.

[480] T. W. Traut. Physiological concentrations of purines and pyrimidines. *Molecular and Cellular Biochemistry*, 140(1):1–22, 1994.

[481] B. K. Tye. MCM Proteins in DNA Replication. *Annual Review of Biochemistry*, 68(1):649–686, 1999.

[482] T. Udhayabanu, A. Manole, M. Rajeshwari, P. Varalakshmi, H. Houlden, and B. Ashokkumar. Riboflavin Responsive Mitochondrial Dysfunction in Neurodegenerative Diseases. *Journal of Clinical Medicine*, 6(5):52, 2017.

[483] M. Uhlén, L. Fagerberg, B. M. Hallström, C. Lindskog, P. Oksvold, A. Mardinoglu, Å. Sivertsson, C. Kampf, E. Sjöstedt, A. Asplund, I. M. Olsson, K. Edlund, E. Lundberg, S. Navani, C. A. K. Szigyarto, J. Odeberg, D. Djureinovic, J. O. Takanen, S. Hober, T. Alm, P. H. Edqvist, H. Berling, H. Tegel, J. Mulder, J. Rockberg, P. Nilsson, J. M. Schwenk, M. Hamsten, K. Von Feilitzen, M. Forsberg, L. Persson, F. Johansson, M. Zwahlen, G. Von Heijne, J. Nielsen, and F. Pontén. Tissue-based map of the human proteome. *Science*, 347(6220), 2015.

[484] M. Ummadi and M. Curic-Bawden. *Protein Hydrolysates in Biotechnology*. Springer Netherlands, Dordrecht, 2010.

[485] T. Valenta, G. Hausmann, and K. Basler. The many faces and functions of Î 2-catenin. *EMBO Journal*, 31(12):2714–2736, 2012.

[486] J. van der Valk, D. Brunner, K. De Smet, A. Fex Svenningsen, P. Honegger, L. E. Knudsen, T. Lindl, J. Noraberg, A. Price, M. L. Scarino, G. Gstraunthaler, Å. Fex Svenningsen, P. Honegger, L. E. Knudsen, T. Lindl, J. Noraberg, A. Price, M. L. Scarino, and G. Gstraunthaler. Optimization of chemically defined cell culture media - Replacing fetal bovine serum in mammalian in vitro methods. *Toxicology in Vitro*, 24(4):1053–1063, 2010.

[487] R. van Wielink, H. C. M. Kant-Eenbergen, M. M. Harmsen, D. E. Martens, R. H. Wijffels, and J. M. Coco-Martin. Adaptation of a Madin-Darby canine kidney cell line to suspension growth in serum-free media and comparison of its ability to produce avian influenza virus to Vero and BHK21 cell lines. *Journal of Virological Methods*, 171(1):53–60, 2011.

[488] F. M. Vaz and R. J. A. Wanders. Carnitine biosynthesis in mammals. *The Biochemical Journal*, 361(Pt 3):417–29, 2002.

[489] N. Vijayasankaran, S. Varma, Y. Yang, M. Mun, S. Arevalo, M. Gawlitzek, T. Swartz, A. Lim, F. Li, B. Zhang, S. Meier, and R. Kiss. Effect of cell culture medium components on color of formulated monoclonal antibody drug substance. *Biotechnology Progress*, 29(5):1270–1277, 2013.

[490] Voet, Voet, and Pratt. *Fundamentals of Biochemistry*. John Wiley Sons, Inc., 4 edition, 2013.

[491] D. Voet and J. G. Voet. *Biochemisty*. John Wiley Sons, Inc, 4 edition, 2011.

[492] T. Wada, T. Hanyu, K. Nozaki, K. Kataoka, T. Kawatani, T. Asahi, and N. Sawamura. Antioxidant activity of Ge-132, a synthetic organic germanium, on cultured mammalian cells. *Biological and Pharmaceutical Bulletin*, 41(5):749–753, 2018.

[493] S. J. Wakil, E. B. Titchener, and D. M. Gibson. Evidence for the participation of biotin in the enzymic synthesis of fatty acids. *BBA - Biochimica et Biophysica Acta*, 29(1):225–226, 1958.

[494] R. J. Walker, S. Weggery, J. J. Bedford, F. J. McDonald, G. Ellis, and J. P. Leader. Lithium-induced reduction in urinary concentrating ability and urinary aquaporin 2 (AQP2) excretion in healthy volunteers. *Kidney International*, 67(1):291–294, 2005.

[495] R. J. Wanders, M. Duran, and F. J. Loupatty. Enzymology of the branched-chain amino acid oxidation disorders: The valine pathway. *Journal of Inherited Metabolic Disease*, 35(1):5–12, 2012.

[496] G. Wang, Q. Jiang, and C. Zhang. The role of mitotic kinases in coupling the centrosome cycle with the assembly of the mitotic spindle. *Journal of Cell Science*, 127(19):4111–4122, 2014.

[497] P. Wang, L. Zhang, W. Zheng, L. Cong, Z. Guo, Y. Xie, L. Wang, R. Tang, Q. Feng, Y. Hamada, K. Gonda, Z. Hu, X. Wu, and X. Jiang. Thermo-triggered Release of CRISPR-Cas9 System by Lipid-Encapsulated Gold Nanoparticles for Tumor Therapy. *Angewandte Chemie - International Edition*, 57(6):1491–1496, 2018.

[498] X. Wang, W. Ying, K. A. Dunlap, G. Lin, M. C. Satterfield, R. C. Burghardt, G. Wu, and F. W. Bazer. Arginine decarboxylase and agmatinase: An alternative pathway

for de novo biosynthesis of polyamines for development of mammalian conceptuses. *Biology of Reproduction*, 90(4):1–15, 2014.

[499] C. Waymouth. Culture media: animal tissue. In P. Altman and D. Dittmer, editors, *Metabolism*, pages 180–187. FASEB, 1968.

[500] C. Waymouth. Osmolality of mammalian blood and of media for culture of mammalian cells. *In Vitro*, 6(2):109–127, 1970.

[501] T. Wei and V. Simko. The corrplot package. *R Core Team*, 2016.

[502] E. P. Wen, R. Ellis, and N. S. Pujar, editors. *Vaccine Development and Manufacturing*. John Wiley Sons, Ltd, 2014.

[503] W. Whitford and J. Manwaring. Lipids in Cell Culture Media. *Fisher application notes*, pages 152–154.

[504] H. Wickham. ggplot2. *Wiley Interdisciplinary Reviews: Computational Statistics*, 2011.

[505] S. R. Wiley, K. Schooley, P. J. Smolak, W. S. Din, C.-P. Huang, J. K. Nicholl, G. R. Sutherland, T. D. Smith, C. Rauch, C. A. Smith, and R. G. Goodwin. Identification and characterization of a new member of the TNF family that induces apoptosis. *Immunity*, 3(6):673–682, 1995. dec.

[506] G. M. Williams and J. M. Gunn. Long-term cell culture of adult rat liver epithelial cells. *Experimental Cell Research*, 89(1):139–142, 1974.

[507] D. R. Wise and C. B. Thompson. Glutamine addiction: a new therapeutic target in cancer. *Trends in Biochemical Sciences*, 35(8):427–433, 2010.

[508] G. T. Wondrak and E. L. Jacobson. Vitamin B6: Beyond Coenzyme Functions. In *Water Soluble Vitamins*, pages 291–300. 2012.

[509] V. V. T. Wong, K. W. Ho, and M. G. S. Yap. Evaluation of insulin-mimetic trace metals as insulin replacements in mammalian cell cultures. *Cytotechnology*, 45(3):107–115, 2004.

[510] V. V. T. Wong, P. M. Nissom, S. L. Sim, J. H. M. Yeo, S. H. Chuah, and M. G. S. Yap. Zinc as an insulin replacement in hybridoma cultures. *Biotechnology and Bioengineering*, 93(3):553–563, 2006.

[511] A. Woo Suk and M. R. Antoniewicz. Parallel labeling experiments with [1,2-13C]glucose and [U-13C]glutamine provide new insights into CHO cell metabolism. *Metabolic Engineering*, 15(1):34–47, 2013.

[512] N. Wressnigg, M. V. W. Van Der Velden, D. Portsmouth, W. Draxler, M. O'Rourke, P. Richmond, S. Hall, W. J. H. McBride, A. Redfern, J. Aaskov, P. N. Barrett, and G. Aichingera. An inactivated Ross River virus vaccine is well tolerated and immunogenic in an adult population in a randomized phase 3 trial. *Clinical and Vaccine Immunology*, 22(3):267–273, 2015.

[513] G. Wu and S. M. Morris. Arginine metabolism: nitric oxide and beyond. *Biochemical Journal*, 336(1):1–17, 1998. nov.

[514] S. C. Wu, C. C. Liu, and W. C. Lian. Optimization of microcarrier cell culture process for the inactivated enterovirus type 71 vaccine development. *Vaccine*, 22(29-30):3858–3864, 2004.

[515] J. Xiong, H. Kawagishi, Y. Yan, J. Liu, Q. S. Wells, L. R. Edmunds, M. M. Fergusson, Z. X. Yu, I. I. Rovira, E. L. Brittain, M. J. Wolfgang, M. J. Jurczak, J. P. Fessel, and

T. Finkel. A Metabolic Basis for Endothelial-to-Mesenchymal Transition. *Molecular Cell*, 69(4):689–698.e7, 2018.

[516] J. Xu, M. Jin, H. Song, C. Huang, X. Xu, J. Tian, N. X. Qian, K. Steger, N. S. Lewen, L. Tao, and Z. J. Li. Brown drug substance color investigation in cell culture manufacturing using chemically defined media: A case study. *Process Biochemistry*, 49(1):130–139, 2014.

[517] P. Xu, X. P. Dai, E. Graf, R. Martel, and R. Russell. Effects of glutamine and asparagine on recombinant antibody production using CHO-GS cell lines. *Biotechnology Progress*, 30(6):1457–1468, 2014.

[518] W. Xu, X. Yu, J. Zhang, S. Bhushan, S. Prasad, K. Prasad, F. Wu, J. Yuan, and H. F. Poon. Soy hydrolysate mimic autocrine growth factors effect of conditioned media to promote single CHO-K1 cell proliferation. *Tissue and Cell*, 58(April):130–133, 2019. jun.

[519] Z. Xu, D. Li, and J. Baohua. Quantification of the stiffness and strength of cadherin ectodomain binding with different ions. *Theoretical and Applied Mechanics Letters*, 4(3):34001, 2014.

[520] M. B. Yaffe and S. J. Smerdon. PhosphoSerine/threonine binding domains: You can't pSERious? *Structure*, 9(3):33–38, 2001.

[521] A. Yamaji-Hasegawa and M. Tsujimoto. Asymmetric Distribution of Phospholipids in Biomembranes. *Biological & Pharmaceutical Bulletin*, 29(8):1547–1553, 2006.

[522] K. Yamauchi, T. Komatsu, A. D. Kulkarni, Y. Ohmori, H. Minami, Y. Ushiyama, M. Nakayama, and S. Yamamoto. Glutamine and arginine affect Caco-2 cell proliferation by promotion of nucleotide synthesis. *Nutrition*, 18(4):329–333, 2002.

[523] M. Yamauchi and M. Sricholpech. Lysine post-translational modifications of collagen. *Essays In Biochemistry*, 52:113–133, 2012. may.

[524] D. Yang, X. Lü, Y. Hong, T. Xi, and D. Zhang. The molecular mechanism of mediation of adsorbed serum proteins to endothelial cells adhesion and growth on biomaterials. *Biomaterials*, 34(23):5747–5758, 2013.

[525] M. Yang and W. J. Brackenbury. Membrane potential and cancer progression. *Frontiers in Physiology*, 4 JUL(July):1–10, 2013.

[526] H. Yao and J. Ye. Long chain Acyl-CoA synthetase 3-mediated phosphatidylcholine synthesis is required for assembly of very low density lipoproteins in human hepatoma Huh7 cells. *Journal of Biological Chemistry*, 283(2):849–854, 2008.

[527] H. Yin, R. L. Kanasty, A. A. Eltoukhy, A. J. Vegas, J. R. Dorkin, and D. G. Anderson. Non-viral vectors for gene-based therapy. *Nature Reviews Genetics*, 15(8):541–555, 2014.

[528] A. Y. Yokomizo, M. M. Antoniazzi, P. L. Galdino, N. Azambuja, S. A. C. Jorge, and C. A. Pereira. Rabies Virus Production in High Vero Cell Density Cultures on Macroporous Microcarriers. *Biotechnology and Bioengineering*, 85(5):506–515, 2004.

[529] H. C. Yoo, Y. C. Yu, Y. Sung, and J. M. Han. Glutamine reliance in cell metabolism. *Experimental and Molecular Medicine*, 52(9):1496–1516, 2020.

[530] F. H. Yu and W. A. Catterall. Overview of the voltage-gated sodium channel family. *Genome Biology*, 4(3), 2003.

[531] I. H. Yuk, G. B. Lin, H. Ju, I. Sifi, Y. Lam, A. Cortez, D. Liebertz, J. M. Berry, and R. M. Schwartz. A serum-free Vero production platform for a chimeric virus vaccine candidate. *Cytotechnology*, 51(3):183–192, 2006.

[532] R. K. Zalups and D. J. Koropatnick. *Cellular and Molecular Biology of Metals*. CRC Press, 2010.

[533] S. P. Zano, C. Pate, M. Frank, C. O. Rock, and S. Jackowski. Correction of a genetic deficiency in pantothenate kinase 1 using phosphopantothenate replacement therapy. *Molecular Genetics and Metabolism*, 116(4):281–288, 2015.

[534] J. Zempleni, S. S. K. K. Wijeratne, and Y. I. Hassan. Biotin. *BioFactors*, 35(1):36–46, 2009. jan.

[535] H. Zhang, H. Wang, M. Liu, T. Zhang, J. Zhang, X. Wang, and W. Xiang. Rational development of a serum-free medium and fed-batch process for a GS-CHO cell line expressing recombinant antibody. *Cytotechnology*, 65(3):363–378, 2013.

[536] J. Zhang, J. Fan, S. Venneti, J. R. Cross, T. Takagi, B. Bhinder, H. Djaballah, M. Kanai, E. H. Cheng, A. R. Judkins, B. Pawel, J. Baggs, S. Cherry, J. D. Rabinowitz, and C. B. Thompson. Asparagine Plays a Critical Role in Regulating Cellular Adaptation to Glutamine Depletion. *Molecular Cell*, 56(2):205–218, 2014. oct.

[537] S. Zhao, Y. Guo, Q. Sheng, and Y. Shyr. Advanced Heat Map and Clustering Analysis Using Heatmap3. *BioMed Research International*, 2014:1–6, 2014.

[538] Y. Zhao, P. Gao, F. Sun, Q. Li, J. Chen, H. Yu, L. Li, X. X. Wei, H. He, Z. Lu, X. X. Wei, B. Wang, Y. Cui, S. Xiong, Q. Shang, A. Xu, Y. Huang, D. Liu, and Z. Zhu. Sodium Intake Regulates Glucose Homeostasis through the PPARδ/Adiponectin-Mediated SGLT2 Pathway. *Cell Metabolism*, 23(4):699–711, 2016.

[539] C. Zhaolie, X. Chengzu, L. Hong, W. Benchuan, and J. Xihua. A novel serum-free medium for the cultivation of Vero cells on microcarriers. *Biotechnology Techniques*, 10(6):449–452, 1996.

[540] Y. Zheng and L. C. Cantley. Toward a better understanding of folate metabolism in health and disease. *Journal of Experimental Medicine*, 216(2):253–266, 2019.

[541] A. Zimmer, R. Mueller, M. Wehsling, A. Schnellbaecher, and J. von Hagen. Improvement and simplification of fed-batch bioprocesses with a highly soluble phosphotyrosine sodium salt. *Journal of Biotechnology*, 186:110–118, 2014.

APPENDICES

Appendix A

Median Concentrations from Media Review Analysis

Table A.1: Median concentrations in millimolar for serum-free media formulations that support adherent, suspension, or both types of culture methods.

Compound	**Adherent**	**Both**	**Suspension**
Ag	9.41e-08	5.00e-07	6.91e-07
Al	2.78e-06	2.34e-06	6.05e-06
α-tocopherol	0.00035242	Na	0.00136316
Ascorbic acid	0.08	0.01	0.07
Ba	6.77e-06	4.78e-06	6.78e-06
β-mercapoethanol	0.11494	N/A	0.01805
Biotin	0.00015811	2.83e-05	0.00040497
Br	3.14e-07	4.71e-07	6.79e-07

Continued on next page

Table A.1: Median concentrations in millimolar for serum-free media formulations that support adherent, suspension, or both types of culture methods.

Compound	**Adherent**	**Both**	**Suspension**
Ca	1.08108108	1.06594478	0.83867511
Cd	2.24e-05	2.24e-05	2.37e-05
Choline chloride	0.06414	0.06414	0.12857
Co	2.89e-06	3.27e-06	1.83e-05
Cr	1.08e-06	4.68e-07	1.04e-06
Cu	6.15e-06	5.91e-06	1.54e-05
D-Ca pantothenate	0.00511195	0.0047	0.00759
Ethanolamine HCl	0.02	0.02	0.1
F	5.79e-05	4.69e-05	6.57e-05
Fe	0.00165786	0.00162376	0.0290961
Folic acid	0.00603	0.00603	0.01134
Ge	2.62e-06	2.39e-06	3.44e-06
Glycine	0.565	0.175	0.17
I	4.97e-07	5.12e-07	7.06e-07
myo-Inositol	0.07637473	0.07848567	0.20474765
K	4.21164572	4.20623924	4.2985371
L-Alanine	0.145	0.24	0
L-Arginine HCl	0.73	0.785	1.84746759
L-Asparagine H2O	0.11	0.225	0.51608969
L-Aspartic acid	0.075	0.075	1.36
L-Cysteine HCl H2O	0.12	0.12	0.33

Continued on next page

Table A.1: Median concentrations in millimolar for serum-free media formulations that support adherent, suspension, or both types of culture methods.

Compound	**Adherent**	**Both**	**Suspension**
L-Cystine 2HCl	0.1	0.255	0.13
L-Glutamic acid	0.06	0.06	0.3
L-Glutamine	0	6.61	4.01
L-Histidine HCl H2O	0.245	0.215	0.48
L-Isoleucine	0.61	0.695	1.87
L-Leucine	0.825	0.725	2.29
L-Lysine	0.52	0.77	1.455
L-Methionine	0.16	0.185	0.77
L-Phenylalanine	0.275	0.355	0.61
L-Proline	0.3	0.445	0.79
L-Serine	0.33	0.485	0.86
L-Threonine	0.37	0.32	2.1
L-Tryptophan	0.365	0.42	0.71670968
L-Tyrosine Na2H2O	0.045	0.09	0.27
L-Valine	0.795	0.79	1.32
Li	0.05897061	N/A	N/A
Mg	0.7593672	0.92850394	1.0029386
Mn	6.71e-07	7.07e-07	7.95e-07
Mo_7O_{24}	9.71e-08	4.53e-06	4.39e-06
Na	147.611802	133.377932	104.620307
Ni	3.58e-07	3.58e-07	4.71e-07

Continued on next page

Table A.1: Median concentrations in millimolar for serum-free media formulations that support adherent, suspension, or both types of culture methods.

Compound	**Adherent**	**Both**	**Suspension**
Niacinamide	0.01745	0.01656	0.02951
Putrescine 2HCl	N/A	0.01	0.02
Pyridoxal HCl	0.00491	0.00982	0.01719
Pyridoxine HCl	0.00071729	0.00013416	0.00696778
Rb	4.25e-07	5.46e-06	7.23e-06
Riboflavin	0.00058	0.00058	0.00100876
SeO_3	1.00e-05	4.97e-05	2.50e-05
SiO_3	1.41e-05	0.00033075	0.00025225
Sn	1.27e-07	1.27e-07	4.88e-07
Thiamine HCl	0.00617974	0.00644	0.00887267
Thymidine	0.01	0.02	0.01414214
Ti	2.48e-06	2.48e-06	2.38e-06
TiO_2	1.00e-05	N/A	N/A
Vitamin A Acetate	0.00032125	0.00043	N/A
Vitamin B_{12}	5.00e-04	0.00045277	0.00097468
Vitamin D	0.00018028	0.00025	N/A
VO_3	2.09e-06	4.59e-06	5.13e-06
Zn	0.00161685	0.00134086	0.00218115
ZrO	4.65e-06	4.65e-06	9.01e-06

Appendix B

Table B.1: Formulation for Millipore Sigma's Chemically Defined Lipid Mixture 1.

Compound	Concentration (μg/mL)
Arachidonic Acid	2
Linoleic Acid	10
Linolenic Acid	10
Myristic Acid	10
Oleic Acid	10
Palmitic Acid	10
Stearic Acid	10
Cholesterol	220
Tween-80	2200
α-tocopherol acetate	70
Pluronic™ F-68	100000

Table B.2: The medium recipe for Formulation 8 from Plackett-Burman Experiment 2

Component	**Concentration (g/L)**
$CaCl_2$	0.0111
$CuSO_4 \cdot 5H_2O$	1.29854×10^{-6}
$Fe(NO_3)_3 \cdot 9H_2O$	0.00005
$FeSO_4 \cdot 7H_2O$	0.000417
$MgCl_2 \cdot 6H_2O$	0.02033
$NiSO_4 \cdot 6H_2O$	2.43381×10^{-7}
$(NH_4)_6Mo_7O_{24} \cdot 4H_2O$	0.00000618
KCl	0.3118
$NaHCO_3$	1.2
NaCl	6.996
Na_2SeO_3	0.000051882
Na_2HPO_4	0.07102
NaH_2PO_4	0.543
V_2O_5	1.00034×10^{-6}
$ZnCl_2$	0.000204429
L-Alanine	0.00445
L-Arginine	0.121774882
L-Asparagine$\cdot H_2O$	0.04
L-Aspartic Acid	0.04
L-Cystine$\cdot$2HCl	0.1756
L-Cysteine$\cdot$HCl$\cdot H_2O$	0.03129
L-Glutamic Acid	0.0147

Continued on next page

Table B.2: The medium recipe for Formulation 8 from Plackett-Burman Experiment 2

Component	**Concentration (g/L)**
L-Glutamine	0.365
Glycine	0.01875
L-Histidine·HCl·H_2O	0.03148
L-Isoleucine	0.055447
L-Leucine	0.05905
L-Lysine·HCl	0.09125
L-Methionine	0.0172
L-Ornithine·HCl	0.11
L-Phenylalanine	0.03548
L-Proline	0.01725
L-Serine	0.02625
L-Threonine	0.05345
L-Tryptophan	0.00902
L-Tyrosine·2Na·$2H_2O$	0.05579
L-Valine	0.05285
D-Biotin	0.000013
Choline Chloride	0.00898
Folic Acid	0.00266
myo-Inositol	0.0126
Niacinamide	0.004
Nicotinic Acid	0.0005
D-Pantothenic Acid·1/2 Ca^{2+}	0.004

Continued on next page

Table B.2: The medium recipe for Formulation 8 from Plackett-Burman Experiment 2

Component	**Concentration (g/L)**
Pyridoxal·HCl	0.002
Pyridoxine·HCl	0.000163
Riboflavin	0.00219
Thiamine·HCl	0.00217
Vitamin B_{12}	0.00068
Adenine·HCl	0.0001716
D-Glucose	4.5
HEPES	3.5745
Hypoxanthine	0.0021
Linoleic Acid	0.000042
Putrescine·2HCl	0.000081
Pyruvic Acid·Na	0.11
DL-Thioctic Acid	0.000105
Thymidine	0.000365
rEGF	0.00004
Ethanolamine HCl	0.00399914
α-tocopherol	0.00018
Pluronic F68	1
Lipid Mix 1	10 mL

Table B.3: The medium recipe for basal medium from Plackett-Burman Experiment 3

Component	**Concentration (g/L)**
$CaCl_2$	0.0116
$CuSO_4 \cdot 5H_2O$	1.29854×10^{-6}
$Fe(NO_3)_3 \cdot 9H_2O$	0.00005
$FeSO_4 \cdot 7H_2O$	0.000417
$MgCl_2 \cdot 6H_2O$	0.00612
$MgSO_4 \cdot 7H_2O$	0.0158
$MnSO_4 \cdot H_2O$	0.000000151
$NiSO_4 \cdot 6H_2O$	2.43381×10^{-7}
$(NH_4)_6Mo_7O_{24}$ $4H_2O$	0.00000618
$CoCl_2 \cdot 6H_2O$	0.000001
V_2O_5	1.00034×10^{-6}
KCl	0.3118
$NaHCO_3$	1.2
NaCl	6.996
$NaSiO_3 \cdot 9H_2O$	0.0000142
Na_2SeO_3	0.0000173
Na_2HPO_4	0.07102
NaH_2PO_4	0.543
$SnCl_2 \cdot 7H_2O$	0.00000011
$ZnCl_2$	0.000204429
L-Alanine	0.00445
L-Alanyl-L-Glutamine	0.869

Continued on next page

Table B.3: The medium recipe for basal medium from Plackett-Burman Experiment 3

Component	**Concentration (g/L)**
L-Arginine	0.121774882
L-Asparagine·H_2O	0.04
L-Aspartic Acid	0.04
L-Cystine·2HCl	0.1756
L-Cysteine·HCl·H_2O	0.05
L-Glutamic Acid	0.00735
Glycine	0.01875
L-Histidine·HCl·H_2O	0.03148
L-Isoleucine	0.055447
L-Leucine	0.05905
L-Lysine·HCl	0.5
L-Methionine	0.0172
L-Ornithine HCl	0.11
L-Phenylalanine	0.03548
L-Proline	0.01725
L-Serine	0.02625
L-Threonine	0.05345
L-Tryptophan	0.00902
L-Tyrosine·2Na·2H_2O	0.05579
L-Valine	0.05285
D-Biotin	0.000013
Choline Chloride	0.00898

Continued on next page

Table B.3: The medium recipe for basal medium from Plackett-Burman Experiment 3

Component	**Concentration (g/L)**
Folic Acid	0.00266
myo-Inositol	0.0126
Niacinamide	0.00202
D-Pantothenic Acid·1/2 Ca	0.011
Pyridoxal·HCl	0.002
Pyridoxine·HCl	0.000031
Riboflavin	0.00219
Thiamine·HCl	0.00217
Vitamin B_{12}	0.0006887
Adenine HCl	0.0001716
D-Glucose	4.5
HEPES	3.5745
Hypoxanthine	0.0021
Linoleic Acid	0.000042
Putrescine·2HCl	0.000081
Pyruvic Acid·Na	0.11
DL-Thioctic Acid	0.000105
Thymidine	0.000365
Glutathione	0.001
rEGF	40
Ethanolamine HCl	0.003
α-tocopherol	0.014

Continued on next page

Table B.3: The medium recipe for basal medium from Plackett-Burman Experiment 3

Component	**Concentration (g/L)**
Pluronic™ F68	10 mL
Lipid Mix 1	10 mL
Nicotininc acid	0.0005

Table B.4: The medium recipe for Formulations 11, 17, 23 from Plackett-Burman Experiment 4

Component (g/L)	**11**	**17**	**23**
$CaCl_2$	0.011	0.011	0.011
$CuSO_4 \cdot 5H_2O$	1.29854×10^{-6}	1.29854×10^{-6}	1.29854×10^{-6}
$Fe(NO_3)_3 \cdot 9H_2O$	0.00005	0.00005	0.00005
$FeSO_4 \cdot 7H_2O$	0.000417	0.000417	0.000417
$MgCl_2 \cdot 6H_2O$	0.00612	0.00612	0.00612
$MgSO_4 \cdot 7H_2O$	0.0158	0.0158	0.0158
$MnSO_4 \cdot H_2O$	0.000000151	0.000000151	0.000000151
$NiSO_4 \cdot 6H_2O$	8.00×10^{-7}	8.00×10^{-7}	8.00×10^{-7}
$(NH_4)_6Mo_7O_{24} \cdot 4H_2O$	0.00001236	0.00001236	0.00001236
$CoCl_2 \cdot 6H_2O$	2.98791×10^{-6}	0.000001	0.000001
V_2O_5	1.00034×10^{-6}	1.00034×10^{-6}	1.00034×10^{-6}
KCl	0.3118	0.3118	0.3118
$NaHCO_3$	1.2	2.2	1.2
NaCl	6.996	6.996	6.996
$NaSiO_3 \cdot 9H_2O$	0.0000142	0.0000142	0.0000142

Continued on next page

Table B.4: The medium recipe for Formulations 11, 17, 23 from Plackett-Burman Experiment 4

Component (g/L)	**11**	**17**	**23**
Na_2SeO_3	0.000051882	0.000051882	0.000051882
Na_2HPO_4	0.07102	0.07102	0.07102
NaH_2PO_4	0.543	0.543	0.543
$SnCl_2 \cdot 7H_2O$	1.41316×10^{-7}	0	1.41316×10^{-7}
$ZnCl_2$	0.000204429	0.000204429	0.000204429
L-Alanine	0.00445	0.00445	0.00445
L-Alanyl-L-Glutamine	0.8689	0.8689	0.8689
L-Arginine	0.121774882	0.193527118	0.121774882
L-Asparagine$\cdot H_2O$	0.04	0.04	0.04
L-Aspartic Acid	0.04	0.04	0.04
L-Cystine$\cdot$2HCl	0.1756	0.1756	0.1756
L-Cysteine$\cdot$HCl$\cdot H_2O$	0.1	0.1	0.1
L-Glutamic Acid	0.00735	0.00735	0.00735
Glycine	0.01875	0.01875	0.01875
L-Histidine$\cdot$HCl$\cdot H_2O$	0.03148	0.03148	0.03148
L-Isoleucine	0.055447	0.055447	0.134503
L-Leucine	0.28034	0.28034	0.1
L-Lysine$\cdot$HCl	0.5	0.2562	0.2562
L-Methionine	0.1	0.2	0.2
L-Ornithine$\cdot$HCl	0.11	0.11	0.11
L-Phenylalanine	0.03548	0.03548	0.03548

Continued on next page

Table B.4: The medium recipe for Formulations 11, 17, 23 from Plackett-Burman Experiment 4

Component (g/L)	**11**	**17**	**23**
L-Proline	0.01725	0.01725	0.01725
L-Serine	0.02625	0.02625	0.02625
L-Threonine	0.19645	0.19645	0.19645
L-Tryptophan	0.00902	0.00902	0.10318
L-Tyrosine·2Na·2H_2O	0.05579	0.05579	0.05579
L-Valine	0.05285	0.05285	0.05285
D-Biotin	0.0000941	0.000026	0.000026
Choline Chloride	0.014	0.014	0.014
Folic Acid	0.004472484	0.004472484	0.004472484
myo-Inositol	0.022469787	0.022469787	0.0126
Niacinamide	0.00202	0.00202	0.00202
D-Pantothenic Acid·1/2 Ca	0.022	0.022	0.022
Pyridoxal·HCl	0.002	0.002	0.002
Pyridoxine·HCl	0.000031	0.000031	0.000031
Riboflavin	0.00219	0.00219	0.00219
Thiamine·HCl	0.00217	0.002403597	0.00217
Vitamin B12	0.00068	0.00068	0.00068
Adenine·HCl	0.0003432	0.0003432	0.001
Guanosine	0.001	0.001	0.001
Uridine	0.00124542	0.000124542	0.00124542
D-Glucose	4.5	4.5	4.5

Continued on next page

Table B.4: The medium recipe for Formulations 11, 17, 23 from Plackett-Burman Experiment 4

Component (g/L)	**11**	**17**	**23**
HEPES	3.5745	3.5745	3.5745
Hypoxanthine	0.01571115	0.0293223	0.0293223
Linoleic Acid	0.000042	0.000042	0.000042
Phenol Red·Na	0.0081	0.0081	0.0081
Putrescine·2HCl	0.000181	0.00161	0.00161
Pyruvic Acid·Na	0.11	0.11	0.11
DL-Thioctic Acid	0.000105	0.000105	0.000105
Thymidine	0.004240658	0.008116315	0.008116315
Glutathione	0.001	0.001	0.001
rEGF	40	40	40
IGF	1.00E-05	1.00E-05	0
Ethanolamine·HCl	0.004	0.004	0.004
α-tocopherol	0.0003	0.0003	0.0003
Pluronic™ F-68	1	1	1
Lipid Mix 1	10 mL	10 mL	10 mL
Nicotininc acid	0.0008	0.0008	0.0008

Appendix C

List of key up regulated and down regulated cell cycle genes

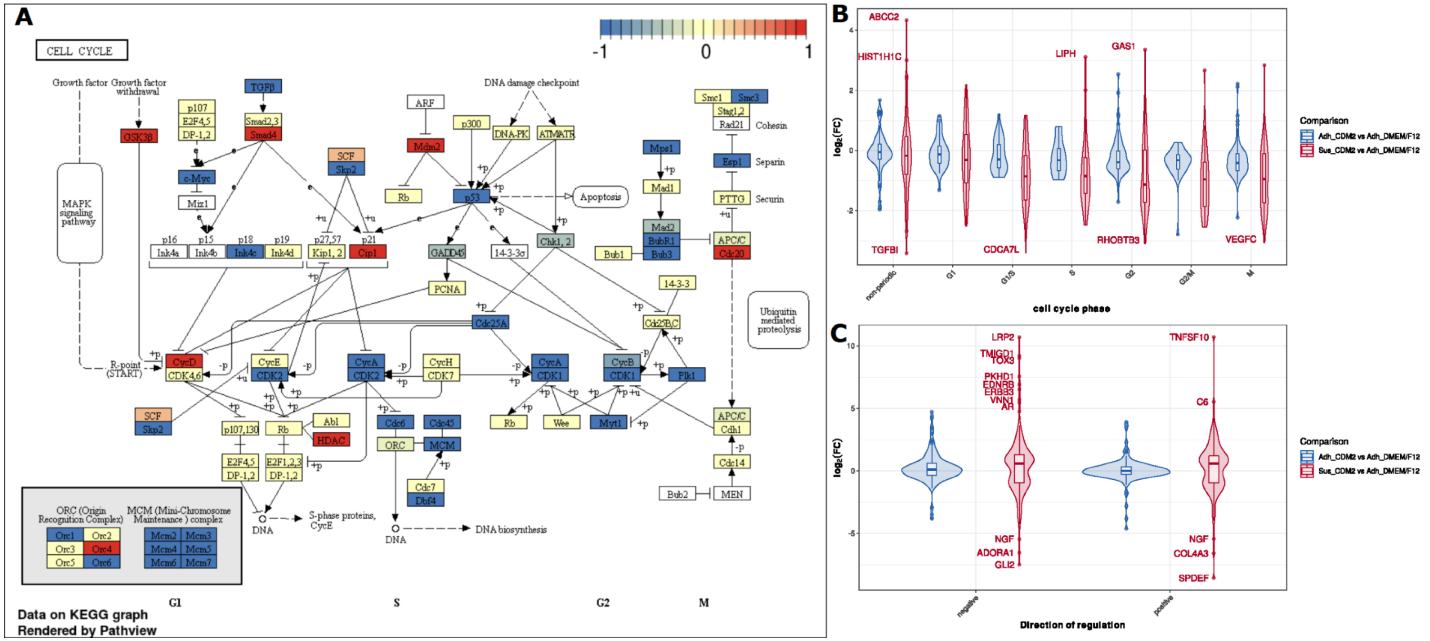

Figure C.1: Expression regulation of cell cycle related genes. **A.** KEGG cell cycle showing differentially regulated genes for the comparison of Sus_CDM2 against Adh_CDM2 rendered with Pathview. The color code determines the direction of significantly differentially regulated genes (FDR < 0.001)according to the legend at the top of the figure. A white background of a text box means that the gene was not identified as expressed. **B.** LFC for the top 500 cell cycle related genes from Cyclebase 3.0 grouped to their peak expression phase. Non-periodic: no known expressional changes during the cell cycle, G1: Gap phase 1 of the cell cycle, G1/S: Gap 1 to synthesis transition phase, S: synthesis phase, G2: Gap phase 2, G2/M: Gap2 to mitosis transition phase, M: mitosis phase. **C.** LFC for genes linked to positive or negative regulation of apoptosis according to Gene Ontology.

Table C.1: Name and description of genes in the cell cycle that were up or downregulated in suspension (Sus_CDM2) cells compared to cells grown adherently in CDM2 (Adh_CDM2). The descriptions were acquired from Genecards or UniProt.

Gene Name	**Regulation**	**Name**	**Description**
GSK3β	Up	Glycogen synthase kinase-3 β	Constituitively active protein kinase that acts as a negative regulator in the hormonal control of glucose, Wnt signaling and regulation of transcription factors and microtubules, by phosphorylating and inactivating glycogen synthase. Plays an important role in ERBB2-dependent stabilization of microtubules at the cell cortex. Through phosphorylation of the anti-apoptotic protein MCL1, may control cell apoptosis in response to growth factors deprivation. Promotes the formation of an anti-apoptotic complex, made of DDX3X, BRIC2 and GSK3B, at death receptors.
Smad4	Up	Mothers against decapentaplegic homolog 4	Common SMAD (co-SMAD) is the coactivator and mediator of signal transduction by TGF-β. Component of the heterotrimeric SMAD2/SMAD3-SMAD4 complex that forms in the nucleus and is required for the TGF-mediated signaling. Also binds zinc.
Mdm2	Up	E3 ubiquitin-protein ligase Mdm2	E3 ubiquitin-protein ligase that mediates ubiquitination of p53/TP53, leading to its degradation by the proteasome. Inhibits p53/TP53- and p73/TP73-mediated cell cycle arrest and apoptosis by binding its transcriptional activation domain. Permits the nuclear export of p53/TP53.
Cdc20	Up	Cell division cycle protein 20 homolog	Required for full ubiquitin ligase activity of the anaphase promoting complex/cyclosome (APC/C).
Cip1	Up	Cyclin-dependent kinase inhibitor 1	May be involved in p53/TP53 mediated inhibition of cellular proliferation in response to DNA damage. Binds to and inhibits cyclin-dependent kinase activity, preventing phosphorylation of critical cyclin-dependent kinase substrates and blocking cell cycle progression.
CycD	Up	Cyclin D	Cyclin which controls both the G1/S and the G2/M transition phases of the cell cycle.
HDAC	Up	Histone deacetylase 1	Responsible for the deacetylation of lysine residues on the N-terminal part of the core histones. Histone deacetylation gives a tag for epigenetic repression and plays an important role in transcriptional regulation, cell cycle progression and developmental events.

Continued on next page

Table C.1: Name and description of genes in the cell cycle that were up or downregulated in suspension (Sus_CDM2) cells compared to cells grown adherently in CDM2 (Adh_CDM2). The descriptions were acquired from Genecards or UniProt.

Gene Name	**Regulation**	**Name**	**Description**
Orc4	Up	Origin recognition complex subunit 4	The origin recognition complex (ORC) subunit. The complex is a highly conserved six subunit protein complex essential for the initiation of the DNA replication in eukaryotic cells. Studies in yeast demonstrated that ORC binds specifically to origins of replication and serves as a platform for the assembly of additional initiation factors such as Cdc6 and Mcm proteins. Gene silencing studies with small interfering RNA demonstrated that this protein plays an essential role in coordinating chromosome replication and segregation with cytokinesis.
LIPH	Up	Lipase H	This gene encodes a membrane-bound member of the mammalian triglyceride lipase family. It catalyzes the production of 2-acyl lysophosphatidic acid (LPA), which is a lipid mediator with diverse biological properties that include platelet aggregation, smooth muscle contraction, and stimulation of cell proliferation and motility.
GAS1	Up	Growth Arrest Specific 1	Growth arrest-specific 1 plays a role in growth suppression. GAS1 blocks entry to S phase and prevents cycling of normal and transformed cells.
SCF	Slightly up	SKP1-CUL1-F-box protein	A multi-protein E3 ubiquitin ligase complex that catalyzes the ubiquitination of proteins destined for 26S proteasomal degradation. Along with the anaphase-promoting complex, SCF has important roles in the ubiquitination of proteins involved in the cell cycle. The SCF complex also marks various other cellular proteins for destruction.
TGF-β	Down	Transforming growth factor beta	Transforming growth factor β (TGF-β) is a multifunctional cytokine belonging to the transforming growth factor superfamily and many other signaling proteins. TGF-β plays a crucial role in the regulation of the cell cycle by blocking progress through G1 phase. In doing so, TGF-β suppresses expression of *c-Myc*, a gene which is involved in G1 cell cycle progression
c-Myc	Down	Myc proto-oncogene protein	This gene is a proto-oncogene and encodes a nuclear phosphoprotein that plays a role in cell cycle progression, apoptosis and cellular transformation. The encoded protein forms a heterodimer with the related transcription factor MAX. This complex binds to the E box DNA consensus sequence and regulates the transcription of specific target genes. Amplification of this gene is frequently observed in numerous human cancers.

Continued on next page

Table C.1: Name and description of genes in the cell cycle that were up or downregulated in suspension (Sus_CDM2) cells compared to cells grown adherently in CDM2 (Adh_CDM2). The descriptions were acquired from Genecards or UniProt.

Gene Name	**Regulation**	**Name**	**Description**
Skp2	Down	S-phase kinase-associated protein 2	Substrate recognition component of a SCF (SKP1-CUL1-F-box protein) E3 ubiquitin-protein ligase complex which mediates the ubiquitination and subsequent proteasomal degradation of target proteins involved in cell cycle progression, signal transduction and transcription. Specifically recognizes phosphorylated CDKN1B/p27kip and is involved in regulation of G1/S transition.
Ink4c	Down	Cyclin Dependent Kinase Inhibitor 2C	This protein has been shown to interact with CDK4 or CDK6, and prevent the activation of the CDK kinases, thus function as a cell growth regulator that controls cell cycle G1 progression.
CDK1	Down	Cyclin-dependent kinase 1	Plays a key role in the control of the eukaryotic cell cycle by modulating the centrosome cycle as well as mitotic onset; promotes G2-M transition, and regulates G1 progress and G1-S transition via association with multiple interphase cyclins. Required in higher cells for entry into S-phase and mitosis.
CDK2	Down	Cyclin-dependent kinase 2	This gene encodes a member of a family of serine/threonine protein kinases that participate in cell cycle regulation. The encoded protein is the catalytic subunit of the cyclin-dependent protein kinase complex, which regulates progression through the cell cycle. Activity of this protein is especially critical during the G1 to S phase transition.
CycA	Down	G2/mitotic-specific cyclin-A	Essential for the control of the cell cycle at the G2/M (mitosis) transition. Interacts with the Cdk1 and Cdk2 protein kinases to form MPF (Cdk/cyclin complex that initiates mitosis called maturation-promoting factor).
Cdc7AL	Down	Cell Division Cycle Associated 7 Like	Participates in MYC-mediated cell transformation and apoptosis; induces anchorage-independent growth and clonogenicity in lymphoblastoid cells. Insufficient to induce tumorigenicity when overexpressed but contributes to MYC-mediated tumorigenesis. May play a role as transcriptional regulator.
Cdc6	Down	Cell division control protein 6 homolog	Involved in the initiation of DNA replication. Also participates in checkpoint controls that ensure DNA replication is completed before mitosis is initiated.

Continued on next page

Table C.1: Name and description of genes in the cell cycle that were up or downregulated in suspension (Sus_CDM2) cells compared to cells grown adherently in CDM2 (Adh_CDM2). The descriptions were acquired from Genecards or UniProt.

Gene Name	**Regulation**	**Name**	**Description**
Cdc45	Down	Cell Division Control Protein 45 Homolog	Required for initiation of chromosomal DNA replication.
Cdc25A	Down	Cell Division Cycle 25A	CDC25A is required for progression from G1 to the S phase of the cell cycle. CDC25A is specifically degraded in response to DNA damage, which prevents cells with chromosomal abnormalities from progressing through cell division. CDC25A is an oncogene, although its exact role in oncogenesis has not been demonstrated.
MCM	Down	Mini-chromosome-maintenance complex	A DNA helicase essential for genomic DNA replication.
Dbf4	Down	DBF4 Zinc Finger	Regulatory subunit for CDC7 which activates its kinase activity thereby playing a central role in DNA replication and cell proliferation. It is also required for the progression of S phase. The complex CDC7-DBF4A selectively phosphorylates MCM2 subunit at 'Ser-40' and 'Ser-53' and then is involved in regulating the initiation of DNA replication during cell cycle.
p53	Down	Tumor Protein p53	Acts as a tumor suppressor in many tumor types; induces growth arrest or apoptosis depending on the physiological circumstances and cell type. Involved in cell cycle regulation as a trans-activator that acts to negatively regulate cell division by controlling a set of genes required for this process. One of the activated genes is an inhibitor of cyclin-dependent kinases. Apoptosis induction seems to be mediated either by stimulation of BAX and FAS antigen expression, or by repression of Bcl-2 expression.
Smc3	Down	Structural Maintenance Of Chromosomes 3	Central component of cohesin, a complex required for chromosome cohesion during the cell cycle. The cohesin complex may form a large proteinaceous ring within which sister chromatids can be trapped. At anaphase, the complex is cleaved and dissociates from chromatin, allowing sister chromatids to segregate. Cohesion is coupled to DNA replication and is involved in DNA repair.

Continued on next page

Table C.1: Name and description of genes in the cell cycle that were up or downregulated in suspension (Sus_CDM2) cells compared to cells grown adherently in CDM2 (Adh_CDM2). The descriptions were acquired from Genecards or UniProt.

Gene Name	**Regulation**	**Name**	**Description**
Mps1	Down	Monopolar Spindle 1 Kinase	This gene encodes a dual specificity protein kinase with the ability to phosphorylate tyrosine, serine and threonine. Associated with cell proliferation, this protein is essential for chromosome alignment at the centromere during mitosis and is required for centrosome duplication. It has been found to be a critical mitotic checkpoint protein for accurate segregation of chromosomes during mitosis.
BubR1	Down	Mitotic spindle checkpoint protein	This gene encodes a kinase involved in spindle checkpoint function. The protein has been localized to the kinetochore and plays a role in the inhibition of the anaphase-promoting complex/cyclosome (APC/C), delaying the onset of anaphase and ensuring proper chromosome segregation. Impaired spindle checkpoint function has been found in many forms of cancer.
Bub3	Down	Mitotic Checkpoint Protein BUB3	This gene encodes a protein involved in spindle checkpoint function. The BUB1/BUB3 complex plays a role in the inhibition of anaphase-promoting complex or cyclosome (APC/C) when spindle-assembly checkpoint is activated and inhibits the ubiquitin ligase activity of APC/C by phosphorylating its activator CDC20.
Esp1	Down	Extra Spindle Pole Bodies Like 1, Separase	Caspase-like protease, which plays a central role in the chromosome segregation by cleaving the SCC1/RAD21 subunit of the cohesin complex at the onset of anaphase.
Myt1	Down	Myelin Transcription Factor 1	Binds to the promoter region of genes encoding proteolipid proteins of the central nervous system.
Plk1	Down	Polo Like Kinase 1	Serine/threonine-protein kinase that performs several important functions throughout M phase of the cell cycle, including the regulation of centrosome maturation and spindle assembly, the removal of cohesins from chromosome arms, the inactivation of anaphase-promoting complex/cyclosome (APC/C) inhibitors, and the regulation of mitotic exit and cytokinesis.
Mcm2-7	Down	Minichromosome Maintenance Complex Component 2	CM2-7 complex (MCM complex) is the putative replicative helicase essential for 'once per cell cycle' DNA replication initiation and elongation in eukaryotic cells. It is required for the entry in S phase and for cell division.

Continued on next page

Table C.1: Name and description of genes in the cell cycle that were up or downregulated in suspension (Sus_CDM2) cells compared to cells grown adherently in CDM2 (Adh_CDM2). The descriptions were acquired from Genecards or UniProt.

Gene Name	**Regulation**	**Name**	**Description**
Orc1,2	Down	Origin Recognition Complex Subunits 1,2	The origin recognition complex (ORC) is a highly conserved six subunit protein complex essential for the initiation of the DNA replication in eukaryotic cells. Studies in yeast demonstrated that ORC binds specifically to origins of replication and serves as a platform for the assembly of additional initiation factors such as Cdc6 and Mcm proteins. Gene silencing studies with small interfering RNA demonstrated that this protein plays an essential role in coordinating chromosome replication and segregation with cytokinesis.
RHOBTB3	Down	Rho Related BTB Domain Containing 3	The protein encoded by this gene belongs to the Rho family of the small GTPase superfamily. The protein plays a role in small GTPase-mediated signal transduction and the organization of the actin filament system.
GADD45	Slightly down	Growth Arrest And DNA Damage Inducible Alpha	This gene is a member of a group of genes whose transcript levels are increased following stressful growth arrest conditions and treatment with DNA-damaging agents. The protein encoded by this gene responds to environmental stresses by mediating activation of the p38/JNK pathway via MTK1/MEKK4 kinase.
Chk1,2	Slightly down	Checkpoint Kinase 1, 2	Serine/threonine-protein kinase which is required for checkpoint-mediated cell cycle arrest and activation of DNA repair in response to the presence of DNA damage or unreplicated DNA. May also negatively regulate cell cycle progression during unperturbed cell cycles. This regulation is achieved by a number of mechanisms that together help to preserve the integrity of the genome.
CycB	Slightly down	Cyclin B1	The protein encoded by this gene is a regulatory protein involved in mitosis. The gene product complexes with p34(cdc2) to form the maturation-promoting factor (MPF). The encoded protein is necessary for proper control of the G2/M transition phase of the cell cycle.
Mad2	Slightly down	Mitotic spindle checkpoint component MAD2	Central component of the spindle assembly checkpoint which is a feedback control that prevents cells with incompletely assembled spindles from leaving mitosis. The mitotic checkpoint complex and presumably the MAD2-CDC20 subcomplex inhibit the ubiquitin ligase activity of the anaphase promoting complex/cyclosome (APC/C) by preventing its activation by CDC20.

Table C.2: A list of the 25 genes that were identified as upregulated in the HPA kidney tissue gene dataset, along with their associated ligand and description of the protein function according to UniProt.

Protein Name	**Protein Name**	**Ligand**	**Protein Function**
BBOX1	Gamma-butyrobetaine hydroxylase 1	Iron, Metal-binding, Zinc	Catalyzes the formation of L-carnitine from gamma-butyrobetaine.
CALB1	Calbindin 1	Calcium, Metal-binding, Vitamin D	Buffers cytosolic calcium. May stimulate a membrane Ca^{2+}- ATPase and a 3',5'-cyclic nucleotide phosphodiesterase.
CLCN5	Chloride voltage-gated channel 5	ATP-binding, Chloride, Nucleotide-binding	Proton-coupled chloride transporter. Functions as antiport system and exchanges chloride ions against protons.
CLTRN	Collectrin, amino acid transport regulator		Plays an important role in amino acid transport by acting as binding partner of amino acid transporters SLC6A18 and SLC6A19, regulating their trafficking on the cell surface and their amino acid transporter activity.
CYS1	Cystin 1		
FMO1	Flavin containing monooxygenase 1	FAD, Flavoprotein, NADP	This protein is involved in the oxidative metabolism of a variety of xenobiotics such as drugs and pesticides.
GGACT	Gamma-glutamylamine cyclotransferase		Contributes to degradation of proteins cross-linked by transglutaminases by degrading the cross-link between a lysine and a glutamic acid residue.
LHX1	LIM homeobox 1	Metal-binding, Zinc	Potential transcription factor. May play a role in early mesoderm formation and later in lateral mesoderm differentiation and neurogenesis.
MIOX	Myo-inositol oxygenase	Iron, Metal-binding	

Continued on next page

Table C.2: A list of the 25 genes that were identified as upregulated in the HPA kidney tissue gene dataset, along with their associated ligand and description of the protein function according to UniProt.

Protein Name	**Protein Name**	**Ligand**	**Protein Function**
NAT8	N-acetyltransferase 8 (putative)		Acetylates the free α-amino group of cysteine S-conjugates to form mercapturic acids. This is the final step in a major route for detoxification of a wide variety of reactive electrophiles which starts with their incorporation into glutathione S-conjugates. The glutathione S-conjugates are then further processed into cysteine S-conjugates and finally mercapturic acids which are water soluble and can be readily excreted in urine or bile. Alternatively, may have a lysine N-acetyltransferase activity catalyzing peptidyl-lysine N6-acetylation of various proteins. Thereby, may regulate apoptosis through the acetylation and the regulation of the expression of PROM1.
NOX4	NADPH oxidase 4	NADP	Constitutive NADPH oxidase which generates superoxide intracellularly upon formation of a complex with CYBA/p22phox. Regulates signaling cascades probably through phosphatases inhibition. May regulate insulin signaling cascade. May play a role in apoptosis, bone resorption and lipolysaccharide-mediated activation of NFKB. May produce superoxide in the nucleus and play a role in regulating gene expression upon cell stimulation.
NPR3	Natriuretic peptide receptor 3	Chloride	Receptor for the natriuretic peptide hormones, binding with similar affinities atrial natriuretic peptide NPPA/ANP, brain natriuretic peptide NPPB/BNP, and C-type natriuretic peptide NPPC/CNP.
PKHD1	PKHD1, fibrocystin/polyductin	Receptor	May be required for correct bipolar cell division through the regulation of centrosome duplication and mitotic spindle assembly. May be a receptor protein that acts in collecting-duct and biliary differentiation.
SLC12A1	Solute carrier family 12 member 1	Chloride, Potassium, Sodium	Renal sodium, potassium and chloride ion cotransporter that mediates the transepithelial NaCl reabsorption in the thick ascending limb and plays an essential role in the urinary concentration and volume regulation.
SLC13A1	Solute carrier family 13 member 1	Sodium	Sodium/sulfate cotransporter that mediates sulfate reabsorption in the kidney.
SLC17A1	Solute carrier family 17 member 1	Sodium	Important for the resorption of phosphate by the kidney. May be involved in actively transporting phosphate into cells via Na^+ cotransport in the renal brush border membrane.

Continued on next page

Table C.2: A list of the 25 genes that were identified as upregulated in the HPA kidney tissue gene dataset, along with their associated ligand and description of the protein function according to UniProt.

Protein Name	**Protein Name**	**Ligand**	**Protein Function**
SLC17A3	Solute carrier family 17 member 3	Sodium	Voltage-driven, multispecific, organic anion transporter able to transport para-aminohippurate (PAH), estrone sulfate, estradiol-17-beta-glucuronide, bumetanide, and ochratoxin A.
SLC22A12	Solute carrier family 22 member 12	Urate	Required for efficient urate re-absorption in the kidney. Regulates blood urate levels. Mediates saturable urate uptake by facilitating the exchange of urate against organic anions.
SLC22A2	Solute carrier family 22 member 2		Mediates tubular uptake of organic compounds from circulation. Mediates the influx of agmatine, dopamine, noradrenaline (norepinephrine), serotonin, choline, famotidine, ranitidine, histamine, creatinine, amantadine, memantine, acriflavine, 4-[4-(dimethylamino)-styryl]-N-methylpyridinium ASP, amiloride, metformin, N-1-methylnicotinamide (NMN), tetraethylammonium (TEA), 1-methyl-4-phenylpyridinium (MPP), cimetidine, cisplatin and oxaliplatin.
SLC34A1	Solute carrier family 34 member 1	Sodium	Involved in actively transporting phosphate into cells via Na^+ cotransport in the renal brush border membrane. Probably mediates 70-80% of the apical influx.
SLC6A18	Solute carrier family 6 member 18		
SLC7A13	Solute carrier family 7 member 13		Mediates the transport L-aspartate and L-glutamate in a sodium-independent manner.
TINAG	Tubulointerstitial nephritis antigen		Mediates adhesion of proximal tubule epithelial cells via integrins α_3-β_1 and α_V-β_3. This is a non catalytic peptidase C1 family protein.
TMEM52B	Transmembrane protein 52B		

Table C.3: List of transporter genes that are downregulated in suspension Vero cells compared to adherent Vero cells that are grown in CDM2 or in DMEM/F12 + 10% FBS. Descriptions of the genes were taken from Human Protein Atlas and UniProt.

Gene Name	**Full Name**	**Gene Summary**
ABCB10	ATP Binding Cassette Subfamily B Member 10	The membrane-associated protein encoded by this gene is a member of the superfamily of ATP-binding cassette (ABC) transporters. ABC proteins transport various molecules across extra- and intra-cellular membranes. This protein is a member of the MDR/TAP subfamily. Members of the MDR/TAP subfamily are involved in multidrug resistance.
SLC15A3	Solute Carrier Family 15 Member 3	Proton-coupled amino-acid transporter that transports free histidine and certain di- and tripeptides. It is also able to transport carnosine.
SLC16A9	Solute Carrier Family 16 Member 9	This gene encodes a protein that is a proton-linked monocarboxylate transporter. It may catalyze the transport of monocarboxylates across the plasma membrane.
SLC18A3	Solute Carrier Family 18 Member A3	This gene is a member of the vesicular amine transporter family. The encoded transmembrane protein transports acetylcholine into secretory vesicles for release into the extracellular space.
SLC20A2	Solute Carrier Family 20 Member 2	This gene encodes a member of the inorganic phosphate transporter family. The encoded protein is a type 3 sodium-dependent phosphate symporter that plays an important role in phosphate homeostasis by mediating cellular phosphate uptake.
SLC25A12	Solute Carrier Family 25 Member 12	Mitochondrial and calcium-binding carrier that catalyzes the calcium-dependent exchange of cytoplasmic glutamate with mitochondrial aspartate across the mitochondrial inner membrane. It may also have a function in the urea cycle.
SLC25A19	Solute Carrier Family 25 Member 19	This gene encodes for a mitochondrial transporter mediating uptake of thiamine pyrophosphate (ThPP) into mitochondria.
SLC25A37	Solute Carrier Family 25 Member 37	SLC25A37 is a solute carrier localized in the mitochondrial inner membrane. It functions as an essential iron importer for the synthesis of mitochondrial heme and iron-sulfur clusters
SLC2A1	Solute Carrier Family 2 Member 1	Facilitative glucose transporter, which is responsible for constitutive or basal glucose uptake. It has a very broad substrate specificity, which can transport a wide range of aldoses including both pentoses and hexoses.

Continued on next page

Table C.3: List of transporter genes that are downregulated in suspension Vero cells compared to adherent Vero cells that are grown in CDM2 or in DMEM/F12 + 10% FBS. Descriptions of the genes were taken from Human Protein Atlas and UniProt.

Gene Name	**Full Name**	**Gene Summary**
SLC2A10	Solute Carrier Family 2 Member 10	Facilitative glucose transporter required for the development of the cardiovascular system.
SLC2A14	Solute Carrier Family 2 Member 14	Members of the glucose transporter (GLUT) family, including SLC2A14, are highly conserved integral membrane proteins that transport hexoses such as glucose and fructose into all mammalian cells.
SLC30A3	Solute Carrier Family 30 Member 3	Gene Ontology (GO) annotations related to this gene include cation transmembrane transporter activity and zinc-transporting ATPase activity.
SLC35F2	Solute Carrier Family 35 Member F2	Putative solute transporter.
SLC37A3	Solute Carrier Family 37 Member 3	May transport cytoplasmic glucose-6-phosphate into the lumen of the endoplasmic reticulum and translocate inorganic phosphate into the opposite direction.
SLC38A10	Solute Carrier Family 38 Member 10	Functions as a sodium-dependent amino acid transporter. Mediates the saturable, pH-sensitive and electrogenic cotransport of neutral amino acids and sodium ions with a stoichiometry of 1:1.
SLC4A11	Solute Carrier Family 4 Member 11	This gene encodes a voltage-regulated, electrogenic sodium-coupled borate cotransporter that is essential for borate homeostasis, cell growth and cell proliferation.
SLC7A5	Solute Carrier Family 7 Member 5	The heterodimer with SLC3A2 functions as sodium-independent, high-affinity transporter that mediates uptake of large neutral amino acids such as phenylalanine, tyrosine, L-DOPA, leucine, histidine, methionine and tryptophan
SLC8A2	Solute Carrier Family 8 Member A2	Mediates the electrogenic exchange of Ca^{2+} against Na^{+} ions across the cell membrane, and thereby contributes to the regulation of cytoplasmic Ca^{2+} levels and Ca^{2+}-dependent cellular processes.
SLC9A3R2	SLC9A3 Regulator 2	Scaffold protein that connects plasma membrane proteins with members of the ezrin/moesin/radixin family and thereby helps to link them to the actin cytoskeleton and to regulate their surface expression. Necessary for cAMP-mediated phosphorylation and inhibition of SLC9A3. May also act as scaffold protein in the nucleus.

Continued on next page

Table C.3: List of transporter genes that are downregulated in suspension Vero cells compared to adherent Vero cells that are grown in CDM2 or in DMEM/F12 + 10% FBS. Descriptions of the genes were taken from Human Protein Atlas and UniProt.

Gene Name	**Full Name**	**Gene Summary**
SLC9A5	Solute Carrier Family 9 Member A5	Involved in pH regulation to eliminate acids generated by active metabolism or to counter adverse environmental conditions. Major proton extruding system driven by the inward sodium ion chemical gradient. Plays an important role in signal transduction.
SLCO3A1	Solute Carrier Organic Anion Transporter Family Member 3A1	Mediates the Na^+-independent transport of organic anions such as estrone-3-sulfate. Mediates transport of prostaglandins E1 and E2, thyroxine (T4), deltorphin II, BQ-123 and vasopressin.
SLCO5A1	Solute Carrier Organic Anion Transporter Family Member 5A1	This gene encodes a 12 transmembrane domain protein that is a member of the solute carrier organic anion transporter superfamily.

Appendix D

List of Differentially Expressed Genes and their Associated KEGG Pathways

Table D.1: A list of the genes that are up or down-regulated in the KEGG pathways that were identified during the RNA-Seq analysis when comparing suspension to adherent Vero cells grown in CDM2.

KEGG ID	Gene Name	Definition	Regulation	Associated Pathways
1.1.1.62	HSD17B1	17β-estradiol 17-dehydrogennase	upregulated	Steroid Hormone Biosynthesis, Metabolic pathways, ovarian steroidogenesis

Continued on next page

Table D.1: A list of the genes that are up or down-regulated in the KEGG pathways that were identified during the RNA-Seq analysis when comparing suspension to adherent Vero cells grown in CDM2.

KEGG ID	Gene Name	Definition	Regulation	Associated Pathways
2.4.1.17	UGT	glucuronosyltransferase	upregulated	Pentose and glucuronate interconversions, Ascorbate and aldarate metabolism, Steroid hormone biosynthesis, Retinol metabolism, Metabolism of xenobiotics by cytochrome P450, Drug metabolism - cytochrome P450, Drug metabolism - other enzymes, Metabolic pathways, Biosynthesis of secondary metabolites, Biosynthesis of cofactors, Bile secretion, Chemical carcinogenesis - DNA adducts, Chemical carcinogenesis - receptor activation
1.14.14.1	CYP1A1	Cytochrome P450 Family 1 subfamily A1	upregulated	Steroid hormone biosynthesis, Tryptophan metabolism, Retinol metabolism, Metabolism of xenobiotics by cytochrome P450, Metabolic pathways, Ovarian steroidogenesis, Chemical carcinogenesis - DNA adducts, Chemical carcinogenesis - receptor activation, Lipid and atherosclerosis
1.1.1.149	E1.1.149	20α-hydroxysteroid dehydrogenase	upregulated	Steroid Hormone Biosynthesis
1.3.1.22	SRD5A1	3-oxo-5-α-steroid 4-dehydrogenase 1	upregulated	Steroid Hormone Biosynthesis
1.1.1.62	HSD17B2	17β-estradiol 17-dehydrogenase / 3α(17β)-hydroxysteroid dehydrogenase (NAD+)	upregulated	Steroid Hormone Biosynthesis, Metabolic pathways, ovarian steroidogenesis

Continued on next page

Table D.1: A list of the genes that are up or down-regulated in the KEGG pathways that were identified during the RNA-Seq analysis when comparing suspension to adherent Vero cells grown in CDM2.

KEGG ID	Gene Name	Definition	Regulation	Associated Pathways
1.1.1.51	E1.1.1.51	3 (or 17) β-hydroxysteroid dehydrogenase	down	Steroid Hormone Biosynthesis, Steroid degradation, Metabolic pathways
2.1.1.6	COMT	catechol O-methyltrasferase	down	Steroid hormone biosynthesis, Tyrosine metabolism, Betalain biosynthesis, Metabolic pathways, Dopaminergic synapse
1.1.1.213	AKR1C2	3α-hydroxysteroid 3-dehydrogenase	down	Steroid Hormone Biosynthesis, Chemical carcinogenesis - DNA adducts
RDH	RDH5	11-cis-retinol dehydrogenase	upregulated	Retinol Metabolism
1.399.23	E.1.3.99.23	all-trans-retinol 13,14-reductase	upregulated	Retinol Metabolism
DHRS	DHRS3	short-chain dehydrogenase/reductase 3	upregulated	Retinol Metabolism, Metabolic pathways, Biosyntheis of cofactors
DGAT	hypothetical protein	diacylglycerol 0-acyltransferase 1	upregulated	Glycerolipid metabolism, retinol metabolism, metabolic pathways, fat digestion and absorption
CYP1A	CYP1A1	Cytochrome P450 Family 1 subfamily A1	upregulated	Steroid hormone biosynthesis, Tryptophan metabolism, Retinol metabolism, Metabolism of xenobiotics by cytochrome P450, Metabolic pathways, Ovarian steroidogenesis, Chemical carcinogenesis - DNA adducts, Chemical carcinogenesis - receptor activation, Lipid and atherosclerosis

Continued on next page

Table D.1: A list of the genes that are up or down-regulated in the KEGG pathways that were identified during the RNA-Seq analysis when comparing suspension to adherent Vero cells grown in CDM2.

KEGG ID	Gene Name	Definition	Regulation	Associated Pathways
CYP3A	CYP3A4	Cytochrome P450 Family 3 subfamily A4	upregulated	Steroid hormone biosynthesis, Linoleic acid metabolism, Retinol metabolism, Metabolism of xenobiotics by cytochrome P450, Drug metabolism - cytochrome P450, Drug metabolism - other enzymes, Metabolic pathways, Bile secretion, Chemical carcinogenesis - DNA adducts, Chemical carcinogenesis - receptor activation
CYP1A1	CYP1A1	Cytochrome P450 Family 1 subfamily A1	upregulated	Steroid hormone biosynthesis, Tryptophan metabolism, Retinol metabolism, Metabolism of xenobiotics by cytochrome P450, Metabolic pathways, Ovarian steroidogenesis, Chemical carcinogenesis - DNA adducts, Chemical carcinogenesis - receptor activation, Lipid and atherosclerosis
CYP4A11	CYP4A	long-chain fatty acid omega-monooxygenase	upregulated	Fatty acid degradation, Arachidonic acid metabolism, Retinol metabolism, Metabolic pathways, PPAR signaling pathway, Vascular smooth muscle contraction, Inflammatory mediator regulation of TRP channels

Continued on next page

Table D.1: A list of the genes that are up or down-regulated in the KEGG pathways that were identified during the RNA-Seq analysis when comparing suspension to adherent Vero cells grown in CDM2.

KEGG ID	Gene Name	Definition	Regulation	Associated Pathways
UGT	hypothetical protein	glucuronosyltransferase	upregulated	Pentose and glucuronate interconversions, Ascorbate and aldarate metabolism, Steroid hormone biosynthesis, Retinol metabolism, Porphyrin and chlorophyll metabolism, Metabolism of xenobiotics by cytochrome P450, Drug metabolism - cytochrome P450, Drug metabolism - other enzymes, Metabolic pathways, Biosynthesis of secondary metabolites, Biosynthesis of cofactors, Bile secretion, Chemical carcinogenesis
1.2.1.36	ALDH1A	retinal dehydrogenase	down	Retinol Metabolism, Metabolic pathways
1.13.11.63	BCMO1, BCDO1	beta-carotene 15,15'-dioxygenase	down	Retinol Metabolism, Metabolic pathways, Biosynthesis of cofactors
UGT2B7	UGT2B7	UDP-glucuronosyltransferase 2B7	down	Pentose and glucuronate interconversions, Ascorbate and aldarate metabolism, Steroid hormone biosynthesis, Retinol metabolism, Porphyrin and chlorophyll metabolism, Metabolism of xenobiotics by cytochrome P450, Drug metabolism - cytochrome P450 ,Drug metabolism - other enzymes, Metabolic pathways, Biosynthesis of cofactors, Bile secretion, Chemical carcinogenesis - DNA adducts, Chemical carcinogenesis - receptor activation

Continued on next page

Table D.1: A list of the genes that are up or down-regulated in the KEGG pathways that were identified during the RNA-Seq analysis when comparing suspension to adherent Vero cells grown in CDM2.

KEGG ID	Gene Name	Definition	Regulation	Associated Pathways
CPT1	CPT1C, CATL1, CPT1-B, CPT1P, CPTI-B, CPTIC, SPG73	carnitine palmitoyltransferase 1C	upregulated	Fatty acid degradation, Fatty acid metabolism, PPAR signaling pathway, AMPK signaling pathway, Thermogenesis, Adipocytokine signaling pathway, Glucagon signaling pathway
CPT2	CPT2, CPT1, CPTASE, IIAE4	carnitine palmitoyltransferase 2	upregulated	Fatty acid degradation, Fatty acid metabolism, PPAR signaling pathway, Thermogenesis, Diabetic cardiomyopathy
1.3.3.6	ACOX1, ACOX, MITCH, PALMCOX, SCOX	acyl-CoA oxidase 1	upregulated	Fatty acid degradation, β-Alanine metabolism, α-Linolenic acid metabolism, Propanoate metabolism, Biosynthesis of unsaturated fatty acids, Metabolic pathways, Carbon metabolism, Fatty acid metabolism, PPAR signaling pathway, cAMP signaling pathway, Peroxisome
1.3.8.7	ACADM, ACAD1, MCAD, MCADH	acyl-CoA dehydrogenase medium chain	upregulated	Fatty acid degradation, Valine, leucine and isoleucine degradation, Metabolic pathways, Fatty acid metabolism, PPAR signaling pathway
4.2.1.17	ECHS1, ECHS1D, SCEH	enoyl-CoA hydratase, short chain 1	upregulated	Fatty acid elongation, Fatty acid degradation, Valine, leucine and isoleucine degradation, Lysine degradation, Tryptophan metabolism, β-Alanine metabolism, Propanoate metabolism, Butanoate metabolism, Metabolic pathways, Carbon metabolism, Fatty acid metabolism

Continued on next page

Table D.1: A list of the genes that are up or down-regulated in the KEGG pathways that were identified during the RNA-Seq analysis when comparing suspension to adherent Vero cells grown in CDM2.

KEGG ID	Gene Name	Definition	Regulation	Associated Pathways
1.1.1.35	EHHADH, ECHD, FRTS3, L-PBE, LBFP, LBP, MFE1, PBFE	enoyl-CoA hydratase and 3-hydroxyacyl CoA dehydrogenase	upregulated	Fatty acid degradation, Valine, leucine and isoleucine degradation, Lysine degradation, Tryptophan metabolism, β-Alanine metabolism, Propanoate metabolism, Butanoate metabolism, Metabolic pathways, Fatty acid metabolism, PPAR signaling pathway, Peroxisome
1.1.1.211	HADHA, ECHA, GBP, HADH, LCEH, LCHAD, MTPA, TP-ALPHA	hydroxyacyl-CoA dehydrogenase trifunctional multienzyme complex subunit α	upregulated	Fatty acid elongation, Fatty acid degradation, Valine, leucine and isoleucine degradation, Lysine degradation, Tryptophan metabolism, β-Alanine metabolism, Propanoate metabolism, Butanoate metabolism, Metabolic pathways, Fatty acid metabolism
2.3.1.16	ACAA2, DSAEC	acetyl-CoA acyltransferase 2	upregulated	Fatty acid elongation, Fatty acid degradation, Valine, leucine and isoleucine degradation, Metabolic pathways, Fatty acid metabolism
1.3.99.-	ACAD8, ACAD-8, ARC42, IBDH	acyl-CoA dehydrogenase family member 8	upregulated	Valine, leucine and isoleucine degradation, Metabolic pathways
5.3.3.8	ECI2, ACBD2, DRS-1, DRS1, HCA88, PECI, dJ1013A10.3	enoyl-CoA delta isomerase 2	upregulated	Fatty acid degradation, Peroxisome

Continued on next page

Table D.1: A list of the genes that are up or down-regulated in the KEGG pathways that were identified during the RNA-Seq analysis when comparing suspension to adherent Vero cells grown in CDM2.

KEGG ID	**Gene Name**	**Definition**	**Regulation**	**Associated Pathways**
1.2.1.3	ALDH2, ALDH-E2, ALDHI, ALDM	aldehyde dehydrogenase 2 family member	upregulated	Glycolysis / Gluconeogenesis, Ascorbate and aldarate metabolism, Fatty acid degradation ,Valine, leucine and isoleucine degradation, Lysine degradation, Arginine and proline metabolism, Histidine metabolism, Tryptophan metabolism, β-Alanine metabolism, Glycerolipid metabolism, Pyruvate metabolism, Pantothenate and CoA biosynthesis, Metabolic pathways, Biosynthesis of cofactors
1.14.14.80	CYP2U1, P450TEC, SPG49, SPG56	cytochrome P450 family 2 subfamily U member 1	upregulated	Fatty acid degradation, Arachidonic acid metabolism, Metabolic pathways

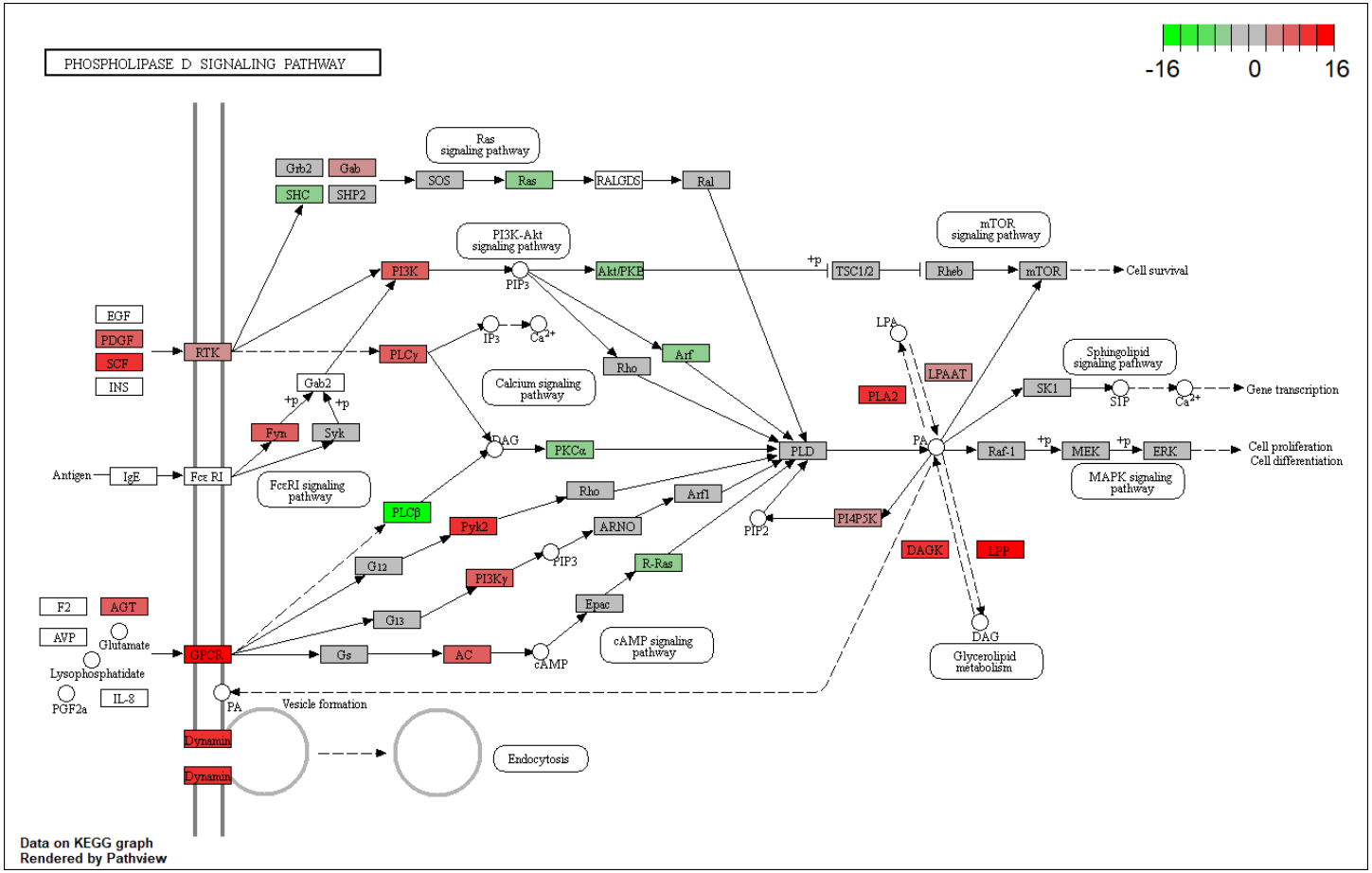

Figure D.1: The expression of genes associated with phospholipase D signalling pathway in suspension compared to adherent Vero cells grown in CDM2 media. Genes that are differentially expressed are highlighted in green (downregulated) and red (upregulated) to demonstrate the changes in suspension cells compared to adherent cells using the Pathview package.

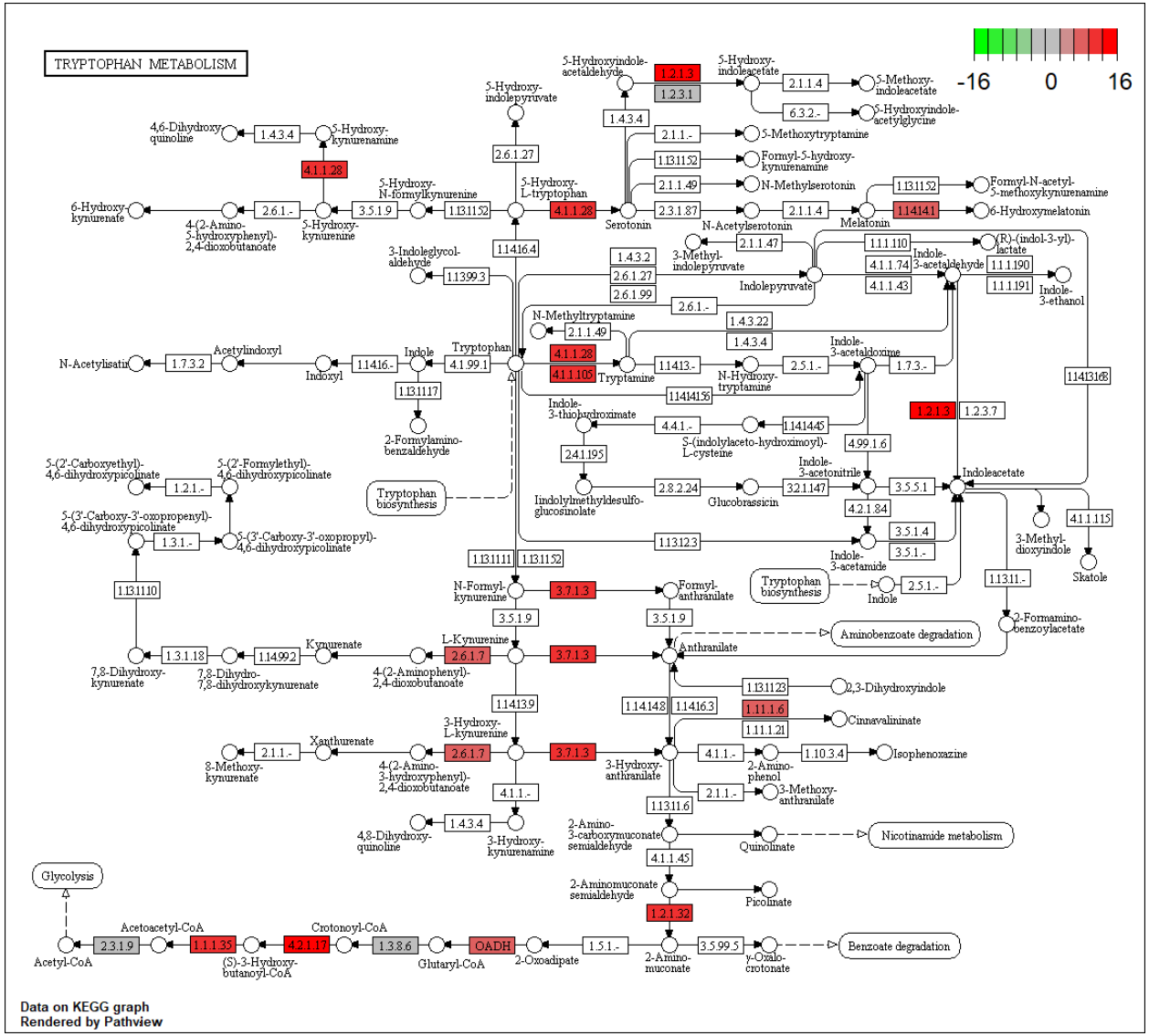

Figure D.2: The expression of genes associated with tryptophan metabolism pathway in suspension compared to adherent Vero cells grown in CDM2 media. Genes that are differentially expressed are highlighted in green (downregulated) and red (upregulated) to demonstrate the changes in suspension cells compared to adherent cells using the Pathview package.

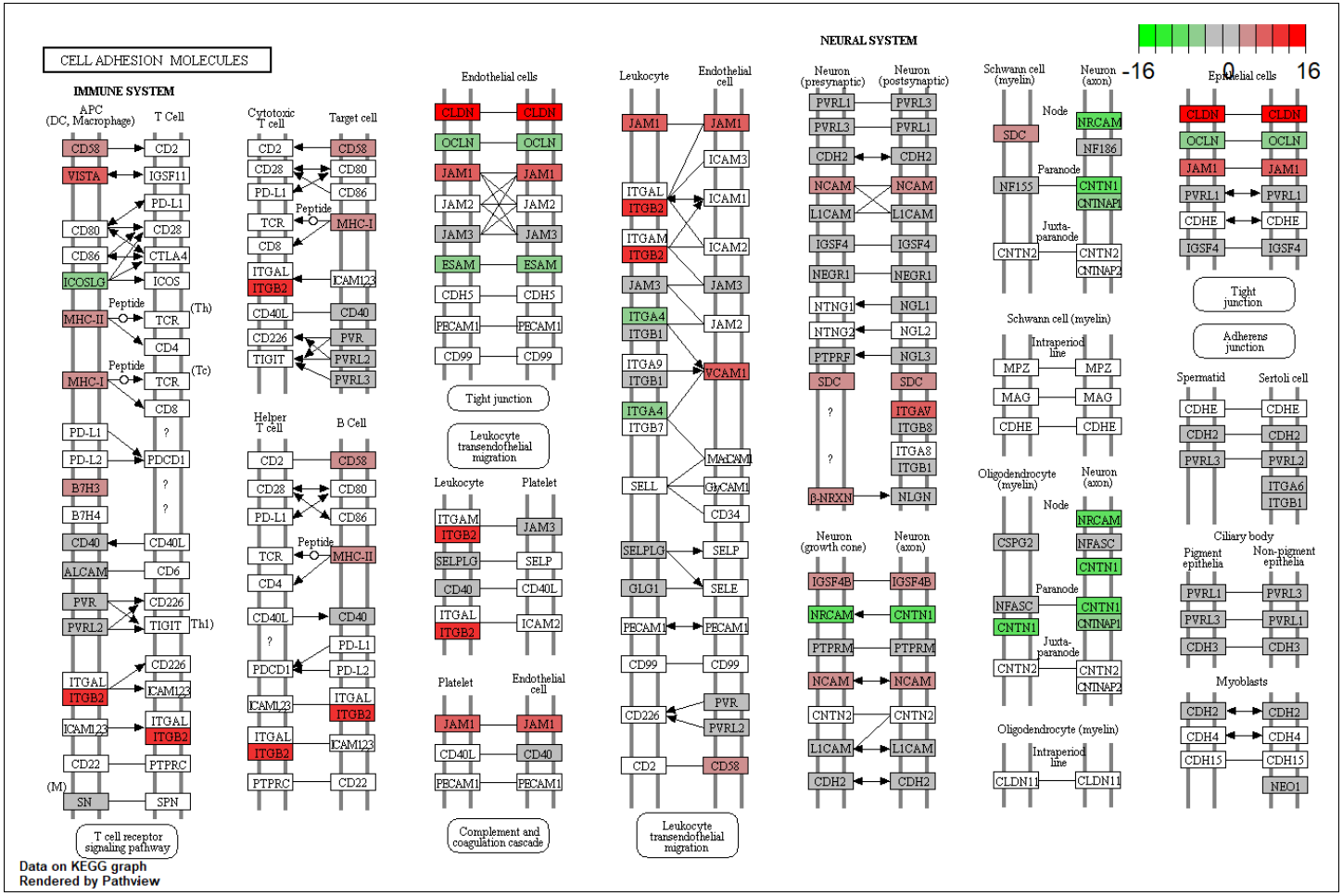

Figure D.3: The expression of genes associated with cell adhesion molecule signalling pathway in suspension compared to adherent Vero cells grown in CDM2 media. Genes that are differentially expressed are highlighted in green (downregulated) and red (upregulated) to demonstrate the changes in suspension cells compared to adherent cells using the Pathview package.

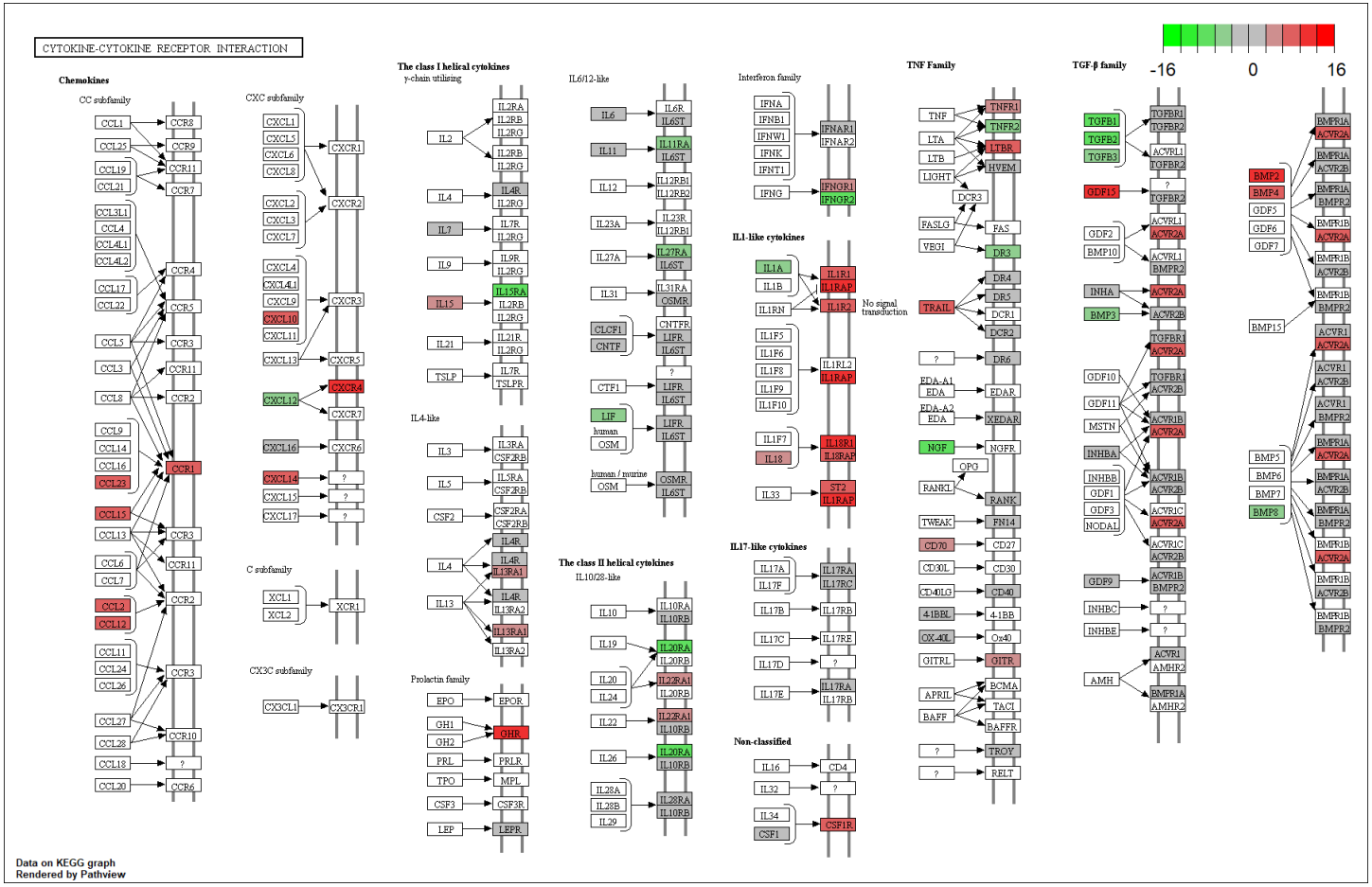

Figure D.4: The expression of genes associated with cytokine-cytokine receptor interaction signalling pathway in suspension compared to adherent Vero cells grown in CDM2 media. Genes that are differentially expressed are highlighted in green (downregulated) and red (upregulated) to demonstrate the changes in suspension cells compared to adherent cells using the Pathview package.

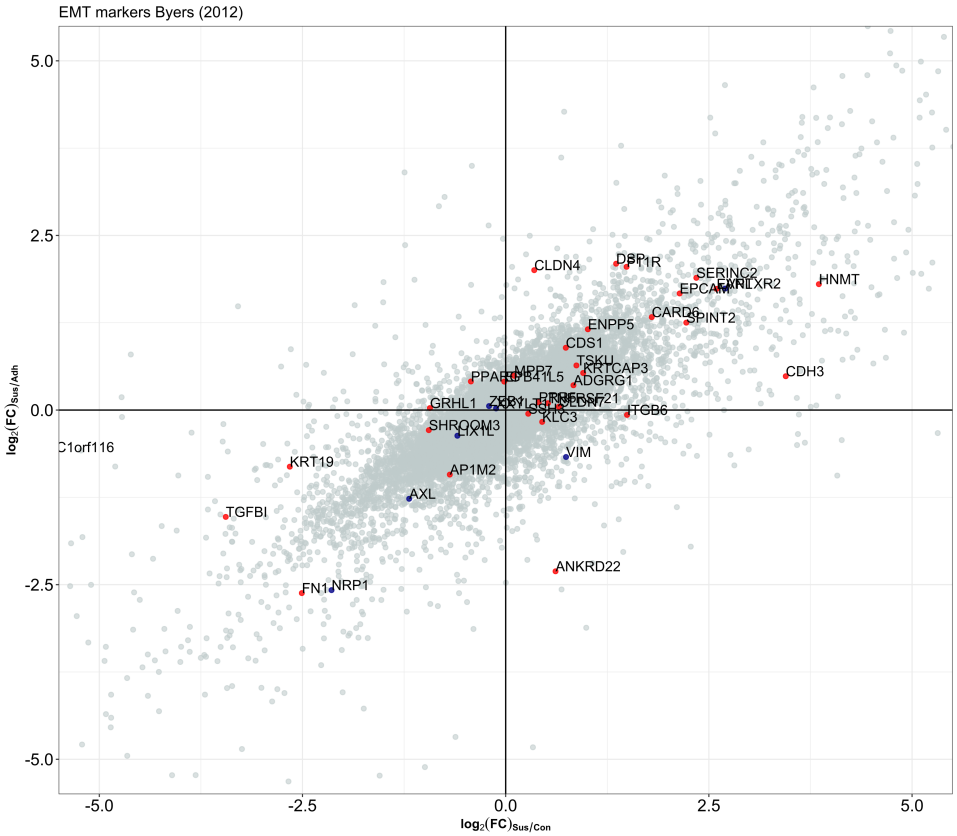

Figure D.5: Mean difference plot of identified pro-mesenchymal (blue) or anti-mesenchymal (red) genes with log fold-change between Sus and Adh (adherent Vero cells grown in CDM2) groups (y-axis), or Sus and Con (adherent Vero cells grown in DMEM/F12 + 10% FBS) (x-axis). Gene targets associated with EMT were identified in Byers *et al.* [60]

Figure D.6: Mean difference plot of identified pro-mesenchymal (blue) or anti-mesenchymal (red) genes with log fold-change between Sus and Adh (adherent Vero cells grown in CDM2) groups (y-axis), or Sus and Con (adherent Vero cells grown in DMEM/F12 + 10% FBS) (x-axis). Gene targets associated with EMT were identified in Kalluri *et al.* [208]

Appendix E

Table E.1: The medium recipe for CDM4. Use Sigma DMEM/F12 media (cat#D9785-10L) (w/o bicarbonate, phenol red, and glutamine, leucine, lysine, methionine) for suspension media for CHO-K1 or Vero cells, or Corning DMEM/F12 for suspension MDCK and HEK293T, or adherent Vero.

Component	**Final Concentration (g/L)**
Metals	
$CaCl_2$	0.116
$CuSO_4$·5H20	0.0000013
$Fe(NO_3)_3$·$9H_2O$	0.00005
$FeSO_4$·$7H_2O$	0.000417
Ferric Citrate	0.0005
$MgCl_2$·$6H_2O$	0.612
$MgSO_4$	0.4884
$MnSO_4$·H_2O	0.000000151
$NiSO_4$·$6H_2O$	0.0000008

Continued on next page

Table E.1: The medium recipe for CDM4. Use Sigma DMEM/F12 media (cat#D9785-10L) (w/o bicarbonate, phenol red, and glutamine, leucine, lysine, methionine) for suspension media for CHO-K1 or Vero cells, or Corning DMEM/F12 for suspension MDCK and HEK293T, or adherent Vero.

Component	**Final Concentration (g/L)**
$(NH_4)_6Mo_7O_{24}{\cdot}4H_2O$	0.00000618
$CoCl_2{\cdot}6H_2O$	0.000002988
V_2O_5	1.00034E-06
KCl	0.3118
$NaHCO_3$	2.2
NaCl	6.9955
$NaSiO_3{\cdot}9H_2O$	0.0000142
Na_2SeO_3	0.00005188
Na_2HPO_4	0.07102
$NaH_2PO_4{\cdot}H_2O$	0.0625
$SnCl_2{\cdot}7H_2O$	0.0000001413
$ZnCl_2$	0.000922
Amino Acids	
L-Alanine	0.00445
L-Arginine	0.2975
L-Asparagine$\cdot H_2O$	0.0475
L-Aspartic Acid	0.04665
Citrulline	0.0037
L-Cystine·2HCl	0.03129

Continued on next page

Table E.1: The medium recipe for CDM4. Use Sigma DMEM/F12 media (cat#D9785-10L) (w/o bicarbonate, phenol red, and glutamine, leucine, lysine, methionine) for suspension media for CHO-K1 or Vero cells, or Corning DMEM/F12 for suspension MDCK and HEK293T, or adherent Vero.

Component	**Final Concentration (g/L)**
L-Cysteine·HCl·H_2O	0.11756
L-Glutamic Acid	0.00735
L-Glutamine	0
GlutaMax	0
Glycine	0.01875
L-Histidine·HCl·H_2O	0.03148
L-Isoleucine	0.133526
L-Leucine	0.1
L-Lysine·HCl	0.4
L-Methionine	0.15
L-Ornithine HCl	0.11
L-Phenylalanine	0.03548
L-Proline	0.01725
L-Serine	0.04625
L-Threonine	0.15
L-Tryptophan	0.08
L-Tyrosine·2Na·$2H_2O$	0.05579
L-Valine	0.05285
Vitamins	

Continued on next page

Table E.1: The medium recipe for CDM4. Use Sigma DMEM/F12 media (cat#D9785-10L) (w/o bicarbonate, phenol red, and glutamine, leucine, lysine, methionine) for suspension media for CHO-K1 or Vero cells, or Corning DMEM/F12 for suspension MDCK and HEK293T, or adherent Vero.

Component	**Final Concentration (g/L)**
α-tocopherol	0.00133
D-Biotin	0.0000295
Choline Chloride	0.01188
Folic Acid	0.004462484
Ethanolamine	0.002
myo-Inositol	0.017277194
Niacinamide	0.00202
Nicotinic Acid	0.0004
D-Pantothenic Acid·1/2 Ca	0.02424
Pyridoxal·HCl	0
Pyridoxine·HCl	0.002313
Retinyl Acetate	
Riboflavin	0.000219
Thiamine·HCl	0.002403597
Vitamin B_{12}	0.000680502
Pyrimidines/Purines	
Adenosine	0.001
Guanosine	0.001
Uridine	0.0006225

Continued on next page

Table E.1: The medium recipe for CDM4. Use Sigma DMEM/F12 media (cat#D9785-10L) (w/o bicarbonate, phenol red, and glutamine, leucine, lysine, methionine) for suspension media for CHO-K1 or Vero cells, or Corning DMEM/F12 for suspension MDCK and HEK293T, or adherent Vero.

Component	**Final Concentration (g/L)**
HT Supplement (100x)	0
Thymidine	0.000365
Hypoxanthine	0.00239
Other	
D-Glucose	4.501
Linoleic Acid	0.000042
Phenol Red·Na	0.0081
Putrescine·2HCl	0.0008455
Pyruvic Acid·Na	0.11
Lipoic Acid	0.0002
Glutathione	0.001
rEGF	0
Pluronic F68	0
Lipid Mix 1	0
Progesterone	0.0032
Spermine	0.0005
Spermidine	0.0014
β-estradiol	2.7238E-06
Prostaglandin E_2	0.00001